

**EFFECT OF GLYCIDYL METHACRYLATE GRAFTED  
NATURAL RUBBER ON PROPERTIES OF PLA/NR  
BLENDS AND PLA/VETIVER/NR COMPOSITES**

**Punmanee Juntuek**

**A Thesis Submitted in Partial Fulfillment of the Requirements for the  
Degree of Doctor of Philosophy in Polymer Engineering  
Suranaree University of Technology  
Academic Year 2011**

ผลของยางธรรมชาติดัดแปรด้วยไกลซีดีลเมทาคริเลทที่มีต่อสมบัติของ  
พอลิเมอร์ผสมระหว่างพอลิแลคติกแอซิดกับยางธรรมชาติ  
และพอลิเมอร์คอมพอสิตระหว่างพอลิแลคติกแอซิด  
ยางธรรมชาติและเส้นใยหญ้าแฝก

นางสาวพันธ์มณี จันทิก

วิทยานิพนธ์นี้เป็นส่วนหนึ่งของการศึกษาตามหลักสูตรปริญญาวิศวกรรมศาสตรดุษฎีบัณฑิต  
สาขาวิชาวิศวกรรมพอลิเมอร์  
มหาวิทยาลัยเทคโนโลยีสุรนารี  
ปีการศึกษา 2554

**EFFECT OF GLYCIDYL METHACRYLATE GRAFTED  
NATURAL RUBBER ON PROPERTIES OF PLA/NR  
BLENDS AND PLA/VETIVER/NR COMPOSITES**

Suranaree University of Technology has approved this thesis submitted in partial fulfillment of the requirements for the Degree of Doctor of Philosophy.

Thesis Examining Committee

\_\_\_\_\_  
(Asst. Prof. Dr. Nitinat Suppakarn)

Chairperson

\_\_\_\_\_  
(Asst. Prof. Dr. Yupaporn Ruksakulpiwat)

Member (Thesis Advisor)

\_\_\_\_\_  
(Asst. Prof. Dr. Pranee Chumsamrong)

Member

\_\_\_\_\_  
(Asst. Prof. Dr. Chaiwat Ruksakulpiwat)

Member

\_\_\_\_\_  
(Asst. Prof. Dr. Chantima Deeprasertkul)

Member

\_\_\_\_\_  
(Assoc. Prof. Dr. Jatuporn Wittayakun )

Member

\_\_\_\_\_  
(Assoc. Prof. Dr. Ittipol Jangchud)

Member

\_\_\_\_\_  
(Prof. Dr. Sukit Limpijumnong)

Vice Rector for Academic Affairs

\_\_\_\_\_  
(Assoc. Prof. Flt. Lt. Dr. Kontorn Chamniprasart)

Dean of Institute of Engineering

พันธุมณี จันทิก : ผลของยางธรรมชาติดัดแปรด้วยไกลซิดิลเมทาคริเลทที่มีต่อสมบัติของพอลิเมอร์ผสมระหว่างพอลิแลคติกแอซิดกับยางธรรมชาติและพอลิเมอร์คอมพอสิตระหว่างพอลิแลคติกแอซิด ยางธรรมชาติและเส้นใยหญ้าแฝก (EFFECT OF GLYCIDYL METHACRYLATE GRAFTED NATURAL RUBBER ON PROPERTIES OF PLA/NR BLENDS AND PLA/VETIVER/NR COMPOSITES) อาจารย์ที่ปรึกษา : ผู้ช่วยศาสตราจารย์ ดร.ยุพาพร รักสกุลวัฒน์, 194 หน้า.

ในงานวิจัยนี้ ยางธรรมชาติดัดแปรด้วยไกลซิดิลเมทาคริเลทถูกใช้เป็นตัวเชื่อมประสานในพอลิเมอร์ผสมระหว่างพอลิแลคติกแอซิดกับยางธรรมชาติและพอลิเมอร์คอมพอสิตระหว่างพอลิแลคติกแอซิด เส้นใยหญ้าแฝกและยางธรรมชาติ ยางธรรมชาติดัดแปรด้วยไกลซิดิลเมทาคริเลทถูกเตรียมโดยใช้วิธีการอิมัลชันพอลิเมอไรเซชัน จากการทดลองพบว่า ไกลซิดิลเมทาคริเลทสามารถกราฟท์ลงบนยางธรรมชาติได้โดยวิธีการอิมัลชันพอลิเมอไรเซชัน สภาวะที่เหมาะสมในการเตรียมยางธรรมชาติดัดแปรด้วยไกลซิดิลเมทาคริเลท คือ อุณหภูมิ 30 องศาเซลเซียส และเวลา 8 ชั่วโมง

จากการศึกษาแสดงให้เห็นว่ายางธรรมชาติดัดแปรด้วยไกลซิดิลเมทาคริเลท เป็นตัวเชื่อมประสานที่มีประสิทธิภาพสำหรับพอลิเมอร์ผสมระหว่างพอลิแลคติกแอซิดกับยางธรรมชาติ เมื่อใช้ยางธรรมชาติดัดแปรเป็นตัวเชื่อมประสานในพอลิเมอร์ผสมของพอลิแลคติกแอซิด พบการกระจายตัวที่ดีขึ้นของเม็ดยางในพอลิแลคติกแอซิด ซึ่งการกระจายตัวที่ดีของเม็ดยางนี้ทำให้ค่าความต้านทานแรงกระแทกและค่าความยืดสูงสุด ณ จุดขาด ของพอลิเมอร์ผสมของพอลิแลคติกแอซิด มีค่ามากขึ้นอย่างมีนัยสำคัญ ขณะที่ค่าความต้านทานการดึงยึดและค่ามอดุลัสลดลงเพียงเล็กน้อย เมื่อเติมยางธรรมชาติดัดแปรในปริมาณ 1 เปอร์เซ็นต์โดยน้ำหนัก พบว่าค่าความต้านทานแรงกระแทกและค่าความยืดสูงสุด ณ จุดขาดเพิ่มขึ้นถึง 2 เท่าและ 2.5 เท่าตามลำดับ ยิ่งกว่านั้นเมื่อเพิ่มเปอร์เซ็นต์การกราฟท์ของยางธรรมชาติดัดแปรเป็น 2.3 ทำให้ค่าความต้านทานแรงกระแทกและค่าความยืดสูงสุด ณ จุดขาดของพอลิเมอร์ผสมของพอลิแลคติกแอซิดเพิ่มขึ้น

นอกจากนี้ยางธรรมชาติดัดแปรด้วยไกลซิดิลเมทาคริเลท ยังถูกใช้เป็นตัวเชื่อมประสานในพอลิเมอร์คอมพอสิตระหว่างพอลิแลคติกแอซิด เส้นใยหญ้าแฝกและยางธรรมชาติอีกด้วย ความเข้ากันได้ของพอลิแลคติกแอซิด เส้นใยหญ้าแฝกและยางธรรมชาติถูกปรับปรุงโดยการเติมยางธรรมชาติดัดแปรด้วยไกลซิดิลเมทาคริเลท เมื่อเติมยางธรรมชาติดัดแปรด้วยไกลซิดิลเมทาคริเลท พบว่าค่าความยืดสูงสุด ณ จุดขาดและค่าความต้านทานแรงกระแทกของพอลิเมอร์คอมพอสิตระหว่างพอลิแลคติกแอซิด เส้นใยหญ้าแฝกและยางธรรมชาติมีค่าเพิ่มขึ้น

ในงานวิจัยนี้ยังได้ศึกษาผลของการขึ้นรูปแบบฉีดและการขึ้นรูปแบบกดอัด ที่มีต่อสมบัติเชิงกลของพอลิเมอร์คอมพอสิตระหว่างพอลิแลคติกแอซิด เส้นใยหญ้าแฝกและยางธรรมชาติ ผลการทดลองพบว่า พอลิเมอร์คอมพอสิตที่ได้จากการขึ้นรูปแบบฉีดมีค่าความต้านทานการดึงยืดและค่าความต้านทานแรงกระแทกสูงกว่าพอลิเมอร์คอมพอสิตที่ได้จากการขึ้นรูปแบบกดอัด

ความสามารถในการย่อยสลายของพอลิเมอร์ผสมของพอลิแลคติกแอซิดและพอลิแลคติกแอซิดคอมพอสิต ทดสอบโดยการนำชิ้นงานฝังในดิน ทำการเปรียบเทียบสมบัติเชิงกล ของพอลิโพรพิลีน พอลิแลคติกแอซิด พอลิเมอร์ผสมของพอลิแลคติกแอซิดและพอลิแลคติกแอซิดคอมพอสิต หลังจากฝังดินเป็นเวลา 180 วัน สมบัติเชิงกลของพอลิโพรพิลีนไม่เปลี่ยนแปลง สำหรับพอลิแลคติกแอซิดและพอลิเมอร์ผสมของพอลิแลคติกแอซิด สมบัติเชิงกลมีค่าลดลงเล็กน้อย ขณะที่สมบัติเชิงกลของพอลิแลคติกแอซิดคอมพอสิตลดลงอย่างมีนัยสำคัญเมื่อเวลาในการฝังดินเพิ่มขึ้น แสดงว่าการเติมเส้นใยหญ้าแฝกมีบทบาทสำคัญต่อการเพิ่มความสามารถในการย่อยสลายของพอลิแลคติกแอซิดคอมพอสิต และยังพบว่าการเติมเส้นใยหญ้าแฝก ในปริมาณ 20 และ 30 เปอร์เซ็นต์ ทำให้น้ำหนักของพอลิแลคติกแอซิดคอมพอสิตลดลงอย่างมีนัยสำคัญเมื่อเวลาในการฝังดินเพิ่มขึ้น



สาขาวิชา วิศวกรรมพอลิเมอร์

ปีการศึกษา 2554

ลายมือชื่อนักศึกษา \_\_\_\_\_

ลายมือชื่ออาจารย์ที่ปรึกษา \_\_\_\_\_

ลายมือชื่ออาจารย์ที่ปรึกษาร่วม \_\_\_\_\_

ลายมือชื่ออาจารย์ที่ปรึกษาร่วม \_\_\_\_\_

PUNMANEE JUNTUEK : EFFECT OF GLYCIDYL METHACRYLATE  
GRAFTED NATURAL RUBBER ON PROPERTIES OF PLA/NR BLENDS  
AND PLA/VETIVER/NR COMPOSITES. THESIS ADVISOR : ASST. PROF.  
YUPAPORN RUKSAKULPIWAT, Ph.D., 194 PP.

## POLYLACTIC ACID/NATURAL RUBBER/BIOCOMPOSITES/VETIVER GRASS FIBER

In this research, glycidyl methacrylate grafted natural rubber (NR-g-GMA) was used as a compatibilizer in PLA/NR blends and PLA/vetiver/NR composites. NR-g-GMA was synthesized using emulsion polymerization method. The result showed that glycidyl methacrylate (GMA) can be grafted onto natural rubber (NR) by emulsion polymerization method. The appropriate temperature and time for preparation of the graft copolymer was 30°C and 8 hours.

From this study, NR-g-GMA was shown to be an effective compatibilizer for PLA/NR blend. With the addition of NR-g-GMA, better dispersion and distribution of NR in PLA matrix can be observed. This led to a significant increase in impact strength and elongation at break without significant loss in tensile strength and modulus of PLA/NR blends with NR-g-GMA. With increasing NR-g-GMA content up to 1% (wt/wt), impact strength and elongation at break of PLA/NR blend increased about 2 times and 2.5 times, respectively. Moreover, with increasing %grafting of NR-g-GMA up to 2.3, the impact strength and elongation at break of PLA/NR/NR-g-GMA were increased.

Moreover, NR-g-GMA was also used as a compatibilizer in PLA/vetiver/NR composites. The compatibility between PLA, vetiver grass fiber and NR was shown to

be improved by using NR-g-GMA. With the addition of NR-g-GMA, elongation at break and impact strength of PLA/vetiver/NR composites were increased.

Furthermore, effect of molding techniques (injection molding and compression molding) on the mechanical properties of PLA/vetiver/NR composites was studied. The result showed that injection molded PLA composites showed higher tensile strength and impact strength than those of compression molded PLA composites.

Finally, the biodegradability of PLA blends and PLA composites was evaluated by soil burial test. The comparisons of mechanical properties of polypropylene (PP), PLA, PLA blends and PLA composites as a function of burial time were made. After burial in soil for 180 days, the mechanical properties of PP did not change. For PLA and PLA blends, the mechanical properties were slightly decreased. In contrast, the mechanical properties of PLA composites were dramatically decreased with increasing burial time. This indicated that vetiver grass fiber showed a significant role in increasing the biodegradability of PLA composites. Moreover, the addition of vetiver grass fiber at 20 and 30% (wt/wt) content led to a significant increase in weight loss of the specimens with increasing burial time.

School of Polymer Engineering

Academic Year 2011

Student's Signature \_\_\_\_\_

Advisor's Signature \_\_\_\_\_

Co-advisor's Signature \_\_\_\_\_

Co-advisor's Signature \_\_\_\_\_

## **ACKNOWLEDGEMENTS**

I would like to thank Suranaree University of Technology, National Innovation Agency, Thailand and Center of Excellence on Petrochemical and Materials Technology for financial support. In addition, I wish to acknowledge the staffs in laboratory division of Mettler-Toledo (Thailand) Co., Ltd. for their kind supporting and providing TGA instrument. I am grateful to all the faculty and staff members of the School of Polymer Engineering and the Center for Scientific and Technological Equipment of Suranaree University of Technology for their help and assistance throughout the period of this study. The grateful thanks and appreciation are given to thesis advisor, Asst. Prof. Dr. Yupaporn Ruksakulpiwat, for her valuable supervision, advice, support and kindness throughout this study. Moreover, I would like to thank Asst. Prof. Dr. Chaiwat Ruksakulpiwat and Asst. Prof. Dr. Pranee Chumsamrong, my co-advisors for advices during my research work.

Finally, I am deeply grateful to my family and friends who support and encourage me towards the course of this study at the Suranaree University of Technology.

Punmanee Juntuek

# TABLE OF CONTENTS

	<b>Page</b>
ABSTRACT (THAI) .....	I
ABSTRACT (ENGLISH).....	III
ACKNOWLEDGEMENT .....	V
TABLE OF CONTENTS .....	VI
LIST OF TABLES.....	XII
LIST OF FIGURES .....	XIV
SYMBOLS AND ABBREVIATIONS.....	XXII
<b>CHAPTER</b>	
<b>I INTRODUCTION .....</b>	<b>1</b>
1.1 General background.....	1
1.2 Research objectives.....	3
1.3 Scopes and limitations of the study .....	3
1.4 References.....	4
<b>II LITERATURE REVIEWS .....</b>	<b>6</b>
2.1 Polylactic acid (PLA) .....	6
2.2 Natural rubber (NR).....	31
2.3 References .....	42

## TABLE OF CONTENTS (Continued)

	<b>Page</b>
<b>III GLYCIDYL METHACRYLATE GRAFTED NATURAL RUBBER</b> .....	<b>50</b>
3.1 Abstract .....	50
3.2 Introduction .....	50
3.3 Experimental .....	53
3.3.1 Materials .....	53
3.3.2 Synthesis of NR-g-GMA .....	53
3.3.3 FT-IR .....	57
3.3.4 NMR .....	57
3.3.5 Tensile tests.....	57
3.3.6 Thermal property .....	58
3.4 Results and discussion .....	59
3.4.1 Characterization of polymers .....	59
3.4.2 Effect of reaction temperature on grafting efficiency, % grafting and % conversion.....	65
3.4.3 Effect of reaction time on grafting efficiency, % grafting and % conversion.....	67
3.4.4 Effect of GMA content on grafting efficiency, % grafting and % conversion.....	69

## TABLE OF CONTENTS (Continued)

	<b>Page</b>
3.4.5 Effect of % grafting on mechanical properties .....	72
3.4.6 Effect of % grafting on thermal properties .....	76
3.5 Conclusions.....	79
3.6 References.....	80
<b>IV EFFECT OF GLYCIDYL METHACRYLATE GRAFTED NATURAL RUBBER ON PHYSICAL PROPERTIES OF POLYLACTIC ACID AND NATURAL RUBBER BLENDS.....</b>	<b>86</b>
4.1 Abstract.....	86
4.2 Introduction.....	87
4.3 Experimental.....	90
4.3.1 Materials .....	90
4.3.2 Blends preparation .....	90
4.3.3 Characterization .....	92
4.4 Results and discussion .....	95
4.4.1 Thermal properties of PLA, NR, PLA/NR and PLA/NR/NR-g-GMA.....	95
4.4.2 Rheological property of PLA, NR, PLA/NR and PLA/NR/NR-g-GMA.....	99

## TABLE OF CONTENTS (Continued)

	<b>Page</b>
4.4.3 Effect of NR content on morphological and mechanical properties of PLA/NR blend.....	100
4.4.4 Effect of NR-g-GMA content on morphological and mechanical properties of PLA/NR blend.....	105
4.4.5 Effect of %grafting of NR-g-GMA on morphological and mechanical properties of PLA/NR blend .....	114
4.5 Conclusions.....	120
4.6 References.....	121
<b>V EFFECT OF GLYCIDYL METHACRYLATE GRAFTED NATURAL RUBBER ON PHYSICAL PROPERTIES OF PLA/VETIVER/NR COMPOSITES.....</b>	<b>126</b>
5.1 Abstract.....	126
5.2 Introduction.....	127
5.3 Experimental.....	128
5.3.1 Materials .....	128
5.3.2 Vetiver grass fibers preparation.....	128

## TABLE OF CONTENTS (Continued)

	<b>Page</b>
5.3.3 Composites preparation .....	129
5.3.4 Characterization .....	130
5.4 Results and discussion .....	132
5.4.1 Gel permeable chromatography .....	132
5.4.2 Mechanical properties .....	133
5.4.3 Morphology.....	139
5.4.4 Thermal properties .....	142
5.4.5 Rheological properties .....	146
5.5 Conclusions.....	149
5.6 References.....	149
<b>VI BIODEGRADABILITY</b> .....	<b>151</b>
6.1 Abstract .....	151
6.2 Introduction .....	151
6.3 Experimental .....	153
6.3.1 Materials .....	153
6.3.2 Composites preparation .....	153
6.3.3 Characterization .....	154
6.4 Results and discussion .....	156



## LIST OF TABLES

Table	Page
2.1	Properties of some commercial PLA ..... 13
2.2	Chemical composition of vetiver grass fiber after treated with 1% (w/v) NaOH for five days ..... 26
2.3	The physical and mechanical properties of vetiver grass fiber after treated with 1% (w/v) NaOH for five days ..... 26
2.4	Physical properties of NR at 20 °C ..... 32
3.1	Formulation for the preparation of NR-g-GMA ..... 55
3.2	Composition of rubber compounds ..... 58
4.1	Blend composition ..... 91
4.2	The standard specimen size for tensile testing ..... 94
4.3	T <sub>g</sub> , T <sub>c</sub> , ΔH <sub>c</sub> , T <sub>m</sub> , ΔH <sub>m</sub> and %X <sub>c</sub> of PLA and PLA blend ..... 98
4.4	MFI of PLA and PLA blends ..... 100
4.5	Tensile strength, modulus and elongation at break of PLA and PLA/NR blends ..... 105
4.6	Tensile strength, modulus and elongation at break of PLA, PLA/NR (90/10) and PLA/NR/NR-g-GMA at various NR-g-GMA contents ..... 113
4.7	Tensile strength, modulus and elongation at break of PLA, PLA/NR (90/10) and PLA/NR/NR-g-GMA at various %grafting of NR-g-GMA ..... 119

## LIST OF TABLES (Continued)

Table	Page
5.1 Composite composition .....	130
5.2 The weight-average molecular weights ( $\overline{M}_w$ ), the number-average molecular weights ( $\overline{M}_n$ ) and the molecular weight distribution (MWD) of PLA and PLA composites .....	133
5.3 Tg, Tc, $\Delta H_c$ , Tm, $\Delta H_m$ and %Xc of PLA and PLA blend.....	146
5.4 MFI of PLA and PLA composites .....	148
6.1 Blends and Composites composition .....	154
6.2 The weight-average molecular weights ( $\overline{M}_w$ ), the number-average molecular weights ( $\overline{M}_n$ ) and the molecular weight distribution (MWD) of PLA and PLA composites before and after burial in soil.....	157
7.1 Blends and Composites composition .....	176
7.2 Impact strength, tensile strength, modulus and elongation at break of PLA, PLA blends and composites .....	175
7.3 Tg, Tc, $\Delta H_c$ , Tm, $\Delta H_m$ and %Xc of PLA blends and PLA composites .....	181

## LIST OF FIGURES

Figure	Page
2.1	Chemical structure of polylactic acid (PLA)..... 6
2.2	Lactic acid stereoisomers..... 7
2.3	The commercial process for chemical synthesis of lactic acid ..... 9
2.4	Synthesis methods for high-molecular-weight PLA ..... 11
2.5	Lactide formation mechanism..... 12
2.6	Compatibilisation of immiscible blends of polymers A and B by block or graft copolymers..... 18
2.7	Cellulose structure..... 23
2.8	Lignin structure ..... 24
2.9	Photograph of vetiver grass..... 25
2.10	Chemical structure of cis 1,4-polyisoprene..... 31
2.11	The represent structure of graft copolymer..... 34
2.12	The represent reaction of copolymerization via unsaturated groups ..... 36
3.1	Digital photographs of the reactor for prepare glycidyl methacrylate graft natural rubber..... 55
3.2	The FTIR spectra of NR and NR/PGMA blend before and after soxhlet extraction..... 56
3.3	FT-IR spectra of NR, PGMA and NR-g-GMA ..... 60
3.4	The probable structure of NR-g-GMA ..... 61

## LIST OF FIGURES (Continued)

Figure	Page
3.5	<sup>1</sup> H-NMR spectrum of unmodified NR (A) and NR-g-GMA (B)..... 63
3.6	<sup>13</sup> C-NMR spectrum of unmodified NR (A) and NR-g-GMA (B)..... 64
3.7	%Grafting at various reaction temperatures with reaction time of 8 hours ..... 66
3.8	Grafting efficiency and %conversion of GMA at various reaction temperatures with reaction time of 8 hours..... 66
3.9	%Grafting at various reaction times..... 68
3.10	Grafting efficiency and %conversion of GMA at various reaction times..... 68
3.11	FT-IR spectra of NR and NR-g-GMA at various GMA contents..... 69
3.12	%grafting and absorbance ratio at various GMA contents ..... 70
3.13	Calibration curve of absorbance ratio and %grafting ..... 71
3.14	Grafting efficiency and %conversion of GMA at various GMA contents ..... 72
3.15	Tensile stress-strain curve of NR and NR-g-GMA..... 73
3.16	Elongation at break of NR and NR-g-GMA at various %grafting ..... 75
3.17	Tensile strength of NR and NR-g-GMA at various %grafting ..... 75
3.18	100% modulus, 300% modulus and 500% modulus of NR and NR-g-GMA at various %grafting..... 76
3.19	DSC curves of NR and NR-g-GMA at various %grafting..... 77
3.20	TGA curves of NR, PGMA and NR-g-GMA at various %grafting..... 78
3.21	DTG curves of NR, PGMA and NR-g-GMA at various %grafting..... 79

## LIST OF FIGURES (Continued)

Figure	Page
4.1 The standard specimen size for impact testing .....	93
4.2 The standard specimen size for tensile testing.....	93
4.3 TGA curves of PLA, PLA/NR (90/10), PLA/NR/NR-g-GMA (B) (90/9/1) and NR.....	96
4.4 DTG curves of PLA, PLA/NR (90/10), PLA/NR/NR-g-GMA (B) (90/9/1) and NR.....	97
4.5 DSC curves of PLA, PLA/NR (90/10) and PLA/NR/NR-g-GMA (B) (90/9/1) .....	98
4.6 Shear viscosity of PLA, PLA/NR (90/10) and PLA/NR/NR-g-GMA(B) (90/9/1) at various shear rate.....	99
4.7 SEM micrographs of impact fractured surface of PLA (a), PLA/NR (95/5) (b), PLA/NR (90/10) (c), PLA/NR (80/15) (d) and PLA/NR (80/20) (e) .....	101
4.8 SEM micrographs of tensile fractured surface of PLA (a), PLA/NR (95/5) (b), PLA/NR (90/10) (c), PLA/NR (80/15) (d) and PLA/NR (80/20) (e) .....	102
4.9 Impact strength of PLA, PLA/NR blends at various NR content .....	104

## LIST OF FIGURES (Continued)

Figure	Page
4.10 SEM micrographs of impact fractured surface of PLA/NR (90/10) (a), PLA/NR/ NR-g-GMA (B) (90/9.8/0.2) (b), PLA/NR/NR- g-GMA (B) (90/9/1) (c), PLA/NR/NR-g-GMA (B) (90/7/3) (d) and PLA/NR/ NR-g-GMA (B) (90/5/5) (e) .....	107
4.11 FT-IR spectra of NR, PLA and PLA/NR-g-GMA(C) blend.....	108
4.12 SEM micrographs of tensile fractured surface of PLA/NR (90/10) (a), PLA/NR/ NR-g-GMA (B) (90/9.8/0.2) (b), PLA/NR/NR-g-GMA (B) (90/9/1) (c), PLA/NR/NR-g-GMA (B) (90/7/3) (d) and PLA/NR/ NR-g-GMA (B) (90/5/5) (e) .....	109
4.13 Impact strength of PLA, PLA/NR (90/10) and PLA/NR/NR-g-GMA at various NR-g-GMA contents .....	110
4.14 Tensile stress–strain curves of PLA, PLA/NR (90/10) and PLA/NR/NR-g- GMA(B) (90/9/1) .....	112
4.15 SEM micrographs of impact fractured surface of PLA/NR (90/10) (a), PLA/NR/NR-g-GMA(A) (90/9/1) (b), PLA/NR /NR-g-GMA (B) (90/9/1) (c), PLA/NR/NR-g-GMA (C) (90/9/1) (d), PLA/NR/- NR-g-GMA (D) (90/9/1) (e) and PLA/NR/NR-g-GMA (E) (90/9/1) (f).....	115

## LIST OF FIGURES (Continued)

Figure	Page
4.16	SEM micrographs of tensile fractured surface of PLA/NR (90/10) (a), PLA/NR/NR-g-GMA (A) (90/9/1) (b), PLA/NR /NR-g-GMA (B) (90/9/1) (c), PLA/NR/NR-g-GMA (C) (90/9/1) (d), PLA/NR/-NR-g-GMA (D) (90/9/1) (e) and PLA/NR/NR-g-GMA (E) (90/9/1) (f).....
	116
4.17	Impact strength of PLA, PLA/NR (90/10) and PLA/NR/NR-g-GMA at various %grafting of NR-g-GMA .....
	118
4.18	Pictures of PLA/NR/NR-g-GMA film.....
	120
5.1	Tensile strength of PLA and PLA composites.....
	136
5.2	Elongation at break of PLA and PLA composites .....
	137
5.3	Impact strength of PLA and PLA composites .....
	138
5.4	SEM micrographs (500x magnification) of impact fractured surface of PLA/vetiver (a), PLA/vetiver/NR (b) and PLA/vetiver/NR/NR-g-GMA(c) prepared from compression molding .....
	139
5.5	SEM micrographs (100x magnification) of tensile fractured surface of PLA/vetiver (a), PLA/vetiver/NR (b), PLA/vetiver/NR/NR-g-GMA (c), PLA/vetiver2/NR/NR-g-GMA(d) and PLA/vetiver3/NR/NR-g-GMA (e) prepared from compression molding and tensile fractured surface of PLA/vetiver (f), PLA/vetiver/NR (g), PLA/vetiver/NR/NR-g-GMA (h), PLA/vetiver2/NR/NR-g-GMA(i) and PLA/vetiver3/NR/NR-g-GMA (j) prepared from injection molding.....
	141

## LIST OF FIGURES (Continued)

Figure	Page
5.6	TGA curves of PLA, PLA/vetiver, PLA/vetiver/NR and PLA/vetiver/NR/NR-g-GMA..... 143
5.7	DTG curves of PLA, PLA/vetiver, PLA/vetiver/NR and PLA/vetiver/NR/NR-g-GMA..... 143
5.8	TGA curves of PLA, PLA/vetiver/NR/NR-g-GMA, PLA/vetiver2/NR- /NR-g-GMA and PLA/vetiver3/NR/NR-g-GMA ..... 144
5.9	DTG curves of PLA, PLA/vetiver/NR/NR-g-GMA, PLA/vetiver2/NR-/NR-g-GMA and PLA/vetiver3/NR/NR-g-GMA ..... 144
5.10	DSC curves of PLA, PLA/vetiver, PLA/vetiver/NR, PLA/vetiver/NR/NR-g-GMA, PLA/vetiver2/NR-/NR-g-GMA and PLA/vetiver3/NR/NR-g-GMA..... 145
5.11	Shear viscosity of PLA, PLA/vetiver, PLA/vetiver/NR and PLA/vetiver/NR/NR-g-GMA at various shear rate ..... 147
5.12	Shear viscosity of PLA/vetiver/NR/NR-g-GMAPLA, PLA/vetiver2/NR/NR-g-GMAPLA and PLA/vetiver3/NR/NR-g-GMAPLA at various shear rate..... 148

## LIST OF FIGURES (Continued)

Figure	Page
6.1	Pictures of PP, PLA, PLA/NR, PLA/NR/NR-g-GMA, PLA/vetiver, PLA/vetiver/NR, PLA/vetiver/NR/NR-g-GMA, PLA/vetiver2/NR/NR-g-GMA and PLA/vetiver3/NR/NR-g-GMA before and after burial in soil for 180 days.....158
6.2	Impact strength of PP, PLA, PLA/NR and PLA/NR/NR-g-GMA..... 160
6.3	Impact strength of PLA/vetiver, PLA/ vetiver /NR, PLA/ vetiver /NR/NR-g-GMA, PLA/ vetiver 2/NR/NR-g-GMA and PLA/ vetiver3 /NR/NR-g-GMA..... 161
6.4	Tensile strength of PP, PLA, PLA/NR and PLA/NR/NR-g-GMA..... 162
6.5	Tensile strength of PLA/vetiver, PLA/ vetiver /NR, PLA/vetiver/NR/NR-g-GMA, PLA/vetiver2/NR/NR-g-GMA and PLA/vetiver 3/NR/NR-g-GMA ..... 163
6.6	Elongation at break of PP, PLA/NR and PLA/NR/NR-g-GMA..... 164
6.7	Elongation at break of PLA, PLA/vetiver, PLA/ vetiver /NR, PLA/vetiver/NR/NR-g-GMA, PLA/vetiver2/NR/NR-g-GMA and PLA/vetiver 3/NR/NR-g-GMA ..... 165
6.8	Weight loss of PLA, PLA blends and PLA composites during the burial in soil..... 167

## LIST OF FIGURES (Continued)

Figure	Page
6.9 SEM micrographs (500x magnification) of surface morphology of PLA/NR/NR-g-GMA before burial in soil (a), PLA/NR/NR-g-GMA after burial in soil (b), PLA/vetiver2/NR/NR-g-GMA before burial in soil (c) and PLA/vetiver2/NR/NR-g-GMA after burial in soil (d) prepared from compression molding .....	168
7.1 TGA curves of PLA blends and PLA composites.....	179
7.2 TGA curves of PLA blends and PLA composites at various CaCO <sub>3</sub> contents.....	179
7.3 DSC curves of PLA, PLA blends and PLA composites (Second heating scan).....	180
7.4 DSC curves of PLA, PLA blends and PLA composites at various CaCO <sub>3</sub> contents (Second heating scan).....	180

## SYMBOLS AND ABBREVIATIONS

°C	=	Degree Celsius
%	=	Percent
wt	=	Weight
v	=	Volume
μm	=	Micrometer
g	=	Gram
cm <sup>3</sup>	=	Cubic centimeter
μm	=	Micrometer
MPa	=	Megapascal
GPa	=	Gigapascal
cal	=	Calorie
kJ	=	Kilojoule
J	=	Joule
s	=	Second
m <sup>2</sup>	=	Squaremeter
cm <sup>2</sup>	=	Square centimeter
phr	=	Parts per hundred of rubber
min	=	Minute
cm <sup>-1</sup>	=	Per centimeter
ppm	=	Parts per million

**SYMBOLS AND ABBREVIATIONS (Continued)**

$\Delta H$	=	Heat of fusion
mg	=	Milligram
rpm	=	Revolution per minute
kg	=	Kilogram
$\%X_c$	=	Degree of crystallinity



# CHAPTER I

## INTRODUCTION

### 1.1 General Background

In the past decade, many investigations were focused on biopolymers because they have less harmful effect on environment compared to fossil fuel based plastics. One of the most important biodegradable polymers is poly (lactic acid) (PLA), whose monomer unit is derived from renewable natural resources such as starch, sugar and cellulose. Moreover, PLA has attracted great attention due to its excellent properties such as high mechanical properties, high stiffness and biocompatibility. However, the inherent brittleness, low-melt viscosity, and low-heat distortion temperature of PLA have restricted its applications (Lunt, 1998); (Martin and Averous, 2001).

In order to improve toughness of PLA, flexible polymers such as polycaprolactone (PCL) (Broz, VanderHart, and Washburn, 2003), polybutylene-succinate (PBS) (Shibata, Inoue, and Miyoshi, 2006) and poly(butylene adipate-co-terephthalate) (PBAT) (Chen, Tan, Chen, Yang, and Wang, 2008) were blended with PLA. However, these flexible polymers come from petroleum resource, whose price tends to increase in the future. Therefore, new materials from renewable resource are interesting choices.

Natural rubber (NR) is one of interesting materials because it has excellent properties such as high strength, high resilience and high elongation at break (Oksman, 2000). Moreover, NR is a natural polymer which comes from renewable

resource. It is also one of the most significant agricultural products of Thailand. From these reasons, NR is used to improve impact strength and flexibility of PLA. The addition of NR in PLA can improve impact strength of PLA (Zhang, Man, Pan, Wang, Jiang, and Dan, 2011). However, to obtain higher impact strength the miscibility between PLA and NR can be improved by adding compatibilizer. Glycidyl methacrylate (GMA) grafted polymers are often used as reactive compatibilizers in polyester blends (Sun, Hu, and Lambla, 1996). It is usually believed that epoxy groups of GMA can react with carboxyl or hydroxyl groups of polyester. Therefore, it is expected that the compatibility of PLA/NR blends can be improved by using glycidyl methacrylate grafted natural rubber (NR-g-GMA) as a compatibilizer.

In order to improve tensile strength of PLA, many studies have been carried out to investigate the addition of natural fibers such as abaca fiber (Teramoto, Urata, Ozawa, and Shibata, 2004), flax fiber (Oksman, Skrifvars, and Selin, 2003); (Oksman, 2000) and kenaf fibers (Ochi, 2008) as reinforcing components. Generally, the tensile strength of PLA is greatly improved when reinforced with fibers. Vetiver grass is one attractive natural fiber that can be used to improve tensile strength of PLA. It is a tropical plant which grows naturally. In Thailand, vetiver grass can be found growing in a wide range of area from highlands to lowlands in various soil conditions, so this lead to low-price of vetiver grass. In our previous study, it was shown that the addition of vetiver grass fiber in polypropylene (PP) led to an increase in tensile strength (Ruksakulpiwat, Suppakarn, Sutapun, and Thomthong, 2007); (Somnuk, Eder, Phinyocheep, Suppakarn, Sutapun, and Ruksakulpiwat, 2007). Therefore, it is expected that the addition of vetiver grass in PLA/NR blends can improve tensile strength and an inexpensive price can be obtained.

## 1.2 Research objectives

The main objectives of this research can be classified as follows:

- (i) To study the preparation of glycidyl methacrylate grafted natural rubber (NR-g-GMA)
- (ii) To study the effects of NR-g-GMA on properties of PLA/NR blends.
- (iii) To study the effects of NR-g-GMA on properties of PLA/vetiver/NR composites.
- (iv) To study the effects of molding techniques including, injection molding and compression molding, on properties of PLA and PLA composites.
- (v) To study biodegradability of PLA, PLA/NR blends and PLA/vetiver/NR composites.

## 1.3 Scopes and limitations of the study

Glycidyl methacrylate grafted natural rubber (NR-g-GMA) was synthesized by emulsion polymerization method. Cumene hydroperoxide (CHP) and tetraethylenepentamine (TEPA) were used to initiate polymerization. Sodiumdodecyl sulphate (SDS) was used as a surfactant. The structures of NR-g-GMA were characterized by  $^1\text{H}$  nuclear magnetic resonance spectroscopy ( $^1\text{H}$  NMR) and Fourier transform infrared spectroscopy (FT-IR). The PLA/NR blends and PLA/vetiver/NR composites were melted blending using an internal mixer. The effects of NR-g-GMA on mechanical, rheological, morphological and thermal properties of PLA/NR blends and PLA/vetiver/NR composites were studied. Heat treatment method was done to obtain heat treated vetiver grass fibers. The effects of vetiver grass fiber content on mechanical, rheological, morphological and thermal properties of PLA/vetiver/NR

composites using NR-g-GMA as a compatibilizer were also studied. The interaction of PLA and NR-g-GMA was evaluated using FT-IR. The morphology of the composites was observed by scanning electron microscopy (SEM). Thermal properties of PLA/NR blends and PLA/vetiver/NR composites were studied by differential scanning calorimetry (DSC) and thermogravimetric analysis (TGA). The mechanical properties of all composites were compared. The rheological property of PLA/vetiver/NR composites was studied using capillary rheometer and melt flow indexer. In addition, the biodegradability of PLA, PLA/NR blends and PLA/vetiver/NR composites was studied.

#### 1.4 References

- Broz, M.E., VanderHart, D.L., and Washburn, N.R. (2003). Structure and mechanical properties of poly (d, l-lactic acid)/poly ( $\epsilon$ -caprolactone) blends. **Biomaterials**. 24: 4181-4190.
- Chen, Y., Tan, L., Chen, L., Yang, Y., and Wang, X. (2008). Study on biodegradable aromatic/aliphatic polyesters. **Braz. J. Chem. Eng.** 25: 321-335.
- Lunt, J. (1998). Large-scale production, properties and commercial applications of polylactic acid polymers. **Polym. Degrad. Stab.** 59: 145-152.
- Martin, O., and Averous, L. (2001). Poly (lactic acid): plasticization and properties of biodegradable multiphase systems. **Polymer**. 42: 6209-6219.
- Ochi, S. (2008). Mechanical properties of kenaf fibers and kenaf/PLA composites. **Mech. Mater.** 40: 446-452.
- Oksman, K. (2000). Mechanical properties of natural fibre reinforced thermoplastic. **Appl. Compos. Mater.** 7: 403-414.

- Oksman, K., Skrifvars, M., and Selin, J.F. (2003). Natural fibres as reinforcement in polylactic acid (PLA) composites. **Compos. Sci. Technol.** 63: 1317-1324.
- Ruksakulpiwat, Y., Suppakarn, N., Sutapun, W., and Thomthong, W. (2007). Vetiver -polypropylene composites: physical and mechanical properties. **Compos. Part A: Appl. Sci. Manufact.** 38: 590-601.
- Shibata, M., Inoue, Y., and Miyoshi, M. (2006). Mechanical properties, morphology, and crystallization behavior of blends of poly (L-lactide) with poly (butylene succinate-co-L-lactate) and poly (butylene succinate). **Polymer.** 47: 3557-3564.
- Somnuk, U., Eder, G., Phinyocheep, P., Suppakarn, N., Sutapun, W., and Ruksakulpiwat, Y. (2007). Quiescent crystallization of natural fibers polypropylene composites. **J. Appl. Polym. Sci.** 106: 2997-3006.
- Sun, Y.J., Hu, G.H., and Lamba, M. (1996). In situ compatibilization of polypropylene and poly (butylene terephthalate) polymer blends by one-step reactive extrusion. **Polymer.** 37: 4119-4127.
- Teramoto, N., Urata, K., Ozawa, K., and Shibata, M. (2004). Biodegradation of aliphatic polyester composites reinforced by abaca fiber. **Polym. Degrad. Stab.** 86: 401-409.
- Zhang, C., Man, C., Pan, Y., Wang, W., Jiang, L., and Dan, Y. (2011). Toughening of polylactide with natural rubber grafted with poly (butyl acrylate). **Polym. Int.** pi. 3118.

## CHAPTER II

### LITERATURE REVIEW

#### 2.1 Poly (lactic acid) (PLA)

Poly (lactic acid) (PLA), synthetic aliphatic polyester derived from biomasses, is an environmental friendly polymer and has been emerging as an alternative to conventional petroleum-based polymeric materials because of its renewability, biodegradability and greenhouse gas neutrality. PLA has high mechanical properties and biocompatibility. It has been proposed as a renewable and degradable plastic for uses in service ware, grocery, waste-composting bags and mulch films, controlled release matrices for fertilizers, pesticides, and herbicides. The products made from PLA is bio-degradable and reverts in less than 60 days in ideal conditions, namely in commercial composting installations. However, PLA is still more expensive than many petroleum-derived commodity plastics and some of other properties such as impact strength are frequently insufficient for various end-use applications (Rudnik, 2008). Molecular structure of PLA is schematically presented in Figure 2.1.

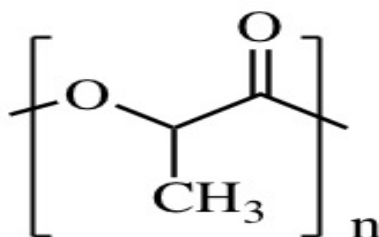


**Figure 2.1** Chemical structure of poly (lactic acid) (PLA).

PLA is most commonly synthesized either through polycondensation of lactic acid (2-hydroxy propionic acid) or ring-opening polymerization of lactide (LA) (the dimer of lactic acids). Lactic acid is one of the simplest chiral molecules and exists as the two stereo isomers: L- lactic acid and D-lactic acid. The D form differs from the L form in its effect on polarized light. The plane is rotated in a clockwise (dextro) direction for D-lactic acid while the L form rotates the plane in anticlockwise (laevo) direction (Lunt, 1998) as shown in Figure 2.2.

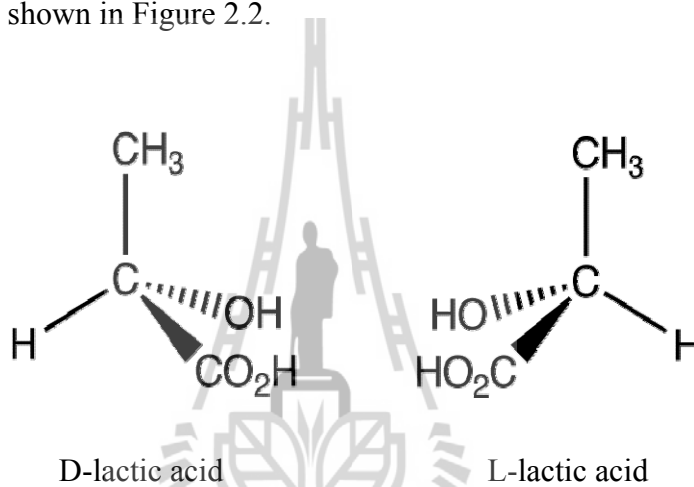


**Figure 2.2** Lactic acid stereoisomers (Lunt, 1998).

Lactic acid was discovered by the Swedish chemist Sheele in 1870 as a sour component of milk, and was first produced commercially by Charles E. Avery at Littleton, Massachusetts, USA, in 1881. Lactic acid can be produced via bacterial fermentation of corn starch, or other starch-rich substances like maize, sugar or wheat, using homolactic organisms (Lunt, 1998). The commercial process for chemical synthesis is based on lactonitrile ( $\text{CH}_3\text{CHOHCN}$ ). Hydrogen cyanide (HCN) is added

to acetaldehyde ( $\text{CH}_3\text{CHO}$ ) in the presence of a base to produce lactonitrile (as illustrated in Figure 2.3). This reaction occurs in liquid phase at high atmospheric pressures. The crude lactonitrile is recovered and purified by distillation. It is then hydrolyzed to lactic acid, either by concentrated  $\text{HCl}$  or by  $\text{H}_2\text{SO}_4$  to produce the corresponding ammonium salt and lactic acid. Lactic acid is then esterified with methanol to produce methyl lactate, which is removed and purified by distillation and hydrolyzed by water under acid catalyst to produce lactic acid and the methanol, which is recycled (Narayanan, Roychoudhury, and Srivastava, 2004). Lactic acid produced by petrochemical route exists as a racemic (optically inactive) mixture of D and L forms. Though chemical synthesis produces a racemic mixture, stereo specific lactic acid can be made by carbohydrate fermentation depending on the strain being used. The organisms that predominantly yield the L-isomer are *Lactobacilli amylophilus*, *L. bavaricus*, *L. casei*, *L. maltaromicus*, and *L. salivarius*. Strains such as *L. delbrueckii*, *L. jensenii*, or *L. acidophilus* yield the D-isomer or mixtures of both (Hartmann, 1998).

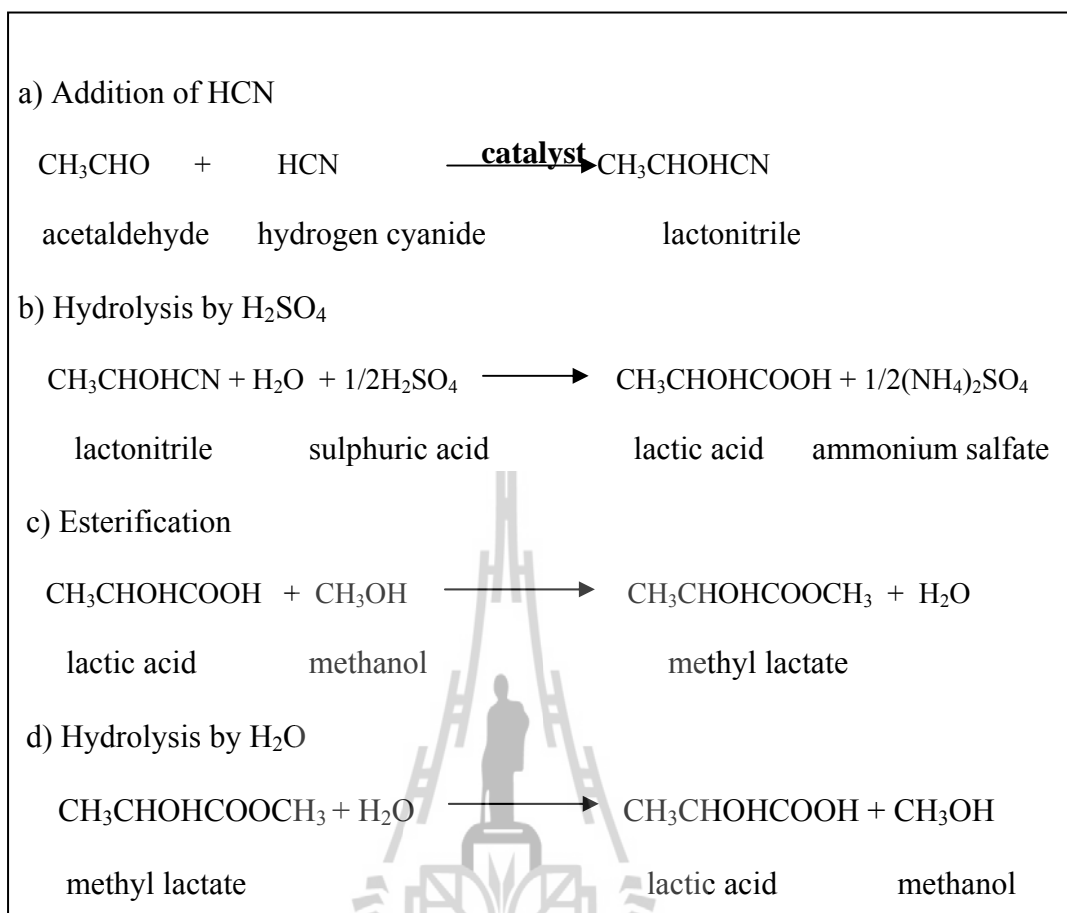


**Figure 2.3** The commercial process for chemical synthesis of lactic acid  
(Narayanan et al., 2004).

High-molecular weight PLA can be produced using several techniques, including azeotropic dehydrative condensation, direct condensation polymerization and polymerization through lactide formation. The commercial high molecular weight PLA resins are generally produced via the lactide ring-opening polymerization route (Auras, Harte, and Selke, 2004); (Garlotta, 2001); (Ikada and Tsuji, 2000). Recently, Cargill Dow used a solvent-free process and a novel distillation process to produce a range of PLA polymers (Gruber, Hall, Kolstad, Iwen, Benson, and Borchardt, 1992). The essential novelty of the process lies in the ability to go from lactic acid to a low-

molecular weight polylactic acid, followed by controlled depolymerization to produce the cyclic dimer, commonly referred to lactide. This lactide is maintained in the liquid form and purified by distillation. Catalytic ring opening of the lactide intermediate results in the production of PLA with controlled molecular weights. The process is continuous with no necessity to separate the intermediate lactide. In contrast, Mitsui Toatsu (Enomoto, Ajioka, and Yamaguchi, 1994) utilises a solvent based process in which a high-molecular-weight polymer is produced by direct condensation using azeotropic distillation to remove the water of condensation continuously. Figure 2.4 illustrates the steps involved in these two processes. Producing the cyclic dimer (lactide) introduces the potential to tailor molecular architecture in the final product. By controlling residence time and temperature in combination with catalyst type and concentration, it is possible to control the ratio and sequencing of D- and L-lactic acid units in the final polymer. Since L-lactic acid can be controllably racemised to D-lactic acid, then during the depolymerisation stage, three forms of lactide are possible (Figure 2.5). Only the L- and D- forms demonstrate optical activity. The meso form is optically inactive. Compositional control of the lactide stream dictates many properties of the final polymer.

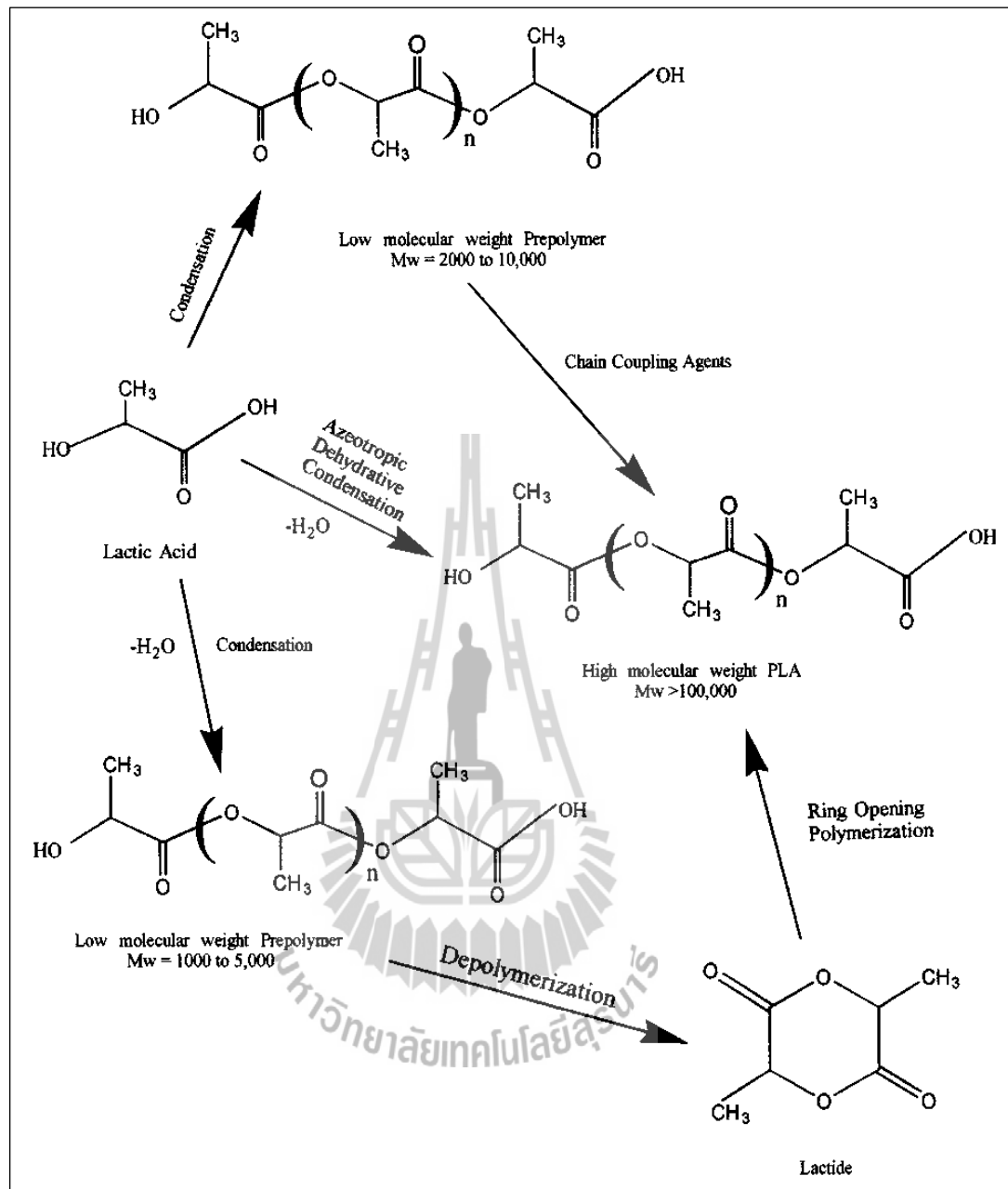


**Figure 2.4** Synthesis methods for high-molecular-weight PLA (Hartmann, 1998).

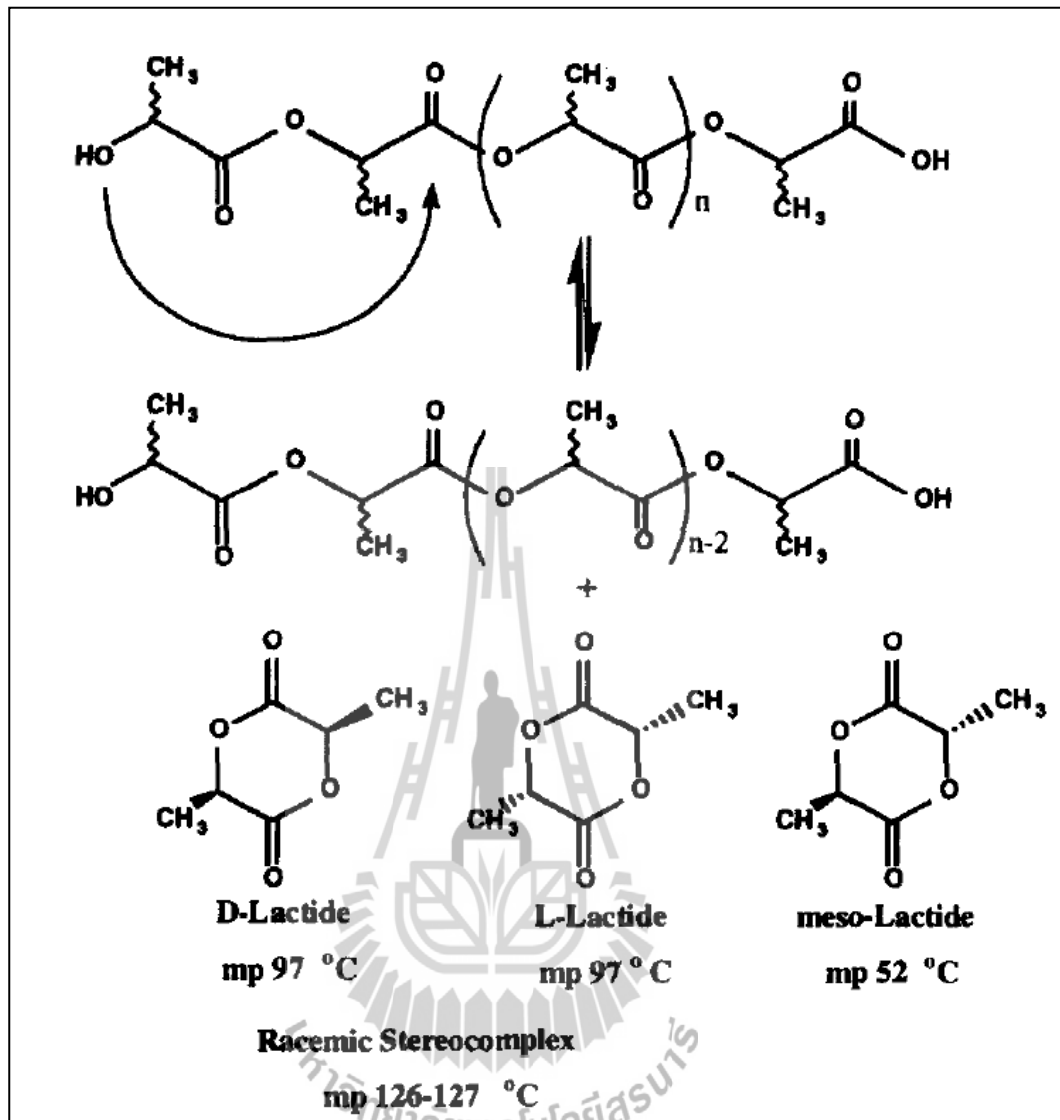


**Figure 2.5** Lactide formation mechanisms (Lunt, 1998).

Poly (lactic acid) homopolymers have some properties as shown in Table 2.1. They require processing temperatures in excess of 185-190°C (Garlotta, 2001). Glass transition temperature ( $T_g$ ) and melting temperature ( $T_m$ ) are strongly affected by overall optical composition, primary structure, thermal history, and molecular weight. Below  $T_g$ , PLA will only behave as a brittle polymer. In order to PLA to be processed on large-scale production lines in applications such as injection molding, blow

molding, thermoforming, and extrusion, the polymer must possess adequate thermal stability to prevent degradation and maintain molecular weight and properties. PLA degradation is dependent on time, temperature, low-molecular-weight impurities, and catalyst concentration. Catalysts and oligomers decrease the degradation temperature and increase the degradation rate of PLA. In addition, they can cause viscosity and rheological changes during processing, and poor mechanical properties (Garlotta, 2001).

**Table 2.1** Properties of some commercial PLA (NatureWork, 2005; Biomer, 2006).

Properties	NatureWork® PLA	Biomer® L9000
Density (g/ml)	1.24	1.25
T <sub>g</sub> (°C)	56.7 - 57.9	n/a
T <sub>m</sub> (°C)	140 - 152	n/a
HDT (°C)	40 - 45 (amorphous) 135 (crystalline)	n/a
Tensile strength (MPa)	53	70
Elongation at break (%)	6	2.4
Flexular Modulus (MPa)	350 - 450	3,600

### 2.1.1 PLA blend

When one tries to mix two polymers in order to get a material with properties somewhere between those of the two polymers, materials made from two polymers mixed together are called polymer blends. The technology of polymer blends has been one of major areas of research and development in polymer science in

the past three decades. A new polymers modification process, based on a simple mechanical mixture of two polymers first appeared when Thomas Hancock (1823) got one mixture of natural rubber (NR-an amorphous cis-1,4-poly isoprene) with gutta-percha (GP-a semi-crystalline trans-1,4-poly isoprene) using a spiked. In 1846, Parkes patented the first polymer blend: NR with GP partially co-dissolved in CS<sub>2</sub>. Blending these two isomers resulted in partially crosslinked (co-vulcanized) materials whose rigidity was controllable by composition. The blends had many applications ranging from picture frames, table-ware, ear-trumpets, to sheathing the first submarine cables.

PLA has excellent properties including tensile strength, thermal plasticity, processing ability and biocompatibility compared to many petroleum-based plastics (Martin and Averous, 2001). However, PLA is very brittle under tensile and bending loads leading to serious physical aging during application (Jun, 2000); (Lunt, 1998). Blending of PLA with other more flexible polymers is interesting technique. The expectation of this operation is the increasing of impact strength while maintains high modulus and tensile strength of PLA blend. For example, PLA is blended with other more flexible polymers such as (butylene adipate-co-terephthalate) (PBAT) (Jiang, Wolcott, and Zhang, 2006); (Chen, Tan, Chen, Yang, and Wang, 2008), poly ( $\epsilon$ -caprolactone) (PCL) (Sarazin, Li, Orts, and Favis, 2008), polybutylene-succinate (PBS) (Shibata, Inoue, and Miyoshi, 2006), poly (3-hydroxybutyrate-co-3-hydroxyhexanoate) (PHBHHx) (Schreck and Hillmyer, 2007) and poly (ethylene oxide) (PEO) (Nijenhuis, Colstee, Grijpma, and Pennings, 1996). It was expected that these polymers can improve mechanical properties of PLA. The experimental results showed that impact strength of the PLA blend was greatly increased. A significant increase in the elongation at break and decrease in tensile strength can be observed.

The stress-extension curve showed the material changed from brittle (PLA) to ductile failure with the addition of flexible polymers. These works demonstrate that blend of PLA and more flexible polymers is a viable technique to expand the property range of PLA materials.

### **2.1.2 Miscibility of PLA blend**

Utracki (1989) defines the polymer blend as a mixture of at least two polymers or copolymers comprising more than 2 wt% of each macromolecular component. Depending on the sign of the free energy of mixing, the components of the blends are miscible and immiscible. Miscibility in the context of polymer blends is defined as the degree of mixing to yield properties (e.g., glass transition temperature, permeability) expected of a single phase material. Polymer blends can be broadly divided into three categories: miscible, partially miscible and immiscible blends. A miscible polymer blend is capable of forming a single phase over certain range of temperature, pressure, and composition also it can be thermodynamically stable, exhibits a single  $T_g$  or optical clarity. An immiscible polymer blend means a multiphase system. Miscibility between PLA/PBAT (Gu, Zhang, Ren, and Zhan, 2008) and PLA/PHBHHx (Gao et al., 2006) were studied. The phase morphology of PLA/PBAT blends was observed by scanning electron microscopy (SEM). An oval cavities and enclosed round PBAT particles are visible on the fractured surfaces. The blend is a kind of immiscible, two-phase system with PBAT dispersing evenly in PLA matrix because of the immiscibility between PLA and PBAT. Miscibility of PLA/PHBHHx blend was studied using differential scanning calorimetry (DSC) analysis. The result indicated that the glass transition temperature ( $T_g$ ) of the PLA

component in PLA/PHBHHx blends were independent of the blend composition, indicating that the blend is immiscible in the molten state.

Zhang, Goh, and Lee (1998) studied the miscibility of poly (L-lactide) (PLLA)/poly (p-vinylphenol) (PVPh) blends by DSC. They found that PLLA/PVPh blends are partially miscible as characterized by shifts in the  $T_g$  of the two component polymers. The  $T_g$  of the PLLA-rich phase increases with increasing PVPh content, while that of the PVPh-rich phase decreases with increasing PLLA content. The apparent melting temperature ( $T_m$ ) of PLLA is significantly decreased with increasing PVPh content.

Broz et al. (2003) studied the miscibility of PLA/PCL blends using DSC and nuclear magnetic resonance spectroscopy (NMR). The DSC and NMR results suggested that PCL still crystallizes at levels very similar to pure PCL. In addition, very little mixing occurs between PLA and the non-crystalline PCL. In fact, phase separation on a distance scale larger than the separation between PCL crystallites is indicated. The results proved that PLA and PCL are not miscible and that some adhesion may occur at the PLA/PCL interface when the majority phase is PCL but not when it is PLA.

### **2.1.3 Compatibilizer for PLA blends**

Polymer blending is a very attractive way to obtain new material. However, most of polymer blends are immiscible and/or incompatible. If useful properties are to be achieved, compatibilization methods must be employed for these blends. Compatibilisation is any physical or chemical process of modification of interfacial properties of an immiscible polymer blend, resulting in formation of the interphase and stabilisation of the desired morphology thus leading to the creation of a

polymer alloy. The compatibilisation must not only ensure a certain morphology and improvement in performance but must be also stable and reproducible, insensitive to forming stresses and repeated processing. A compatible polymer blend indicates a commercially attractive polymer mixture, normally homogeneous to the eye, frequently with some enhanced properties compared to those of the individual components. Various techniques were used to improve compatibility of polymer blend such as adding of non-reactive compatibilizer (graft or block copolymers), adding of a reactive polymer or functionalised polymer, in situ reactive compatibilisation, compatibilisation by transesterification and dynamic vulcanization. A compatibilizer, can be added to the polymer mixture as a third component or generated '*in situ*' during reactive compatibilisation process. It can be a grafted copolymer or, most often, a block copolymer, see Figure 2.6. The added compatibilizer should migrate to the interface, reducing the interfacial tension coefficient and the size of the phase domains (a finer dispersion of the minor component), as well as creating improved adhesion in the solid state. Intensified phase interactions and control phase morphology lead to improvements in mechanical properties of the blends. An additional function of compatibilizers is stabilisation of the blend morphology against coalescence and agglomeration of the dispersed particles that can take place during the following processing and forming steps. Most of polymer blends are highly immiscible leading to poor mechanical properties.

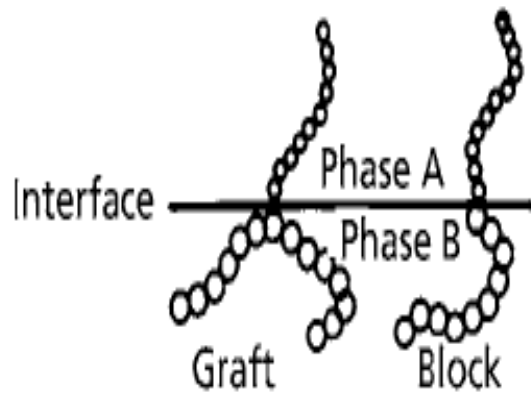


**Figure 2.6** Compatibilisation of immiscible blends of polymers A and B by block or graft copolymers (Cornelia, Anand, and Kulshereshta, 2002).

Miscibility of polymer blend was improved by many researchers. As an example, Wang, Ma, Gross, and McCarthy (1998) studied reactive compatibilization of biodegradable blends of PLA and PCL. Mechanical property measurements indicated that the elongation at break of the PLA/PCL blends was improved significantly when compared to that of pure PLA especially for the reactively compatibilized blends. Degradation studies showed that the enzymatic degradation rate (or normalized weight loss) of the reactively compatibilized blends were much higher than that of pure PLA and PCL, while the degradation rate of physical blends are between those of pure PLA and PCL.

Li and Shimizu (2009) also improved the toughness of PLLA through reactive blending with acrylonitrile-butadiene-styrene copolymer (ABS). The results showed that uncompatibilized blends of PLLA and ABS have morphology with big phase size and weak interface. The blends exhibited poor mechanical properties with low elongation at break and low impact strength. Styrene/acrylonitrile/glycidyl methacrylate copolymer (SAN-GMA) was found to be an effective reactive

compatibilizer for PLLA/ABS blend by the presence of ethyltriphenyl phosphonium bromide (ETPB) as a catalyst. The results showed significant improvement in the dispersion of rubber particles as well as the clearly shifted glass transition temperature of both PLLA and ABS. Compatibilized PLLA/ABS blends exhibit an increase of impact strength and elongation at break with a slight loss in the modulus and tensile strength.

Oyama (2009) toughened PLA by reactive blending with poly (ethylene-glycidyl methacrylate) (EGMA). This study demonstrated a dramatic improvement in the mechanical characteristics of PLA by its reactive blending with EGMA. The results showed that very high performance of PLA blends was obtained by reactive blending of PLA and EGMA. The elongation at break of PLA blends showed 40 times higher than that of neat PLA. Annealed PLA/EGMA blends had impact strengths over 50 times higher than the neat PLA. Here, it is considered that the epoxy group in EGMA reacts with both the carboxyl groups and the hydroxyl groups located at the PLA chain ends during melt-mixing leading to an improvement in miscibility and mechanical properties of PLA blend.

Shibata, Teramoto, and Inoue (2007) studied mechanical properties, morphologies, and crystallization behavior of plasticized PLLA/poly (butylene succinate-co-L-lactate) (PBSL) blends. The blends of PLLA with PBSL containing the lactate unit of 3 mol% and Rikemal PL710 (RKM) which is a plasticizer mainly composed of diglycerine tetraacetate. The RKM content in PLLA/PBSL/RKM blends was 0-20 wt%, and the PLLA/PBSL weight ratio was 100/0 to 80/20. Although elongation at break in the tensile test did not increase by the addition of 10 wt% RKM to PLLA, the addition of a small amount of PBSL to the PLLA/RKM blend caused a

considerable increase of the elongation. The SEM and DSC analysis revealed that all the PLLA/PBSL/RKM blends were immiscible blends where the PBSL particles were finely dispersed, and they suggested that there was some compatibility between PLLA-rich phase and PBSL-rich phase in the amorphous state when the RKM content is 20 wt%. As a result of investigation of the crystallization behavior by DSC and polarized optical microscopic measurements, it was revealed that the addition of RKM caused the acceleration of crystalline growth rate at a lower annealing temperature, and the addition of PBSL mainly enhanced the formation of PLLA crystal nucleus.

Huneault and Li (2007) investigated the properties and interfacial modification of blends of PLA and glycerol-plasticized thermoplastic starch (TPS). A twin-screw extrusion process was used to gelatinize the starch, devolatilize the water to obtain a water-free TPS and then to blend into the PLA matrix. The investigated TPS concentration ranged from 27 to 60 wt%. In the absence of interfacial modification, the TPS/PLA blend morphology observed through SEM was very coarse with TPS particles sizes between 5 and 30  $\mu\text{m}$ . They improved miscibility of these blends by free-radical grafting of maleic anhydride (MA) onto the PLA and then reacting the modified PLA with the starch macromolecules. Blends comprising MA-grafted PLA showed much finer dispersed phase size, in the 1-3  $\mu\text{m}$  range and exhibited a dramatic improvement in ductility. Elongation at break of modified blends was in the 100-200% range compared to 5-20% for non-modified control and for the pure PLA. They suggested that this improvement was due to a more homogeneous blend and smaller TPS particle sizes and possibly due to an improvement of interfacial adhesion between the TPS and PLA phases.

Chen et al. (2006) also investigated PLLA/starch blends. They used poly (L-lactide)-g-starch copolymer (PLLA-g-St) as a compatibilizer. The results showed that the use of PLLA-g-St as a compatibilizer in PLLA/starch blends can improve the performances without changing their whole biodegradability. PLLA-g-St is a good compatibilizer for the blend of hydrophobic PLLA and hydrophilic granular corn starch. The PLLA-g-St effectively improved the interfacial adhesion and the mechanical properties of the composites. The PLLA-g-St compatibilized PLLA/Starch blends showed better mechanical properties and stronger medium-resistance in comparison with the simple starch/PLLA blend.

Ho, Wang, Lin, and Lee (2008) used a thermoplastic polyolefin elastomer-graft-poly lactide (TPO-PLA) as a compatibilizer for PLA/starch blends. TPO-PLA was prepared by grafting poly lactide onto maleic anhydride-functionalized TPO (TPO-MAH) in the presence of 4-dimethylaminopyridine (DMAP). A Molau test and the SEM images of cryo-fractured surface of PLA/TPO binary blends and PLA/TPO/TPO-PLA ternary blends, indicated that the particle size dispersed in PLA matrix substantially decreased as the concentration of the compatibilizers increased, until the content exceeded the critical micelle concentration. Compatibilizing the PLA/TPO (80/20) blend with TPO-PLA copolymer reduced the tensile strength and tensile modulus because of the natural elastic property with low strength and modulus. However, the enhanced interfacial adhesion strength markedly increased the elongation at break and tensile toughness. Moreover, the result indicated that a TPO-PLA copolymer is more efficient than TPO-MAH in compatibilizing the PLA/TPO (80/20) blend. The PLA/TPO (80/20) blend with TPO-PLA showed smaller particle

size, narrower size distribution and higher elongation at break and greater tensile toughness.

Su, Li, Liu, Hu, and Wu (2009) studied the compatibility and interaction of PLA and glycidyl methacrylate grafted poly (ethylene octane) (GMA-g-POE denoted as mPOE) blend. They found that all the PLA/mPOE blends exhibit two distinct glass transition temperatures. These peaks approached each other with increasing mPOE content, indicating that the PLA/mPOE blend is a partially compatible polymer pair. The reaction between the epoxy groups of the mPOE and the carboxyl end-groups of the PLA enhanced the compatibility between the PLA and mPOE. The T<sub>g</sub> of the mPOE in the PLA/mPOE blends was smaller than that of the pure mPOE. It was attributed to the negative pressure imposed on the dispersed rubber phase, resulting from differential contraction due to the thermal shrinkage mismatch upon cooling from the melt state.

#### **2.1.4 Natural fibers reinforced PLA**

Natural fibers are subdivided based on their origins, whether they are derived from plants, animals, or minerals. The chemical compositions as well as the structure of fibers are fairly complicated. Most plant fibers are composed of cellulose, hemicelluloses, lignin, waxes, and some watersoluble compound. Cellulose, hemicelluloses and lignin are the major constituents. The amount of cellulose in lignocellulosic system depends on the species and age of the plant. Cellulose is a hydrophilic glucan polymer consisting of a linear chain of 1, 4- $\beta$  anhydroglucose unite, which contain alcoholic hydroxyl group (Figure 2.7). These hydroxyl groups form intermolecular and intramolecular hydrogen bonds with the macromolecule itself and also with other cellulose macromolecules or polar molecules. Therefore, all

natural fibers are hydrophilic in nature. Although the chemical structure of cellulose from different natural fiber is the same, the degree of polymerization varies.

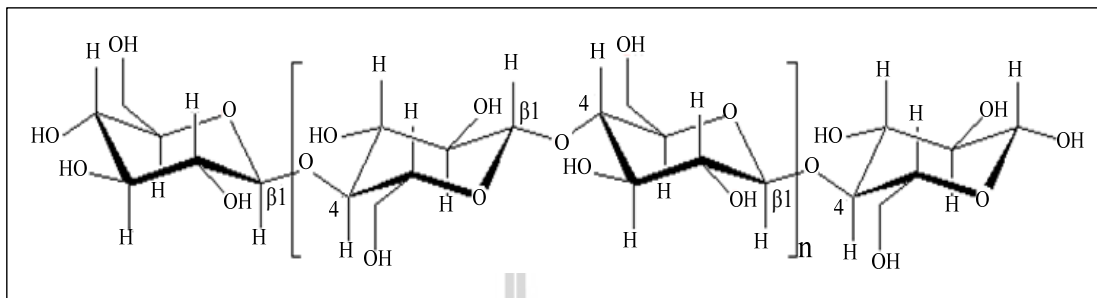


**Figure 2.7** Cellulose structure (Mohanty, Misra, and Drzal, 2005).

Hemicelluloses are polysaccharides composed of 5-ring and 6-ring carbon ring sugars. The polymer chains are much shorter and branched, containing pendant side groups giving rise to its noncrystalline nature. Hemicelluloses form the supportive matrix for cellulose microfibrils. Hemicelluloses are very hydrophilic and soluble in alkali and easily hydrolyzed in acid.

During the biological synthesis of plant walls, polysaccharide such as cellulose and hemicelluloses are produced, and simultaneously lignin fills the spaces between the polysaccharide fibers, cementing them together. This lignification process causes a stiffening of cell walls, and the carbohydrate is protected from chemical and physical damage. A probable structure of lignin is represented in Figure 2.8. Although the exact mode of linkages of lignin with cellulose in lignocellulosic natural fiber is not well known, lignin is believed to be linked with the carbohydrate through two types of linkages, one alkali sensitive and the other alkali resistant. The alkali sensitive linkages form an ester-type combination between lignin hydroxyls and carboxyls of hemicellulose uronic acid.

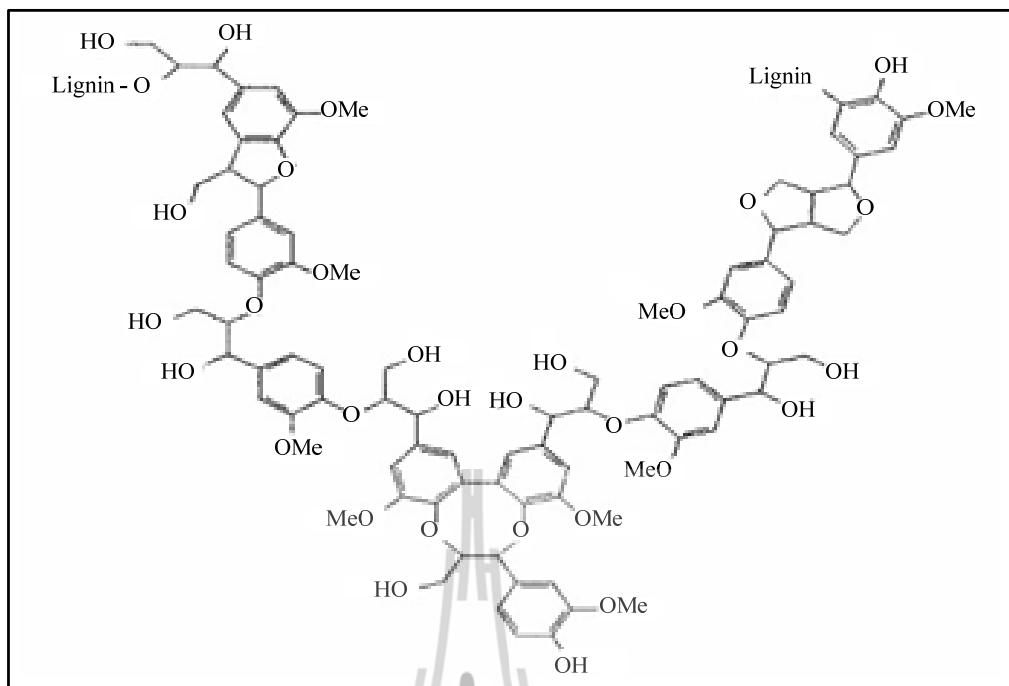


**Figure 2.8** Lignin structure (Mohanty et al., 2005).

Waxes make up the part of the fiber, which can be extracted with organic solutions. These waxy materials consist of different types of alcohols, which are insoluble in water as well as in several acids (palmitic acid, oleaginous acid, stearic acid) (Bledzki and Gassan, 1999).

The mechanical properties of plant fibers are much lower when compared to those of the most widely used competing reinforcing glass fibers. However, a value of low density, the specific properties, strength, and stiffness plant fibers were high compared to the glass fibers. Moreover, natural fibers have several advantages, such as low cost, ease of separation, biodegradability, renewability, recyclability and locally availability (Lee and Wang, 2006). In order to expand the use of agro-fibers for composites, it is useful to have the information on fiber characteristics and the factors, which affect performance of the fiber. Vetiver grass

(*Vetiveria zizanioides*) as shown in Figure 2.9 belongs to the same grass family as maize, sorghums, sugarcane and lemon grass. Vetiver grass is well known as a useful plant for erosion control. Chemical composition, physical and mechanical properties of vetiver fiber are shown in Table 2.2 and 2.3, respectively. In Thailand, His Majesty the King Bhumipol Adulyadej has initiated and supported the use of vetiver grass for soil and water conservation since 1991. Various activities on other applications of this grass have been promoted since then. Normally, leaves of the vetiver grass are cut every few months to keep vetiver row in order and left as a residue. Vetiver grass has many advantages including low cost, low density, biodegradability and renewability. Therefore, vetiver grass fiber was used as a filler in PP composites (Somnuk, Eder, Phinyocheep, Suppakarn, Sutapun, and Ruksakulpiwat, 2007); (Ruksakulpiwat, Suppakarn, Sutapun, and Thomthong, 2007).



**Figure 2.9** Photograph of vetiver grass (*Vetiveria zizanioides*).

**Table 2.2** Chemical composition of vetiver fiber after treated with 1% (wt/v) NaOH for five days (Ruksakulpiwat et al., 2007).

Chemical compositions	Vetiver grass fiber (wt%)
C	97.30
SiO <sub>2</sub>	1.17
K <sub>2</sub> O	0.21
P <sub>2</sub> O <sub>5</sub>	0.12
SO <sub>3</sub>	0.05
Al <sub>2</sub> O <sub>3</sub>	0.05
MgO	0.07
Cl	0.02
MnO	0.04
Na <sub>2</sub> O	0.01
Others	0.07

**Table 2.3** The physical and mechanical properties of vetiver fiber after treated with 1% (wt/v) NaOH for five days (Ruksakulpiwat et al., 2007).

Properties	Vetiver grass fiber
Density (g/cm <sup>3</sup> )	1.5
Diameter (μm)	100-200
Tensile strength (MPa)	247-723
Young's modulus (GPa)	12.0-49.8
Elongation at break (%)	1.6-2.4

Natural plant fibers have many advantages such as renewability, low density and high specific strength. Therefore, the use of natural plant fibers as reinforcement in fiber-reinforced plastics to replace synthetic fibers such as glass fiber is recently receiving attention. For example, flax fibers were used as reinforcement for PLA in order to improve its mechanical properties (Oksman, Skrifvars, and Selin, 2003); (Oksman, 2000). The results showed that the composite strength was about 50% better compared to similar PP/flax fiber composites, which are used today in many automotive panels. The study of interfacial adhesion showed that adhesion needed to be improved to optimize the mechanical properties of the PLA/flax composites. Bax and Mussig (2008) reinforced PLA with Cordenka rayon fibers and flax fibers, respectively. The highest impact strength and tensile strength were found for Cordenka reinforced PLA at a fiber-mass proportion of 30%. The highest Young's modulus was found for the composite made of PLA and flax. A poor adhesion between the matrix and the fibers was shown for both composites.

Bodros, Pillin, Montrelay, and Baley (2007) also used flax fiber reinforced PLA and PLLA. They found that the tensile properties were improved. The tensile strength and Young's modulus of PLLA and PLA flax composites were greater than those of similar PP/flax fiber composites. The specific tensile strength and modulus of flax fiber/PLLA composite have proved to be very close to those of glass fiber polyester composites.

Ochi (2008) studied mechanical properties of kenaf fibers and kenaf/PLA composites. It was found that tensile and flexural strength and elastic moduli of the kenaf fiber-reinforced composites increased linearly up to a fiber content of 50%. The biodegradability of kenaf/PLA composites was examined for

four weeks using a garbage-processing machine. Experimental results showed that the weight of composites decreased 38% after four weeks of composting.

The addition of natural fiber in PLA resulting in an increase of the mechanical properties of PLA such as modulus, tensile and flexural strength but the composite still suffer from poor interfacial adhesion. In order to improve interfacial adhesion between fiber and PLA, it is useful to have the information on fiber characteristics and factors which affect performance of the fibers.

Mwaikambo and Ansell (1999) proved that alkalization of plant fibers (hemp, sisal, jute and kapok) effectively changed the surface topologies of the fibers and their crystallographic structures. However, the concentration of sodium hydroxide (NaOH) for alkalization must be taken into consideration. Moreover, they have reported that removal of surface impurities on plant fibers may be an advantage for fiber to matrix adhesion. This may facilitate both mechanical interlocking and the bonding reaction due to the exposure of fibril to chemicals such as resins and dyes.

Ray and Sarkar (2000) conducted a research on the characterization of alkali-treated jute fibers for physical and mechanical properties. The alkali treatment of jute fibers with 5% NaOH solution showed that most of the changes occurred within 2-4 hours of treatment. The weight loss due to losing their cementing capacity in the fiber structure, separating the fibers from the strands, and dissolution of hemicellulose was maximized at these treatment hours. The loss of hemicellulose led to closer packing of its cellulose chains. On further treatment with alkali solution from 4-8 hours, the crystallinity of the fibers has found to be improved. The tenacity and modulus of the fibers were improved by 45 and 79%, respectively, and the percent breaking strain was decreased by 23% after 8 hours of treatment. This indicated that

fibers become stiffer and more brittle with increasing the crystallinity of the fibers. The rate of change of tenacity, modulus, and breaking strain showed the possibility of two different mechanisms before and after 4 hours of treatment. The first mechanism was the loss of hemicellulose as a cementing material at the beginning up to 4 hours of treatment contributed to the closer packing of the cellulose chains. The second mechanism was a slow improvement in crystallinity with further closer packing of the cellulose chains beyond 4 hours of treatment. This caused the fibers stiffer and stronger.

Valadez-Gonzalez, Cervantes-Uc, Olayo, and Herrera-Franco (1999) used silane and alkaline treatment to enhance both the matrix fiber adhesion and the chemical surface modification in order to improve the physicochemical interactions at the fiber-matrix interphase. It was found that the alkaline treatment has two effects on the fiber. First it increases the surface roughness that results in a better mechanical interlocking and second it raises the amount of exposed cellulose on the fiber surface, thus increasing the number of possible reactive sites. Moreover, the fiber preimpregnation allowed a better fiber wetting which in a normal fiber-polymer mixing procedure would not be possible because of the high polymer viscosity. Thus, the preimpregnation enhanced the mechanical interlocking between fiber and matrix. The fiber-surface silanization resulted in better interfacial load transfer efficiency, but it did not improve the wetting of the fiber.

The effect of fiber surface-treatments on the properties of biocomposites from poly (lactic acid) (PLA) and kenaf fibers were studied by Huda, Drzal, Mohanty, and Misra (2008). The kenaf fibers were modified by using alkalization and silane-treatments. From this investigation, they found that the alkali-

followed by silane-treated fiber (FIBNASI) reinforced composite also significantly improved mechanical properties. The heat deflection temperature (HDT) of the PLA laminated composites is significantly higher than that of neat PLA resin. Moreover, morphological studies by SEM demonstrated that better adhesion between the fiber and the matrix was achieved.

Teramoto, Urata, Ozawa, and Shibata (2004) studied the effect of chemical treatment abaca fibers on biodegradation of aliphatic polyester composites. The composites of aliphatic polyesters PCL, poly (3-hydroxybutyrate-co-3-hydroxyvalerate) (PHBV), poly (butylene succinate) (PBS), and PLA with 10 wt. % untreated or acetic anhydride-treated (AA-) abaca fibers were prepared and their biodegradability was evaluated by the soil-burial test. In case of PCL composites, the presence of untreated abaca or AA-abaca did not pronouncedly affect the weight loss because PCL itself has a relatively high biodegradability. However, the addition of abaca fibers caused the acceleration of weight loss in case of PHBV and PBS composites. Especially, when untreated abaca was used, the PHBV and PBS composite specimens were crumbled within 3 months. This result was a marked contrast to the fact that neat PHBV and PBS specimens retain the original shape even after 6 months. Although no weight loss was observed for neat PLA and PLA/AA-abaca composite, the PLA/untreated abaca composite showed 10% weight loss at 60 days, which was caused by the preferential degradation of the fiber.

## 2.2 Natural rubber (NR)

Natural rubber (NR) is an unsaturated hydrocarbon polymer that was originally derived from a milky colloidal suspension, or latex, found in the sap of some plants. The major commercial source of natural rubber latex is the Para rubber tree, *Hevea brasiliensis* (Euphorbiaceae). This is largely because it responds to wounding by producing more latex. The purified form of NR contains 93–95% cis-1,4-polyisoprene (as shown in Figure 2.10) and has 11,000-20,000 isoprene units in a polymer chain. Typically, a few percent of other materials, such as proteins, fatty acids, resins and inorganic materials are found in natural rubber. Because of some good properties such as high strength, outstanding resilience, and high elongation at break, it is used extensively in many applications and products.

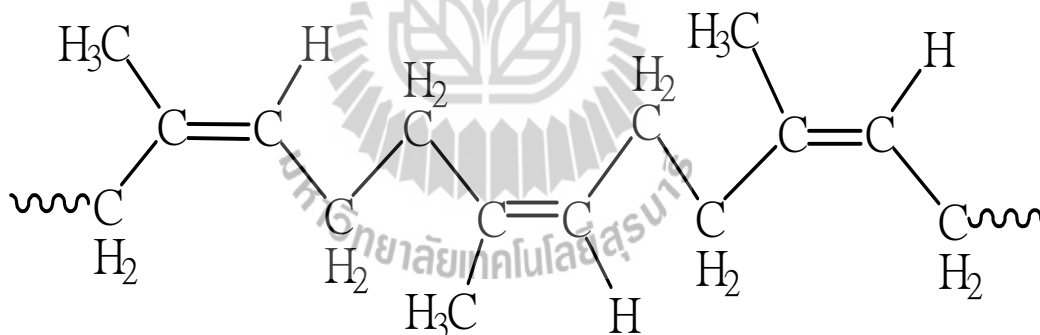


**Figure 2.10** Chemical structure of cis 1, 4-polyisoprene.

### 2.2.1 Physical properties of NR

Natural rubber latex (NRL) is a cloudy white liquid, similar in appearance to cow milk. It is collected by cutting a thin strip of bark from the tree and allowing the latex to exude into a collecting vessel over a period of hours. The composition of NRL consists of 30-40% rubber particles, 55-65% water, and small

amounts of protein, sterol glycosides, resins, ash, and sugars. Physical properties of NR may vary slightly due to the non-rubber constituents present and to the degree of crystallinity. When natural rubber is held below 100 °C crystallization occurs, resulting in a change of density from 0.92 to about 0.95. Listed in Table 2.4 are some average physical properties of NR (Hofmann, 1989).

**Table 2.4** Physical properties of NR latex at 20 °C.

Physical property	Value
Density	0.93
Refractive index	1.52
Coefficient of cubical expansion	0.00062/°C
Cohesive energy density	63.7 cal./cm <sup>3</sup>
Heat of combustion	44.16 kJ/g
Thermal conductivity	0.00032 cal./s./cm <sup>2</sup> /°C
Dielectric constant	2.37
Power factor (1,000 cycles)	0.15-0.2

### 2.2.2 NR as a toughening agent for brittle polymer

The improvement of impact strength of brittle polymers can be done by incorporating an elastomeric material. NR and its derivative are attractive materials because it has excellent flexibility and can be obtained from renewable resource. Thus many researches have been conducted on using NR as toughening agent for brittle polymers.

Phinyocheep, Saelao, and Buzare (2007) studied the properties of poly (ethylene terephthalate) (PET)/NR blends. They showed that toughness of the PET/NR blend increased with increasing amount of NR. The impact strength of the PET/NR (80/20 wt%) blend increased up to seven-fold when compared to that of pure PET.

Tanrattanakul, Sungthong, and Raksa (2008) used epoxidized natural rubber (ENR) as a toughening agent for nylon 6 (PA6). NR was used to compare with ENR, it was found that NR and ENR decreased yield stress and tensile strength but slightly increased elongation at break of PA6. NR slightly decreased impact strength of PA6, whereas this property increased up to six fold by blending with ENR. The impact strength of the blends increased with increasing ENR content. Rubber particle diameter also increased but was still much smaller than natural rubber particles. Compounded ENR increased tensile properties but decreased impact strength of the blends.

Asaletha, Kumaran, and Thomas (1999) prepared the thermoplastic elastomers (TPEs) from blends of natural rubber and polystyrene (NR/PS). Morphology and properties of these blends were studied. They found that, in both melt mixing and solution casting techniques the mechanical properties and morphology of the blends were dependent on the processing conditions. Three different solvents namely chloroform, benzene and carbon tetrachloride were used as the casting solvents. Differences in mechanical and morphological properties were observed in each case which in turn depends upon the interaction of the solvent with the constituent homopolymers. The changes in morphology in different casting solvents are associated with the different level of interactions of the blend component

with the solvent. In the case of melt mixed samples, the tensile and tear strength decreased with an increase of rubber content, whereas the impact strength increased with an increase of rubber content. The same trend was observed in the case of solution casted blends.

### 2.3 Graft copolymer

Graft copolymers are a special type of branched copolymer in which the side chains are structurally distinct from the main chain. The illustration in Figure 2.11 depicts a special case where the main chain and side chains are composed of distinct homopolymers. However, the individual chains of a graft copolymer may be homopolymers or copolymers.

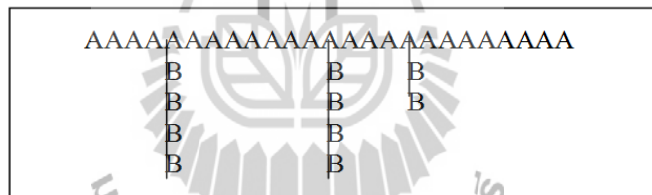


**Figure 2.11** The represent structure of graft copolymer.

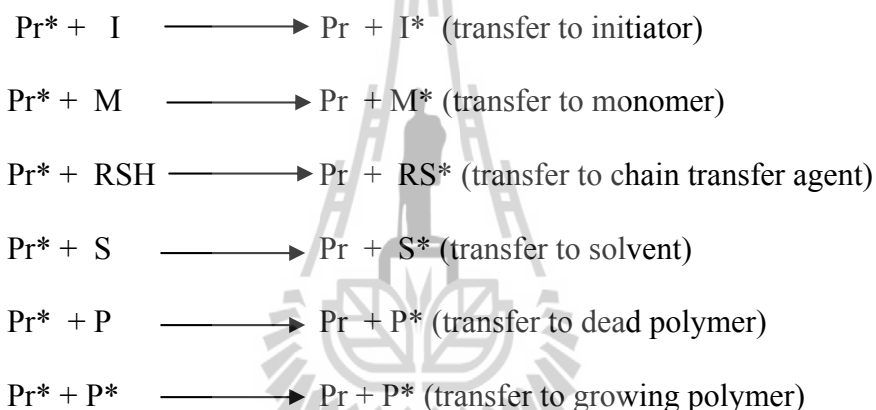
Where A units refer to the main chain or backbone and B units is the side chain of graft copolymer. It is well known that graft copolymers of vinyl monomers such as styrene, acrylonitrile, methylmethacrylate can be directly used to improve compatibility, impact, and low temperature properties of thermoplastics. Moreover, it can be employed as compatibilizers for promoting the interaction between immiscible phases in the blends.

### 2.3.1 Graft copolymerization techniques

The synthesis of graft copolymers is much more diverse, but can be dividing into groups of related process.

#### 2.3.1.1 Chain Transfer

In a free radical polymerization, chain transfer, is an important reaction. Chain transfer from growing polymer ( $\text{Pr}^*$ ) to a monomer, solvent, or other growing chain can take place. The chain transfer mechanisms are shown by the following equation.



These reactions are also a part of the free radical reaction system. Moreover, these reactions are important mechanism for to synthesis graft copolymer.

#### 2.3.1.2 Copolymerization via unsaturated groups

Copolymerization via unsaturated groups is the reaction of growing chain ( $\text{Pr}^*$ ) at unsaturated site or double bond of unsaturated polymer as shown in Figure 2.12. This technique should be applicable to isoprene and butadiene copolymer.

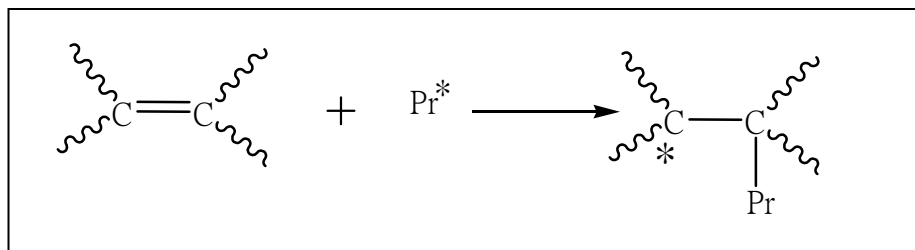


**Figure 2.12** The represent reaction of copolymerization via unsaturated groups.

### 2.3.1.3 High Energy Reaction Technique

During high- energy irradiation in vacuum, e.g., from a  $\text{Co}^{60}$  source, some main chain degradation of natural rubber and other polyisoprene occurs. Irradiation synthesis may be carried out in solution, either in contact with liquid monomer or in contact with monomer in the vapor phase, or in emulsion or suspension. The polymer may be preirradiated in the absence of air to produce free radical for later monomer addition, but the life of these radical is short as a result of mobility within the polymer matrix. Irradiation at very low temperature makes it possible to use the trapped radical technique for variety of polymer.

### 2.3.1.4 Photochemical Technique

Macromolecules containing photosensitive groups which absorb energy from ultraviolet frequencies often degrade by radical processes. Therefore, only a few type of monomer can be used this technique. The drgradative process as a rule is fairly slow, but by the addition of photosensitizer, such as xanthone, benzyl, benzoin, and 1-chloroanthraquinone, the rate can be speeded up to enable graft copolymerization to take place in the presence of monomers. This can be done in the case of natural rubber in the latex phase with reasonably high of graft copolymer.

### **2.3.1.5 Redox polymerization**

Redox polymerization is among the most popular techniques for grafting reaction especially for NR. In a redox polymerization, a hydroperoxide or similar group is reduced to a free radical plus an anion, while the metal ion or others oxidizing agent is oxidized to higher valency state and at the same time a monomer is added. When the reducible group is attached to polymeric chain, the free radical grafting sites thus formed on the macromolecular backbone act as initiators for graft copolymerization. This technique is suitable for graft copolymer at low temperature, and usually carried out in aqueous solution, suspension, or emulsion.

### **2.3.2 Graft copolymerization of NR by emulsion polymerization**

Emulsion polymerization has developed into widely used process for the production of synthetic latexes since its first introduction on an industrial scale in the mid-1930s. Today, millions of tons of synthetic polymer latexes are prepared by the emulsion polymerization process for use as commodity polymers in a wide variety of application such as synthetic rubber, high impact polymers, latex foam, latex paints and paper coating (Chern, 2008). Emulsion polymerization is a type of radical polymerization that usually starts with an emulsion incorporating water, monomer, and surfactant. The most common type of emulsion polymerization is an oil-in-water emulsion, in which droplets of monomer (the oil) are emulsified (with surfactants) in a continuous phase of water. A monomer is dispersed or emulsified in a solution of surfactant and water forming relatively large droplets of monomer in water (Lovell and El-Aasser, 1997).

Water is a chief ingredient in emulsion polymerization. As the continuous phase, although inert, it acts to maintain a low viscosity and provide for

good heat transfer. The water also act as the medium of transfer of monomer from droplet, the locus of initiator decomposition and oligomer formation and the medium of dynamic exchange of surfactant between the phase. The Smith-Ewart-Harkins theory for the mechanism of free-radical emulsion polymerization is summarized by the following steps.

First excess surfactant creates micelles in the water, after that small amounts of monomer diffuse through the water to the micelle, and then a water-soluble initiator is introduced into the water phase where it reacts with monomer in the micelles (This characteristic differs from suspension polymerization where an oil-soluble initiator dissolves in the monomer, followed by polymer formation in the monomer droplets themselves.). The total surface area of the micelles is much greater than the total surface area of the fewer, larger monomer droplets, therefore the initiator typically reacts in the micelle and not the monomer droplet. Monomer in the micelle quickly polymerizes and the growing chain terminates. At this point the monomer-swollen micelle has turned into a polymer particle. When both monomer droplets and polymer particles are present in the system more monomer from the droplets diffuses to the growing particle, where more initiators will eventually react. Eventually the free monomer droplets disappear and all remaining monomer is located in the particles. Depending on the particular product and monomer, additional monomer and initiator may be continuously and slowly added to maintain their levels in the system as the particles growth. The final product is a dispersion of polymer particles in water. It can also be known as a polymer colloid, a latex, or commonly and inaccurately as an 'emulsion' (Lovell and El-Aasser, 1997).

Most type of NR copolymer is graft copolymer. The backbone of this copolymer is polyisoprene and the side chain is the other polymer. According to the status of NR from the natural source is latex form, the emulsion polymerization is a suitable method for modifying NR. Moreover, low viscosity, good heat transfer and faster rate of polymerization can be obtained from this method. Thus graft copolymerization of NR using emulsion polymerization has attracted great attention in many researches.

Kongparakul, Prasassarakich, and Rempel (2008) grafted methyl methacrylate (MMA) onto natural rubber using a cumene hydroperoxide (CHP) and tetraethylenepentamine (TEPA) as a redox initiator. Sodiumdodecyl sulphate (SDS) was used as a surfactant. The reaction was performed at 50 °C for 8 h. The graft copolymer latex was precipitated using ethanol. The composite polymers were recovered and dried to a constant weight in vacuum. To remove free homopolymer, PMMA, the residue was extracted in acetone for 24 h. The results showed that the grafted product consisted of 24.8% ungrafted NR, 22.7% free PMMA, and 52.5% grafted NR. The MMA conversion and grafting efficiency were 83.2% and 51.6%, respectively.

Pukkate, Kitai, Yamamoto, Kawazura, Sakdapipanich, and Kawahara (2007) studied the effect of graft-copolymerization of polystyrene (PS) onto urea-deproteinized natural rubber (U-DPNR) latex. The conversion and grafting efficiency for the grafted U-DPNR were compared with those for a control sample prepared from enzymatic deproteinized natural rubber (E-DPNR) with styrene. Graft-copolymerization of U-DPNR and E-DPNR latices was carried out with styrene as a monomer, using tert-butyl hydroperoxide (*t*-BHP)/TEPA as an initiator. The highest

conversion and grafting efficiency of styrene for U-DPNR-g-PS copolymer were achieved at 1.5 mol/kg-rubber feed of styrene to be about 90 and 90% wt/wt, respectively, as in the case of EDPNR, since nitrogen content of U-DPNR was about 0.02% wt/wt as well as E-DPNR.

Oliveira, Guimaraes, Cavaille, Chazeau, Gilbert, and Santosa (2005) studied poly (dimethylaminoethyl methacrylate) (DMAEMA) grafted NR from seeded emulsion polymerization. The polymerization is initiated by a redox couple where one component (TEPA) is hydrophilic and the other (CHP) is hydrophobic. This should promote grafting at the interface between hydrophobic natural rubber particles and the hydrophilic DMAEMA. They found that the modifying NR by exposure to radicals from the redox initiator in the absence of monomer leads, not surprisingly, to an increase of cross-linking. In the presence of DMAEMA, there is a competition between crosslinking, homogeneous aqueous-phase polymerization and grafting, and leads to less crosslinking for the same radical flux. SEM result suggests that the grafted layer in these high-DMAEMA samples is a shell around the natural rubber core. They also studied the grafting reaction of DMAEMA onto NR. They found that the couple of initiators present in the graft copolymerization of DMAEMA in NR particles seem to be appropriate to create sites of grafting by the abstraction reaction over addition to allylic double bonds acting predominantly at the water/particle interface.

Lee, Subramaniam, Fellows, and Gilbert (2002) grafted PMMA onto NR by seed emulsion polymerization using two different redox systems, CHP/TEPA and *t*-BHP/TEPA. Polymerization and phase mixing was promoted by the addition of vinyl *neo*-decanoate (VneoD). They found that PMMA can graft onto NR by seed

emulsion polymerization. The CHP/TEPA system was more efficient than *t*-BHP/TEPA for the grafting of secondary polymers in modified NR.

### 2.3.3 Graft copolymer of NR as a compatibilizer for NR blends

Sabbagh (2003) enhanced the miscibility of NR and ethylene-propylene diene rubber (EPDM) blend by the addition of compatibilizers such as copolymer of EPDM and maleic anhydride (EPDM-g-MAH), polybutadiene rubber (BR), chlorinated rubber, chlorosulfonated polyethylene and polyvinylchloride (PVC). It was found that the incorporation of compatibilizers into NR/EPDM blends greatly enhances their compatibility and greatly improves the rheological properties of rubber blends. The compatibilizers are able to create a well-dispersed bicontinuous phase that exhibits rheological properties very similar to those obtained for compatible blends having one glass transition.

Nakason, Saiwaree, Tatun, and Kaesaman (2006) studied reactive blending of maleated natural rubber (MNR) with poly (methyl methacrylate) (PMMA). They found that the shear stress and shear viscosity of MNR/PMMA blends increased until reaching the maximum at a MNR content of 60 wt%. Increasing MNR higher than this value caused a decrease of the shear stress and viscosity. SEM micrographs were also analyzed. They observed decreasing sizes of dispersed PMMA domains as the maleic anhydride (MA) concentration increased. Moreover, they found that the increasing of MA in MNR caused increasing levels of chemical interaction between the MNR and PMMA phases. As a consequence, decreasing sizes of the PMMA domains dispersed in the MNR matrix were observed.

Hinchiranan, Suppaibulsuk, Promprayoon, and Prasassarakich (2007) improved properties of modified acrylic sheet via addition of graft natural rubber

(GNR). The results showed that the addition of GNR 0.5-4 parts to the acrylic sheets showed the improvement of the mechanical properties. Tensile strength, elongation at break and Charpy impact strength of the modified acrylic sheet were considerably increased due to the compatibility of the graft product with PMMA. This implied that the graft copolymer of NR and copolymer of styrene and methacrylate (ST-co-MMA) can be used as the impact modifier and the compatibilizer in acrylic plastics. However, the hardness of the modified acrylic sheet containing GNR decreased with the increase of the rubber content. The morphology of the fractured surfaces of the specimens containing graft natural rubber also confirmed better compatibility that caused the higher impact strength of the modified acrylic sheet.

## 2.4 References

- Asaletha, R., Kumaran, M.G., and Thomas, S. (1999). Thermoplastic elastomers from blends of polystyrene and natural rubber: morphology and mechanical properties. **Euro. Polym. J.** 35: 253-271.
- Auras, R., Harte, B., and Selke, S. (2004). An overview of polylactides as packaging materials. **Macromol. Bio. sci.** 4: 835-64.
- Bax, B., and Mussig, J. (2008). Impact and tensile properties of PLA/Cordenka and PLA/flax composites. **Compos. Sci. Technol.** 68: 1601-1607.
- Bledzki, A. K., and Gassan, J. (1999). Composites reinforced with cellulose based fibres. **Prog. Polym. Sci.** 24: 221-274.
- Bodros, E., Pillin, I., Montrelay, N., and Baley, C. (2007). Could biopolymers reinforced by randomly scattered flax fibre be used in structural applications. **Compos. Sci. Technol.** 67: 462-470.

- Broz, M.E., VanderHart, D.L., and Washburn N.R. (2003). Structure and mechanical properties of poly (d, l-lactic acid)/poly ( $\epsilon$ -caprolactone) blends. **Biomaterials**. 24: 4181-4190.
- Chen, L., Qiu, X., Xie, Z., Hong, Z., Sun, J., Chen, X., and Jing, X. (2006). Poly (L-lactide)/starch blends compatibilized with poly (L-lactide)-g-starch copolymer. **Carbo. Polym.** 65: 75-80.
- Chen, Y., Tan, L., Chen, L., Yang, Y., and Wang, X. (2008). Study on biodegradable aromatic/aliphatic polyesters. **Braz. J. Chem. Eng.** 25: 321-335.
- Chern, C. S. (2008). **Emulsion polymerization**. Hoboken: John Wiley & Sons.
- Cornelia, V., Anand, K., Kulshreshtha, A. K., and Gina, G (2002). **Handbook of Polymer Blends and Composites**. Smithers Rapra Technology.
- Enomoto, K., Ajioka, M. and Yamaguchi, A., **US Patent** 5,310,865 (to Misui Tuatsu), 1994.
- Garlotta, D. (2001). A literature review of poly (lactic acid). **J. Polym. Environ.** 9: 63-84.
- Gao, Y., Kong, L., Zhang, L., Gong, Y., Chen, G., Zhao, N., and Zhang, X. (2006). Improvement of mechanical properties of poly (DL-lactide) films by blending of poly (3-hydroxybutyrate-co-3-hydroxyhexanoate). **Euro.Polym. J.** 42: 764-775.
- Gruber, P. R., Hall, E. S., Kolstad, J. J., Iwen, M. L., Benson, R. D. and Borchardt, R. L., **US Patent** 5142,023. (to Cargill), 1992.
- Gu, S.Y., Zhang, K., Ren, J., and Zhan, H. (2008). Melt rheology of polylactide/poly (butylene adipate-co-terephthalate) blends. **Carbohydr. Polym.** 74: 79-85.

- Hancock, T., **Brit. Patent** 004,768, 1823.
- Hartmann, M. H., (1998). **Biopolymers from Renewable Resources**. Berlin: Springer-Verlag.
- Hinchiranan, N., Suppaibulsuk, B., Promprayoon, S., and Prasassarakich, P. (2007). Improving properties of modified acrylic sheet via addition of graft natural rubber. **Mater.Lett.** 61: 3951-3955.
- Ho, C.H., Wang, C.H., Lin, C. I., and Lee, Y. D. (2008). Synthesis and characterization of TPO–PLA copolymer and its behavior as compatibilizer for PLA/TPO blends. **Polymer.** 49: 3902-3910.
- Hofmann, W. (1989). **Rubber technology handbook**. Vienna: Hanser.
- Huda, M. S., Drzal, L. T., Mohanty, A. K., and Misra, M. (2008). Effect of fiber surface-treatments on the properties of laminated biocomposites from poly (lactic acid) (PLA) and kenaf fibers. **Compos. Sci. Technol.** 68: 424-432.
- Huneault, M.A., and Li, H. (2007). Morphology and properties of compatibilized polylactide/thermoplastic starch blends. **Polymer.** 48: 270-280.
- Ikada, Y., and Tsuji, H. (2000). Biodegradable polyesters for medical and ecological applications. **Macromol. Rapid. Commun.** 21: 117-32.
- Jiang, L., Wolcott, M.P., and Zhang, J. (2006). Study of biodegradable polylactide/poly(butylene adipate-co-terephthalate) Blends. **Biomacromolecules.** 7: 199-207.
- Jun, C.L. (2000). Reactive Blending of Biodegradable Polymers: PLA and Starch. **J. Polym. Environ.** 8: 33-37.

- Kongparakul, S., Prasassarakich, P., and Rempel, G.L. (2008). Catalytic hydrogenation of methyl methacrylate-g-natural rubber (MMA-g-NR) in the presence of OsHCl (CO) (O<sub>2</sub>) (PCy<sub>3</sub>)<sub>2</sub>. **Appl. Catal. A-Gen.** 344: 88-97.
- Lee, D.Y., Subramaniam, N., Fellows, C.M., and Gilbert R. G. (2002). Structure–Property Relationships in Modified Natural Rubber Latexes Grafted with Methyl Methacrylate and Vinyl neo-Decanoate. **J. Polym. Sci.: Part A: Polym. Chem.** 40: 809-822.
- Lee, S.-H., and Wang, S. (2006). Biodegradable polymers/bamboo fiber biocomposite with bio-based coupling agent. **Compos. Part A.** 37: 80-91.
- Li, Y., and Shimizu, H. (2009). Improvement in toughness of poly (L-lactide) (PLLA) through reactive blending with acrylonitrile–butadiene–styrene copolymer (ABS): Morphology and properties. **Euro. Polym. J.** 45: 738-746.
- Lovell, P.A., and El-Aasser, M. S. (1997). **Emulsion Polymerization and Emulsion Polymers**, John Wiley & Sons.
- Lunt, J. (1998). Large-scale production, properties and commercial applications of polylactic acid polymers. **Polym. Degrad. Stab.** 59: 145-152.
- Martin, O., and Averous, L. (2001). Poly (lactic acid): plasticization and properties of biodegradable multiphase systems. **Polymer.** 42: 6209-6219.
- Mohanty, A. K., Misra, M., and Drzal, L. T. (2005). **Natural fiber, Biopolymer, and Biocomposites**. Boca Raton: Taylor & Francis Group.
- Mwaikambo, L.Y., and Ansell, M.P. (1999). The effect of chemical treatment on the properties of hemp, sisal, jute, and kapok for composite reinforcement. **Die. Angew. Makromol. Chem.** 272: 108-116.

- Nakason, C., Saiwaree, S., Tatun, S., and Kaesaman, A. (2006). Rheological, thermal and morphological properties of maleated natural rubber and its reactive blending with poly (methyl methacrylate). **Polym. Test.** 25: 656-667.
- Narayanan, N., Roychoudhury, P.K., and Srivastava, A. (2004). L (+) lactic acid fermentation and its product polymerization, **Electron. J. Biotechnol.** 7: 167.
- Nijenhuis, A. J., Colstee, E., Grijpma, D. W., and Pennings, A. J. (1996). High molecular weight poly (L-lactide) and poly (ethylene oxide) blends: thermal characterization and physical properties. **Polymer.** 37: 5849-5857.
- Ochi, S. (2008) Mechanical properties of kenaf fibers and kenaf/PLA composites. **Mech. Mater.** 40: 446-452.
- Oksman, K. (2000). Mechanical Properties of Natural Fibre Mat Reinforced Thermoplastic. **Appl. Compos. Mater.** 7: 403-414.
- Oksman, K., Skrifvars, M., and Selin, J.F. (2003). Natural fibres as reinforcement in polylactic acid (PLA) composites. **Compos. Sci. Technol.** 63: 1317-1324.
- Oliveira, P.C., Guimaraes, A., Cavaille, J.Y., Chazeau, L., Gilbert, R.G., and Santosa, A. M. (2005). Poly (dimethylaminoethyl methacrylate) grafted natural rubber from seeded emulsion polymerization. **Polymer.** 46: 1105-1111.
- Oyama, H.T. (2009). Super-tough poly (lactic acid) materials: Reactive blending with ethylene copolymer. **Polymer.** 50: 747-775.
- Parkes, A., **Brit. Patent** 1,147, 25, 1846.
- Phinyocheep, p., Saelao, J., and Buzare, J.Y. (2007). Mechanical properties, morphology and molecular characteristics of poly (ethylene terephthalate) toughened by natural rubber. **Polymer.** 48: 5702-5712.

- Pukkate, N., Kitai, T., Yamamoto, Y., Kawazura, T., Sakdapipanich, J., and Kawahara, S. (2007). Nano-matrix structure formed by graft-copolymerization of styrene onto natural rubber. **Euro. Polym. J.** 43: 3208-3214.
- Ray, D., and Sarkar, B.K. (2000). Characterization of alkali-treated jute fibers for physical and mechanical properties. **J. Appl. Polym. Sci.** 80: 1013-1020.
- Ray, D., Sakar, B.K., and Rana, A.K. (2002). Study of the thermal behavior of alkali treated jute fibers. **J. Appl. Polym. Sci.** 85: 2594-2599.
- Rudnik, E. (2008). **Compostable polymer material**. Amsterdam: Elsevier.
- Ruksakulpiwat, Y., Suppakarn, N., Sutapun, W., and Thomthong, W. (2007). Vetiver -polypropylene composites: Physical and Mechanical Propertie. **Compos. Part A: Appl. Sci. Manufact.** 38: 590-601.
- Sabbagh, S.H.E. (2003). Compatibility study of natural rubber and ethylene-propylene diene rubber blends. **Polym. Test.** 22: 93-100.
- Sarazin, P., Li, G., Orts, W.J., and Favis, B.D. (2008). Binary and ternary blends of polylactide, polycaprolactone and thermoplastic starch. **Polymer.** 49: 599-609.
- Schreck, K.M., and Hillmyer, M.A. (2007). Block copolymers and melt blends of polylactide with Nodax<sup>TM</sup> microbial polyesters: Preparation and mechanical properties. **J. Biotechnol.** 132: 287-295.
- Shibata, M., Inoue, Y., and Miyoshi, M. (2006). Mechanical properties, morphology, and crystallization behavior of blends of poly (L-lactide) with poly (butylene succinate-co-L-lactate) and poly (butylene succinate). **Polymer.** 47: 3557-3564.

- Shibata, M., Teramoto., and Inoue, Y. (2007). Mechanical properties, morphologies, and crystallization behavior of plasticized poly (L-lactide)/poly (butylene succinate-co-L-lactate) blends. **Polymer**. 48: 2768-2777.
- Somnuk, U., Eder, G., Phinyocheep, P., Suppakarn, N., Sutapun, W., and Ruksakulpiwat, Y. (2007). Quiescent crystallization of natural fibers polypropylene composites, **J. Appl. Polym. Sci.** 106: 2997-3006.
- Su, Z., Li, Q., Liu, Y., Hu, G. H., and Wu, C. (2009). Compatibility and Phase Structure of Binary Blends of Poly (Lactic acid) and Glycidyl methacrylate grafted Poly (ethylene octane). **Euro. Polym.J.** 45: 2428-2433.
- Tanrattanakul, V., Sungthong, N., and Raksa, P. (2008). Rubber toughening of nylon 6 with epoxidized natural rubber. **Polym. Test.** 27: 794-800.
- Teramoto, N., Urata, K., Ozawa, K., and Shibata, M. (2004). Biodegradation of aliphatic polyester composites reinforced by abaca fiber. **Polym. Degrad. Stab.** 86: 401-409.
- Utracki, L. A. (1989) **Polymer Alloys and Blends**, Hanser Publishers, Munich, Germany.
- Valadez-Gonzalez, A., Cervantes-Uc, J.M., Olayo, R., and Herrera-Franco, P.J. (1999). Effect of fiber treatment fiber surface treatment on the fiber-matrix bond strength of natural fiber reinforced composites. **Compos. Part B: Eng.** 30: 309-320.

Wang, L., Ma, W., Gross, R. A. and McCarthy, S. P. (1998). Reactive compatibilization of biodegradable blends of poly (lactic acid) and poly ( $\epsilon$ -caprolactone). **Polym. Degrad. Stab.** 59: 161-168.

Zhang, L., Goh, S. H., and Lee, S. Y. (1998). Miscibility and crystallization behaviour of poly (L-lactide)/poly (p-vinylphenol) blends. **Polymer.** 39: 4841-4847.



# CHAPTER III

## GLYCIDYL METHACRYLATE GRAFTED

### NATURAL RUBBER

#### 3.1 Abstract

Glycidyl methacrylate (GMA) was grafted onto natural rubber (NR) using emulsion polymerization method. The structures of copolymers were characterized by  $^1\text{H}$  nuclear magnetic resonance spectroscopy ( $^1\text{H-NMR}$ ), solid state  $^{13}\text{C-NMR}$  spectroscopy and Fourier transform infrared spectrometer (FT-IR). The %grafting obtained from the gravimetric method and the absorbance ratio were compared. Effects of reaction temperature, GMA content, and reaction time on %grafting, grafting efficiency and %conversion of GMA monomer were determined. Effect of %grafting on mechanical properties of the graft copolymer was studied. Experimental results showed that the appropriate reaction time was 8 hours at a reaction temperature of  $30^\circ\text{C}$ . Moreover, tensile strength and modulus of the graft copolymer increased with increasing %grafting. However, elongation at break of the graft copolymer decreased with increasing %grafting.

#### 3.2 Introduction

Natural rubber (NR) is an unsaturated elastomer obtained from renewable resource. Its good properties, such as high resilience, high elongation at break and

fatigue resistance makes it become an interesting biomaterial (Mark, 1970). However, NR is very sensitive to heat, oxidation reaction and solvent, mainly due to the double bond in its chain and its nonpolar character (Derouet, Intharapat, Tran, Gohier, and Nakason, 2009). Moreover, it has low tensile modulus and tensile strength which causes limitation in variety of applications. To overcome these drawbacks, chemical modification of NR has been widely studied. Various methods have been used to improve properties of NR such as maleated natural rubbers (Nakason, Kaesaman, Samoh, Homsin, and Kiatkamjornwong, 2002), epoxidized natural rubber (Bradbury and Perera, 1985) and graft copolymer of NR. In order to graft NR, various types of monomers such as styrene (Pukkate, Kitai, Yamamoto, Kawazura, Sakdapipanich, and Kawahara, 2007), dimethylaminoethyl methacrylate (DMAEMA) (Oliveira, Guimaraes, Cavaille, Chazeau, and Gilbert, 2005), methacrylic acid (Nakason, Kaesaman, and Supasanthitikul, 2004), and methyl methacrylate (MMA) (Oliveira, Oliveira, Garcia, Barboza, Zavaglia, and Santos, 2005) have been widely used. Oliveira et al. (2005) found that tensile strength of NR was improved by grafting DMAEMA onto NR. George, Britto, and Sebastain (2003) studied mechanical properties of NR grafted MMA. They found that modulus of the films was increased with increasing MMA content. Glycidyl methacrylate (GMA) is one of interesting acrylate monomers because of its relatively low toxicity, polarity and lower price compared to others acrylate monomers (Laine, Legare, Monnet, and Cassagnau, 2008). Furthermore, it has an epoxy group in its chemical structure which exhibits a large number of chemical reactions by opening of their oxirane ring. Copolymers of GMA have been used for various industrial applications such as non-linear optics (Zhang and Tanaka, 2001), polymer membranes (Zhang, Cai, Cai, Yu,

and Loang, 1999), bioactive bone cement (Shinzato et al., 2000), paper strength additives (Zhang and Tanaka, 2001) and leather adhesives (Senthil Kumar, Balaji, and Nanjundan, 2001); (Wang, Tanaka, Kita, and Okamoto, 1998). Moreover, GMA grafted polymers such as styrene/acrylonitrile/glycidyl methacrylate copolymer (SAN-GMA) (Li and Shimizu, 2009), poly (ethylene-glycidyl methacrylate) (EGMA) (Oyama, 2009) and glycidyl methacrylate grafted poly (ethylene octane) (GMA-g-POE) (Su, Li, Liu, Hu, and Wu, 2009) can be employed as compatibilizers for promoting the interaction between immiscible phases in the polymer blends. These studies demonstrated an improvement in the mechanical characteristics of polymer by its reactive blending with graft copolymer of GMA.

According to the status of NR from the natural source which is in latex form, the emulsion polymerization is a suitable method for modifying NR. Moreover, low viscosity, good heat transfer and faster rate of polymerization can be obtained from this method. Thus graft copolymerization of NR using emulsion polymerization has attracted great attention from many researchers (Hinchiranan, Suppaibulsuk, Promprayoon, and Prasassarakich, 2007); (Lee, Subramaniam, Fellows, and Gilbert, 2002); (Arayaprane, Prasassarakich, and Rempel, 2002). To initiate polymerization reaction, various methods were used including high energy reaction technique (Perera, 1999); (Perera and Rowen, 2000), photochemical technique (Sruanganurak, Sanguansap, and Tangboriboonrat, 2006) and redox polymerization (Sanguansap, Thonggoom, and Tangboriboonrat, 2006). Redox polymerization is among the most popular techniques for grafting reaction especially for NR. This initiation system was very effective for emulsion polymerization in the NR latex, because it worked well

with the present of ammonia and was not sensitive to oxygen (Schneider, Pith, and Lambla, 1996).

In this work, graft copolymer of GMA onto NR was synthesized by emulsion polymerization. Cumene hydroperoxide (CHP) and tetraethylenepentamine (TEPA) were used as initiators. It was expected that mechanical properties of NR can be improved by grafting GMA onto NR. Moreover, glycidyl methacrylate grafted natural rubber (NR-g-GMA) may be used for many applications such as a compatibilizer.

### **3.3 Experimental**

#### **3.3.1 Materials**

NR latex containing 61.05% dried rubber was purchased from Thaihua Latex Co., Ltd. glycidyl methacrylate (GMA) and tetraethylene-pentamine (TEPA) were obtained from Aldrich. GMA was purified to remove inhibitor by basic alumina pack column (Aldrich) before used. Sodium dodecyl sulfate (SDS) and cumene hydroperoxide (CHP, 80%) were purchased from Fluka.

#### **3.3.2 Synthesis of NR-g-GMA**

The graft reactions were carried out in a three neck round bottom flask reactor of 250 mL with agitation speed of 100 rpm under nitrogen atmosphere, using distilled water as continuous phase (Figure 3.1). The formulation which used for the preparation of GMA grafted onto NR using emulsion polymerization at various reaction temperature and reaction time are shown in Table 3.1. In each reaction, NR latex was added first. The distilled water, surfactant and GMA were then added, respectively. The content of surfactant used in this study was higher than critical micelle concentration (CMC) of sodium dodecyl sulfate (SDS) in pure water at 25 °C

(0.0082 M) (Mukerjee and Mysels, 1971). After that CHP was added and then  $5 \times 10^{-4}$  g/mL solution of TEPA was added at a rate of 0.08 mL/min for 6 hours. Hydroquinone was added to stop the reaction and then the emulsion samples were poured on petidish and dried in an oven at 70 °C for 48 hours to remove water and unreacted monomers. After that, the film samples were obtained. Then they were cleaned with excess of 20% methanol in water and then extracted with acetone in a soxhlet for 24 hours. Acetone was expected to extract unreacted GMA and polyglycidyl methacrylate (PGMA). This technique was used to extract PGMA from samples by several researchers. Kunita, Rinaldi, Giroto, Radovanovic, Muniz, and Rubira (2005) reported the method of grafting glycidyl methacrylate onto polypropylene. They removed the unreact GMA monomer and GMA homopolymer from the graft copolymer by using soxhlet extraction for 12 hours and acetone was used as a solvent. Jiao, Liu, and Qi (2009) also removed PGMA from poly-glycidyl methacrylate graft  $\text{Al}_2\text{O}_3$  (PGMA/ $\text{Al}_2\text{O}_3$ ) by using acetone in a soxhlet extractor for 20 hours. This extraction is known to be sufficient for removing almost all homopolymer in the film. To confirm the effectiveness of soxhlet extraction, NR were melt blended with PGMA at the ratio of 83.3/16.7% (wt/wt) by using an internal mixer (Hakke Rheomix, 3000p) at the temperature of 170 °C with a rotor speed of 60 rpm for 10 min. NR/PGMA blend before and after soxhlet extraction were characterized by FT-IR spectrophotometer. The FT-IR spectra of NR/PGMA blend before and after soxhlet extraction are shown in Figure 3.2. Polyglycidyl methacrylate (PGMA) showed a strong peak at  $1716 \text{ cm}^{-1}$ , which corresponded to carbonyl group (C=O). This characteristic peak did not exist in FT-IR spectrum of NR. For NR/PGMA blend sample, C=O stretching ( $1729 \text{ cm}^{-1}$ ) of PGMA can be observed.

After soxhlet extraction of NR/PGMA, this characteristic peak (C=O) disappeared indicating that PGMA can be extracted from samples.



**Figure 3.1** Digital photograph of the reactor for preparation of glycidyl methacrylate graft natural rubber.

**Table 3.1** Formulation for the preparation of GMA grafted onto NR using emulsion polymerization at various reaction temperature and reaction time.

Ingredients	Mass of ingredients (g)
Natural rubber latex (NRL)	8
GMA	variable
CHP	0.015
TEPA	0.015
SDS	0.3
Distilled water	100

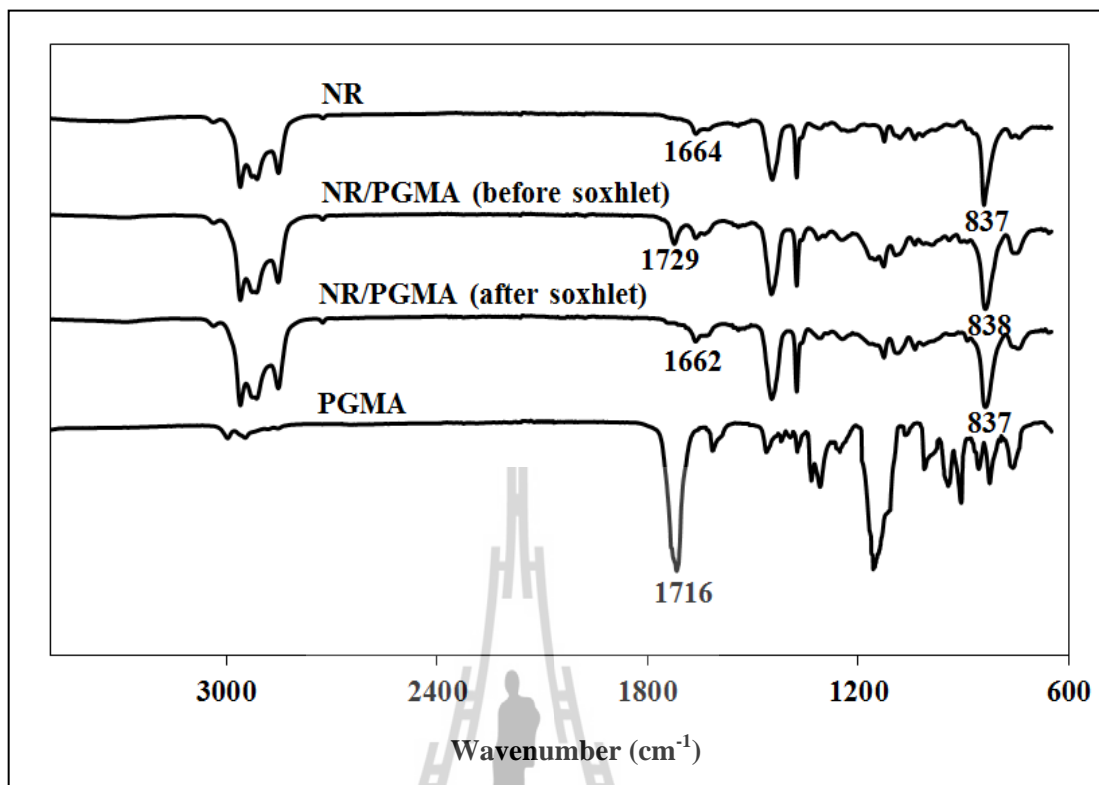


**Figure 3.2** The FT-IR spectra of NR and NR/PGMA blend before and after soxhlet extraction.

After extraction the undissolved part of sample was dried in an oven at 70 °C for 24 hours to a constant weight and characterized by FT-IR, <sup>1</sup>H-NMR and <sup>13</sup>C-NMR. Weight of GMA grafted was obtained from the difference between weight of extracted sample and weight of NR. Weight of GMA homopolymer was obtained from the difference between weight of initial sample and extracted sample. Grafting efficiency, %grafting and %conversion of GMA monomer are defined and calculated as follows (Vijayakumar, Rami, and Joseph, 1985):

$$\text{Grafting efficiency} = \left( \frac{\text{Weight of GMA grafted}}{\text{Weight of GMA grafted} + \text{Weight of GMA homopolymer}} \right) \times 100$$

$$\% \text{grafting} = \left( \frac{\text{Weight of GMA grafted}}{\text{Weight of NR}} \right) \times 100$$

$$\% \text{conversion} = \left( \frac{\text{Weight of GMA grafted} + \text{Weight of GMA homopolymer}}{\text{Weight of GMA monomer}} \right) \times 100$$

### 3.3.3 FT-IR

The structural characterization of NR, PGMA and NR-g-GMA was conducted by using a Spectrum one FT-IR spectrophotometer. Spectra were obtained at 4 cm<sup>-1</sup> resolution in the wavenumber range from 4000 to 650 cm<sup>-1</sup>. All samples were dried in an oven at 70 °C for 24 hours before testing.

### 3.3.4 NMR

<sup>1</sup>H-NMR spectra of polymer samples including NR and NR-g-GMA were run on a Varian model Inova 300 NMR spectrophotometer at 30 °C and 300 MHz using CDCl<sub>3</sub> as a solvent and TMS as an internal standard. Solid state <sup>13</sup>C-NMR measurements were performed at room temperature on a Bruker Biospin DPX-300 at 75 MHz.

### 3.3.5 Tensile tests

Rubber compounds were prepared by two-roll mill at room temperature. During compounding NR was added first. Zinc oxide, stearic acid, benzothiazyl disulfide (MBTS) and sulfur were added accordingly. To prepare

glycidyl methacrylate grafted natural rubber (NR-g-GMA) compound, the same compounding method was applied. The composition of the rubber compounds is shown in Table 3.2. Vulcanizing conditions (temperature and time) were previously determined by a Monsanto Moving Die Rheometer (MDR GT2000E). Rubber compounds were vulcanized at 150 °C in a compression molding machine. Tensile properties were obtained according to ASTM D412–98a using an Instron universal testing machine (UTM, model 5565) with a load cell of 5 kN at a crosshead speed of 500 mm/min.

**Table 3.2** Composition of the rubber compounds.

Ingredients	Content (phr)
NR or NR-g-GMA	100
Zinc oxide	5
Stearic acid	1
Benzothiazyl disulfide (MBTS)	1
Sulfur	2.5

### 3.3.6 Thermal property

Thermo gravimetric analysis (TGA) was performed using a TA Instrument thermo gravimetric analyzer (TGA, Mettler Toledo model TGA/DSC 1) by heating the sample from room temperature to 600 °C at a heating rate of 20 °C/min under a nitrogen atmosphere. The sample with a weight between 5 to 10 mg was used for each run. Differential scanning calorimetry (DSC : Mettler Toledo Version

STARe SW 8.1) was used to obtain thermal properties of specimens by heating the specimens from -80 °C to 50 °C at the rate of 10 °C/min.

### 3.4 Results and discussion

#### 3.4.1 Characterization of polymers

The FT-IR spectra of NR, polyglycidyl methacrylate (PGMA) and glycidyl methacrylate grafted natural rubber (NR-g-GMA) are shown in Figure 3.3. The FT-IR spectra of NR showed absorption bands at 840, 1449 and 1664  $\text{cm}^{-1}$  which were corresponded to the characteristic vibrations of =C-H stretching,  $\text{CH}_2$  stretching and C=C stretching, respectively. Polyglycidyl methacrylate (PGMA) showed peak at 907  $\text{cm}^{-1}$  which was the characteristic vibration of epoxy groups (Nanjundan, Unnithan, Selvamalar, and Penlidis, 2005). A strong peak at 1716  $\text{cm}^{-1}$  was corresponded to carbonyl group (C=O) and a strong peak at 1153  $\text{cm}^{-1}$  was attributed to C-O stretching of the ester group (Hirose, Hatakeyama, Izuta, and Hatakeyama, 2002). For NR-g-GMA sample, C=O stretching (1723  $\text{cm}^{-1}$ ) and C-O stretching (1149  $\text{cm}^{-1}$ ) of GMA can be observed. The C-H stretching (837  $\text{cm}^{-1}$ ),  $\text{CH}_2$  stretching (1446  $\text{cm}^{-1}$ ) and C=C stretching (1664  $\text{cm}^{-1}$ ) of NR were also appeared in the FT-IR spectra. Moreover, it was found that the C=O stretching of GMA was shift to a higher frequency when grafting GMA onto NR. This may be attributed to bond strength of carbonyl group (C=O) is stronger and the environment around C=O was changed by grafting GMA onto NR (Mayo, Miller, and Hannah, 2004). These indicated the occurrence of grafting reaction in NR-g-GMA sample. In addition, it is well known that free radical initiators may promote grafting in two different ways including abstraction allylic hydrogen (C=C-C-H) and addition to allylic double bond

( $\text{H}_2\text{C}=\text{CH}-\text{CH}_2$ ). The allylic double bond is an electron withdrawing group and it will withdraw electron from allylic hydrogen which results in the decrease of electron density of allylic hydrogen. Therefore allylic hydrogen is more acidic than hydrogen atom at other sites resulting in the easily abstraction. Moreover, Oliveira et al. reported that the CHP in the presence of the base TEPA can form radicals by the abstraction reaction over the addition to allylic double bonds. Figure 3.4 shows the probable structure of NR-g-GMA obtained from this grafting method.

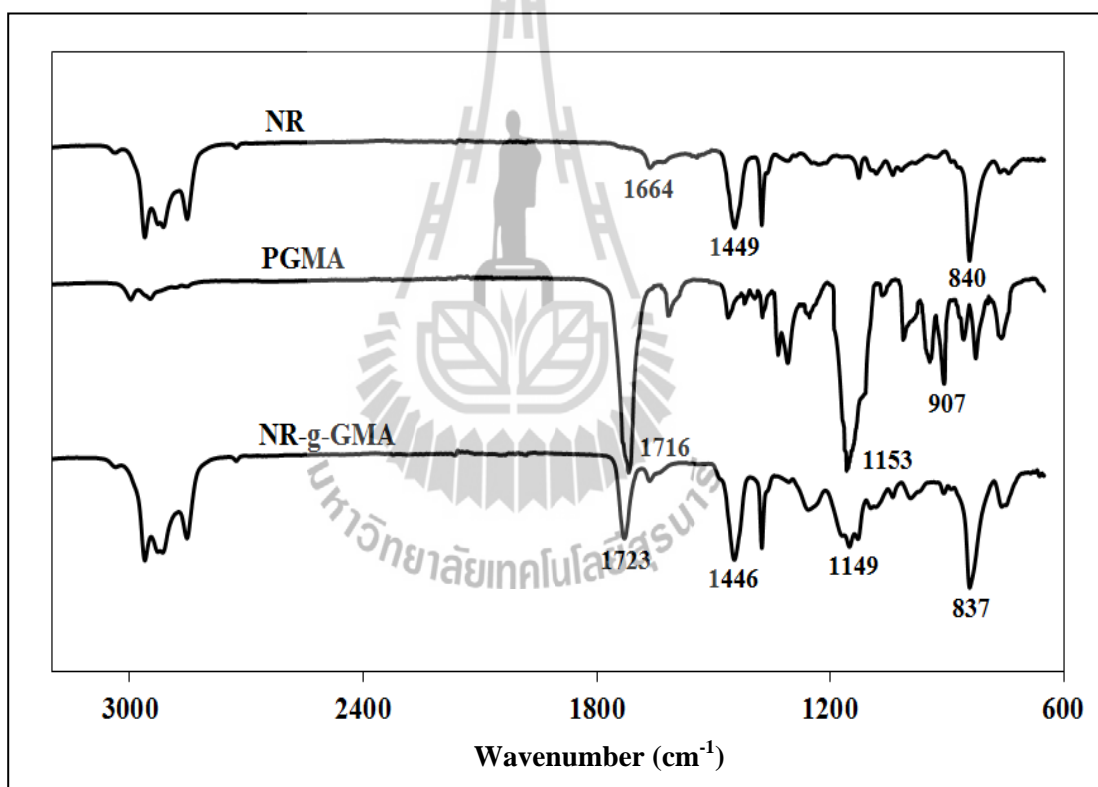


**Figure 3.3** FT-IR spectra of NR, PGMA and NR-g-GMA.

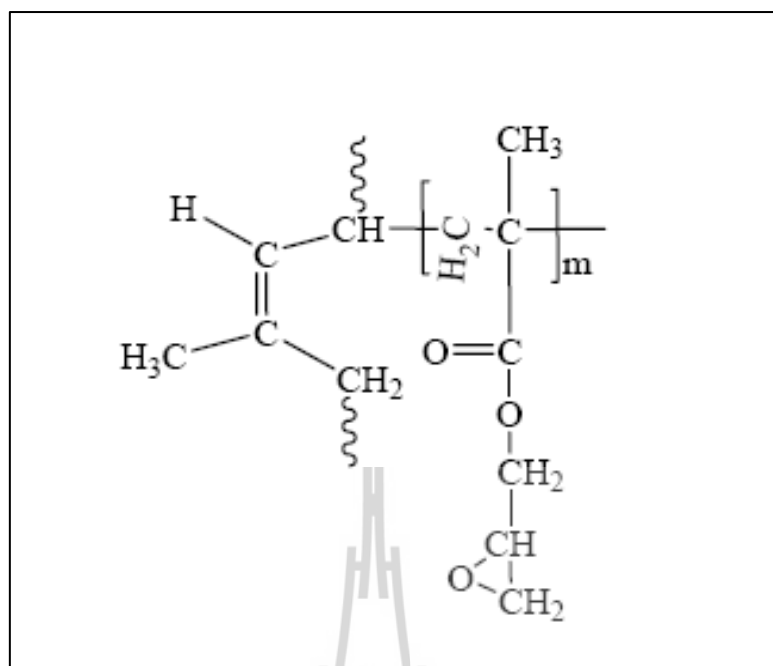


**Figure 3.4** The probable structure of NR-g-GMA.

The structures of NR and NR-g-GMA and their  $^1\text{H-NMR}$  spectra are shown in Figure 3.5. The protons peaks of NR were denoted by a, b, c and the proton peaks of grafted GMA were denoted by 1-5. The  $^1\text{H-NMR}$  spectrum of unmodified NR is shown in Figure 3.5 (A). The unsaturated methyne proton (a, 1H of =CH) showed a signal at 5.1 ppm. The signal at 2.1 ppm might be attributed to the methylene protons (b, 4H of  $(\text{CH}_2)_2$ ) and signal at 1.7 ppm was corresponded to the singlet resonance of the methyl proton (c, 3H of  $\text{CH}_3$ ). The  $^1\text{H}$  NMR spectrum of NR-g-GMA is shown in Figure 3.5 (B). The methyl protons of GMA (1, 3H of  $\text{CH}_3$ ) showed signals at 0.93 and methylene protons of GMA (2, 2H of  $\text{CH}_2$ ) showed signals at 1.29 ppm. The methylenoxy protons in GMA unit (3, 2H of  $-\text{CH}_2-\text{O}-$ ) showed signal at 3.8 ppm. The methoxy protons resonance of GMA (4, 5, 3H of epoxy group) appeared at about 2.9 ppm (Vijayanand, Kato, Satokawa, Kishimoto, and Kojima,

2009). These indicated that GMA can be grafted onto natural rubber. Nevertheless, some signals in  $^1\text{H-NMR}$  spectrum showed low intensity and was not clear, which might be attributed to the fact that NR-g-GMA only swell in  $\text{CDCl}_3$  solvent. So  $^{13}\text{C-NMR}$  spectroscopy was used to confirm the structure of NR-g-GMA.

The solid state  $^{13}\text{C-NMR}$  spectrum of NR sample is shown in Figure 3.6 (A). The  $^{13}\text{C}$  peaks of NR were denoted by a, b, c, d, and e. The signal at 135, 126, 33, 27 and 24 ppm were assigned to olefinic carbons (a, b,  $\text{C}=\text{C}$ ), methylene carbons (c, d,  $\text{CH}_2$ ) and methyl carbon (e,  $\text{CH}_3$ ) of NR, respectively. Figure 3.6 (B) shows the solid state  $^{13}\text{C}$  NMR spectrum of the NR-g-GMA. The  $^{13}\text{C}$  peaks of the grafted GMA were denoted by 1-7. The peaks at 19, 55, 50 and 180 ppm were assigned to methyl carbon (1,  $\text{CH}_3$ ), methylene carbons (2,  $\text{CH}_2$ ), backbone quaternary carbon (3,  $\text{—}\overset{\text{O}}{\underset{\text{O}}{\text{C}}}\text{—}$ ) and carbonyl carbon (4,  $\text{C}=\text{O}$ ) of GMA, respectively. The methylenoxy carbon (5,  $\text{—CH}_2\text{—O—}$ ) in GMA unit showed signal at 68 ppm. The methyne (6,  $\text{CH}$ ) and methylene (7,  $\text{CH}_2$ ) carbons of the epoxy group (  $\text{H}_2\text{C—}\overset{\text{O}}{\triangle}\text{—CH—}$  ) showed signals at about 45 ppm. These confirmed that GMA can be grafted onto natural rubber. Furthermore, the intensity of signals at 126 and 135 of olefinic carbons of NR before and after grafting with GMA were quite similar. This indicated that the initiator seems to be appropriate to create sites of grafting by the abstraction reaction over the addition to allylic double bonds.

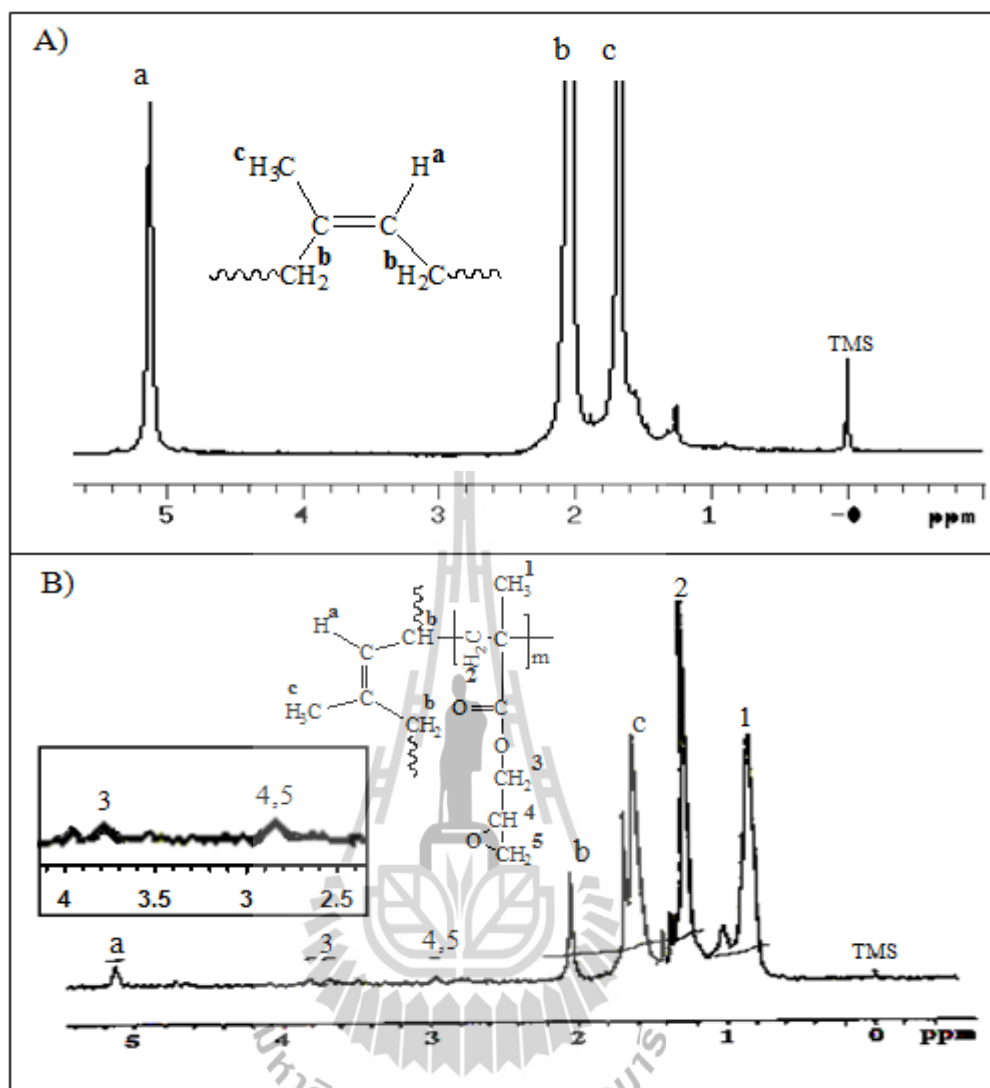


**Figure 3.5**  $^1\text{H-NMR}$  spectrum of unmodified NR (A) and NR-g-GMA (B).

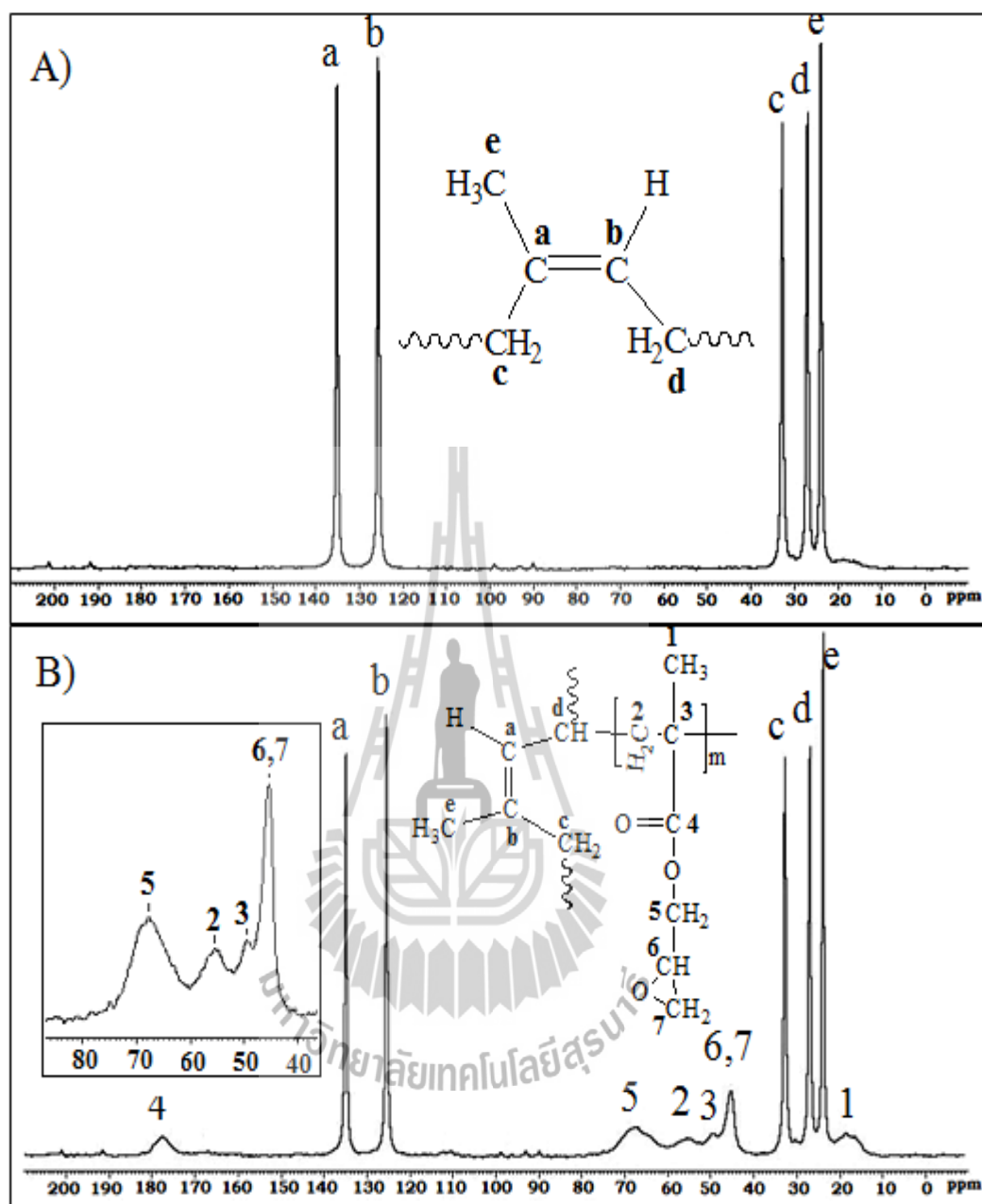


**Figure 3.6**  $^{13}\text{C}$ -NMR spectrum of unmodified NR (A) and NR-g-GMA (B).

### **3.4.2 Effect of reaction temperature on grafting efficiency, %grafting and %conversion**

In order to study the effect of reaction temperature on grafting efficiency, %grafting and %conversion, the graft copolymerization was carried out at 10, 30, 50 and 70 °C using GMA content at 40 phr and the reaction time for 8 hours. The effect of reaction temperature on %grafting is shown in Figure 3.7. %Grafting increased from 26 to 34% with increasing temperature from 10 to 30 °C and it remained constant at 34% above this temperature. Figure 3.8 shows the effect of reaction temperature on grafting efficiency and %conversion. The result showed that at 10 °C %conversion was 73% and increased to 99% at the temperature of 30 °C. The %conversion remained constant above this temperature. Nakason, Kaesaman, and Yimwan (2003) prepared graft copolymers from deproteinized and high ammonia concentrated natural rubber lattices with methyl methacrylate. The graft copolymerization was carried out at four different temperatures ranging from 40 to 70 °C. They found that a higher temperature caused a higher %conversion. The highest grafting efficiency was observed at a reaction temperature of 50 °C. The increasing %conversion at higher temperature might be attributed to an increase in the initiator decomposition. Therefore, an increased number of radicals and rate of polymerization occurred. Moreover, it was found that grafting efficiency was not affected by the reaction temperature between 10-70 °C.

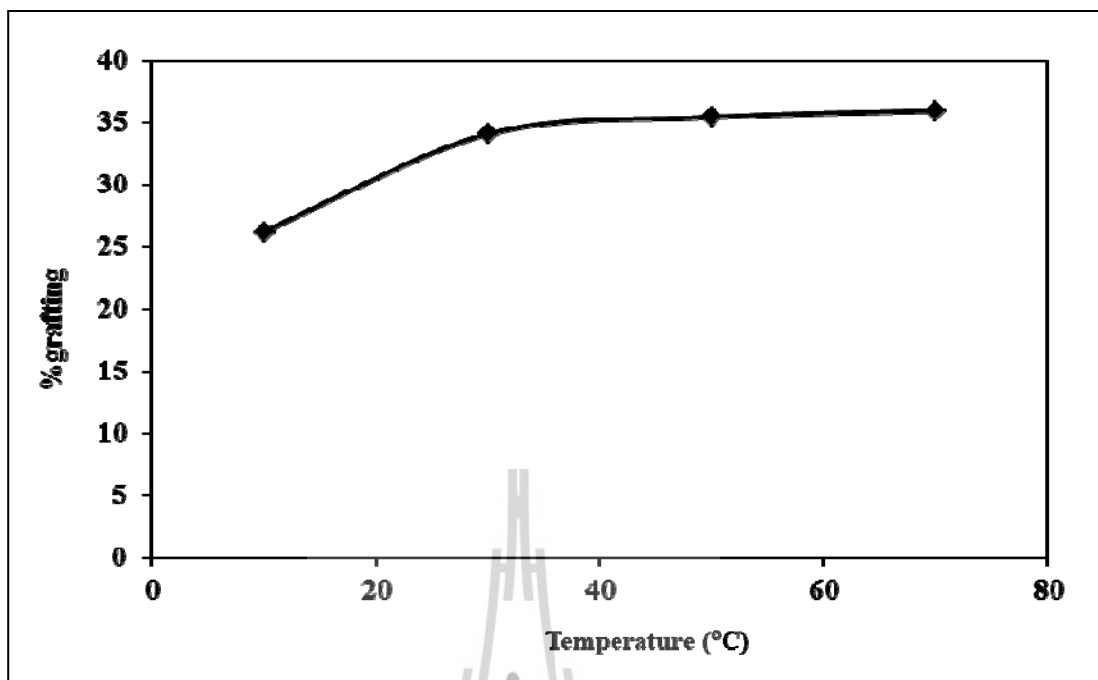


Figure 3.7 %Grafting at various reaction temperatures with reaction time of 8 hours.

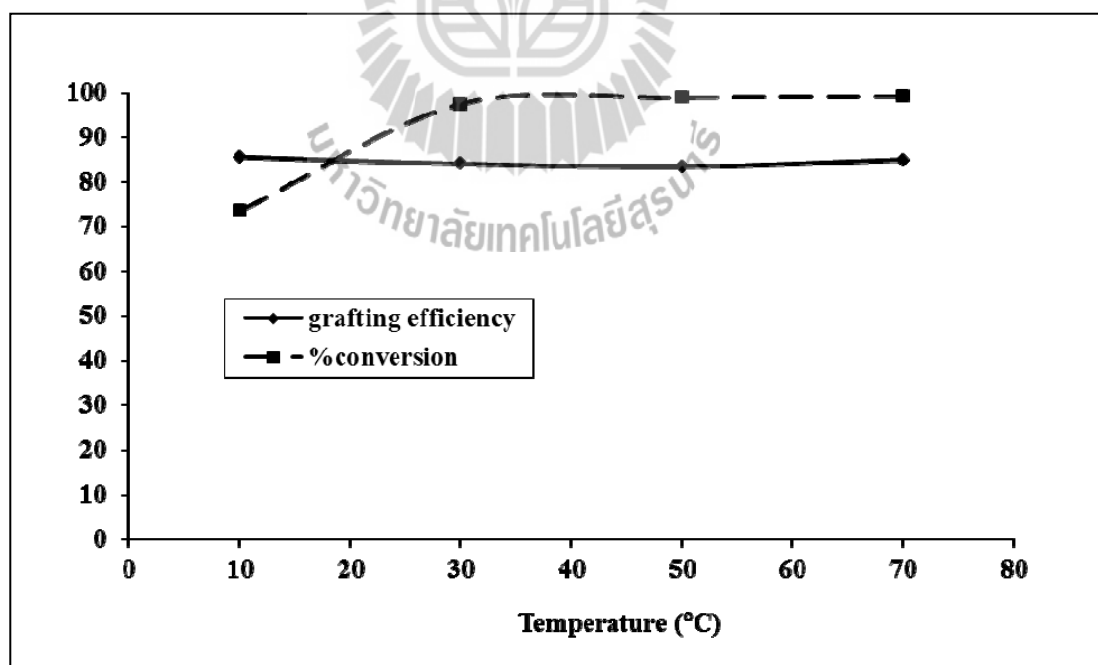


Figure 3.8 Grafting efficiency and %conversion of GMA at various reaction temperatures with reaction time of 8 hours.

### **3.4.3 Effect of reaction time on grafting efficiency, %grafting and %conversion**

In order to study the effect of reaction time on grafting efficiency, %grafting and %conversion, the graft reaction was carried out at 30 °C using GMA content at 40 phr. The graft samples were trapped from the reactor at different times. The reaction was terminated by using hydroquinone. The effect of reaction time on %grafting is shown in Figure 3.9. The %grafting increased with increasing reaction time and %grafting remained constant with the reaction time longer than 8 hours. Figure 3.10 shows the effect of reaction time on %conversion and grafting efficiency. The %conversion increased from 50 to 99% with increasing reaction time from 1 to 8 hours. This indicated that the reaction might be completed at reaction time of 8 hours. So the appropriate condition for the preparation of the graft copolymer was found to be a reaction temperature of 30°C with reaction time of 8 hours, which led to a high %conversion and high %grafting. Moreover, it was observed that grafting efficiency is not affected by the reaction time.

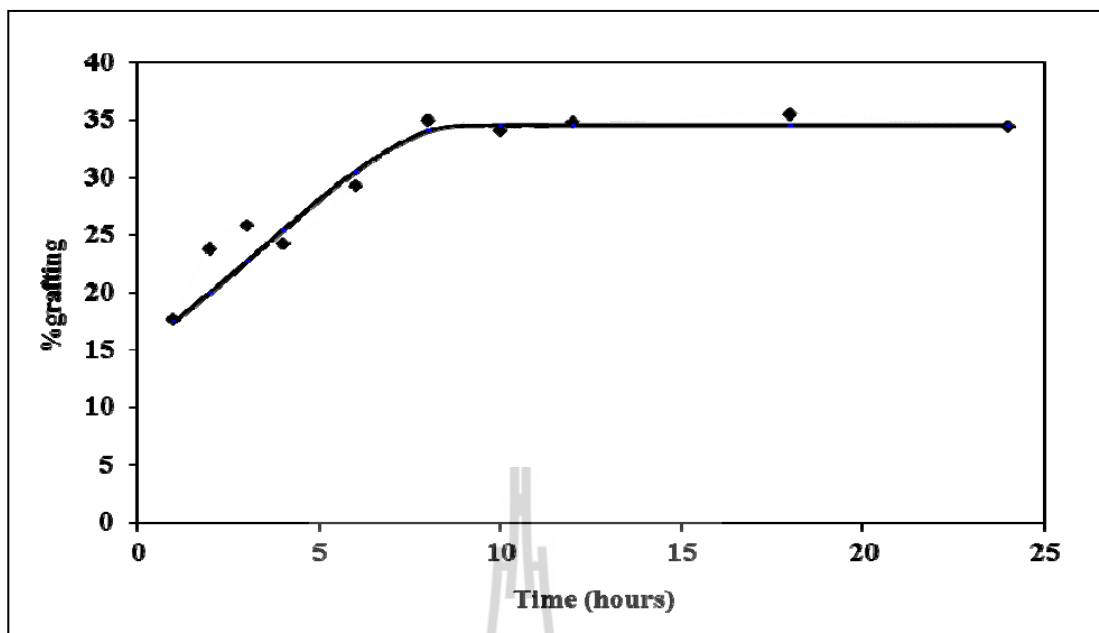


Figure 3.9 %Grafting at various reaction times with reaction temperature of 30 °C.

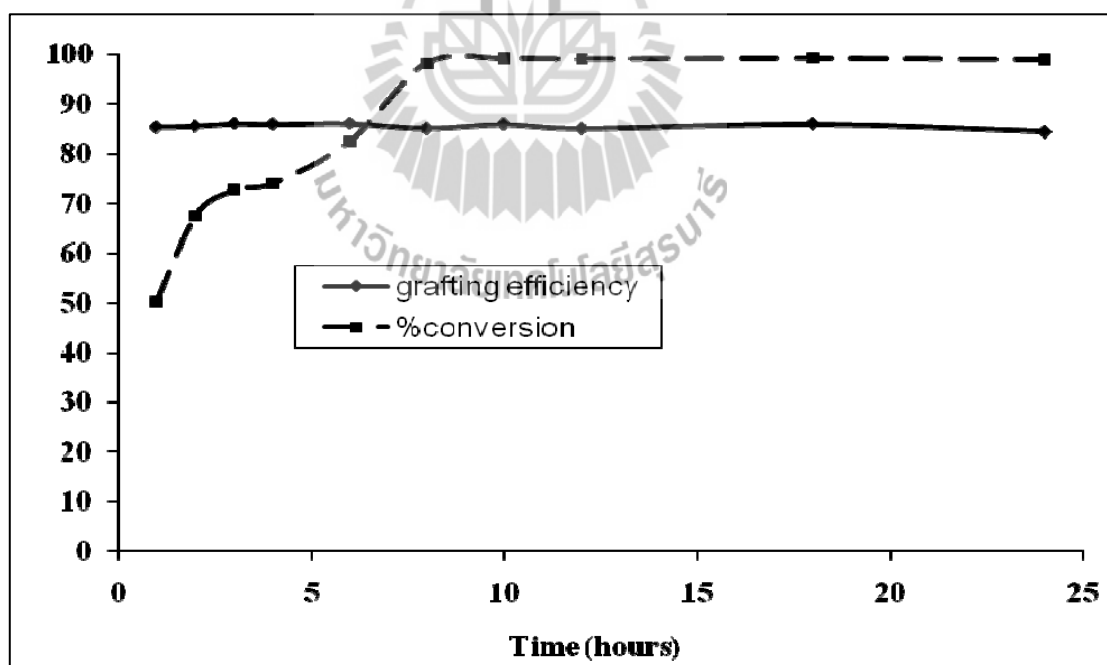
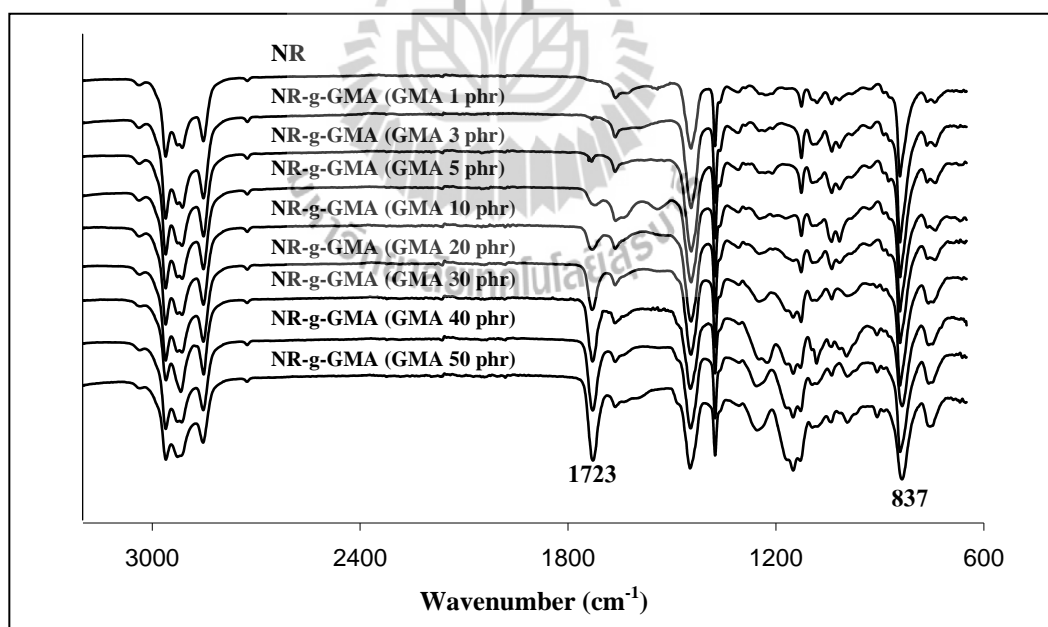


Figure 3.10 Grafting efficiency and %conversion of GMA at various reaction times with reaction temperature of 30 °C.

### 3.4.4 Effect of GMA content on grafting efficiency, %grafting and %conversion

GMA contents were varied from 1-50 phr to study the effect of GMA content on grafting efficiency, %grafting and %conversion. The grafting reaction was prepared at 30 °C for 8 hours. The FT-IR spectra of NR and NR-g-GMA at various GMA contents are shown in Figure 3.11. The single peak at  $837\text{ cm}^{-1}$  was attributed to =C-H stretching ( $837\text{ cm}^{-1}$ ) of NR which was used as an internal standard. The single peak at  $1723\text{ cm}^{-1}$  was attributed to the carbonyl groups of GMA (C=O). The result showed that the area of this characteristic peak increased with increasing GMA content. The level of the grafted GMA was estimated by using the absorbance ratio of IR peaks at  $1723\text{ cm}^{-1}$  to  $837\text{ cm}^{-1}$ .



**Figure 3.11** FT-IR spectra of NR and NR-g-GMA at various GMA contents.

Figure 3.12 shows the %grafting obtained from the gravimetric method and the absorbance ratio at various GMA contents. It can be seen that the %grafting and absorbance ratio showed the same trend. Figure 3.13 shows the calibration curve of absorbance ratio and %grafting. The absorbance ratio is linearly related to the quantity of GMA on NR-g-GMA and can be expressed by the equation  $y = 49.635X$ . X is the absorbance ratio and y is %grafting. Moreover, the coefficient of determination ( $R^2$ ) is 0.9841. This indicated that the simple absorbance ratio method can be used to determine the %grafting of NR-g-GMA.

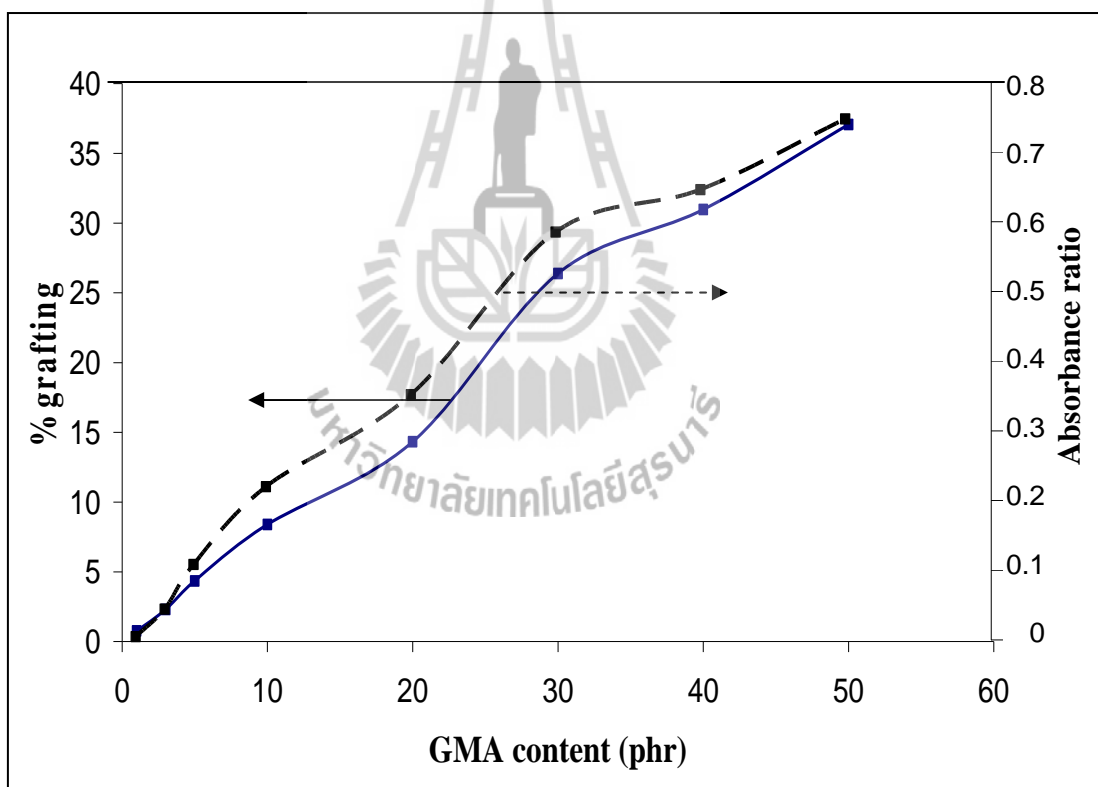


**Figure 3.12** %grafting and absorbance ratio at various GMA contents with reaction temperature of 30 °C and reaction time of 8 hours.

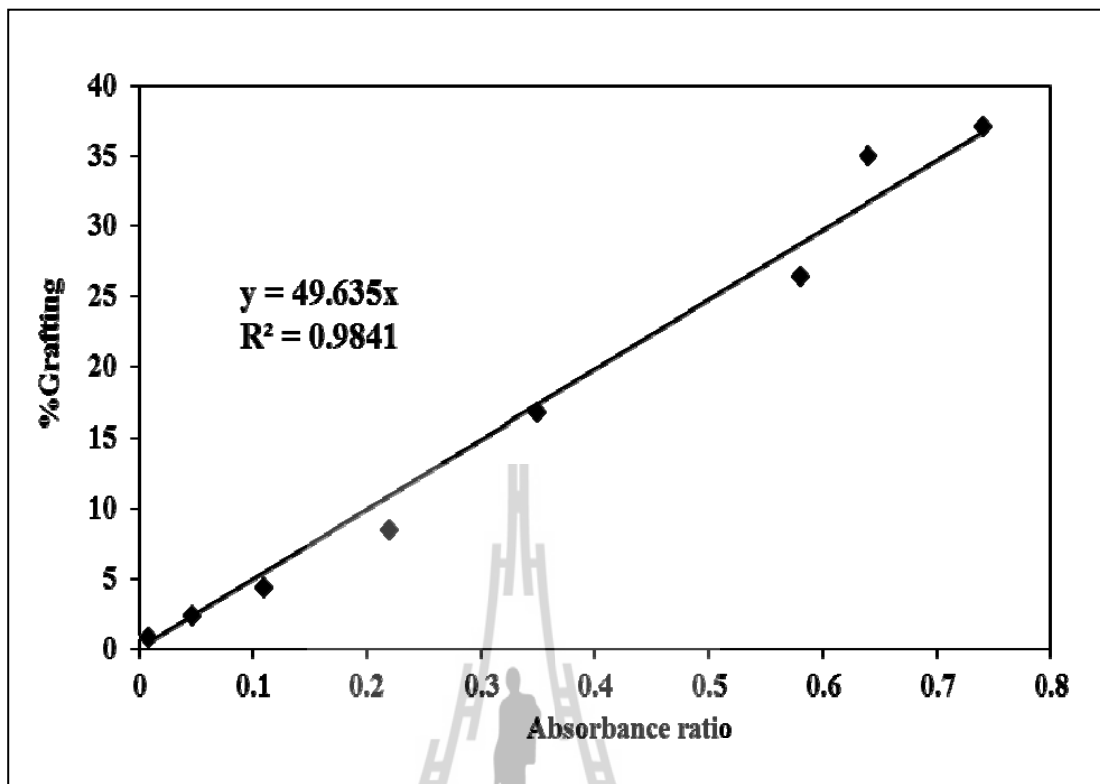


**Figure 3.13** Calibration curve of absorbance ratio and %grafting.

Figure 3.14 shows the effect of GMA content on grafting efficiency and %conversion. The %conversion of GMA at the content of 1-50 phr were about 99% indicating the good polymerization reaction of GMA from this grafting method. Furthermore, it can be seen that %grafting and grafting efficiency increased with increasing GMA content. Whereas, above 40 phr of GMA, grafting efficiency decreased. Yinghai, Yanzhe, Zhenghao, and Kuilin (2002) prepared graft copolymer of butyl acrylate onto casien. The experimental results showed that grafting efficiency increased with increasing butyl acrylate content. Grafting efficiency was decreased at high content of butyl acrylate content. This might be attributed to the chain transfer

reaction of radicals to monomer leading to the formation of homopolymer during the grafting reaction.

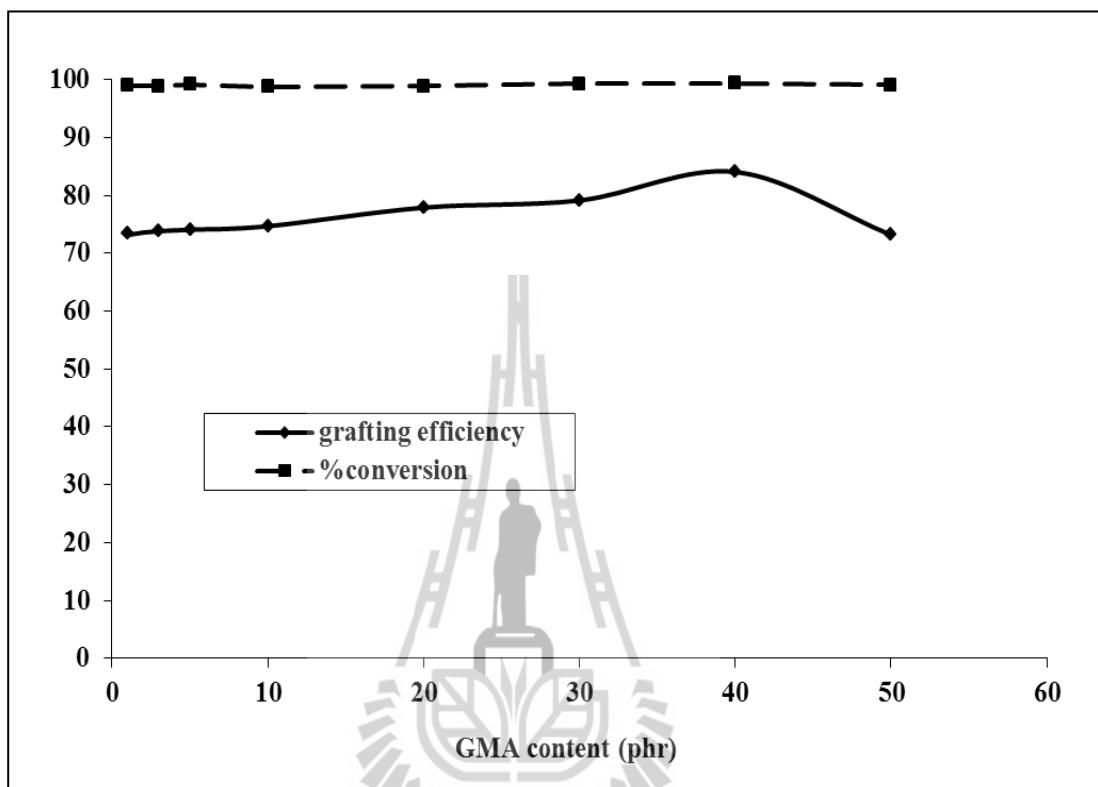


**Figure 3.14** Grafting efficiency and %conversion of GMA at various GMA contents with reaction temperature of 30 °C and reaction time of 8 hours.

### 3.4.5 Effect of %grafting on mechanical properties

Figure 3.15 represents the tensile stress–strain curve of NR and NR-g-GMA at various %grafting. All NR-g-GMA samples show higher stress level than NR. This may be related to the higher crosslinking density of NR-g-GMA than that of NR caused by epoxy moiety from GMA. This can be observed by the increase in the difference in maximum torque (MH) and minimum torque (ML) of MDR curing curve of NR-g-GMA at % grafting of 16.70 (25 dN·m) compared with that of NR (12

dN·m) as shown in Table A4. The difference between maximum torque and minimum torque (MH-ML), or torque difference, is indirectly related to crosslink density of a rubber vulcanizates (Teh et al., 2004). Oliveira et al. (2005) also reported the higher stress level of NR graft polydimethylaminoethyl methacrylate (NR-g-PDMAEMA) than that of NR. Moreover, They mentioned that the hardening of NR-g- PDMAEMA much higher than that of NR, this effect might be enhanced by the crystallization of the NR during the stretching, which is known to depend on the crosslink density and to increase the stress level at large deformation.

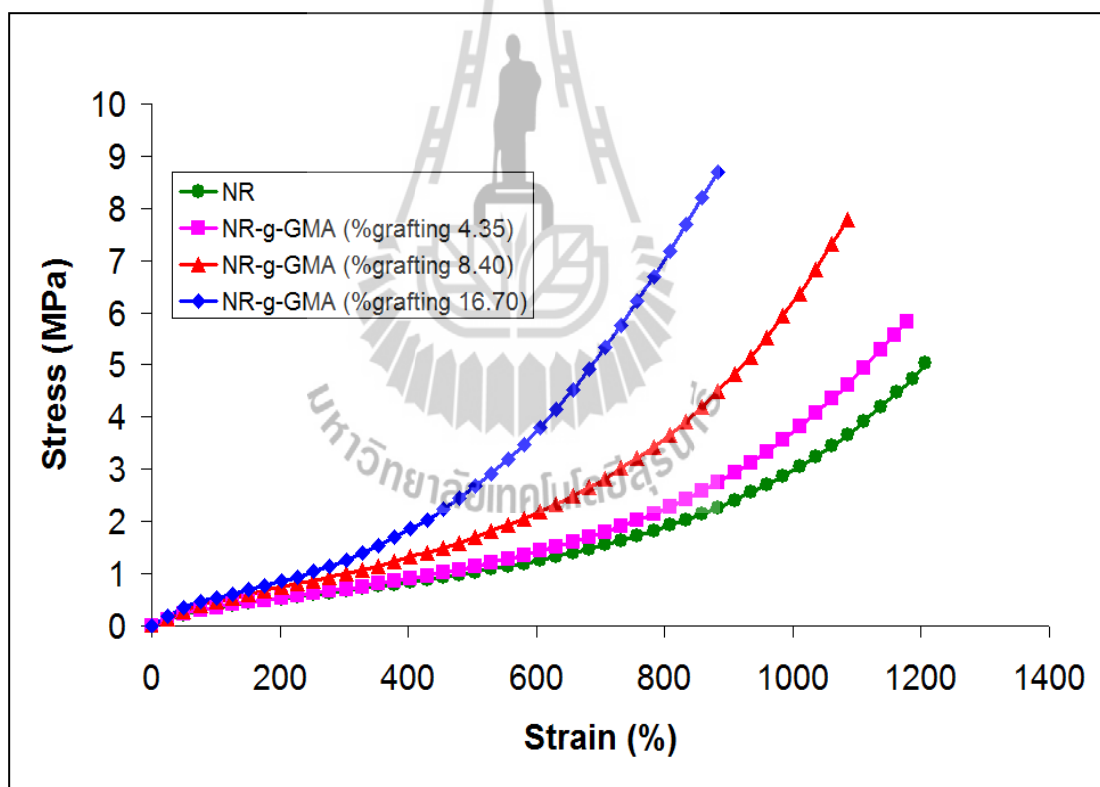


**Figure 3.15** Tensile stress-strain curves of NR and NR-g-GMA at various %grafting.

Elongation at break and tensile strength of NR and NR-g-GMA obtained from Figure 3.15 are shown in Figure 3.16 and 3.17 respectively. With increasing %grafting up to 16.70, tensile strength was significantly increased about 70% compared to that of NR whereas elongation at break slightly decreased. The decrease of elongation at break at high %grafting was due to the restriction of molecular chain movement of NR on stretching caused by GMA and higher crosslink density of NR-g-GMA as mentioned above. Figure 3.18 shows 100%modulus, 300%modulus and 500%modulus of NR and NR-g-GMA. The modulus of NR-g-GMA dramatically increased compared with that of NR. This may be attributed to the higher crosslinking density of NR-g-GMA as mentioned above. By grafting GMA onto NR the attractive force between latex particles in dry film was increased contributing to the high modulus of film. Moreover, polyglycidyl methacrylate (PGMA) is a rigid polymer, it may act as a reinforcing agent in NR resulting in an increase modulus with increasing GMA content in NR-g-GMA. It is noteworthy to point out that NR-g-GMA prepared in this study exhibited excellent improved tensile strength and modulus with insignificant loss in elongation at break compared to NR. With these superior mechanical properties, NR-g-GMA can be used in various applications such as seal, adhesive and coating.

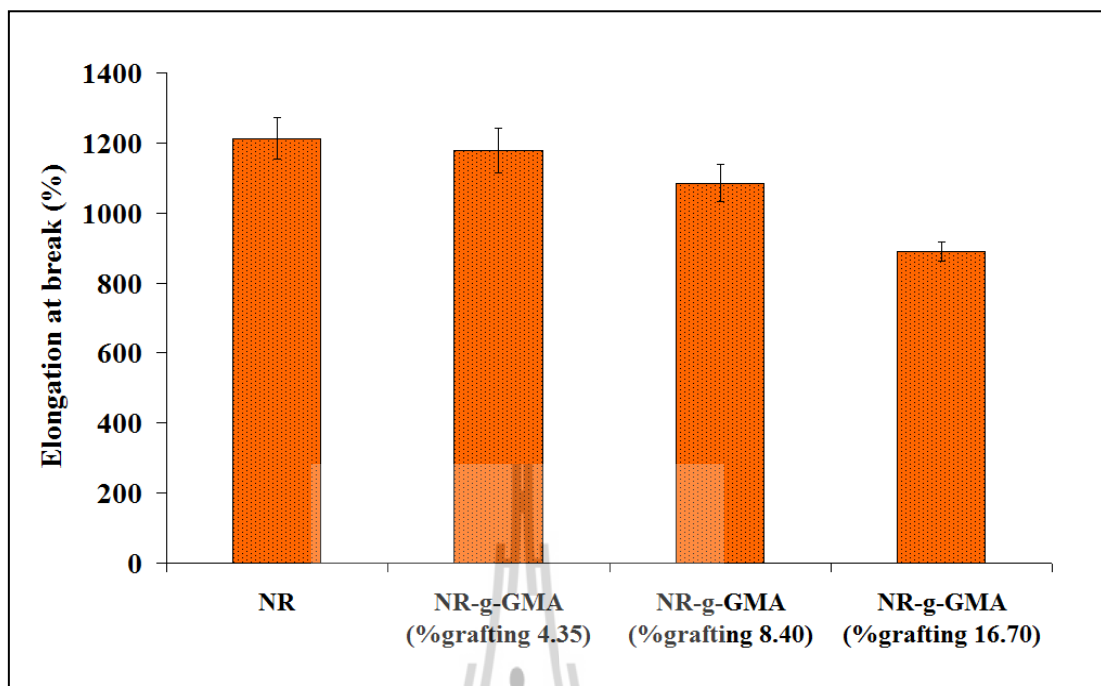


**Figure 3.16** Elongation at break of NR and NR-g-GMA at various %grafting.

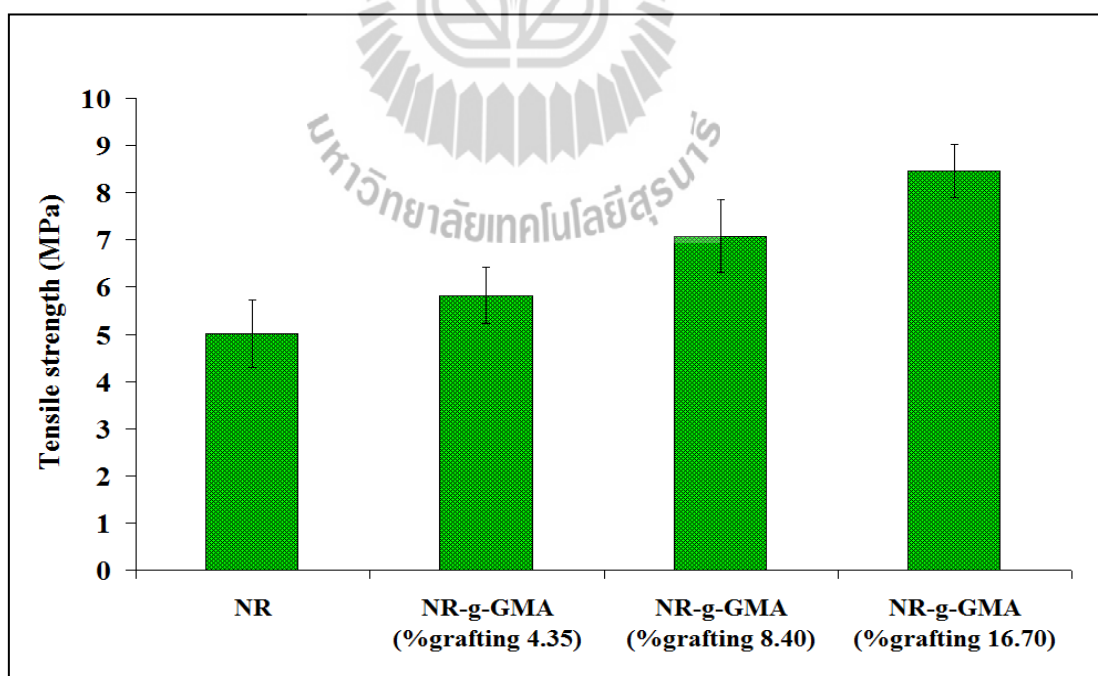


**Figure 3.17** Tensile strength of NR and NR-g-GMA at various %grafting.

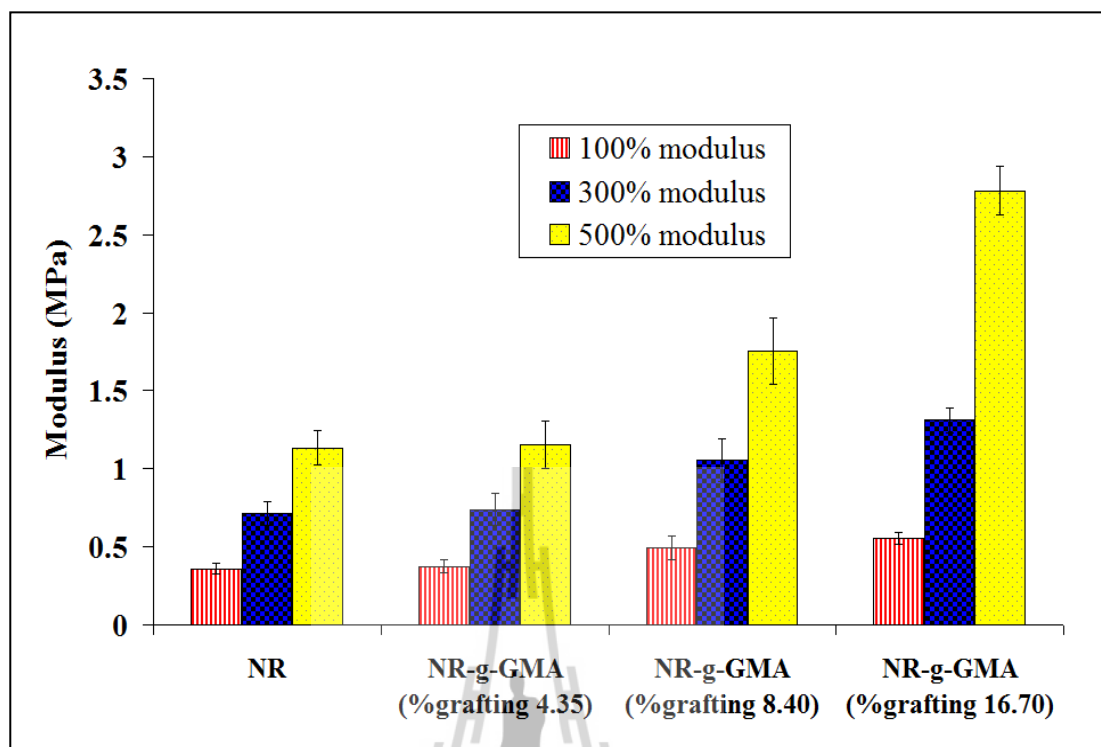


**Figure 3.18** 100% modulus, 300% modulus and 500% modulus of NR and NR-g-GMA at various %grafting.

### 3.4.6 Effect of %grafting on thermal properties

DSC curves of NR and NR-g-GMA at various %grafting are shown in Figure 3.19. From the DSC curves, it was found that  $T_g$  of NR was  $-62.0$  °C.  $T_g$  of NR-g-GMA was shifted to higher temperature compared to that of NR. This could be due to the restriction of molecular chain movement of NR caused by GMA. TGA and DTG curves of NR and NR-g-GMA at various %grafting are illustrated in Figure 3.20 and 3.21, respectively. NR showed only single step of weight loss with an onset temperature of  $305.3$  °C. The degradation of PGMA started at lower temperature than NR but completed at higher temperature. For NR-g-GMA at %grafting of 4.35, 16.7 and 34.60, the TGA curves also showed single step of weight loss. With these graft

copolymers, a shift of the TGA curve toward the high temperatures was observed when %grafting was increased. The onset temperature of NR-g-GMA was lower than NR, this corresponds to the degradation of weak linkages in backbone pendant group that occurred at lower decomposition temperature than that of NR backbone. On the other hand, the degradation of NR-g-GMA was completed at higher temperature than NR. This indicated that thermal stability of NR can be improved by grafting GMA onto NR.

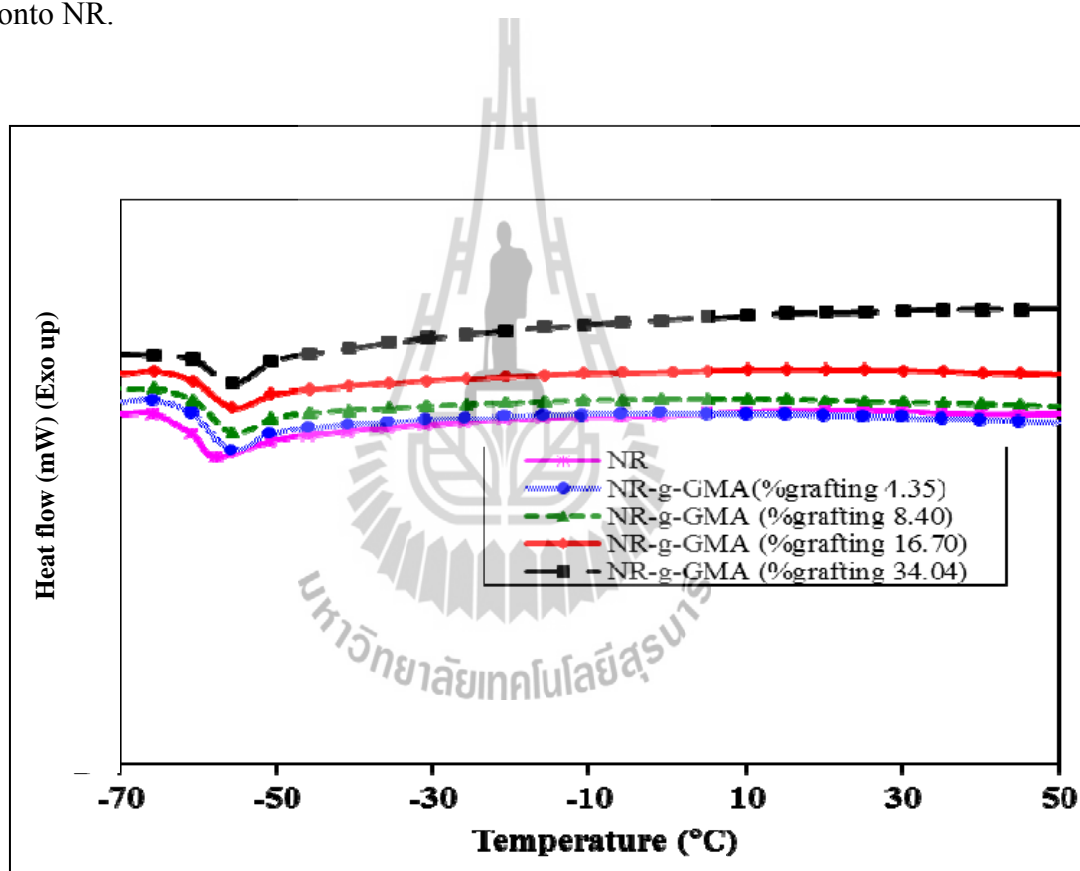


**Figure 3.19** DSC curves of NR and NR-g-GMA at various %grafting.

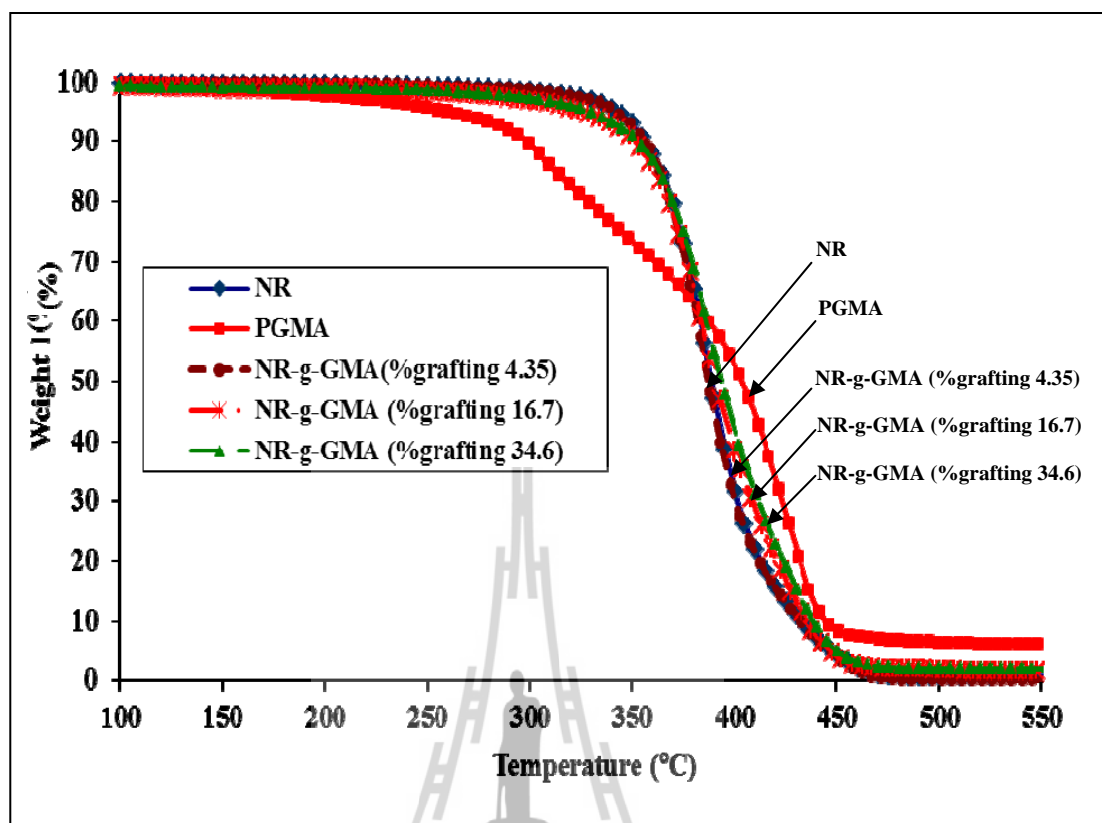
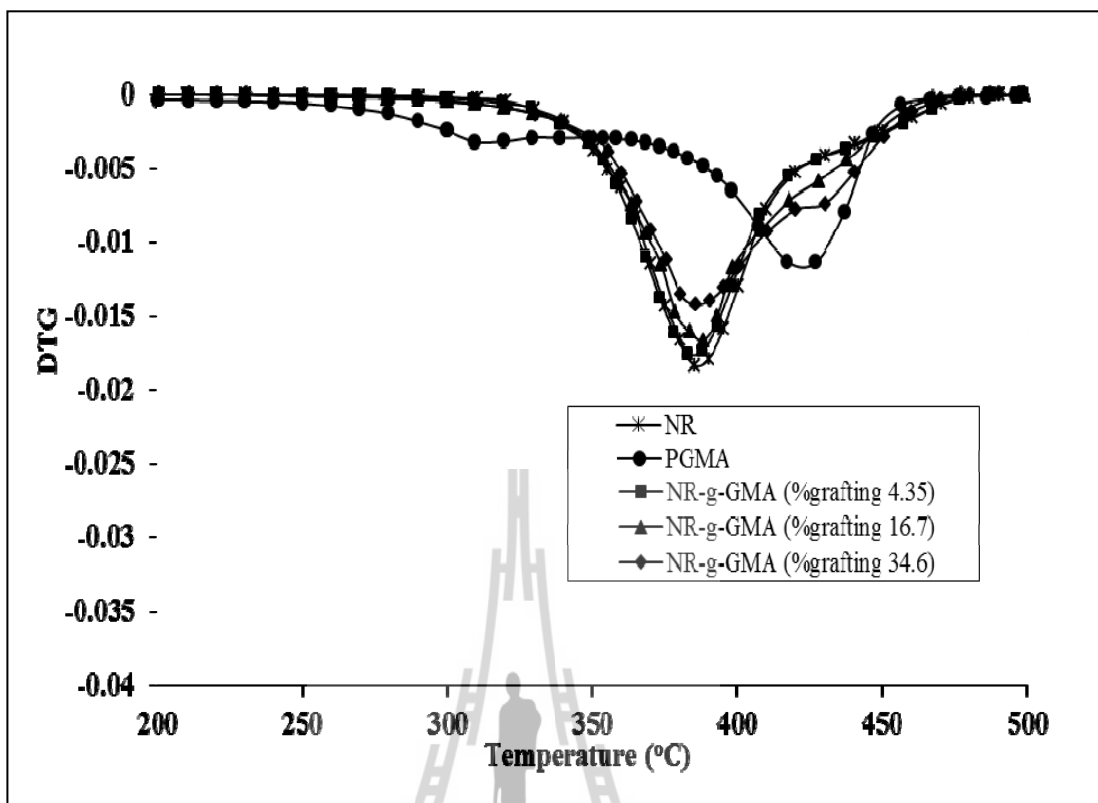


Figure 3.20 TGA curves of NR, PGMA and NR-g-GMA at various %grafting.



**Figure 3.21** DTG curves of NR, PGMA and NR-g-GMA at various %grafting.

### 3.5 Conclusions

GMA can be grafted onto NR by emulsion polymerization method using cumene hydroperoxide (CHP) and tetraethylenepentamine (TEPA) as the initiators. It was observed that %grafting and grafting efficiency were increased with increasing GMA content. However, above 40 phr of GMA content, grafting efficiency decreased. Grafting efficiency was not affected by reaction time and reaction temperature between 10-70 °C. The %grafting and %conversion increased with increasing reaction time and remained constant with the reaction time longer than 8 hours. The % conversion at the reaction temperature of 10 °C was 73% and increased to 99% at the reaction temperature of 30 °C. This indicated that the appropriate

condition for preparation of the graft copolymer was found to be a reaction temperature of 30 °C with the reaction time of 8 hours. With increasing %grafting, the tensile strength and modulus significantly increased with insignificantly decrease in elongation at break.

### 3.6 References

- Arayapranee, W., Prasassarakich, P., and Rempel, G. L. (2002). Synthesis of Graft Copolymers from Natural Rubber Using Cumene Hydroperoxide Redox Initiator. **J. Appl. Polym. Sci.** 83: 2993-3001.
- Bradbury, J. H., and Perera, M.C.S. (1985). Epoxidation of natural rubber studied by nmr spectroscopy. **J. Appl. Polym. Sci.** 30: 3347-3364.
- Derouet, D., Intharapat, P., Tran, Q. N., Gohier, F., and Nakason, C. (2009). Graft copolymers of natural rubber and poly (dimethyl (acryloyloxymethyl) phosphonate) (NR-g-PDMAMP) or poly (dimethyl (methacryloyloxyethyl) phosphonate) (NR-g-PDMMEP) from photopolymerization in latex medium. **Eur. Polym. J.** 45: 820-836.
- George, V., Britto, I. J., and Sebastain, M. S. (2003). Studies on radiation grafting of methyl methacrylate onto natural rubber for improving modulus of latex film. **Radiat. Phys. Chem.** 66: 367-372.
- Hinchiranan, N., Suppaibulsuk, B., Promprayoon, S., and Prasassarakich, P. (2007). Improving properties of modified acrylic sheet via addition of graft natural rubber. **Mater. Lett.** 61: 3951-3955.
- Hirose, S., Hatakeyama, T., Izuta, Y., and Hatakeyama, H. (2002). TG-FTIR studies on lignin-based polycaprolactones. **J. Therm. Anal. Calor.** 70: 853-860.

- Jiao, W., Liu, Y., and Qi, G. (2009). Studies on mechanical properties of epoxy composites filled with the grafted particles PGMA/Al<sub>2</sub>O<sub>3</sub>. **Compos. Sci. Technol.** 69: 391-395.
- Kunita, M. H., Rinaldi, A. W., Giroto, E. M., Radovanovic, E., Muniz, E. C., and Rubira, A. F. (2005). Grafting of glycidyl methacrylate onto polypropylene using supercritical carbon dioxide. **Eur. Polym. J.** 41: 2176-2182.
- Laine, C., Legare, V. B., Monnet, C., and Cassagnau, P. (2008). Free radical polymerization of glycidyl methacrylate in plasticized Poly(vinyl chloride). **Eur. Polym. J.** 44: 3177-3190.
- Lee, D. Y., Subramaniam, N., Fellows, C. M., and Gilbert, R. G. (2002). Structure–Property Relationships in Modified Natural Rubber Latexes Grafted with Methyl Methacrylate and Vinyl *neo*-Decanoate. **J. Polym. Sci.** 40: 809-822.
- Li, Y., and Shimizu, H. (2009). Improvement in toughness of poly(L-lactide) (PLLA) through reactive blending with acrylonitrile–butadiene–styrene copolymer (ABS): Morphology and properties. **Euro. Polym. J.** 45: 738-746.
- Mark, H. F. (1970). **Encyclopedia of Polymer Science and Engineering**. Wiley: New York.
- Mukerjee, P., and Mysels, K. J. (1971). **Critical Micelle Concentration of Aqueous Surfactant Systems**. NSRDS-NBS 36, US. Government Printing Office, Washington, D.C.
- Mayo, D.W., Miller, F.A., and Hannah R.W. (2004). **Course Notes On The Interpretation of Infrared and Raman Spectra**. John Wiley & Sons Inc : New Jersey.

- Nakason, C., Kaesaman, A., Samoh, Z., Homsin, S., and Kiatkamjornwong, S. (2002). Rheological properties of maleated natural rubber and natural rubber blends. **Polym. Test.** 21: 449-455.
- Nakason, C., Kaesaman, A., and Supasanthitikul, P. (2004). The grafting of maleic anhydride onto natural rubber. **Polym. Test.** 23: 35-41.
- Nakason, C., Kaesaman, A., and Yimwan, N. (2003). Preparation of graft copolymers from deproteinized and high ammonia concentrated natural rubber latices with methyl methacrylate. **J. Appl. Polym. Sci.** 87: 68-75.
- Nanjundan, S., Unnithan, C. S., Selvamalar, C. S. J., and Penlidis, A. (2005). Homopolymer of 4-benzoylphenyl methacrylate and its copolymers with glycidyl methacrylate: synthesis, characterization, monomer reactivity ratios and application as adhesives. **J. React. Funct. Polym.** 62: 11-24.
- Oliveira, P. C., Oliveira, A. M., Garcia, A., Barboza, J. C. S., Zavaglia, C., and Santos, A. M. (2005). Modification of natural rubber: A study by <sup>1</sup>H NMR to assess the degree of graftization of polyDMAEMA or polyMMA onto rubber particles under latex form in the presence of a redox couple initiator. **Eur. Polym. J.** 41: 1883-1892.
- Oliveira, P. C., Guimaraes, A., Cavaille, J. Y., Chazeau, L., and Gilbert, R. G. (2005). Poly (dimethylaminoethyl methacrylate) grafted natural rubber from seeded emulsion polymerization. **Polymer.** 46: 1105 -1111.
- Oyama, H. T. (2009). Super-tough poly (lactic acid) materials: Reactive blending with ethylene copolymer. **Polymer.** 50: 747-775.
- Perera, M. C. S. (1999). Structure and Dynamics of MG Rubber Studied by Dynamic Mechanical Analysis and Solid-State NMR. **J. Polym. Sci.** 37: 1141-1153.

- Perera, M. C. S., and Rowen, C. C. (2000). Radiation degradation of MG rubber studied by dynamic mechanical analysis and solid state NMR. **Polymer**. 41: 323-334.
- Pukkate, N., Kitai, T., Yamamoto, Y., Kawazura, T., Sakdapipanich, J., and Kawahara, S. (2007). Nano-matrix structure formed by graft copolymerization of styrene onto natural rubber. **Eur. Polym. J.** 43: 3208-3214.
- Sruanganurak, A., Sanguansap, K., and Tangboriboonrat, P. (2006). Layer-by-layer assembled nanoparticles: A novel method for surface modification of natural rubber latex film Colloids and Surfaces A: Physicochem. **Eng. Aspects**. 289: 110-117.
- Sanguansap, K., Thonggoom, R., and Tangboriboonrat, P. (2006). Surface modification of natural rubber film by polymerization of methyl methacrylate in water-based system. **Eur. Polym. J.** 42: 2334-2342.
- Schneider, M., Pith, T., and Lambla, M. (1996). Preparation and Morphological Characterization of Two- and Three-Component Natural Rubber-Based Latex Particles. **J. Appl. Polym. Sci.** 62: 273-290.
- Shinzato, S., Kobayashi, M., Mousa, W.F., Kamimura, M., Nee, M., Choju, K., Kokubo, T., and Nakamura, T. (2000). Bioactive bone cement : Effect of surface curing properties on bone-bonding strength. **J. Biomed. Mater. Res.** 53: 51-61.
- Senthil Kumar, U., Balaji, R., and Nanjundan, S. (2001). Copolymerization of 2-(N-Phthalimido) ethyl Methacrylate with Glycidyl Methacrylate: Synthesis, Characterization, and Monomer Reactivity Ratios. **J. Appl. Polym. Sci.** 81: 96-103.

- Su, Z., Li, Q., Liu, Y., Hu, G.H., and Wu, C. (2009). Compatibility and phase structure of binary blends of poly (lactic acid) and glycidyl methacrylate grafted poly (ethylene octane). **Euro. Polym. J.** 45: 2428-2433.
- Teh, P.L., Mohd-Ishak, Z. A., Hashim, A.S., Karger-Kocsis, J., and Ishiaku, U. S. (2004). Effects of epoxidized natural rubber as a compatibilizer in melt compounded natural rubber–organoclay nanocomposites. **Eur. Polym. J.** 40: 2513-2521.
- Vijayakumar, M. T., Rami, R. C., and Joseph, K. T. (1985). Grafting of poly (glycidyl methacrylate) onto alginic acid. **Eur. Polym. J.** 21: 415-419.
- Vijayanand, P. S., Kato, S., Satokawa, S., Kishimoto, M., and Kojima, T. (2009). Synthesis, Characterization and thermal properties of homo and copolymers of 3, 5-dimethoxyphenyl methacrylate with glycidyl methacrylate: Determination of monomer reactivity ratios. **J. React. Funct. Polym.** 69: 333-340.
- Wang, H., Tanaka, W., Kita, H., and Okamoto, K. (1998). Preparation of Plasma-Grafted Polymer Membranes and Their Morphology and Pervaporation Properties toward Benzene/Cyclohexane Mixtures. **J. Appl. Polym. Sci.** 36: 2247-2259.
- Yinghai, L., Yanzhe, Z., Zhenghao, L., and Kuilin, D. (2002). Graft copolymerization of butyl acrylate onto casein initiated by potassium diperiodatonickelate (IV) in alkaline medium. **Eur. Polym. J.** 38: 1619-1625.
- Zhang, X., and Tanaka, H. (2001). Influence of Retention System and Curing on Paper Wet Strength Improvement by a Copolymer Containing Glycidyl Groups. **J. Appl. Polym. Sci.** 81: 2791-2797.

- Zhang, L., Cai, Z., Cai, Q.Z., Yu, Q., and Loang, Z. (1999). Photocrosslinked Polymer and Interpenetrating Polymer Network for Nonlinear Optics. **J. Appl. Polym. Sci.** 71: 1081-1087.
- Zhang, X., and Tanaka, H. (2001). Copolymerization of Glycidyl Methacrylate with Styrene and Applications of the Copolymer as Paper-Strength Additive. **J. Appl. Polym. Sci.** 80: 334-339.



# CHAPTER IV

## EFFECT OF GLYCIDYL METHACRYLATE GRAFTED NATURAL RUBBER ON PHYSICAL PROPERTIES OF POLYLACTIC ACID AND NATURAL RUBBER BLENDS

### 4.1 Abstract

Natural rubber (NR) was melt blended with polylactic acid (PLA) at various ratios using an internal mixer. The impact strength and elongation at break of PLA/NR blend dramatically increased with increasing NR content up to 10% (wt/wt). Glycidyl methacrylate grafted natural rubber (NR-g-GMA) was used as a compatibilizer for PLA/NR blend. The effects of content and %grafting of NR-g-GMA on mechanical properties of PLA/NR blend were studied. The experimental result showed that the addition of NR-g-GMA in PLA/NR blend significantly improved impact strength and elongation at break of PLA/NR blend compared to that of neat PLA and PLA/NR blend without NR-g-GMA. The impact strength and elongation at break of PLA/NR blend increased with increasing NR-g-GMA content up to 1% (wt/wt). Moreover, with increasing %grafting of NR-g-GMA in PLA/NR blend up to 2.3 the impact strength and elongation at break of the blend increased. Morphological and thermal property of PLA, PLA/NR and PLA/NR/NR-g-GMA were elucidated as well.

## 4.2 Introduction

Poly (lactic acid) (PLA) is a synthetic aliphatic polyester derived from biomass. Due to its renewability, biodegradability and greenhouse gas neutrality, it has been emerging as an alternative to conventional petroleum-based polymeric materials. However, the inherent brittleness, low-melt viscosity, low-heat distortion temperature and low crystallization rate of PLA led to its restricted applications (Lunt, 1998). In order to improve its property, it is now common practice to modify PLA by physical blending. For example, PLA was blended with other more flexible polymers such as polycaprolactone (PCL) (Broz, Vanderhart, and Washburn, 2003); (Sarazin, Li, Orts, and Favis, 2008); (Wu, Zhang, Zhang, and Zhou, 2008) polybutylenesuccinate (PBS) (Yokohara and Yamaguchi 2008), poly (butylene succinate-co-L-lactate) (PBSL) (Shibata, Inoue, and Miyoshi, 2006) and poly (butylene adipate-co-terephthalate) (PBAT) (Gu, Zhang, Ren, and Zhan, 2008); (Long, Michael, and Jinwen, 2006). Generally, these blends showed considerably higher toughness than pure PLA. However, a significant decrease in tensile strength and modulus of the blends can be observed. As a consequence, the improvement of mechanical properties of PLA blends is still necessary to obtain material with optimum performance. Moreover, these flexible polymers come from petroleum resource, whose price tends to increase in the future. Therefore, new material from renewable resource has received a lot of attention from researchers. Natural rubber (NR) is an interesting candidate to use as an impact modifier for PLA because it has excellent properties such as high strength, high resilience and high elongation at break (Mark, 1970).

NR has been used to improve mechanical properties of other polymers such as poly (ethylene terephthalate) (PET) (Phinyocheep, Saelao, and Buzare, 2007), polystyrene (PS) (Asaletha, Kumaran, and Thomus, 1999) and polypropylene (PP) (Oh, Isayev, and Rogunova, 2003). The improvement in impact strength of these polymers when adding NR was reported. However, Carvalho et al. found that the elongation at break of thermoplastic starch (TPS)/NR blend was increased when using NR content from 2.5-5% (wt/wt) and decreased when using higher NR content (Carvalho, Job, Alves, Curvelo, and Gandini, 2003). The difference in polarity of TPS and NR led to a phase separation and the blends became brittle at high NR content. The phase separation of NR blends due to the difference in polarity and molecular weight was also reported by several researchers (Chuayjuljit, Moolsin, and Potiyaraj, 2005); (Carone, Kopcak, Goncalves, and Nunes, 2000); (Dahlan, Khairul Zaman, and Ibrahim, 2002). In case of PLA/NR blend, the difference in the polarity and molecular weight of PLA and NR may result in the poor compatibility between PLA and NR. Thus, the compatibility between PLA and NR need to be improved in order to obtain the blend with higher impact property.

Generally, there are two ways to improve compatibility of polymer blend. One is to induce a chemical reaction, leading to a modification of the polymer interface in two-phase blends. Another way is to add a third component called compatibilizer which increases the interaction between immiscible phases. The third component can be block or graft copolymer which can interact with both phases. The compatibilization of PLA blends has been extensively studied (Coltelli, Bronco, and China, 2010); (Gao et al., 2006); (Zhang, Goh, and Lee, 1998). The elongation at break of the reactively compatibilized PLA/PCL blends was improved significantly

when compared to that of pure PLA (Wang, Ma, Gross, and McCarthy, 1998). The compatibility of PLA/starch blends was improved by using various compatibilizers such as maleic anhydride (MA) grafted PLA (PLA-g-MA) (Huneault and Li, 2007), poly (L-lactide)-g-starch copolymer (PLLA-g-St) (Chen et al., 2006) and thermoplastic polyolefin elastomer-graft-poly lactide (TPO-PLA) (Ho, Wang, Lin, and Lee, 2008). Glycidyl methacrylate (GMA) grafted polymers such as styrene/acrylonitrile/glycidyl methacrylate copolymer (SAN-GMA) (Li and Shimizu 2009) and glycidyl methacrylate grafted poly (ethylene octane) (GMA-g-POE) (Su, Li, Liu, Hu, and Wu, 2009) are often used as compatibilizer for PLA blends. Oyama toughened PLA by reactive blending with poly (ethylene-glycidyl methacrylate) (EGMA) (Oyama, 2009). This study demonstrated a dramatic improvement in the mechanical characteristics of PLA by its reactive blending with EGMA. The elongation at break of PLA blends showed 40 times higher than that of neat PLA. Moreover, grafted copolymers of GMA were used as compatibilizer in other polyester blends such as PET/PP blend (Pracella, and Chionna, 2003), PCL/cellulose acetate (CA) blend (Rosa, Guedes, and Bardi, 2007) and high-density polyethylene (HDPE)/PET blend (Pietrasanta, Robin, Torres, and Boutevin, 1999). It is usually believed that epoxy groups of GMA can react with carboxyl or hydroxyl groups of polyester.

From Chapter 3, GMA was successfully grafted onto NR by emulsion polymerization to obtain glycidyl methacrylate grafted natural rubber (NR-g-GMA). When PLA was mixed with NR-g-GMA to form blends, it was expected that the epoxy group in NR-g-GMA can react with the carboxyl groups located at the PLA chain ends during melt-mixing. This should enhance compatibility between PLA and

NR. Thus, the toughness of PLA/NR blend should be improved by using NR-g-GMA as a compatibilizer. The effect of NR-g-GMA on mechanical, thermal and morphological properties of PLA/NR blends was elucidated in this study.

## **4.3 Experimental**

### **4.3.1 Materials**

Thai natural rubber (grade STR 5L) was purchased from Thaihua Latex Co., Ltd. A commercial grade of PLA (PLA 4042D) was purchased from NatureWorks LLC. NR-g-GMA at various %grafting was prepared in our laboratory. The synthesis and characterization of NR-g-GMA including the calculation to find %grafting of GMA monomer were given in details in previous chapter. NR-g-GMA at various %grafting including 0.76, 2.30, 4.35, 8.40 and 16.70 were used in this study and they were denoted by NR-g-GMA (A), NR-g-GMA (B), NR-g-GMA (C), NR-g-GMA (D) and NR-g-GMA (E) respectively.

### **4.3.2 Blends preparation**

PLA blends were prepared by using an internal mixer (Hakke Rheomix, 3000p) at the temperature of 170°C with a rotor speed of 60 rpm for 10 min. Before mixing, PLA was dried in an oven at 70 °C for 4 hours to eliminate moisture. NR was cut into a small size and dried in an oven at 70 °C for 24 hours to eliminate moisture. The compositions of all blends are shown in Table 4.1. In each batch, half of PLA was added first. After melting PLA (2 minutes), NR were then added prior to addition of remaining PLA. After mixing in an internal mixer, the blend specimens were prepared by compression molding (LabTech, LP20-B) at 165 °C for 10 minutes.

**Table 4.1** Blend compositions.

<b>Symbols</b>	<b>PLA (wt%)</b>	<b>NR (wt%)</b>	<b>NR-g-GMA (wt%)</b>
PLA	100	-	-
PLA/NR (95/5)	95	5	-
PLA/NR (90/10)	90	10	-
PLA/NR (85/15)	85	15	-
PLA/NR (80/20)	80	20	-
PLA/NR/NR-g-GMA (A) (90/9/1)	90	9	1
PLA/NR/NR-g-GMA (B) (90/9/1)	90	9	1
PLA/NR/NR-g-GMA (C) (90/9/1)	90	9	1
PLA/NR/NR-g-GMA (D) (90/9/1)	90	9	1
PLA/NR/NR-g-GMA (E) (90/9/1)	90	9	1
PLA/NR/NR-g-GMA (B) (90/9.8/0.2)	90	9.8	0.2
PLA/NR/NR-g-GMA (B) (90/7/3)	90	7	3
PLA/NR/NR-g-GMA (B) (90/5/5)	90	5	5

### 4.3.3 Characterization

#### 4.3.3.1 Thermal property

Thermo gravimetric analysis (TGA) was performed using a TA Instrument thermogravimetric analyzer (TGA, Mettler Toledo model TGA/DSC 1) by heating the sample from room temperature to 600 °C at a heating rate of 20 °C/min under a nitrogen atmosphere. The sample with a weight between 5 to 10 mg was used for each run. Differential scanning calorimetry (DSC : Mettler Toledo Version STARe SW 8.1) was used to obtain thermal properties of specimens by heating the specimens from 30 °C to 200 °C at the rate of 5 °C/min (First heating scan). After keeping the specimens at 200 °C for 3 min they were cooled to 30 °C at 5 °C/min. Then they were heated again to 200 °C at 5 °C/min (Second heating scan). The degree of crystallinity, % $X_C$ , of the blends can be obtained by:

$$\%X_C = \frac{\Delta H_m}{\Delta H_{mo}(\phi_{PLA})} \times 100$$

In which  $\Delta H_m$  was the measured melting enthalpy,  $\Delta H_{mo}$  was the melting enthalpy of purely crystalline sample (93 J/g for PLA) and  $\phi_{PLA}$  was the PLA weight fraction in the blends (Cheung et al., 2008).

#### 4.3.3.2 Rheological property

Shear viscosities at the shear rate range of 10 to 10,000 s<sup>-1</sup> of neat PLA and PLA blends were measured using the Kayeness capillary rheometer (model D5052m). Melt flow index (MFI) of PLA, PLA/NR blend and PLA composite were characterized using a melt flow indexer (Kayeness, 4004). All samples were measured at 170°C with a load of 2.16 kg.

#### 4.3.3.3 Mechanical properties

The unnotched Izod impact test was performed according to ASTM D256 using an Atlas testing machine (model BPI). The standard specimen size for impact testing is 10 mm×3.3 mm×55 mm (Figure 4.1). Tensile properties were obtained according to ASTM D638 using an Instron universal testing machine (UTM, model 5565) with a load cell of 5 kN at a crosshead speed of 2 mm/min. The specimen geometry for tensile testing is shown in Figure 4.2 and the standard specimen size is shown in Table 4.2.

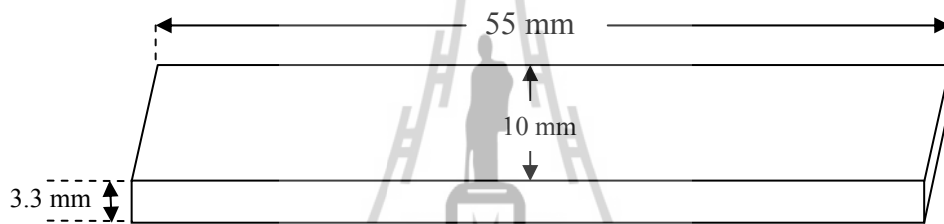


**Figure 4.1** The standard specimen size for impact testing.

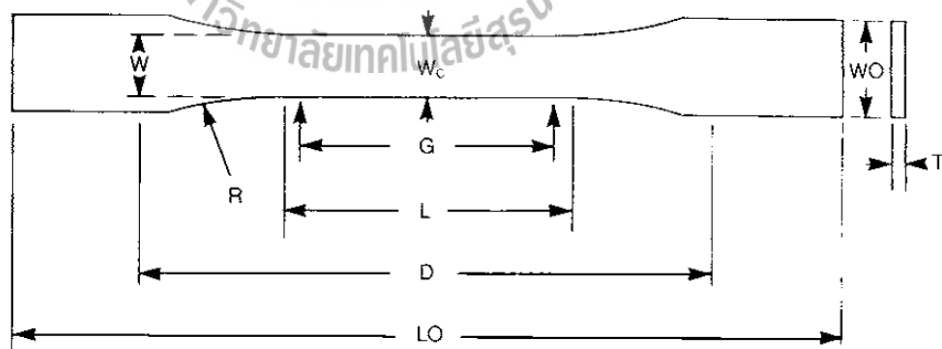


**Figure 4.2** The specimen dimensions for tensile testing.

**Table 4.2** The standard specimen size for tensile testing.

<b>Dimensions (see drawings)</b>	<b>Type V (ASTM D638)</b>
<i>W</i> —Width of narrow section	3.18 ± 0.03 mm
<i>L</i> —Length of narrow section	9.53 ± 0.08 mm
<i>WO</i> —Width overall (min)	9.53 ± 0.08 mm
<i>LO</i> —Length overall	63.5 mm
<i>G</i> —Gage length	7.62 ± 0.02 mm
<i>D</i> —Distance between grips	25.4 ± 0.2 mm
<i>R</i> —Radius of fillet	12.7 ± 0.08 mm

#### 4.3.3.4 Interaction of PLA and NR-g-GMA

PLA was melt blended with NR-g-GMA(C) at the ratio of PLA/NR-g-GMA(C) 90/10 wt/wt by using an internal mixer (Hakke Rheomix, 3000p) at the temperature of 170°C with a rotor speed of 60 rpm for 10 min. The interaction between PLA and NR-g-GMA(C) blend (PLA/NR-g-GMA(C)) was evaluated using Fourier transform infrared (FT-IR) spectrometer (Spectrum one). The spectra were obtained at 4 cm<sup>-1</sup> resolution in the wavenumber range from 4000 to 650 cm<sup>-1</sup>. The FT-IR samples were prepared by casting polymer films. All samples were dried in an oven at 70°C for 24 hours before testing.

#### 4.3.3.5 Morphological property

The morphologies of the impact fractured surface and tensile fractured surface of compression molded samples were examined using a scanning electron microscope (SEM, model JEOL 6400). The specimens were coated with gold

prior to the examination. Acceleration voltage of 20 kV was used to collect SEM images of the samples.

## **4.4 Results and discussion**

### **4.4.1 Thermal properties of PLA, NR, PLA/NR and PLA/NR/NR-g-GMA**

TGA and DTG curves of PLA, PLA/NR (90/10), PLA/NR/NR-g-GMA (B) (90/9/1) and NR are shown in Figure 4.3 and Figure 4.4, respectively. It is evident that the thermal degradation of PLA and NR showed only a single step of weight loss. The onset degradation temperatures of PLA and NR were 290.8 °C and 305.3°C, respectively. The final degradation temperature of PLA and NR were noticed at 409.7 °C and 490.6 °C, respectively. This indicated the higher thermal stability of NR compared to that of PLA. The onset degradation temperature of PLA/NR (90/10) was 294.2 °C, which is about 4 °C higher than PLA. The slightly increase in thermal stability of PLA/NR (90/10) has been attributed to the higher thermal stability of NR. Moreover, PLA/NR/NR-g-GMA (B) (90/9/1) showed higher onset degradation temperatures (301.6 °C) than that of PLA/NR (90/10). The increase in thermal stability of PLA/NR when using NR-g-GMA as compatibilizer might be attributed to the higher interaction and better dispersion of NR in PLA matrix. An increase in thermal stability of PLA due to the good interaction between the blend components was also reported in other PLA blends and composites. Girija, Sailaja, and Giridhar (2005) studied thermal properties of polyethylene terephthalate (PET) and PLA blend. The thermal degradation of the blends was studied using thermogravimetry. They found that thermal stability of PLA was increased by the

addition of PET to PLA. Moreover, Feijoo, Cabedo, Gim, Lagaron, and Saura (2005) prepared the amorphous PLA-montmorillonite nanocomposites. Melt blending of PLA with clay particles was conducted on an internal mixer (Rheomix-Haake) with a rotation speed of 20 rpm for 4 min, then at 60 rpm for another 4 min, at a temperature of 150 °C. Compositions with 4 % (wt/wt) organically modified montmorillonite (OMM) were compounded. The experimental result showed that the thermal stability of PLA composite was increased when the interaction and dispersion of the components was improved.

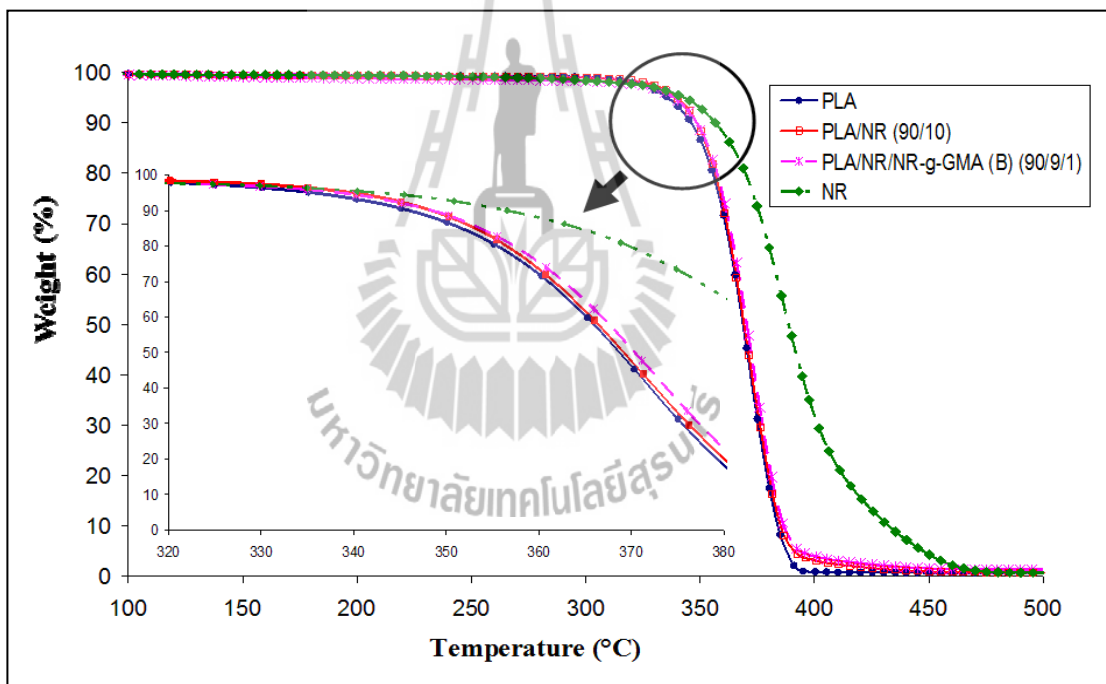


**Figure 4.3** TGA curves of PLA, PLA/NR (90/10), PLA/NR/NR-g-GMA (B) (90/9/1) and NR.

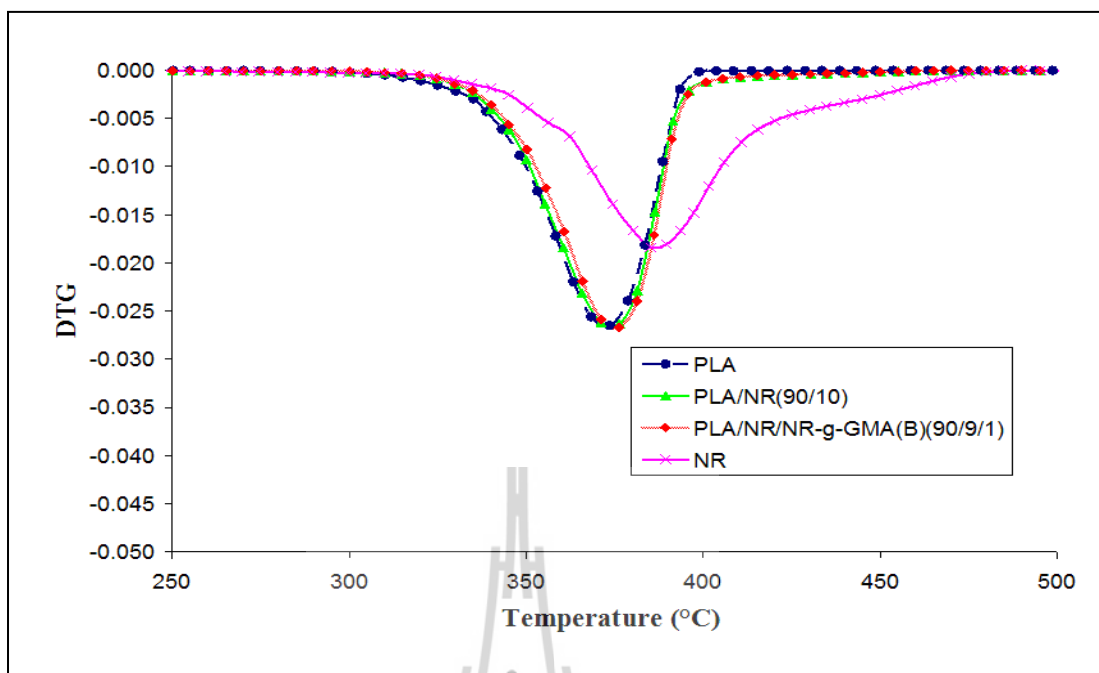


**Figure 4.4** DTG curves of PLA, PLA/NR (90/10), PLA/NR/NR-g-GMA (B) (90/9/1) and NR.

DSC curves of PLA and PLA blends obtained from the second heating scan are shown in Figure 4.5. The glass transition temperature ( $T_g$ ), the crystallization temperature ( $T_c$ ) (indicated by exothermic peak) and melting temperature ( $T_m$ ) (indicated by endothermic peak) of PLA and PLA blends could be observed. The double melting endotherms for neat PLA were observed. This indicated that several crystallite forms of PLA were taken place. From the DSC curves, it was found that  $T_g$  of PLA blend was not changed comparing to that of neat PLA.  $T_m$  of PLA blends was shifted to higher temperature compared to that of neat PLA. Moreover, degree of crystallinity ( $\%X_C$ ) of PLA blends was lower than that of neat PLA (Table 4.3). This could be due to the fact that the addition of NR in PLA may hinder the migration and diffusion of PLA molecular chains to the surface of the nucleus in the blends.

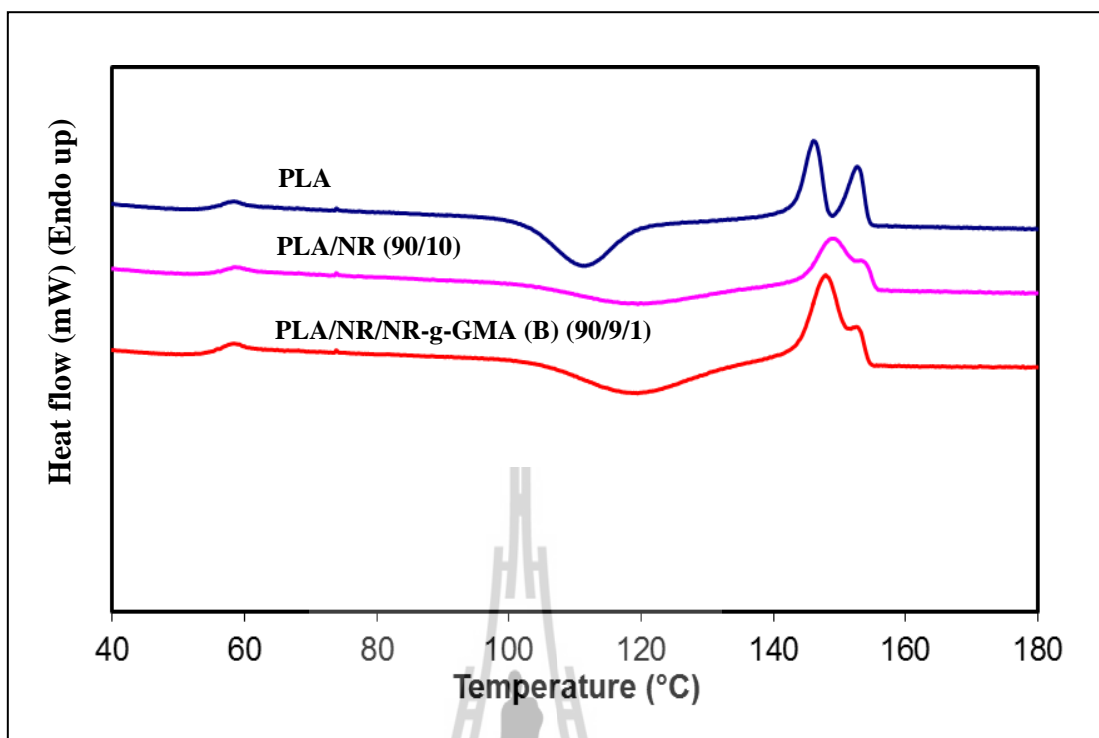


**Figure 4.5** DSC curves of PLA, PLA/NR (90/10) and PLA/NR/NR-g-GMA (B) (90/9/1).

**Table 4.3**  $T_g$ ,  $T_c$ ,  $\Delta H_c$ ,  $T_m$ ,  $\Delta H_m$  and  $\%X_c$  of PLA and PLA blends.

Samples	$T_g$ (°C)	$T_c$ (°C)	$\Delta H_c$ (J/g)	$T_m$ (°C)		$\Delta H_m$ (J/g)	$\%X_c$
				1	2		
PLA	57.3	111.5	30.0	146.0	152.7	29.8	32.1
PLA/NR (90/10)	57.2	119.4	26.7	149.1	-	22.5	26.9
PLA/NR/NR-g-GMA (B) (90/9/1)	57.2	119.4	26.1	147.9	-	25.4	30.4

#### 4.4.2 Rheological property of PLA, NR, PLA/NR and PLA/NR/NR-g-GMA

Figure 4.6 presents the shear viscosity of PLA, PLA/NR (90/10) and PLA/NR/NR-g-GMA (B) (90/9/1) at various shear rate. It can be seen that the viscosity of PLA and PLA blends decreased with increasing in shear rate, indicating pseudoplastic nature of the PLA and PLA blends. The pseudoplasticity is due to the fact that the molecules which under high shear become deformation resulting in a reduction of viscosity. Shear viscosities of PLA/NR and PLA/NR blend with NR-g-GMA were quite similar and they were lower than those of neat PLA. Moreover, MFI of the PLA blends with and without NR-g-GMA was higher than that of neat PLA (as shown in Table 4.4). The reduction in viscosity when adding NR in PLA may be attributed to the ability of NR molecule that can penetrate into PLA matrix. This made PLA matrix slip and flow easier.

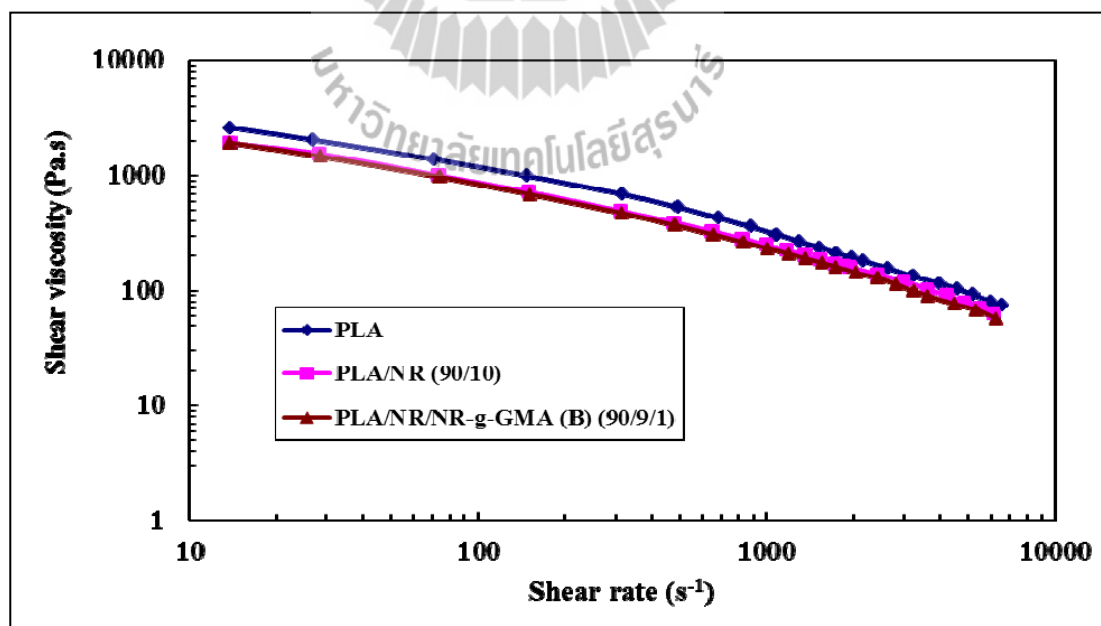


**Figure 4.6** Shear viscosity of PLA, PLA/NR (90/10) and PLA/NR/NR-g-GMA (B) (90/9/1) at various shear rate.

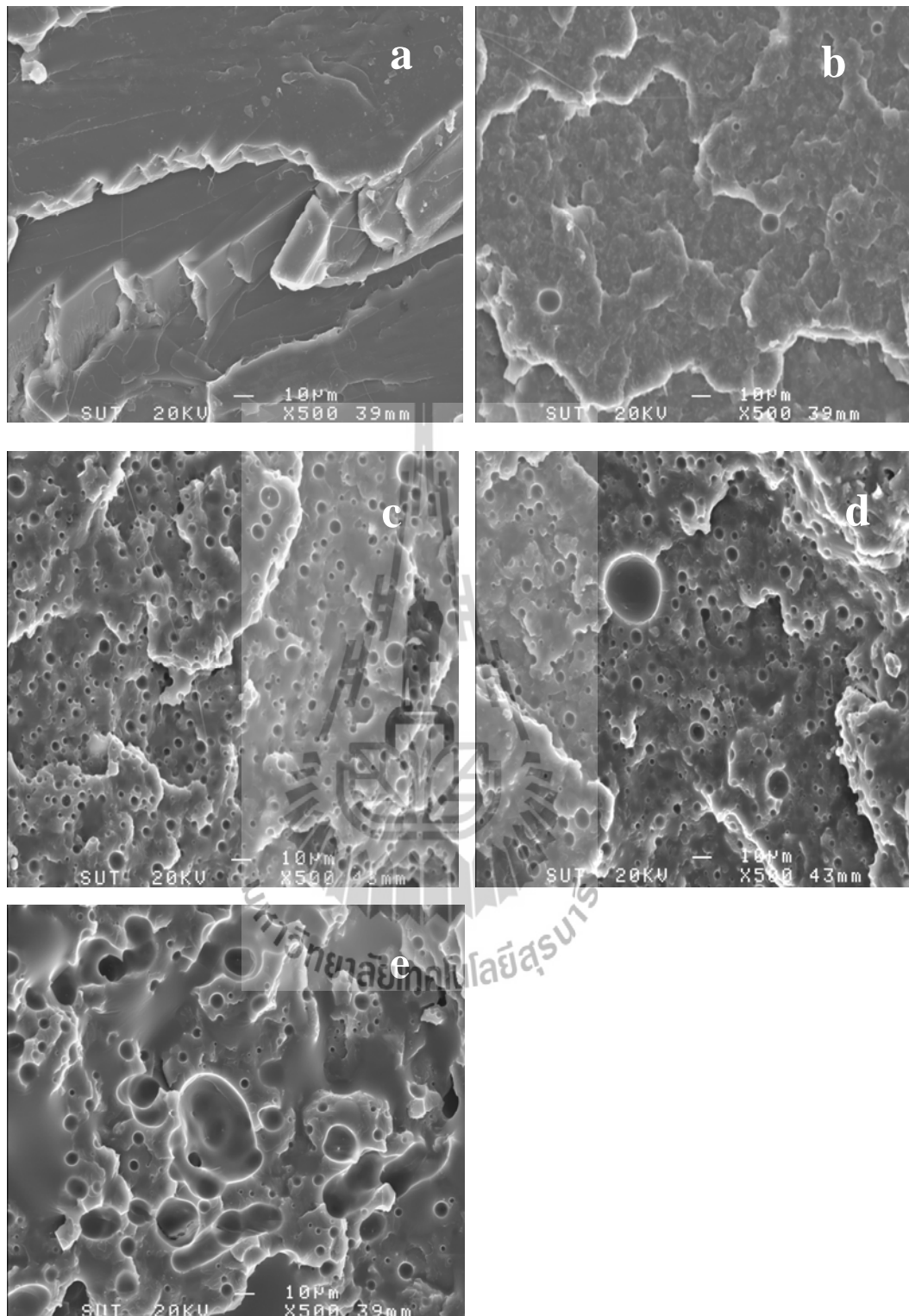
**Table 4.4** MFI of PLA and PLA blends.

Samples	MFI(g/10min)	STDEV
PLA(internal)	7.21	0.26
PLA/NR(90/10)	9.26	0.35
PLA/NR/NR-g-GMA (B) (90/9/1)	9.48	0.44

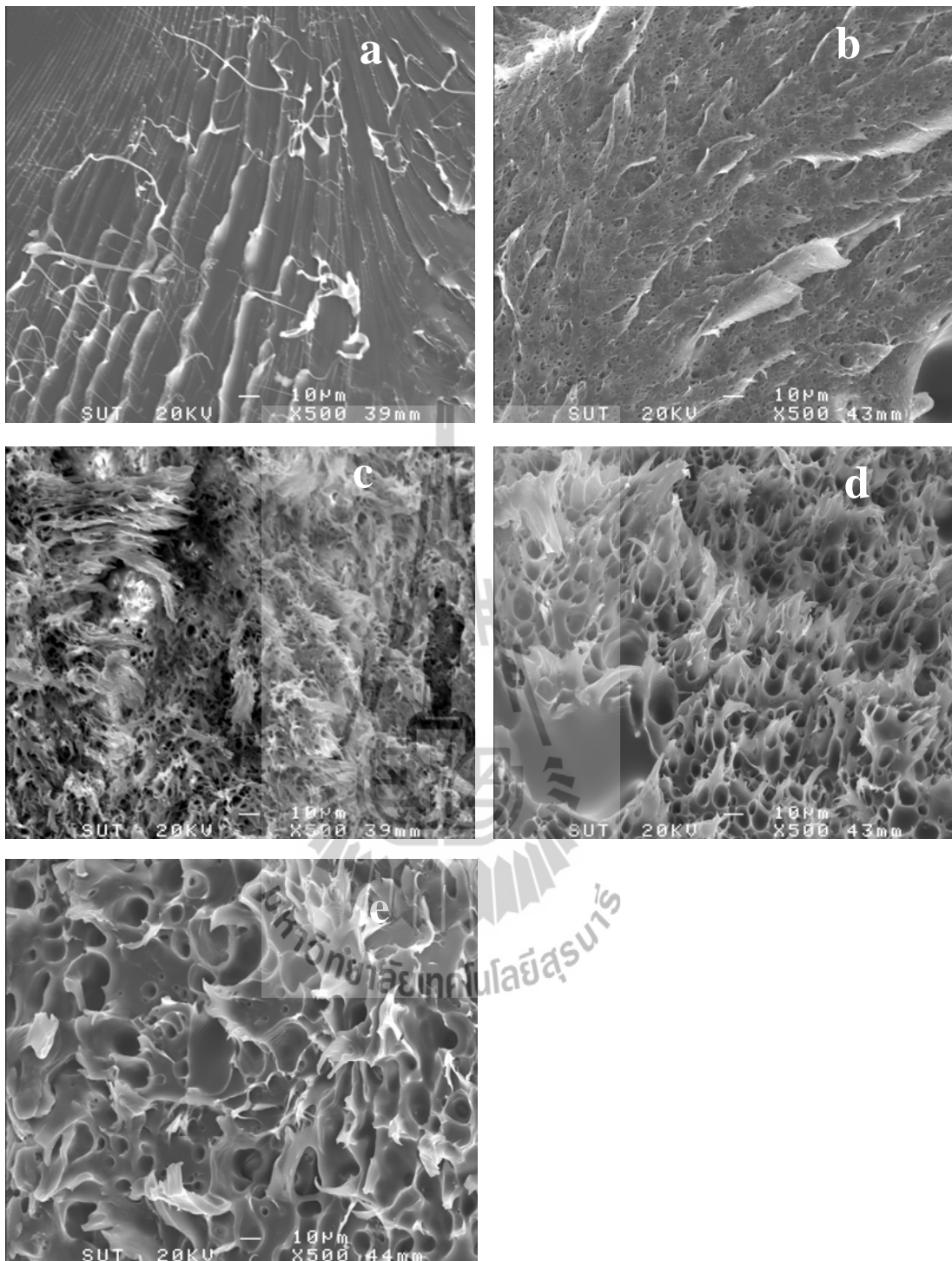
#### 4.4.3 Effect of NR content on morphological and mechanical properties of PLA/NR blend

Figure 4.7 (a-e) shows SEM micrographs of impact fractured surface of PLA and PLA/NR blends with increasing NR contents from 5 to 20% (wt/wt). The micrographs of the blends showed two phases with irregular domain size and shape. This indicates that PLA/NR blends are completely immiscible where NR domains are dispersed in PLA matrix. When 10 % (wt/wt) NR was added the domain size of NR was about 5 to 10  $\mu\text{m}$  (as shown in Figure 4.7 (c)). In case of PLA/NR (80/15 and 80/20), the average domain size of NR was much larger than 10  $\mu\text{m}$  (Figure 4.7 (d and e)). This implied that the coagulation of NR phase appeared at high NR content. Generally, in an immiscible blend system especially at high content of dispersed phase, polymers always coagulate individually due to their different chemical structures and high molecular weights (Chen, Chueh, Tseng, Huang, and Lee (2003)).

Figure 4.8 (a-e) shows SEM micrographs of tensile fractured surface of PLA and PLA/NR blends with increasing NR contents from 5 to 20% (wt/wt). For PLA/NR, more and longer fibrils can be observed from the surfaces when using NR content of 5 and 10% (wt/wt) as shown in Figure 4.8 (b and c). This can be used as an evidence of ductile fractures.



**Figure 4.7** SEM micrographs of impact fractured surface of PLA (a), PLA/NR (95/5) (b), PLA/NR (90/10) (c), PLA/NR (80/15) (d) and PLA/NR (80/20) (e).



**Figure 4.8** SEM micrographs of tensile fractured surface of PLA (a), PLA/NR (95/5) (b), PLA/NR (90/10) (c), PLA/NR (80/15) (d) and PLA/NR (80/20) (e).

Figure 4.9 shows the impact strength of PLA, PLA/NR blends at various NR contents. The impact strength of neat PLA was 19.06 kJ/m<sup>2</sup>. Impact strength of PLA/NR blends increased with increasing NR content up to 10% (wt/wt). When the NR content reached 10% (wt/wt), impact strength of the PLA/NR blend was 39.52 kJ/m<sup>2</sup>, which is about 2 times higher than that of neat PLA. However, when NR content was increased to 15% (wt/wt) impact strength of PLA/NR blend was decreased to 29.98 kJ/m<sup>2</sup> but it was still higher than that of neat PLA. With further increased NR content to 20% (wt/wt) impact strength of PLA/NR blend was decreased to 11.26 kJ/m<sup>2</sup> which was lower than that of neat PLA. This suggests that the optimum content of NR in PLA is 10% (wt/wt). Tensile strength, modulus and elongation at break of PLA and PLA/NR blends at various NR contents are shown in Table 4.5. Modulus and tensile strength of PLA/NR decreased with increasing NR content. The reduction in these mechanical properties was due to the result of the rubbery nature of NR. This behavior was also found in NR blend with other polymers such as nylon 6 (PA6) (Carone et al., 2000). Elongation at break was increased from 10.84% for neat PLA to 74.51% for PLA/NR (90/10). With increasing NR content to 15% and 20% (wt/wt), elongation at break of PLA/NR blends was decreased. There are many factors concerning with the effectiveness of rubber toughened polymer such as interfacial adhesion between rubber particles and matrix, type and concentration of rubber, blending method, processing conditions and rubber particle size and shape. It is generally accepted that rubber particle size and interfacial adhesion between blend components take the key role in determining the mechanical performance of a polymer blend. For example, a large particle size and weak adhesion would result in poor mechanical properties in the blends. This kind of phase separation dramatically

affects the physical and mechanical properties of the blend (Todo, Park, Takayama, and Arakawa, 2007).

The decrease in elongation at break and impact strength of PLA/NR blends at high NR content might be due to the enlargement of the dispersed NR caused by the coagulation of NR phase as previously shown in SEM micrographs. Stress concentration usually takes place in the vicinity of the dispersed phase due to the difference of elastic modulus between the dispersed phases (NR) and the surrounding matrix (PLA), and initiates localized micro-damages in this region resulting in the reduction of mechanical properties such as strength and toughness at high NR content. This behavior was also observed in the PLA/PCL blends (Todo et al., 2007).

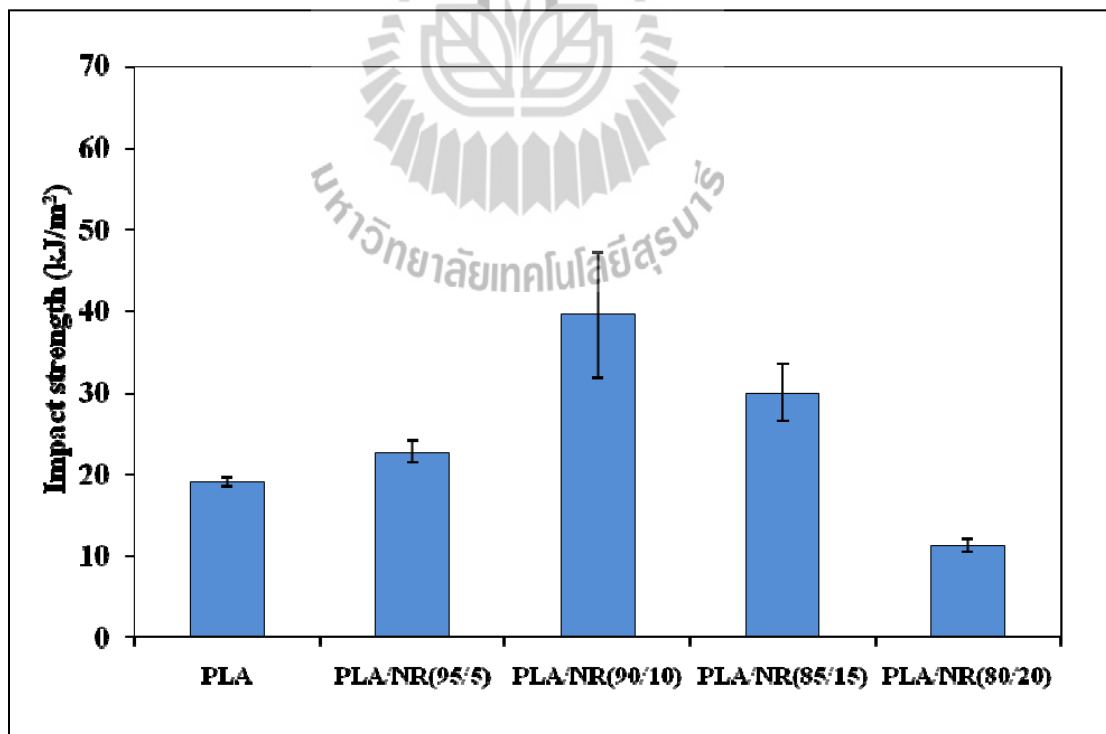


**Figure 4.9** Impact strength of PLA, PLA/NR blends at various NR content.

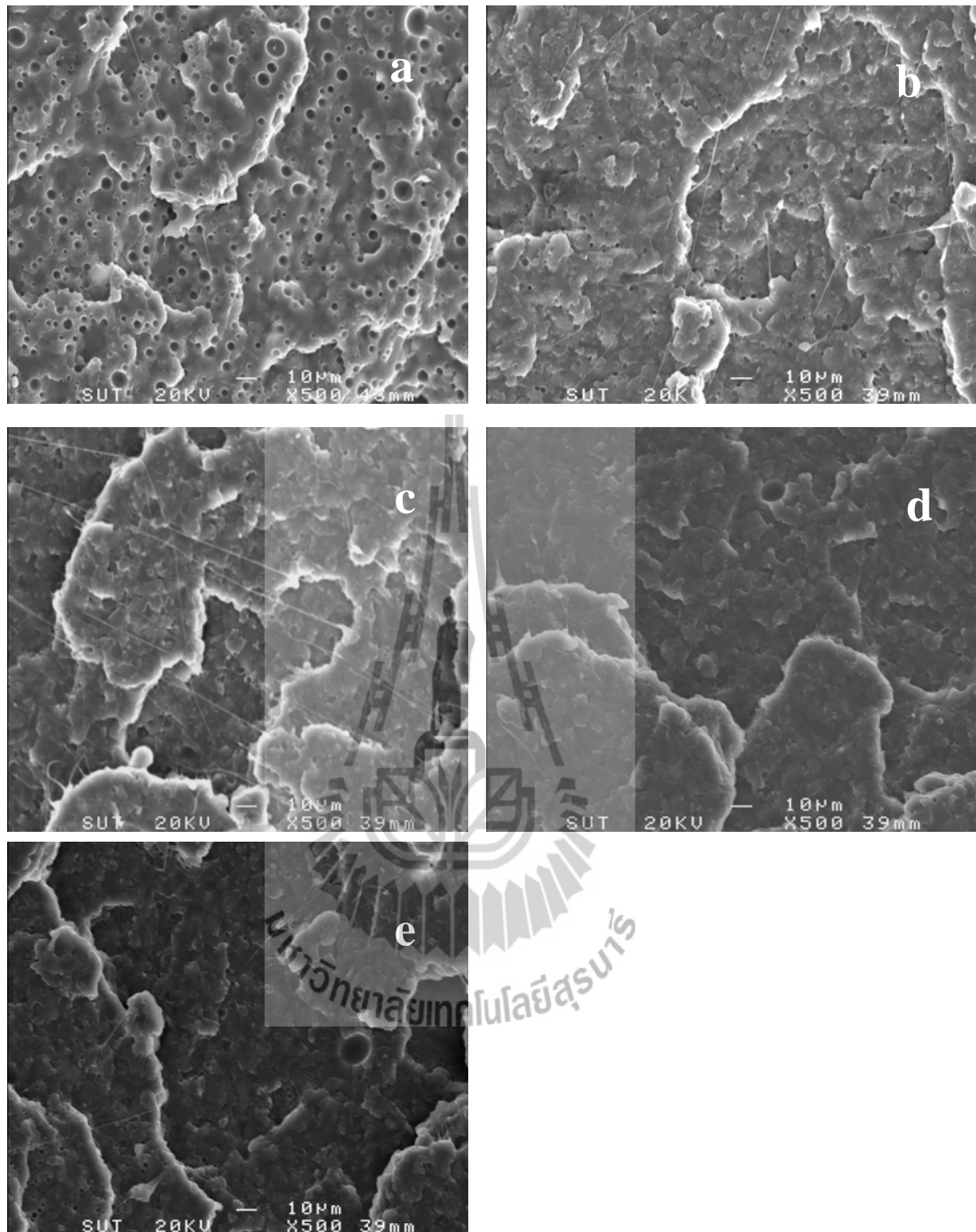
**Table 4.5** Tensile strength, modulus and elongation at break of PLA and PLA/NR blends.

Samples	Tensile strength (MPa)	Elongation at break (%)	Modulus (GPa)
PLA	52.99±0.65	10.84±1.64	0.63±0.04
PLA/NR (95/5)	41.04±1.60	25.75±4.79	0.62±0.02
PLA/NR(90/10)	29.66±1.56	74.51±9.06	0.51±0.04
PLA/NR(85/15)	28.91±0.89	23.39±1.59	0.50±0.02
PLA/NR(80/20)	18.23±1.28	7.43±0.30	0.36±0.02

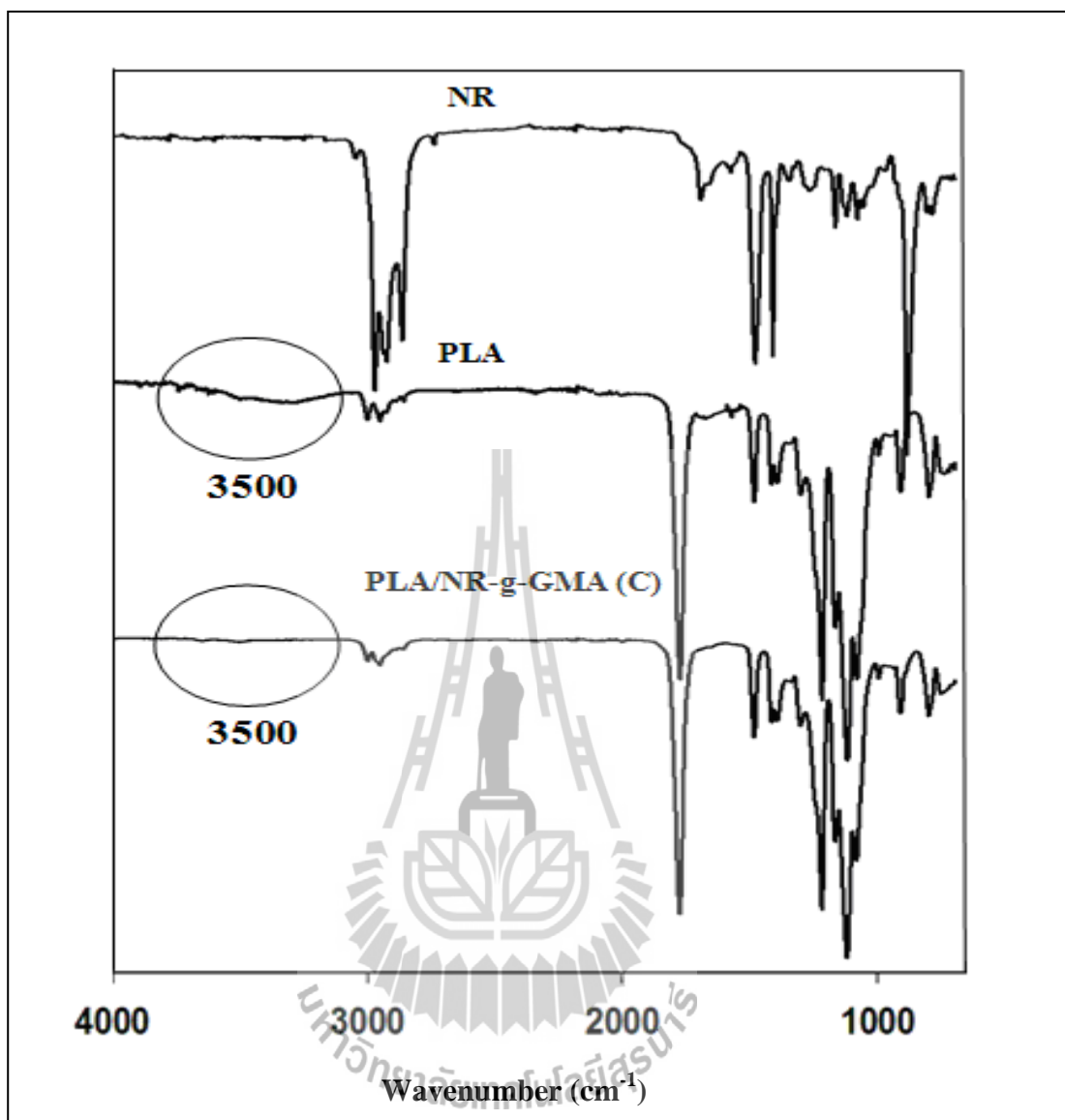
#### 4.4.4 Effect of NR-g-GMA content on morphological and mechanical properties of PLA/NR blend

To study the effect of NR-g-GMA content and %grafting on morphological and mechanical properties of PLA/NR blends, PLA content was fixed at 90 wt% according to the highest impact strength of PLA/NR (90/10). The rest portion (10 wt%) was NR and NR-g-GMA. The ratio of NR to NR-g-GMA was varied (9.8/0.2, 9/1, 7/3, 5/5 wt%) as shown in Table 4.1. Figure 4.10 (a-e) shows SEM micrographs of impact fractured surface of PLA/NR blends containing 0.2 to 5% (wt/wt) of NR-g-GMA. The %grafting was fixed at 2.3. When 1% (wt/wt) of NR-g-GMA was added the domain sizes of NR (as shown in Figure 4.10 (c)) were much smaller than that of PLA/NR (90/10) without NR-g-GMA (Figure 4.10 (a)). This indicated that the compatibility between PLA and NR was improved when NR-g-GMA was used as compatibilizer. Due to the grafting of GMA onto NR, the polarity of NR is changed and it enhances the compatibility between PLA and NR

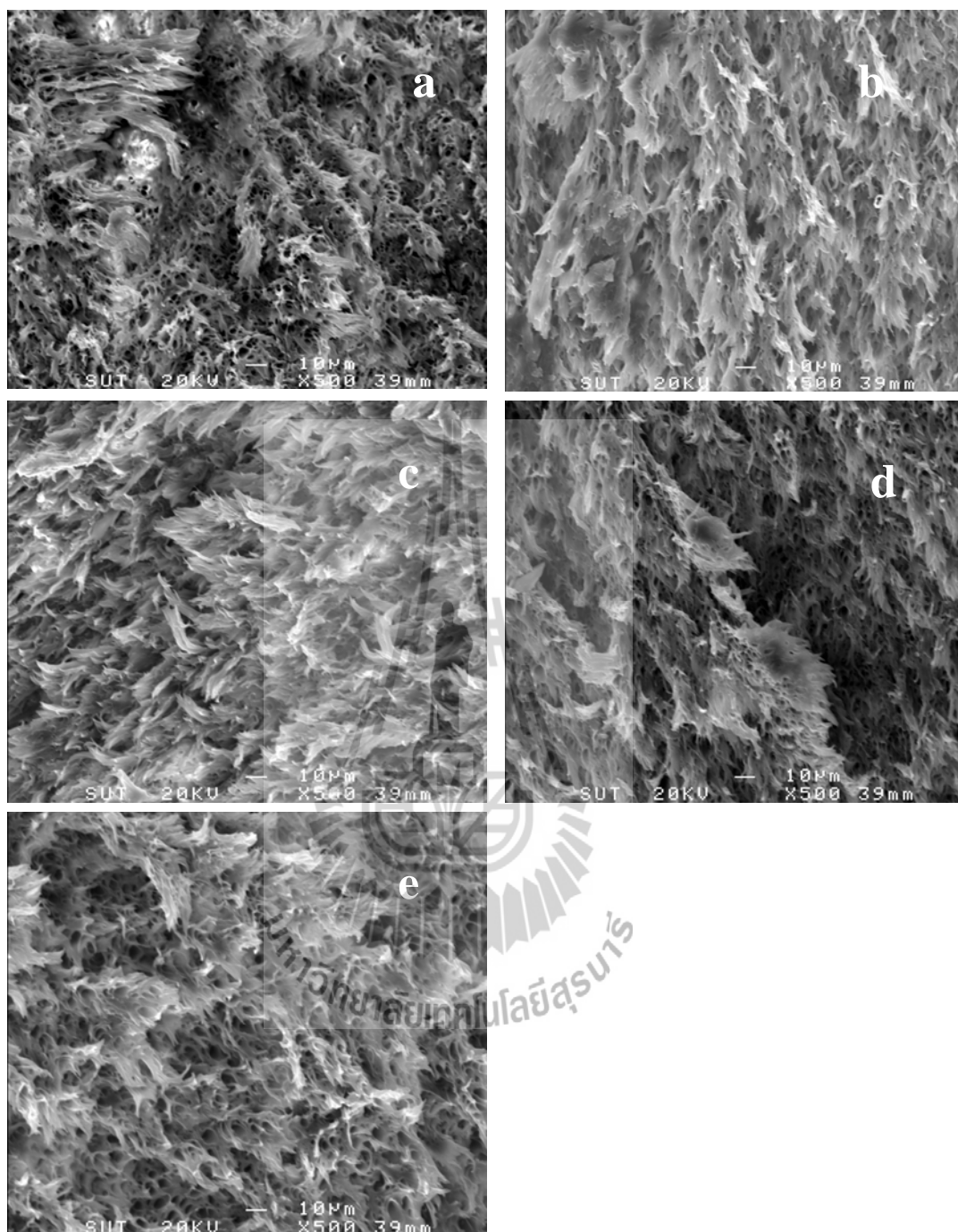
based on the principle of dissolution in a similar material structure. In addition, GMA contains an ester group which is more compatible with PLA. Moreover, the chemical reaction between epoxy group of GMA and carboxyl groups of PLA may occur. The interaction between PLA and NR-g-GMA(C) was investigated by FT-IR spectroscopy as shown in Figure 4.11. PLA shows a band centered at about  $3500\text{ cm}^{-1}$  in the hydroxyl-stretching region, which attributed to the end carboxyl group of PLA. When PLA was mixed with NR-g-GMA to form blends, the peak at  $3500\text{ cm}^{-1}$  disappears. This can be considered that the epoxy group in NR-g-GMA reacted with the carboxyl groups located at the PLA chain ends during melt-mixing. Su, Li, Liu, Hu and Wu (2009) also investigated the chemical reaction between epoxy group of GMA and carboxyl groups of PLA using FT-IR spectroscopy. They found that the peak at  $3504\text{ cm}^{-1}$  of PLA was disappeared after blending PLA with copolymer of GMA. This indicated that the epoxy group of GMA reacted with the carboxyl groups of PLA. This results in the improvement of compatibility between PLA and NR. However, some large domain size of NR was appeared when NR-g-GMA content was increased to 3 and 5% (wt/wt). This may be attributed to the formation of a third phase in the system at high NR-g-GMA content. Figure 4.12 (a-e) shows the tensile fractured surface of PLA/NR blends with NR-g-GMA contents of 0.2-5% (wt/wt). It was observed that the elongated fibrils of PLA/NR blend with NR-g-GMA were longer than that of PLA/NR blend without NR-g-GMA. This confirms that the addition of NR-g-GMA improved toughness of PLA/NR blend.



**Figure 4.10** SEM micrographs of impact fractured surface of PLA/NR (90/10) (a), PLA/NR/ NR-g-GMA (B) (90/9.8/0.2) (b), PLA/NR/NR-g-GMA (B) (90/9/1) (c), PLA/NR/NR-g-GMA (B) (90/7/3) (d) and PLA/NR/ NR-g-GMA (B) (90/5/5) (e).

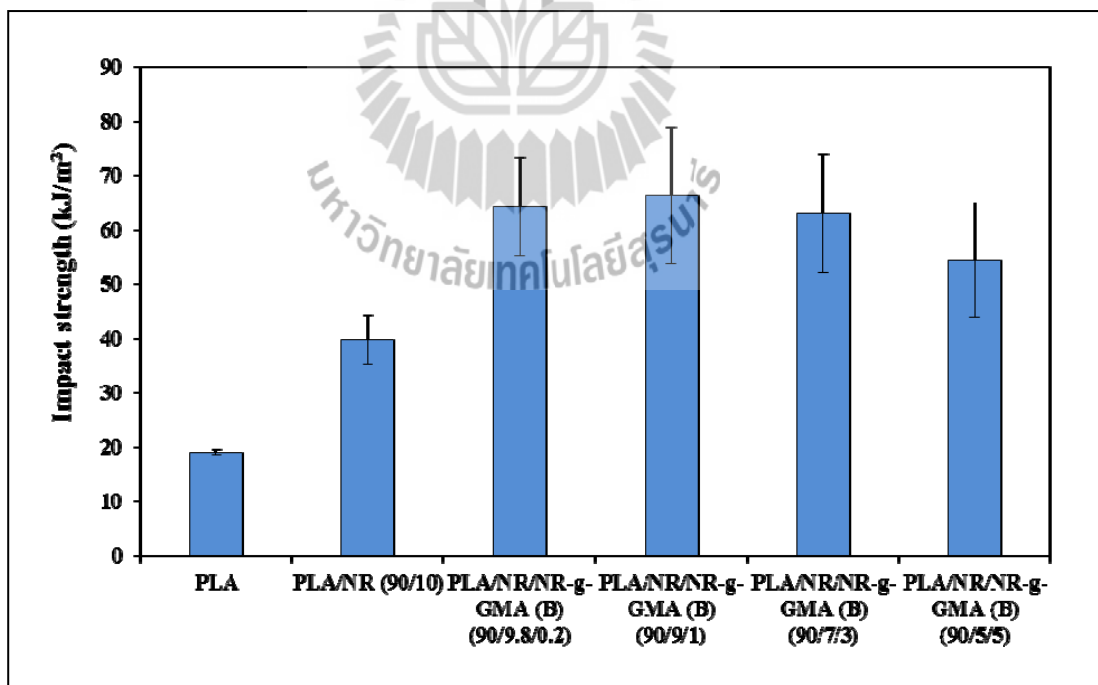


**Figure 4.11** FT-IR spectra of NR, PLA and PLA/NR-g-GMA(C) blend.



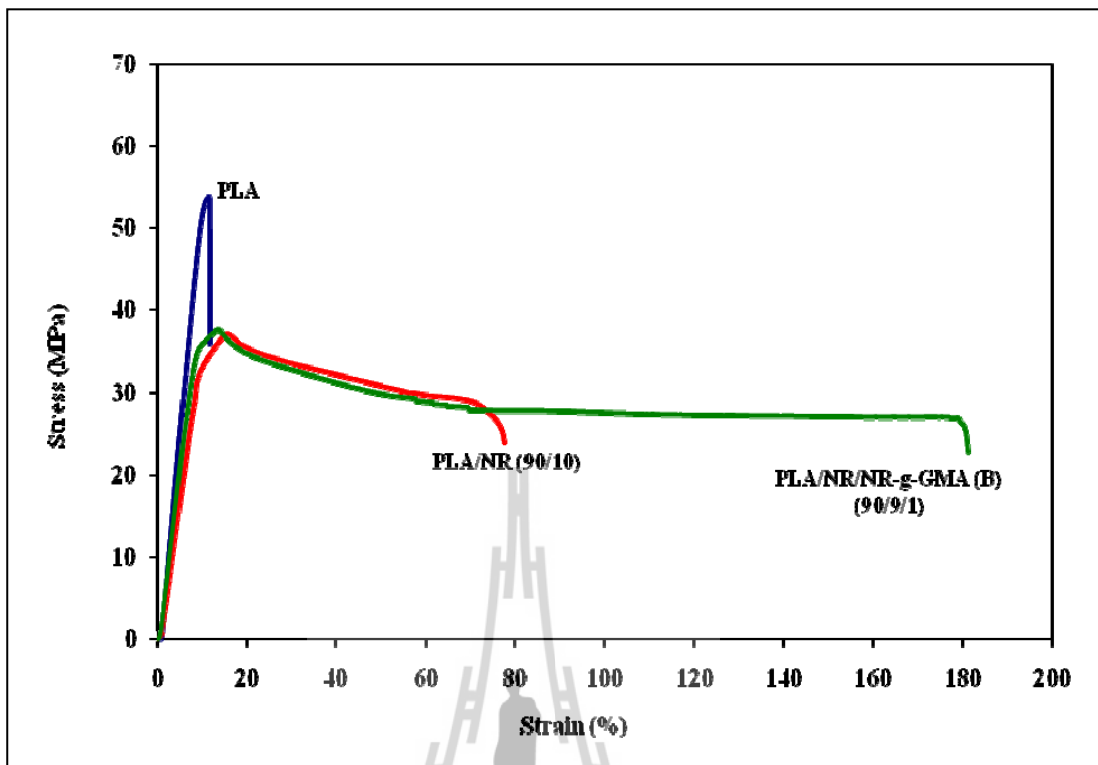
**Figure 4.12** SEM micrographs of tensile fractured surface of PLA/NR (90/10) (a), PLA/NR/ NR-g-GMA (B) (90/9.8/0.2) (b), PLA/NR/NR-g-GMA (B) (90/9/1) (c), PLA/NR/NR-g-GMA (B) (90/7/3) (d) and PLA/NR/ NR-g-GMA (B) (90/5/5) (e).

Figure 4.13 shows the impact strength of PLA, PLA/NR blends at various NR-g-GMA contents. The impact strength of PLA/NR blends increased dramatically with increasing NR-g-GMA content to 1% (wt/wt). The impact strength of PLA/NR blend with NR-g-GMA content of 1 % was 66.36 kJ/m<sup>2</sup>, which is about 3.5 times higher than that of neat PLA. In contrast, the impact strength of PLA/NR blends without NR-g-GMA was only about 2 times higher than that of neat PLA. This is the result from an improvement in compatibility between PLA and NR via reactive blending as explained earlier. With increasing NR-g-GMA content to 3 and 5% (wt/wt), impact strength of PLA/NR blends was slightly decreased to 62.99 and 54.28 kJ/m<sup>2</sup>, respectively. However, these values were still higher than that of neat PLA and PLA/NR blend without NR-g-GMA.



**Figure 4.13** Impact strength of PLA, PLA/NR (90/10) and PLA/NR/NR-g-GMA at various NR-g-GMA contents.

Tensile stress-strain curves of neat PLA and PLA blends are shown in Figure 4.14. The result showed that type of fracture of neat PLA is brittle fracture. PLA/NR blend exhibited plastic flow and higher elongation at break compared to that of neat PLA. This indicated that PLA/NR blend was soft and ductile. Effects of NR-g-GMA content on mechanical properties of PLA/NR blend are illustrated in Table 4.6. Elongation at break PLA/NR blend increased up to 179.37% with increasing NR-g-GMA content up to 1% (wt/wt), which is 2.5 times higher than that of PLA/NR blend without NR-g-GMA (74.51%). The ductility of this material was clearly much higher than that of neat PLA and PLA/NR blends without NR-g-GMA. Elongation at break of PLA/NR blends decreased with increasing NR-g-GMA content to 3 and 5% (wt/wt). However, it was still higher than PLA/NR blend without NR-g-GMA. Modulus of PLA/NR blends insignificantly change compared to PLA/NR blend without NR-g-GMA. The decrease in elongation at break of PLA/NR at high NR-g-GMA content might be due to the appearance of some large domain size as previously shown by SEM micrographs.



**Figure 4.14** Tensile stress–strain curves of PLA, PLA/NR (90/10) and PLA/NR/NR-g-GMA (B) (90/9/1).

**Table 4.6** Tensile strength, modulus and elongation at break of PLA, PLA/NR (90/10) and PLA/NR/NR-g-GMA at various NR-g-GMA contents.

<b>Samples</b>	<b>Tensile strength (Mpa)</b>	<b>Elongation at break (%)</b>	<b>Modulus (Gpa)</b>
PLA	52.99±0.65	10.84±1.64	0.63±0.04
PLA/NR(90/10)	29.66±1.56	74.51±9.06	0.51±0.04
PLA/NR/NR-g-GMA (B) (90/9.8/0.2)	28.78±1.80	165.14±19.03	0.51±0.03
PLA/NR/NR-g-GMA (B) (90/9/1)	27.56±1.35	179.37±21.27	0.50±0.02
PLA/NR/NR-g-GMA (B) (90/7/3)	27.02±0.80	161.40±18.46	0.52±0.04
PLA/NR/NR-g-GMA (B) (90/5/5)	26.34±1.60	123.57±7.91	0.54±0.03

#### **4.4.5 Effect of %grafting of NR-g-GMA on morphological and mechanical properties of PLA/NR blend**

Figure 4.15 (a-e) shows SEM micrographs of impact fractured surface of PLA/NR with increasing %grafting of NR-g-GMA from 0.76 to 16.7. The domain sizes of NR at %grafting of 2.30 (Figure 4.15 C) were much smaller than that of PLA/NR (90/10) (Figure 4.15 (a)). However, at %grafting of 8.4 and 16.7 (Figure 4.15 (e and f)), the domain sizes of NR were larger than that of at %grafting of 2.30 (Figure 4.15 (c)). Tensile fractured surface of PLA/NR blends with increasing %grafting of NR-g-GMA is shown in Figure 4.16 (a-e). It was found that elongated fibrils of PLA/NR blend with NR-g-GMA at high %grafting were shorter than those of PLA/NR blend with NR-g-GMA at low %grafting (%grafting 0.76 and 2.30). Polyglycidyl methacrylate (PGMA) is a hard and brittle polymer. By grafting GMA onto NR the hardness of NR was increased. This is due to the restriction of molecular chain movement of NR caused by GMA. Moreover, as mentioned in Chapter 3, the hardness of NR-g-GMA increased with increasing %grafting of NR-g-GMA. This made it difficult to disperse in PLA matrix at mixing condition used in this work, so the large domain sizes of NR occurred at high %grafting of NR-g-GMA.

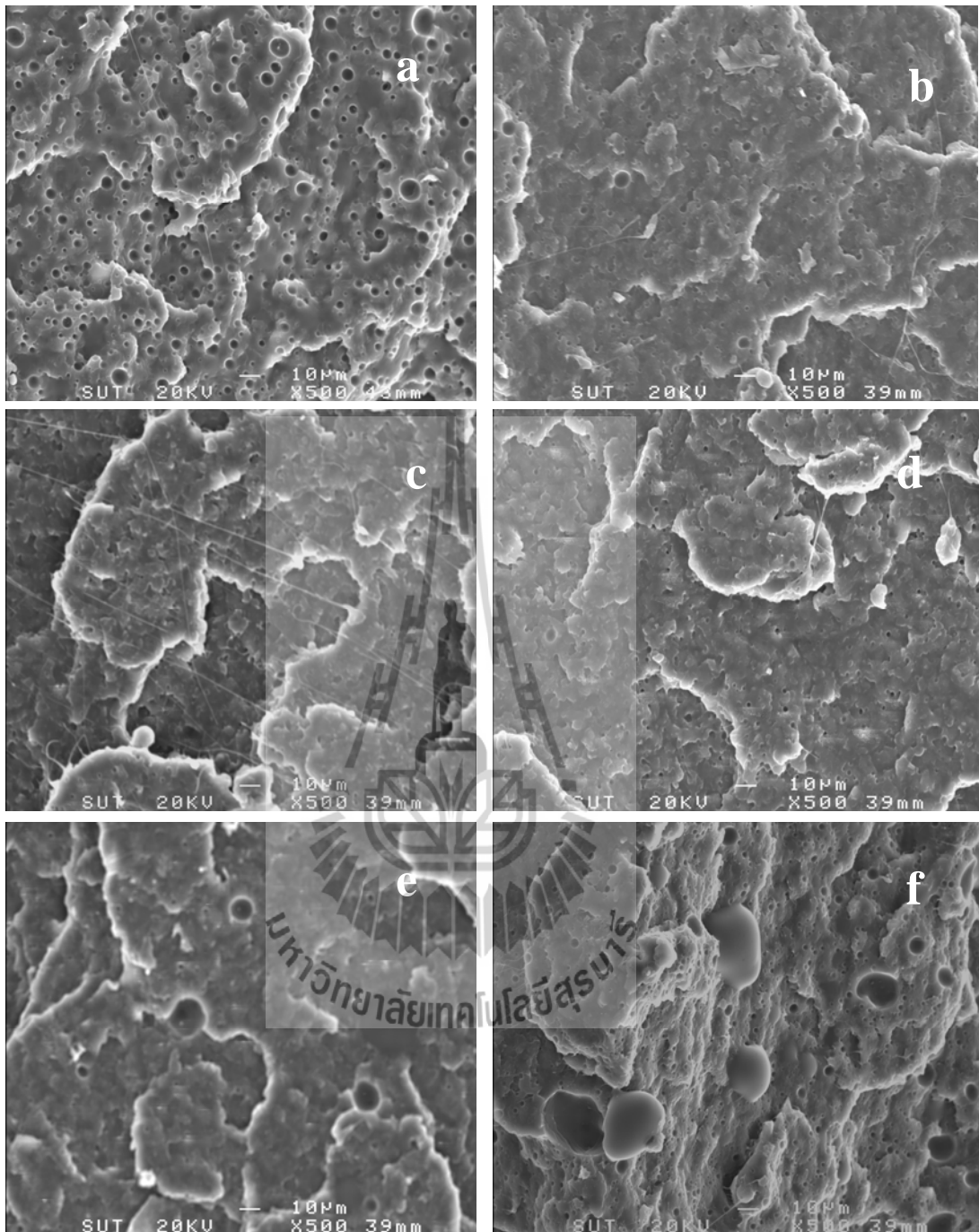


**Figure 4.15** SEM micrographs of impact fractured surface of PLA/NR (90/10) (a), PLA/NR/NR-g-GMA(A) (90/9/1) (b), PLA/NR /NR-g-GMA (B) (90/9/1) (c), PLA/NR/NR-g-GMA (C) (90/9/1) (d), PLA/NR/NR-g-GMA (D) (90/9/1) (e) and PLA/NR/NR-g-GMA (E) (90/9/1) (f).

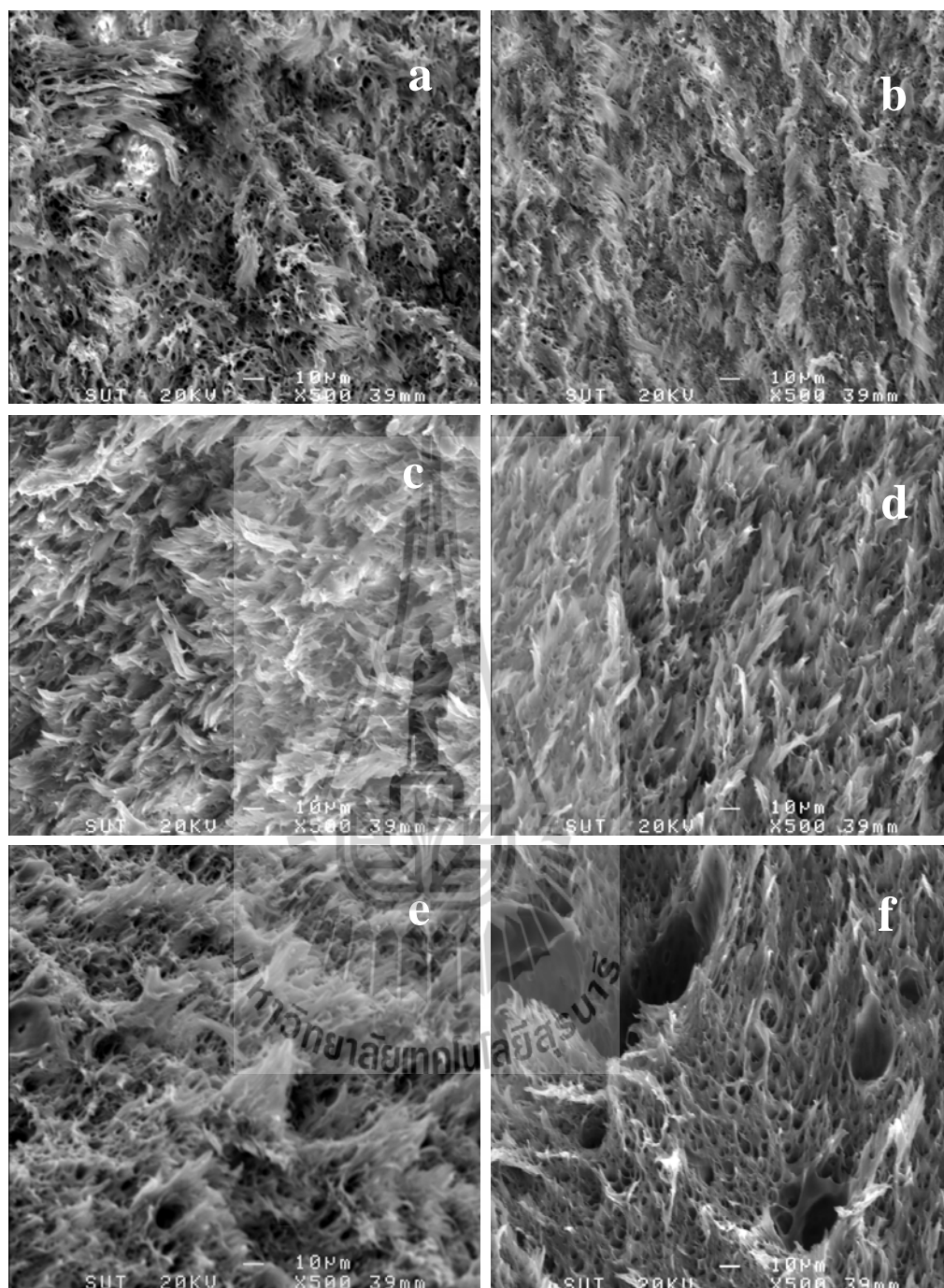


**Figure 4.16** SEM micrographs of tensile fractured surface of PLA/NR (90/10) (a), PLA/NR/NR-g-GMA (A) (90/9/1) (b), PLA/NR /NR-g-GMA (B) (90/9/1) (c), PLA/NR/NR-g-GMA (C) (90/9/1) (d), PLA/NR/NR-g-GMA (D) (90/9/1) (e) and PLA/NR/NR-g-GMA (E) (90/9/1) (f).

The impact strength of PLA, PLA/NR blends with NR-g-GMA at various %grafting is shown in Figure 4.17. Impact strength of PLA/NR blends was increased to 66.36 kJ/m<sup>2</sup> with increasing %grafting of NR-g-GMA to 2.30. When %grafting of NR-g-GMA was increased to 4.35 impact strength was decreased to 54.24 kJ/m<sup>2</sup>. This value was still higher than that of PLA/NR blend without NR-g-GMA. When %grafting of NR-g-GMA was increased to 16.7, impact strength was decreased to 29.46 kJ/m<sup>2</sup>. This value was much lower than that of PLA/NR blend without NR-g-GMA. The domain sizes of NR at high %grafting of NR-g-GMA were much larger than at low %grafting. Also poor distribution of NR particles can be observed. These caused the decrease in impact strength of PLA/NR/NR-g-GMA at high %grafting of NR-g-GMA. From this result, it can be suggested that NR-g-GMA exhibits compatibilization effect when using at low %grafting. Comparisons between mechanical properties of PLA, PLA/NR (90/10) and PLA/NR/NR-g-GMA at various %grafting of NR-g-GMA are shown in Table 4.7. It was observed that elongation at break of PLA/NR blends increased to 179.37 % for the blend containing NR-g-GMA with %grafting of 2.30 without significant loss in tensile strength and modulus. However, with increasing %grafting of NR-g-GMA in PLA/NR blend to 4.35, 8.40 and 16.7 the elongation at break of the blend was decreased. This might be attributed to the large domain sizes of NR at high %grafting which initiates the localized micro-damages. Consequently, the reduction of elongation at break at high %grafting of NR-g-GMA was observed.

Furthermore, it was found that PLA/NR blend with NR-g-GMA can be used to produce commercial blown film using commercial blown film extruder. Blown films of PLA/NR/NR-g-GMA was performed on a blown film extrusion

machine (ILIE Plastic, EP-HA 45 mm) at the temperature range of 150-170°C. Figure 4.18 shows the pictures of PLA/NR/NR-g-GMA film. It was found that a stable film bubble is formed and film gauge can be controlled. The film with the thickness of 15-20 micrometers was shown to be transparent.

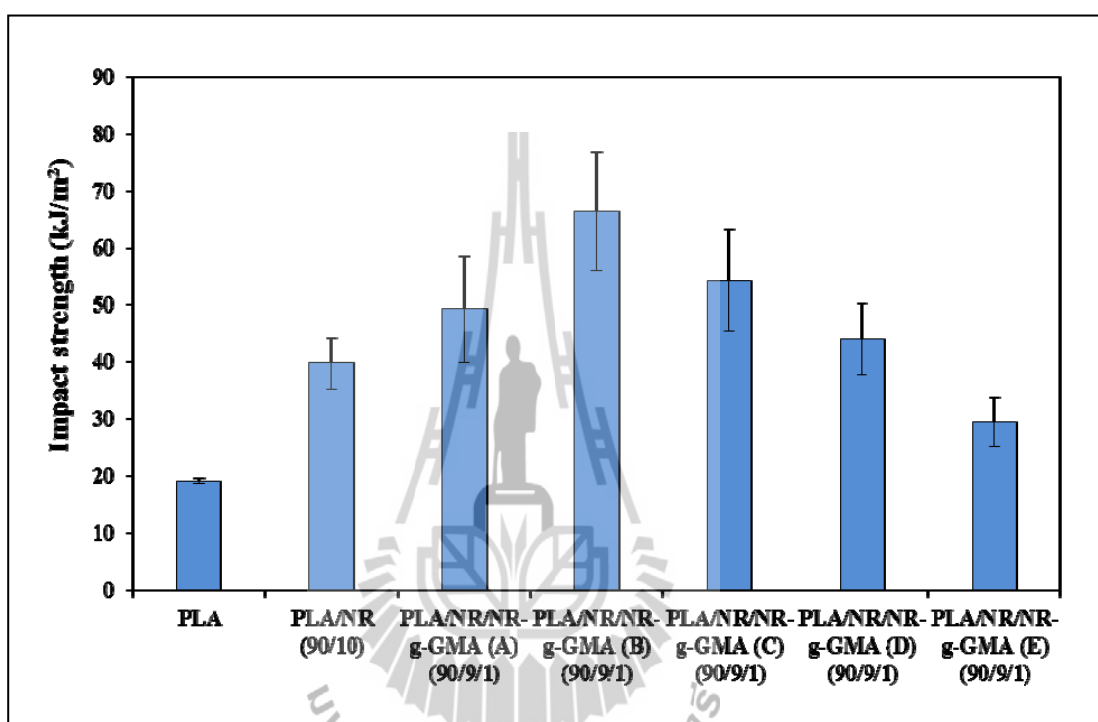


**Figure 4.17** Impact strength of PLA, PLA/NR (90/10) and PLA/NR/NR-g-GMA at various %grafting of NR-g-GMA.

**Table 4.7** Tensile strength, modulus and elongation at break of PLA, PLA/NR (90/10) and PLA/NR/NR-g-GMA at various %grafting of NR-g-GMA.

<b>Samples</b>	<b>Tensile strength (Mpa)</b>	<b>Elongation at break (%)</b>	<b>Modulus (Gpa)</b>
PLA	52.99±0.65	10.84±1.64	0.63±0.04
PLA/NR (90/10)	29.66±1.56	74.51±9.06	0.51±0.04
PLA/NR/NR-g-GMA (A) (90/9/1)	27.41±0.70	82.09±10.00	0.51±0.10
PLA/NR/NR-g-GMA (B) (90/9/1)	27.56±1.35	179.37±21.27	0.50±0.02
PLA/NR/NR-g-GMA (C) (90/9/1)	27.46±0.66	159.08±21.27	0.53±0.02
PLA/NR/NR-g-GMA (D) (90/9/1)	28.53±1.68	86.79±18.87	0.50±0.06
PLA/NR/NR-g-GMA (E) (90/9/1)	29.49±1.95	52.35±6.74	0.51±0.03



**Figure 4.18** Pictures of PLA/NR/NR-g-GMA film.

#### 4.5 Conclusions

NR-g-GMA was shown to be an effective compatibilizer for PLA/NR blend. From FT-IR results, it was confirmed that the epoxy group in NR-g-GMA can react with the carboxyl groups of PLA chain ends during blending. This results in improved compatibility between PLA and NR. With the addition of NR-g-GMA, better dispersion and distribution of NR in PLA matrix can be observed by SEM micrographs. This led to a significant increase in impact strength and elongation at break without significantly loss in tensile strength and modulus of PLA/NR blend with NR-g-GMA. Moreover, an increase in thermal stability of PLA/NR when using NR-g-GMA as compatibilizer was observed. The effects of content and %grafting of NR-g-GMA on mechanical properties of PLA/NR blend were elucidated. With

increasing NR-g-GMA content up to 1% (wt/wt), impact strength and elongation at break of PLA/NR blend increased about 2 times and 2.5 times, respectively. Moreover, with increasing %grafting of NR-g-GMA up to 2.3, the impact strength and elongation at break of PLA/NR/NR-g-GMA were increased. The degree of crystallinity ( $%X_C$ ) of PLA/NR blends with and without NR-g-GMA was lower than that of neat PLA. This could be due to the fact that the addition of NR in PLA may hinder the migration and diffusion of PLA molecular chains to the surface of the nucleus in the blends.

#### 4.6 References

- Asaletha, A., Kumaran, M.G., and Thomus, S. (1999). Thermoplastic elastomers from blends of polystyrene and natural rubber: morphology and mechanical properties. **Euro. Polym. J.** 35: 253-271.
- Broz, M. E., Vanderhart, D. L., and Washburn, N. R. (2003). Structure and mechanical properties of poly (D,L-lactic acid)/poly ( $\epsilon$ -caprolactone) blends. **Biomaterials.** 24: 4181-4190.
- Carone Jr, E., Kopcak, U., Goncalves, M. C., and Nunes, S. P. (2000). In situ compatibilization of polyamide6/natural rubber blends with maleic anhydride. **Polymer.** 41: 5929-5935.
- Carvalho, A.J.F., Job, A.E., Alves, N., Curvelo, A. A. S., and Gandini, A. (2003). Thermoplastic starch/natural rubber blends. **Carbohydr. Polym.** 53: 95-99.

- Chen, C. C., Chueh, J. Y., Tseng, H., Huang, H. M., and Lee, S. Y. (2003). Preparation and characterization of biodegradable PLA polymeric blends. **Biomaterials**. 24: 1167-1173.
- Chen, L., Qiu, X., Xie, Z., Hong, Z., Sun, J., Chen, X., and Jing, X. (2006). Poly (L-lactide)/starch blends compatibilized with Poly (L-lactide)-g-starch copolymer. **Carbohydr. Polym.** 65: 75-80.
- Cheung, H.-Y., Lau, K.-T., Tao, X.-M., and Hui, D. (2008). A potential material for tissue engineering: Silkworm silk/PLA biocomposite. **Comp. Part B: Eng.** 39: 1026-1033.
- Chuayjuljit, S., Moolsin, S., and Potiyaraj, P. (2005). Use of natural rubber-g-polystyrene as a compatibilizer in casting natural rubber/polystyrene blend films. **J. Appl. Polym. Sci.** 95: 826-831.
- Coltelli, M. B., Bronco, S., and Chinea, C. (2010). The effect of free radical reactions on structure and properties of poly (lactic acid) (PLA) based blends. **Polym. Degrad. Stab.** 95: 332-341.
- Dahlan, H. M., Khairul Zaman, M. D., and Ibrahim, A. (2002). The morphology and thermal properties of liquid natural rubber (LNR)-compatibilized 60/40 NR/LLDPE blends. **Polym. Test.** 21: 905-911.
- Feijoo, J. L., Cabedo, L., Gim, E., Lagaron, J. M., and Saura, J. J. (2005). Development of amorphous PLA-montmorillonite nanocomposites. **J. Mater. Sci. Lett.** 40: 1785-1788.

- Gao, Y., Kong, L., Zhang, L., Gong, Y., Chen, G., Zhao, N., and Zhang, X. (2006). Improvement of mechanical properties of poly(DL-lactide) films by blending of poly (3-hydroxybutyrate-co-3-hydroxyhexanoate). **Euro. Polym. J.** 42: 764-775.
- Girija, B.G., Sailaja, R.R.N., and Giridhar, M. (2005). Thermal degradation and mechanical properties of PET blends. **Polym. Degrad. Stab.** 90: 147-153.
- Gu, S.Y., Zhang, K., Ren, J., and Zhan, H. (2008). Melt rheology of Polylactide/poly (butylenes adipate-co-terephthalate) blends. **Carbohydr. Polym.** 74: 79-85.
- Ho, C.H., Wang, C.H., Lin, C. I., and Lee, Y. D. (2008). Synthesis and characterization of TPO-PLA and its behavior as compatibilizer for PLA/TPO blends. **Polymer.** 49: 3902-3910.
- Huneault, M. A., and Li, H. (2007). Morphology and properties of compatibilized polylactide/thermoplastic starch blends. **Polymer.** 48: 270-280.
- Li, Y., and Shimizu, H. (2009). Improvement in toughness of poly (L-lactide) (PLLA) through reactive blending with acrylonitrile-butadiene-styrene copolymer (ABS): morphology and properties. **Euro. Polym. J.** 45: 738-746.
- Long, J., Michael, P. W., and Jinwen, Z. (2006). Study of Biodegradable Polylactide/- Poly (butylenes adipate-co-terephthalate) Blends. **Biomacromolecules.** 7:199-207.
- Lunt, J. (1998). Large-scale production, properties and commercial applications of polylactic acid polymers. **Polym. Degrad. Stab.** 59: 145-152.
- Mark, H. F. (1970). **Encyclopedia of Polymer Science and Engineering.** Wiley: NewYork.

- Oh, J.S., Isayev, A. I., and Rogunova, M. A. (2003). Continuous ultrasonic process for insitu compatibilization of polypropylene/natural rubber blends. **Polymer**. 44: 2337-2349.
- Oyama, H. T.( 2009). Super-tough poly (lactic acid) materials: Reactive blending with ethylene copolymer. **Polymer**. 50: 747-775.
- Phinyocheep, P., Saelao, J., and Buzare, J. Y. (2007). Mechanical properties, morphology and molecular characteristics of poly(ethylene terephthalate) toughened by natural rubber. **Polymer**. 48: 5702-5712.
- Pietrasanta, Y., Robin, J. J., Torres, N., and Boutevin, B. (1999). Reactive compatibilization of HDPE/PET blends by glycidyl methacrylate functionalized polyolefins. *Macromol. Chem. Phys.* 200: 142-149.
- Pracella, M., and Chionna, D. (2003). Reactive compatibilization of blends of PET and PP modified by GMA grafting. **Macromol. Symp.** 198: 161-171.
- Rosa, D.S., Guedes, C.G.F., and Bardi, M.A.G. (2007). Evaluation of thermal, mechanical and morphological properties of PCL/CA and PCL/CA/PE-g-GMA blends. **Polym. Test.** 26: 209-215.
- Sarazin, P., Li, G., Orts, W. J., and Favis, B. D. ( 2008). Binary and ternary blends of polylactide, polycaprolactone and thermoplastic starch. **Polymer**. 49: 599-609.
- Shibata, M., Inoue, Y., and Miyoshi, M. (2006). Mechanical properties, morphology, and crystallization behavior of blends of poly (L-lactide) with poly (butylene succinate-co-L-lactate) and poly (butylene succinate). **Polymer**. 47: 3557-3564.

- Su, Z., Li, Q., Liu, Y., Hu, G.H., and Wu, C. (2009). Compatibility and phase structure of binary blends of poly (lactic acid) and glycidyl methacrylate grafted poly(ethylene octane). **Euro. Polym. J.** 45: 2428-2433.
- Todo, M., Park, S.D., Takayama, T., and Arakawa, K. (2007). Fracture micromechanisms of bioabsorbable PLLA/PCL polymer blends. **Eng. Fract. Mech.** 74: 1872-1883.
- Wang, L., Ma, W., Gross, R. A., and McCarthy, S. P. (1998). Reactive compatibilization of biodegradable blends of poly (lactic acid) and poly ( $\epsilon$ -caprolactone). **Polym. Degrad. Stab.** 59: 161-168.
- Wu, D., Zhang, Y., Zhang, M., and Zhou, W. (2008). Phase behavior and its viscoelastic response of polylactide/poly ( $\epsilon$ -caprolactone) blend. **Euro. Polym. J.** 44: 2171-2183.
- Yokohara, T., and Yamaguchi, M. (2008). Structure and properties for biomass-based polyester blends of PLA and PBS. **Euro. Polym. J.** 44: 677-685..
- Zhang, L., Goh, S. H., and Lee, S. Y. (1998). Miscibility and crystallization behaviour of poly (L-lactide)/poly (p-vinylphenol) blends. **Polymer.** 39: 4841-4847.

# **CHAPTER V**

## **EFFECT OF GLYCIDYL METHACRYLATE GRAFTED NATURAL RUBBER ON PHYSICAL PROPERTIES OF PLA/VETIVER/NR COMPOSITES**

### **5.1 Abstract**

Two types of processing method (injection molding and compression molding) were used to prepare PLA and PLA composites. Molecular weight and molecular weight distribution of PLA before and after processing were compared. After processing, molecular weight of PLA was lower. Moreover, after adding vetiver grass fiber into PLA (PLA/vetiver), molecular weight of PLA in PLA/vetiver was lower than that of neat PLA. However, tensile strength of injection molded PLA/vetiver was higher than that of neat PLA. Nevertheless, the impact strength of PLA/vetiver was lower than that of neat PLA. To improve the impact strength of PLA/vetiver, natural rubber (NR) was used to obtain PLA/vetiver/NR. Furthermore, the effect of using glycidyl methacrylate grafted natural rubber (NR-g-GMA) as compatibilizer on mechanical properties of PLA composite was elucidated. The addition of NR and NR-g-GMA in PLA composite led to an increase in impact strength and elongation at break of PLA composites. Comparisons between the

physical properties of PLA and PLA composites prepared from injection molding and compression molding were made.

## 5.2 Introduction

In recent years, the development of biocomposites from biodegradable polymers and natural fibers such as abaca fiber (Teramoto, Urata, Ozawa, and Shibata, 2004), flax fiber (Oksman, Skrifvars, and Selin, 2003) and kenaf fiber (Ochi, 2008) have attracted great interests. This is because they could allow complete degradation in soil or by composting process and do not emit any toxic components. Moreover, it is expected that the addition of natural fibers in biodegradable polymers can lower the price of biodegradable polymers.

Vetiver grass fiber is one of attractive natural fibers that can be used to improve mechanical properties of biodegradable polymers. It is a tropical plant which grows naturally. In Thailand, vetiver grass can be found growing in a wide range of area from highlands to lowlands in various soil conditions. Moreover, Somnuk, Eder, Phinyocheep, Suppakarn, Sutapun, and Ruksakulpiwat (2007) found that vetiver grass fiber can be used to improve mechanical properties of polypropylene (PP).

Nevertheless, the addition of natural fibers into polymer can improve strength and modulus of the composite but the composite still suffers from low toughness. In order to improve toughness of PLA, natural rubber (NR) was shown to be an effective impact modifier for PLA as discussed in previous chapter. However, PLA blend with NR produced by conventional melt-processing usually exhibit poor mechanical properties, mainly due to the poor miscibility between PLA and NR. The miscibility between PLA and NR can be improved by adding compatibilizer. Glycidyl

methacrylate (GMA) grafted polymers are often used as reactive compatibilizer in polyester blends (Sun, Hu, and Lambla, 1996). Therefore, it is expected that the mechanical properties of PLA composite can be improved by using glycidyl methacrylate grafted natural rubber (NR-g-GMA) as a compatibilizer. Compression molding and injection molding were used to prepare specimens. The molecular weight, mechanical properties and morphology of PLA and PLA composites prepared from injection molding and compression molding were compared.

## **5.3 Experimental**

### **5.3.1 Materials**

Thai natural rubber (grade STR 5L) was purchased from Thaihua Latex Co., Ltd. A commercial grade PLA (PLA 4042D) was purchased from NatureWorks LLC. NR-g-GMA was synthesized in our laboratory. The %grafting of NR-g-GMA was fixed at 2.30. The details on synthesis and characterization of the NR-g-GMA were given in Chapter 3. Vetiver grass (*Vetiveria Zizanioides*) was obtained from Chaiyaphum, Thailand. The ages of vetiver grass are around 6–8 months. Sodium hydroxide (NaOH) (laboratory grade) was purchased from Italmar (Thailand) Co., Ltd.

### **5.3.2 Vetiver grass fibers preparation**

To obtain the vetiver grass fiber, vetiver grass was washed by water to get rid of dirt and dried by sunlight for one day. The washed vetiver leaves were ground by a Retsch grinder machine and then sieved into the length of 2 mm. Vetiver grass fiber was firstly washed by water to eliminate dirt and then dried in an oven at 70°C for 24 hours. Vetiver grass fiber, with 2 mm in length and its aspect ratio of 6.15

was modified by heat treatment method. Vetiver grass fiber was dried in an oven at temperature of 180°C for 4 hours.

### 5.3.3 Composites preparation

PLA composites were prepared at various compositions as shown in Table 5.1. Before mixing, PLA was dried in an oven at 70 °C for 4 hours to eliminate moisture. The ratio of PLA to NR was fixed at 90/10 (wt/wt) in order to get the optimum mechanical properties according to previous study (Chapter 4). The ratio of NR-g-GMA to PLA was fixed at 1% (wt/wt). All compositions of each PLA composite were mixed using an internal mixer (Hakke Rheomix, 3000p) at temperature of 170 °C with a rotor speed of 60 rpm for 10 min. In each batch, half of PLA was added first. After PLA was melted (2 minutes), NR and vetiver grass fiber were then added, respectively. Finally, the rest portion of PLA was added. Compression molding machine (LabTech, LP20-B) and injection molding machine (Chuan Lih Fa, CLF 80P) were used to prepare the specimens. The melting temperature of 165 °C and mold temperature of 25 °C were used in both processing methods. For injection molding process, injection speed of 90%, injection pressure of 90% and holding pressure of 50% were used.

**Table 5.1** Composite compositions.

<b>Symbols</b>	<b>PLA (wt%)</b>	<b>Vetiver grass fiber (wt%)</b>	<b>NR (wt%)</b>	<b>NR-g-GMA (wt%)</b>
PLA	100	-	-	-
PLA/vetiver	90	10	-	-
PLA/vetiver/NR	81	10	9	-
PLA/vetiver/NR/NR-g-GMA	81	10	8.1	0.9
PLA/vetiver2/NR/NR-g-GMA	72	20	7.2	0.8
PLA/vetiver3/NR/NR-g-GMA	63	30	6.3	0.7

### 5.3.4 Characterization

#### 5.3.4.1 Gel Permeable Chromatography

The molecular weight of sample was measured at 35 °C by Gel Permeable Chromatography (GPC, Agilent1200) using chloroform as a solvent (a flow rate of 0.5 ml/min) and calibration with polystyrene standards (Polyscience Co.).

#### 5.3.4.2 Mechanical properties

The unnotched Izod impact test was performed according to ASTM D256 using an Atlas testing machine (model BPI). Tensile properties were obtained according to ASTM D638 using an Instron Universal Testing Machine (UTM, model 5565) with a load cell of 5 kN.

#### 5.3.4.3 Morphological property

The morphologies of the impact fractured surfaces and tensile fractured surfaces of compression molded samples were examined using a Scanning Electron Microscope (SEM, model JEOL 6400). The specimens were coated with

gold prior to the examination. Acceleration voltage of 20 kV was used to collect SEM images of the samples.

#### 5.3.4.4 Thermal property

Thermogravimetric analysis (TGA) was performed using a thermo gravimetric analyzer (TGA, Mettler Toledo model TGA/DSC 1) by heating the sample from room temperature to 600 °C at a heating rate of 20 °C/min under a nitrogen atmosphere. The sample with a weight between 5 to 10 mg was used for each run. Differential scanning calorimetry (DSC: Mettler Toledo Version STARe SW 8.1) was used to obtain thermal properties of specimens by heating the specimens from 30 °C to 200 °C at the rate of 5 °C/min (First heating scan). After keeping the specimens at 200 °C for 3 min they were cooled to 30 °C at 5 °C/min. Then they were heated again to 200 °C at 5 °C/min (Second heating scan). The degree of crystallinity,  $\%X_C$ , of PLA composites can be obtained by:

$$\%X_C = \frac{\Delta H_m}{\Delta H_{m0}(\phi_{PLA})} \times 100$$

In which  $\Delta H_m$  was the measured melting enthalpy,  $\Delta H_{m0}$  was the melting enthalpy of purely crystalline sample (93 J/g for PLA) and  $\phi_{PLA}$  was the PLA weight fraction in the composites (Cheung et al., 2008).

#### 5.3.4.5 Rheological property

Shear viscosities at the shear rate range of 10 to 10,000 s<sup>-1</sup> of PLA and PLA composites were measured using the Kayeness capillary rheometer (model D5052m). Melt flow index (MFI) of PLA, PLA/NR blend and PLA composite

were characterized using a melt flow indexer (Kayeness, 4004). All samples were measured at 170 °C with a load of 2.16 kg.

## 5.4 Results and discussion

### 5.4.1 Gel Permeable Chromatography

Table 5.2 shows the weight-average molecular weights ( $\overline{M}_w$ ), the number-average molecular weights ( $\overline{M}_n$ ) and the molecular weight distribution (MWD) of PLA and PLA composite. The results show that  $\overline{M}_w$  and  $\overline{M}_n$  of PLA after processing from both compression molding and injection molding were decreased compared to those of neat PLA. This indicated that PLA was degraded after processing. Moreover, it was found that  $\overline{M}_w$  and  $\overline{M}_n$  of PLA processed by injection molding were lower than those of PLA processed by compression molding. Generally, shear rate in injection molding is much higher than in compression molding. The higher shear rate creates more viscous heating in polymer melt. PLA is very sensitive to heat. When it gets more heat, it could possibly be more degraded. The addition of vetiver grass fiber resulted in a decrease in  $\overline{M}_w$  and  $\overline{M}_n$  of PLA. This may be attributed to the hydroxyl groups in vetiver grass fiber which may induce the degradation of PLA.

**Table 5.2** The weight-average molecular weights ( $\overline{M}_w$ ), the number-average molecular weights ( $\overline{M}_n$ ) and the molecular weight distribution (MWD) of PLA and PLA composites.

Samples	$\overline{M}_w$	$\overline{M}_n$	MWD
PLA (neat)	174096	86773	2.006
PLA (before molding)	150665	63641	2.367
PLA (after compression)	128582	56024	2.295
PLA (after injection)	101690	44813	2.269
PLA/vetiver (after compression)	98995	41459	2.388
PLA/vetiver (after injection)	91601	31448	2.913

#### 5.4.2 Mechanical properties

Figure 5.1, Figure 5.2 and Figure 5.3 show tensile strength, elongation at break and impact strength of PLA and PLA composites prepared by injection molding and compression molding, respectively. It was found that the injection molded PLA showed slightly lower tensile strength, elongation at break and impact strength than compression molded PLA. This might due to the degradation of PLA during injection molding process. This was indicated by the lower molecular weight of injection molded PLA than that of compression molded PLA. With the addition of vetiver grass fiber into PLA, tensile strength of injection molded PLA/vetiver were slightly higher than that of PLA. This is because the tensile strength of vetiver grass fiber (247–723 MPa) is much higher than that of PLA (Ruksakulpiwat, Suppakarn, Sutapun, and Thomthong, 2007). However, compression molded PLA/vetiver showed lower tensile strength than that of PLA. This may caused by the lower molecular

weight of PLA after processing and the non orientation of vetiver grass fiber in PLA/vetiver from compression molding. Generally, there are many factors influencing the tensile strength of fiber reinforced composite. These include the tensile strength of fiber, the orientation of fiber and the interfacial adhesion between fiber and matrix. In this study, it showed that the orientation of fiber in composite played an important role. The higher orientation of vetiver grass fiber along flow direction in injection molding than compression molding led to the higher tensile strength and impact strength of PLA composites from injection molding. However, elongation at break of injection molded PLA composites was lower than that of compression molded PLA composites. This may be due to more degradation of injection molded PLA composite than compression molded PLA composites.

Furthermore, it was observed that elongation at break and impact strength of PLA/vetiver were lower than those of neat PLA prepared from both injection molding and compression molding. This may due to the fact that the addition of vetiver grass fiber was possibly increased the number of void in PLA composites. So these voids were served as a local area for crack initiation and caused the failure at lower stress. With an addition of NR in PLA/vetiver, elongation at break and impact strength of PLA/vetiver/NR from both injection molding and compression molding were improved. Natural rubber (NR) and ethylene propylene diene monomer (EPDM) rubber at various contents were also shown to use as an impact modifier for the natural fiber polypropylene composites (Ruksakulpiwat, Srideea, Suppakarn, and Sutapun, 2009). The composites were prepared by using an injection molding. It was found that the addition of NR or EPDM in natural fiber-PP composite can improve the impact strength and elongation at break of the composites. The PP composites with

EPDM rubber show slightly higher tensile strength and impact strength than the PP composites with NR. However, from this study tensile strength of PLA/vetiver/NR from both injection molding and compression molding were lower than that of PLA/vetiver. When using NR-g-GMA as a compatibilizer in PLA/vetiver/NR, it was observed that elongation at break and impact strength of PLA/vetiver/NR/NR-g-GMA from both injection molding and compression molding were higher than those of PLA/vetiver/NR without significant lost in tensile strength. This indicated that the miscibility of PLA/vetiver/NR can be improved by using NR-g-GMA as a compatibilizer.

To study the effect of vetiver grass fiber content on mechanical properties of PLA composites, fiber content was varied from 10% to 30% (wt/wt) in vetiver grass fiber-PLA composite with NR and using NR-g-GMA as a compatibilizer. With increasing vetiver grass fiber content from 10% (PLA/vetiver/NR/NR-g-GMA) to 20% (PLA/vetiver2/NR/NR-g-GMA), tensile strength of injection molded PLA composite slightly increased. For compression molding, tensile strength as well as elongation at break and impact strength of PLA composite decreased with increasing vetiver grass fiber content. Moreover, it was shown that elongation at break and impact strength of injection molded PLA composites also decreased with increasing vetiver grass fiber content. This may be due to the fact that an increase in vetiver grass fiber content was possibly increased the number of void and agglomeration in PLA composites. So these void and agglomeration were served as a local area for crack initiation and caused the failure at lower stress. Somnuk et.al (2007) also observed this behavior in vetiver grass fiber - PP composite.

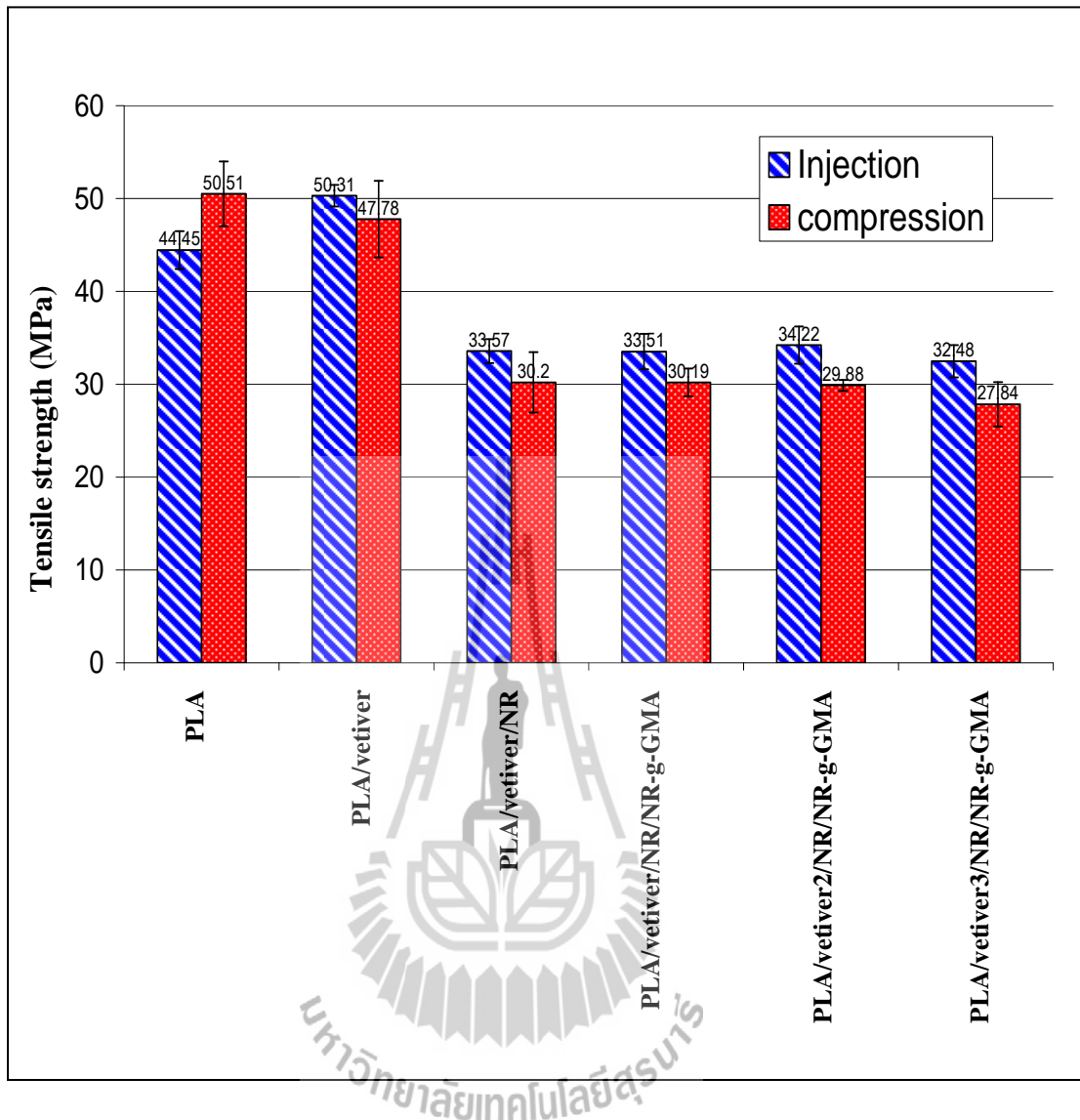


**Figure 5.1** Tensile strength of PLA and PLA composites prepared from different processing methods.

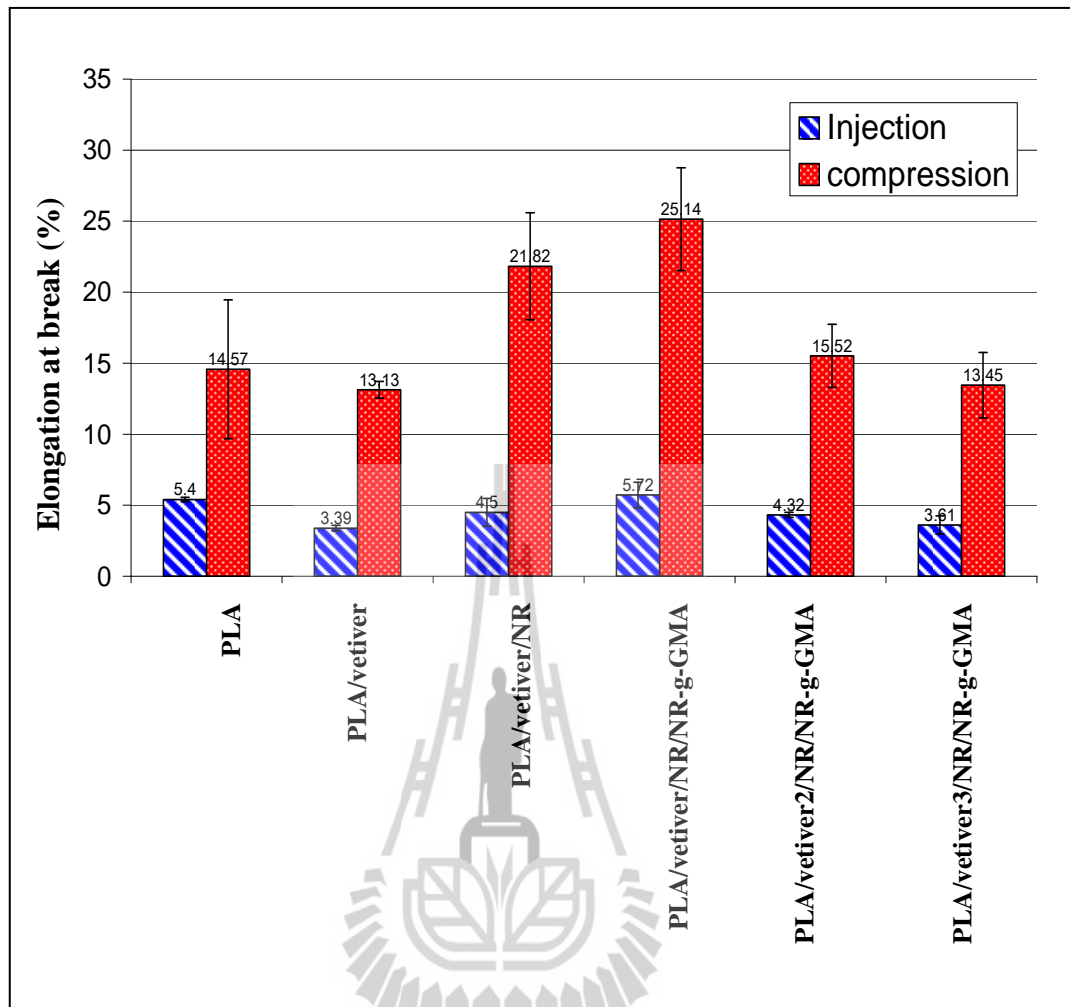


**Figure 5.2** Elongation at break of PLA and PLA composites prepared from different processing methods.

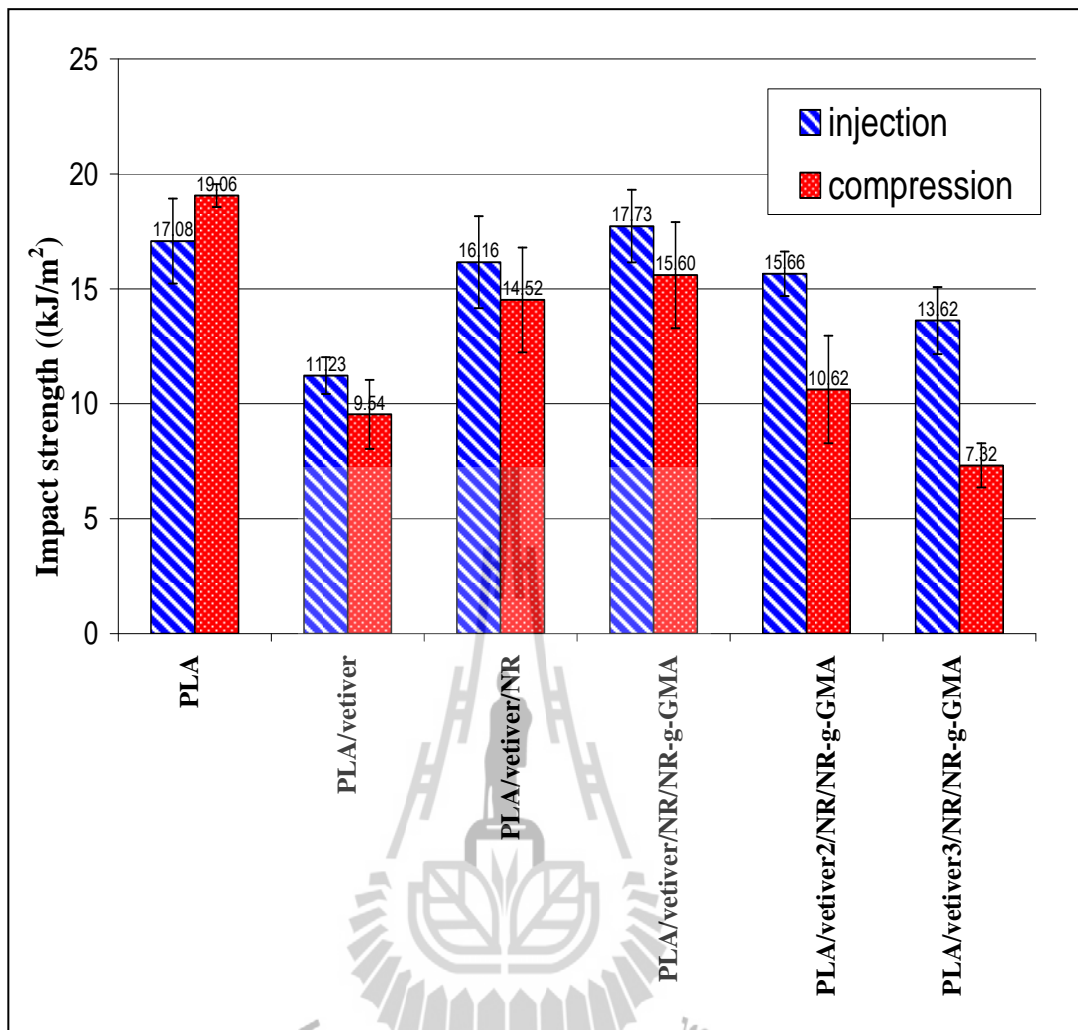


**Figure 5.3** Impact strength of PLA and PLA composites prepared from different processing methods.

### 5.4.3 Morphology

SEM micrographs (500x magnification) of impact fractured surface of PLA and PLA composites prepared by compression molding are shown in Figure.5.4 (a-c). The impact fractured surface of PLA/vetiver/NR (Figure.5.4 (b)) showed the gaps between matrix and vetiver grass fiber. Moreover, the large domain sizes of NR were also observed. This indicated less interfacial adhesion between PLA, vetiver grass fiber, and NR particles. On the other hand, with the addition of NR-g-GMA, the micrograph of PLA/vetiver/NR/NR-g-GMA (Fig.5.4 (c)) shows no gaps between matrix and vetiver grass fiber. Furthermore, the domain sizes of NR in PLA/vetiver/NR/NR-g-GMA were much smaller than that of NR in PLA/vetiver/NR. This indicated the better interfacial adhesion between PLA, vetiver grass fiber, and NR particles.

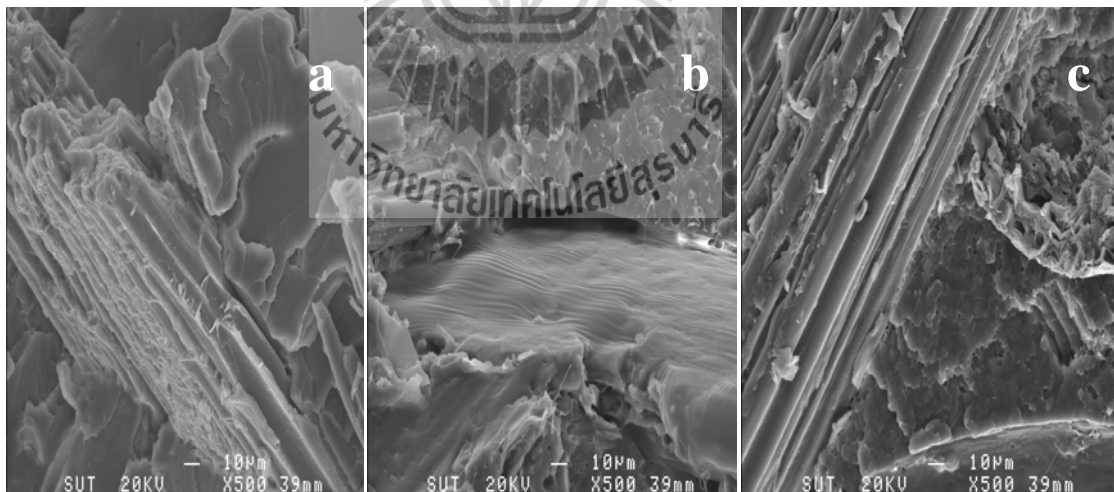


**Figure 5.4** SEM micrographs (500x magnification) of impact fractured surface of PLA/vetiver (a), PLA/vetiver/NR (b) and PLA/vetiver/NR/NR-g-GMA(c) prepared from compression molding.

SEM micrographs (100x magnification) of tensile fractured surface of PLA composites prepared by compression molding and injection molding are shown in Figure 5.5. It can be clearly seen that most of vetiver grass fiber in PLA composites prepared by compression molding were pulled out from the matrix, with the large cavities created. Moreover, vetiver grass fiber in PLA composites from injection molding were more aligned than those from compression molding. This led to higher tensile strength of injection molded PLA composite than that of compression molded PLA composite. The tensile fractured surface of PLA/vetiver/NR showed the gaps between matrix and vetiver grass fiber. This indicated less interfacial adhesion between PLA, vetiver grass fiber, and NR particles. On the other hand, with the addition of NR-g-GMA, the micrograph of PLA/vetiver/NR/NR-g-GMA from both injection molding and compression molding showed the smaller gaps between matrix and vetiver grass fiber. Furthermore, PLA/vetiver/NR/NR-g-GMA shows less vetiver grass fiber pull out compared to PLA/vetiver/NR indicating better interfacial adhesion between PLA, vetiver grass fiber, and NR particles. With increasing vetiver grass fiber content to 20 and 30 %, the agglomeration of vetiver grass fiber can be observed in PLA composites. This resulted in a decrease in mechanical properties of PLA composites with increasing vetiver grass fiber content.

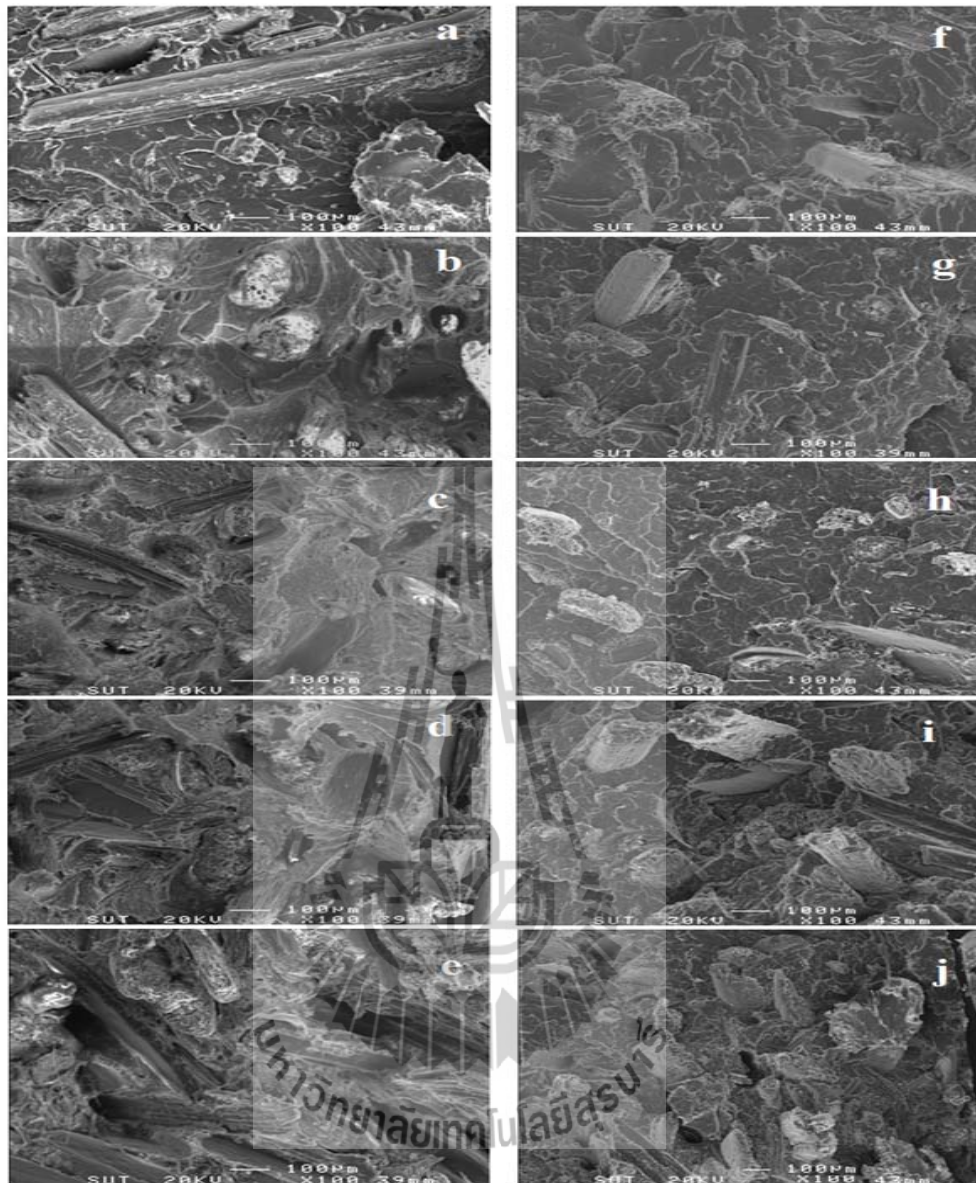


**Figure 5.5** SEM micrographs (100x magnification) of tensile fractured surface of PLA/vetiver (a), PLA/vetiver/NR (b), PLA/vetiver/NR/NR-g-GMA (c), PLA/vetiver2/NR/NR-g-GMA(d) and PLA/vetiver3/NR/NR-g-GMA (e) prepared from compression molding and tensile fractured surface of PLA/vetiver (f), PLA/vetiver/NR (g), PLA/vetiver/NR/NR-g-GMA (h), PLA/vetiver2/NR/NR-g-GMA(i) and PLA/vetiver3/NR/NR-g-GMA (j) prepared from injection molding.

#### 5.4.4 Thermal properties

TGA and DTG curves of PLA, PLA/vetiver, PLA/vetiver/NR and PLA/vetiver/NR/NR-g-GMA are shown in Figure 5.6 and Figure 5.7, respectively. Thermal degradation of PLA and PLA composites showed only single step of weight loss. TGA and DTG thermograms revealed that the onset degradation temperature of PLA composites was lower than that of neat PLA. The onset degradation temperature of PLA/vetiver/NR was higher than PLA/vetiver. The slightly increase in thermal stability of PLA composite with NR has been attributed to the higher thermal stability of NR. Moreover, PLA/vetiver/NR/NR-g-GMA showed higher onset degradation temperatures than that of PLA/vetiver/NR. Figure 5.8 and 5.9 show TGA and DTG curves of PLA and PLA composites at various vetiver grass fiber contents. The experimental result showed that onset degradation temperature of PLA composites decreased with increasing vetiver grass fiber contents due to the low thermal stability of vetiver grass fiber (Somnuk et al., 2007).

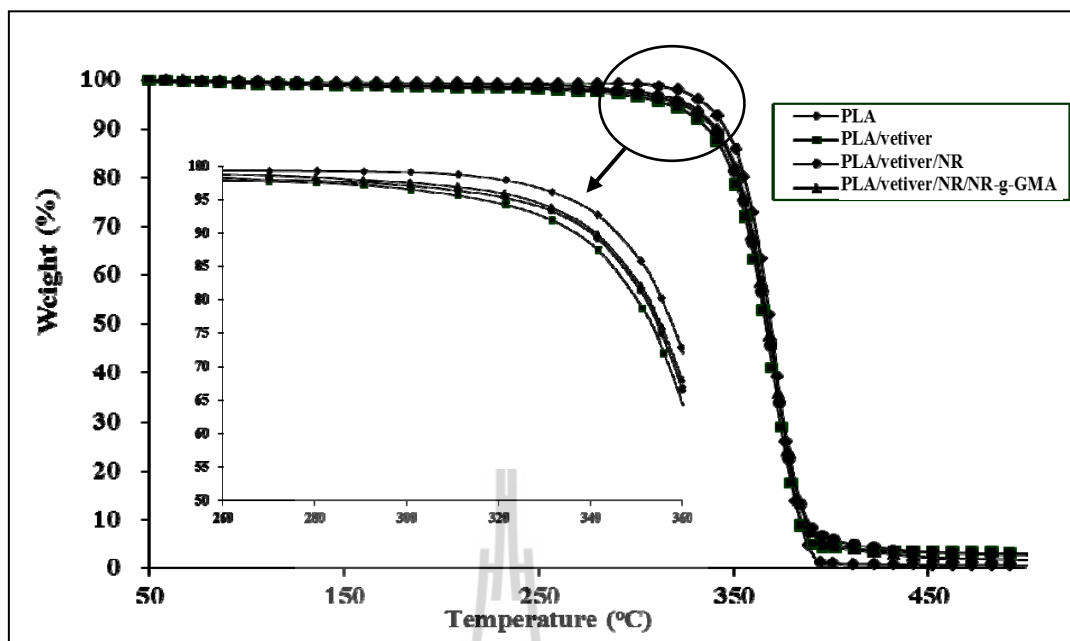


**Figure 5.6** TGA curves of PLA, PLA/vetiver, PLA/vetiver/NR and PLA/vetiver/NR/NR-g-GMA.

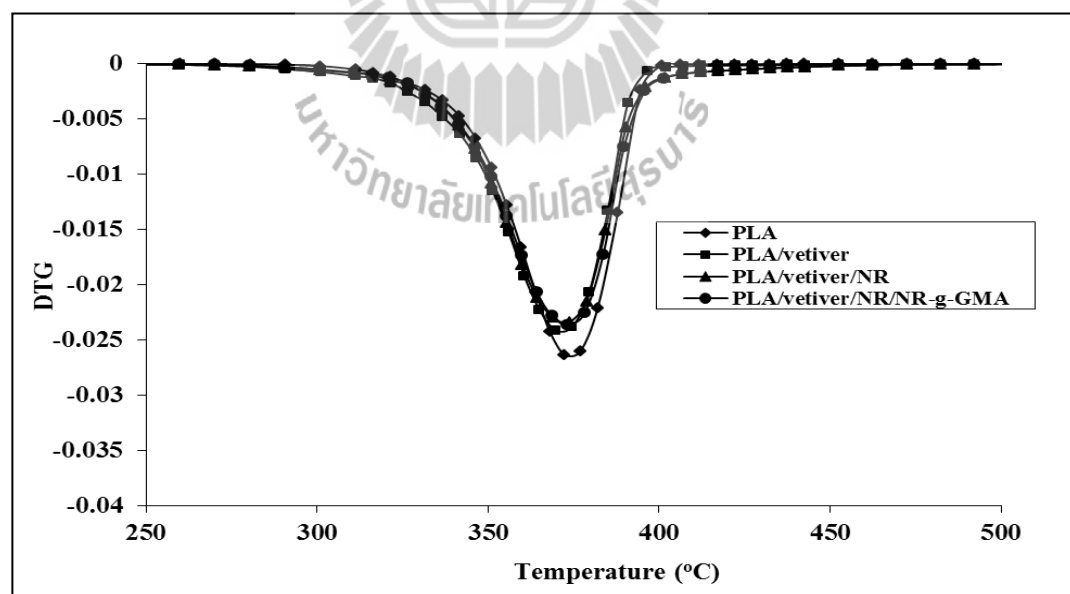


**Figure 5.7** DTG curves of PLA, PLA/vetiver, PLA/vetiver/NR and PLA/vetiver/NR/NR-g-GMA.

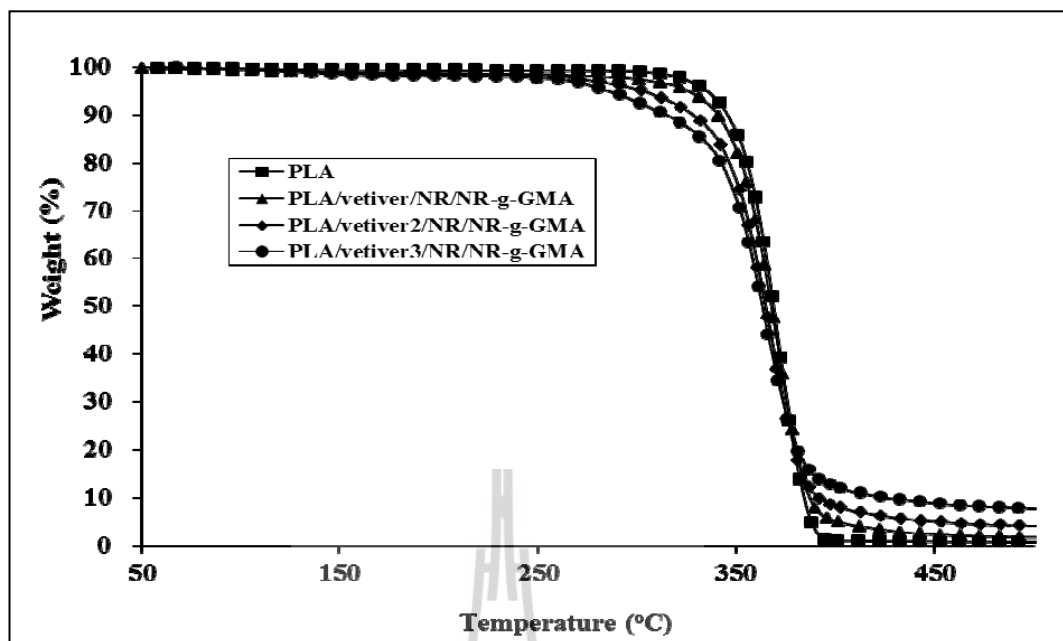


Figure 5.8 TGA curves of PLA, PLA/vetiver/NR/NR-g-GMA, PLA/vetiver2/NR/NR-g-GMA and PLA/vetiver3/NR/NR-g-GMA.

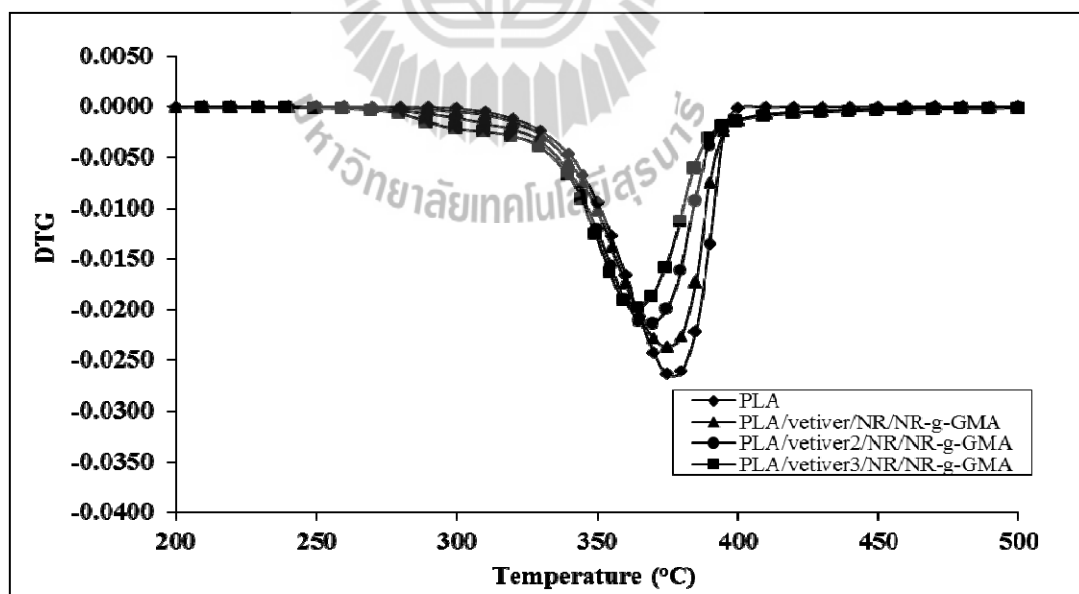
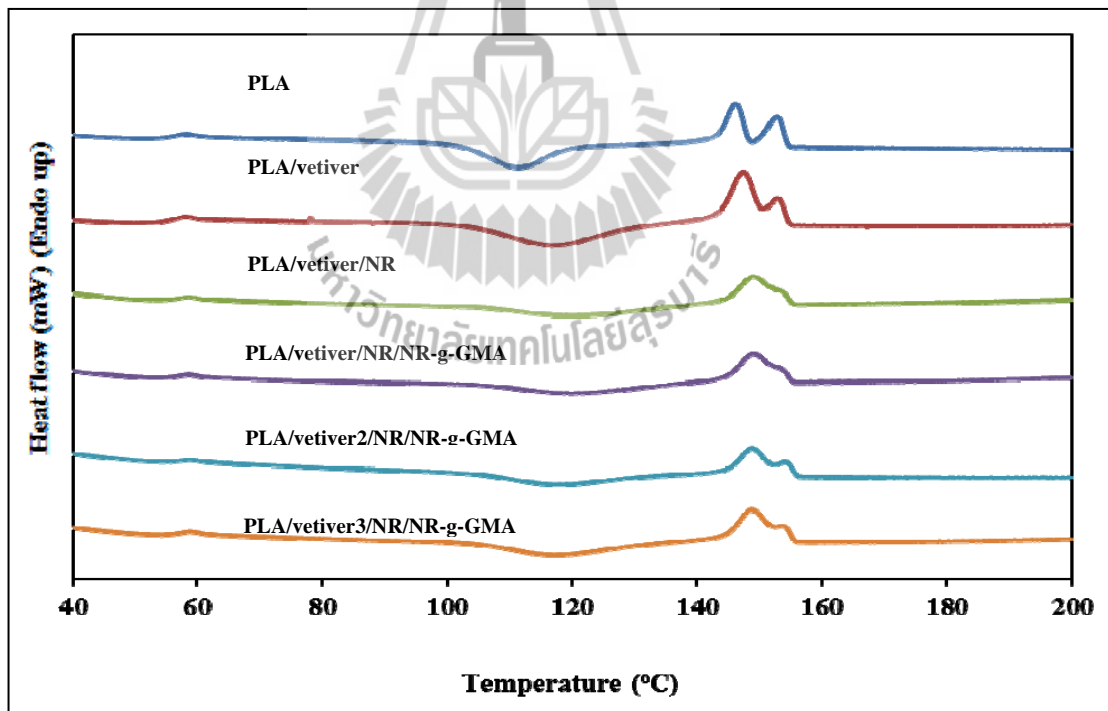


Figure 5.9 DTG curves of PLA, PLA/vetiver/NR/NR-g-GMA, PLA/vetiver2/NR/NR-g-GMA and PLA/vetiver3/NR/NR-g-GMA.

DSC curves of PLA and PLA composites obtained from the second heating scan are shown in Figure 5.10. The glass transition temperature ( $T_g$ ), the crystallization temperature ( $T_c$ ) (indicated by exothermic peak) and melting temperature ( $T_m$ ) (indicated by endothermic peak) of PLA and PLA composites could be observed. From the DSC curves, it was found that  $T_g$  of PLA composites were not changed compared to that of neat PLA.  $T_m$  of PLA composites were shifted to higher temperature compared to that of neat PLA. Moreover, Degree of crystallinity ( $\%X_C$ ) of PLA composites was lower than that of neat PLA (Table 5.3). This could be due to the fact that the addition of vetiver grass fiber in PLA may hinder the migration and diffusion of PLA molecular chains in the composite.



**Figure 5.10** DSC curves of PLA, PLA/vetiver, PLA/vetiver/NR PLA/vetiver/NR /NR-g-GMA, PLA/vetiver2/NR-/NR-g-GMA and PLA/vetiver3/NR/NR-g-GMA.

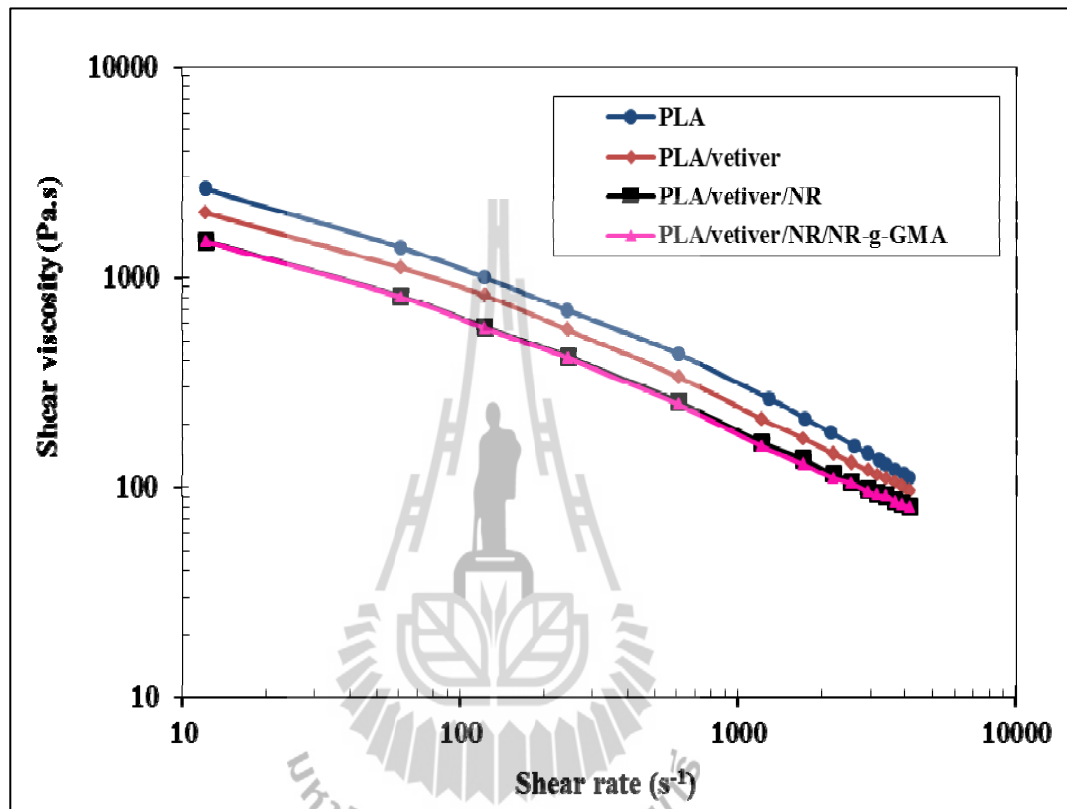
**Table 5.3** T<sub>g</sub>, T<sub>c</sub>, ΔH<sub>c</sub>, T<sub>m</sub>, ΔH<sub>m</sub> and %X<sub>C</sub> of PLA and PLA composites.

Samples	T <sub>g</sub> (°C)	T <sub>c</sub> (°C)	ΔH <sub>c</sub> (J/g)	T <sub>m</sub> (°C)		ΔH <sub>m</sub> (J/g)	%X <sub>C</sub>
				1	2		
PLA	57.3	111.5	30.0	146.0	152.7	29.8	32.1
PLA/vetiver	56.6	116.7	22.2	147.4	-	22.7	27.1
PLA/vetiver/NR	56.5	119.6	19.1	148.8	-	22.3	29.6
PLA/vetiver/NR/NR-g-GMA	56.7	119.3	23.6	149.3	-	21.5	28.3
PLA/vetiver2/NR/NR-g-GMA	57.9	117.8	17.5	148.8	-	18.3	27.3
PLA/vetiver3/NR/NR-g-GMA	58.3	117.3	16.7	148.8		15.9	27.2

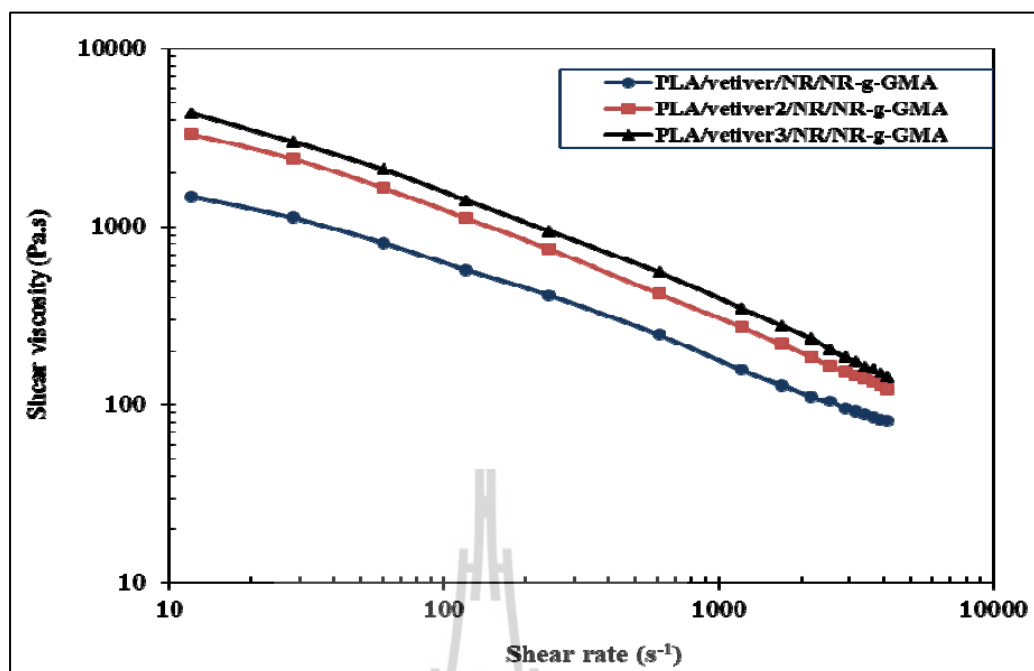
#### 5.4.5 Rheological properties

Figure 5.11 shows shear viscosity of PLA, PLA/vetiver, PLA/vetiver/NR and PLA/vetiver/NR/NR-g-GMA at various shear rates. It revealed that viscosity of PLA/vetiver was considerably lower than that of neat PLA. This may be attributed to the hydroxyl groups in vetiver grass fiber which may induce the degradation of PLA. Moreover, it was found that shear viscosities of PLA/vetiver/NR and PLA/vetiver/NR/NR-g-GMA were quite similar and they were lower than those of PLA/vetiver. Furthermore, it was observed that shear viscosities of PLA/vetiver/NR/NR-g-GMA increase with increasing vetiver grass fiber content (Figure 5.12). Because of the higher content of vetiver fiber, the more perturbed the

normal flow of polymer and the more hindered mobility of chain segments in the melt flow was occurred. Moreover, MFI of the PLA composite with NR-g-GMA decreased with increasing vetiver grass fiber content (as shown in Table 5.4).



**Figure 5.11** Shear viscosity of PLA, PLA/vetiver, PLA/vetiver/NR and PLA/vetiver/NR/NR-g-GMA at various shear rate.



**Figure 5.12** Shear viscosity of PLA/vetiver/NR/NR-g-GMA, PLA/vetiver2/NR/NR-g-GMA and PLA/vetiver3/NR/NR-g-GMA at various shear rate.

**Table 5.4** MFI of PLA and PLA composites.

Samples	MFI(g/10min)	STDEV
PLA	7.21	0.26
PLA/vetiver	8.04	0.50
PLA/vetiver/NR	8.98	0.27
PLA/vetiver/NR/NR-g-GMA	8.98	0.13
PLA/vetiver2/NR/NR-g-GMA	5.65	0.32
PLA/vetiver3/NR/NR-g-GMA	4.37	0.22

## 5.5 Conclusions

Molecular weight of PLA decreased after processing. PLA prepared from injection molding showed lower molecular weight compared to PLA prepared from compression molding. After adding vetiver grass fiber into PLA, molecular weight of PLA from both compression molding and injection molding was lower than that of neat PLA. Injection molded PLA showed lower tensile strength, elongation at break and impact strength. However, it was observed that injection molded PLA composites showed higher tensile strength and impact strength than those of compression molded PLA composites. This is due to the higher orientation of vetiver grass fiber in injection molding than in compression molding as shown in SEM micrographs. The addition of NR led to higher impact strength and elongation at break but lower tensile strength of the composites. NR-g-GMA was shown to be an effective compatibilizer for PLA composites in this study. PLA/vetiver/NR/NR-g-GMA from both injection molding and compression molding showed higher elongation at break and impact strength than PLA/vetiver/NR. With increasing vetiver grass fiber content from 10% to 20%, tensile strength of injection molded PLA composite slightly increased. For compression molded specimens, tensile strength as well as elongation at break and impact strength of PLA composite decreased with increasing vetiver grass fiber content.

## 5.6 References

Cheung, H.-Y., Lau, K.-T., Tao, X.-M., and Hui, D. (2008). A potential material for tissue engineering: Silkworm silk/PLA biocomposite. **Comp. Part B: Eng.** 39: 1026-1033.

- Oksman, K., Skrifvars, M., and Selin, J.F. (2003). Natural fibres as reinforcement in poly(lactic acid (PLA) composites. **Compos. Sci. Technol.** 63:1317-1324.
- Ochi, S. (2008) Mechanical properties of kenaf fibers and kenaf/PLA composites. **Mech. Mater.** 40: 446-452.
- Ruksakulpiwat, Y., Suppakarn, N., Sutapun, W., and Thomthong, W. (2007). Vetiver–Polypropylene Composites: Physical and Mechanical Properties. **Compos. Part A: Appl. Sci. Manufact.** 38: 590-601.
- Ruksakulpiwat, Y., Srideea, J., Suppakarn, N., and Sutapun, W. (2009): Improvement of impact property of natural fiber–polypropylene composite by using natural rubber and EPDM rubber. **Compos. Part B.** 40: 619-622.
- Somnuk, U., Eder, G., Phinyocheep, P., Suppakarn, N., Sutapun, W., and Ruksakulpiwat, Y. (2007). Quiescent crystallization of natural fibers polypropylene composites, **J. Appl. Polym. Sci.** 106:2997-3006.
- Sun, Y.J., Hu, G.H., and Lambla, M. (1996). In situ compatibilization of polypropylene and poly(butylene terephthalate) polymer blends by one-step reactive extrusion. **Polymer.** 37: 4119-4127.
- Teramoto, N., Urata, K., Ozawa, K., and Shibata, M. (2004). Biodegradation of aliphatic polyester composites reinforced by abaca fiber. **Polym. Degrad. Stab.** 86: 401-409.

# CHAPTER VI

## BIODEGRADABILITY

### 6.1 Abstract

In this study, vetiver grass fiber was used as a filler in PLA/NR blend. Glycidyl methacrylate grafted natural rubber (NR-g-GMA) was used as a compatibilizer in the PLA composites. The PLA composites with various ratios of vetiver grass fiber were mixed in an internal mixer. The biodegradability of PLA and PLA composites was evaluated by soil burial test. The effect of vetiver grass fiber on biodegradability and mechanical properties of PLA and PLA composites were studied. It was shown that vetiver grass fiber showed a significant role in the biodegradability of PLA composites. Mechanical properties of PLA composites dramatically decreased after burial in soil compared to those of pure PLA. Moreover, the addition of vetiver grass fiber at 20 and 30% (wt/wt) content led to a significant increase in weight loss of the specimens with increasing burial time.

### 6.2 Introduction

Recently, poly(lactic acid) (PLA) becomes a material of large interest because of its potential biodegradability. However, PLA is very brittle under tensile and bending loads led to restricted applications (Lunt, 1998). In order to improve its property, it is now a common practice to modify PLA by physical blending. For example, PLA was blended with other more flexible polymers such as

polycaprolactone (PCL) (Broz, VanderHart, and Washburn, 2003); (Sarazin, Li, Orts, and Favis, 2008); (Wu, Zhang, Zhang, and Zhou, 2008), polybutylenesuccinate (PBS) (Yokohara, and Yamaguchi, 2008), poly(butylene succinate-co-L-lactate) (PBSL) (Shibata, Inoue, and Miyoshi, 2006) and poly(butylene adipate-co-terephthalate) (PBAT) (Gu, Zhang, Ren, and Zhan, 2008); (Long, Michael, and Jinwen, 2006). From Chapter 4, natural rubber (NR) was used to improve the toughness of PLA. It was shown that with the addition of NR up to 10% (wt/wt), impact strength and elongation at break of the blends dramatically increased. Furthermore, by adding NR-g-GMA as a compatibilizer for PLA/NR blend, the impact strength and elongation at break was significantly increased. This indicated that the miscibility of PLA/NR blends can be improved by using NR-g-GMA as a compatibilizer. However, tensile strength and modulus of PLA/NR blend with and without NR-g-GMA were decreased, which can greatly limit its engineering applications. In order to improve tensile strength of PLA, many studies have been carried out to investigate the addition of natural fibers such as abaca fiber (Teramoto, Urata, Ozawa, and Shibata, 2004), flax fiber (Oksman, Skrifvars, and Selin, 2003) and kenaf fiber (Ochi, 2008). This is because they could allow complete degradation in soil or by composting process and do not emit any toxic components. Moreover, it is expected that the addition of natural fibers in biodegradable polymers can lower the price of biodegradable polymers. Generally, the tensile strength of PLA is greatly improved when reinforced with fibers. Vetiver grass fiber is one of attractive natural fibers to be used as reinforcing filler for polymer composites. It is a tropical plant which grows naturally in various soil conditions. Somnuk et.al found that the addition of vetiver grass fiber in polypropylene (PP) composites greatly improved mechanical properties of PP

composites (Somnuk, Eder, Phinyocheep, Suppakarn, Sutapun, Ruksakulpiwat, 2007); (Ruksakulpiwat, Suppakarn, Sutapun, and Thomthong, 2007). Moreover, it was shown that the addition of vetiver grass fiber in PLA composites can improve mechanical properties of the composites (Chapter 5). In this study, the effect of vetiver grass fiber on biodegradability of PLA composites was elucidated. Comparisons among the biodegradability of commercial PP, commercial PLA, PLA/NR and PLA/NR/vetiver composite were made.

## **6.3 Experimental**

### **6.3.1 Materials**

A commercial grade of PP (PP700J) and a commercial grade of PLA (PLA 4042D) were purchased from Siam Chemical Group Co. Ltd. and NatureWorks LLC, respectively. Thai natural rubber (grade STR 5L) was purchased from Thaihua Latex Co., Ltd. NR-g-GMA with %grafting of 2.30 was synthesized in our laboratory. The details on synthesis and characterization of NR-g-GMA were given in Chapter 3. Vetiver grass fiber, with 2 mm in length and aspect ratio of 6.15 was modified by heat treatment at the temperature of 180°C for 4 hours before mixing.

### **6.3.2 Composites preparation**

PLA blend and PLA composites were prepared at various compositions as shown in Table 6.1. Before mixing, PLA was dried in an oven at 70 °C for 4 hours to eliminate moisture. The ratio of PLA to NR was fixed at 90/10 (wt/wt) in order to get the optimum mechanical properties according to Chapter 4. The ratio of NR-g-GMA to PLA was fixed at 1% (wt/wt). All compositions of each PLA blend and PLA composite were mixed using an internal mixer (Hakke Rheomix,

3000p) at temperature of 170 °C with a rotor speed of 60 rpm for 10 min. Compression molding machine (LabTech, LP20-B) was used to prepare the specimens. The melting temperature of 165 °C and mold temperature of 25 °C were used.

**Table 6.1** Blends and composites composition.

Symbols	PLA (wt%)	NR (wt%)	NR-g-GMA (wt%)	Vetiver grass fiber (wt%)
PLA	100	-	-	-
PLA/NR	90	10	-	-
PLA/NR/NR-g-GMA	90	9	1	-
PLA/vetiver	90	-	-	10
PLA/vetiver/NR	81	9	-	10
PLA/vetiver/NR/NR-g-GMA	81	8.1	0.9	10
PLA/vetiver2/NR/NR-g-GMA	72	7.2	0.8	20
PLA/vetiver3/NR/NR-g-GMA	63	6.3	0.7	30

### 6.3.3 Characterization

#### 6.3.3.1 Biodegradability test

Biodegradability was determined by measuring molecular weight of polymer, weight loss, tensile strength, elongation at break and impact strength of the compression molded specimens buried in soil. Soil used in the test was 1:1 mixture of black soil and leaf mold for gardening. Water was supplied at intervals

of 2 days, and the soil was kept not to be dried. Each specimen was dug out of the soil after the burial for 30, 60, 90, 120, 150, and 180 days, respectively. Obtained specimens were washed with water and dried to a constant weight at 40 °C. The changes in the physical appearance of the specimens were visually observed and recorded using a digital camera, SAMSUNG Digital Camera with four megapixels. The weight loss ( $W_{loss}$ ) was calculated using the formula:

$$W_{loss} = \frac{W_{initial} - W_{final}}{W_{initial}} \times 100$$

Where  $W_{initial}$  and  $W_{final}$  are the weights of specimen before and after burial in soil.

#### **6.3.3.2 Gel Permeable Chromatography**

The polymer molecular weight was measured at 35 °C by Gel Permeable Chromatography (GPC, Agilent1200) using chloroform as solvent (a flow rate of 0.5 ml/min) and calibration with polystyrene standards (Polyscience Co.).

#### **6.3.3.3 Mechanical properties**

Unnotched Izod impact test was performed according to ASTM D256 using an Atlas testing machine (model BPI). Tensile properties were obtained according to ASTM D638 using an Instron universal testing machine (UTM, model 5565) with a load cell of 5 kN.

#### 6.3.3.4 Morphological property

The surface morphology and tensile fractured surface of compression molded and injection molded samples of the samples before and after burial in soil were examined using a scanning electron microscope (SEM, model JEOL 6400). The specimens were coated with gold prior to the examination. Acceleration voltage of 20 kV was used to collect SEM images of the samples.

### 6.4 Results and discussion

Table 6.2 shows the weight-average molecular weights ( $\overline{M}_w$ ), the number-average molecular weights ( $\overline{M}_n$ ) and the molecular weight distribution (MWD) of PLA, PLA blend and PLA composite before and after burial in soil for 180 days. The experimental results show that  $\overline{M}_w$  and  $\overline{M}_n$  of PLA and PLA composite after burial in soil were lower than  $\overline{M}_w$  and  $\overline{M}_n$  of PLA and PLA composite before burial in soil. The decreased molecular weight of PLA may be attributed to the hydrolysis of the aliphatic ester linkage of PLA, as well as to the change of low molecular weight materials such as oligomer and monomer (Ratto, Stenhouse, Auerbach, Mitchell, and Farrell, 1999); (Tserki, Matzinos, and Panayiotou, 2003). This indicated that PLA and PLA composite were degraded after burial in soil.

**Table 6.2** The weight-average molecular weights ( $\overline{M}_w$ ), the number-average molecular weights ( $\overline{M}_n$ ) and the molecular weight distribution (MWD) of PLA and PLA composites before and after burial in soil.

Samples	Before burial in soil			After burial in soil		
	$\overline{M}_w$	$\overline{M}_n$	MWD	$\overline{M}_w$	$\overline{M}_n$	MWD
PLA (neat)	174096	86773	2.006	-	-	-
PLA (before molding)	150665	63641	2.367	-	-	-
PLA (after compression)	128582	56024	2.295	104900	45867	2.287
PLA (after injection)	101690	44813	2.269	98238	44155	2.225
PLA/vetiver (after compression)	98995	41459	2.388	88533	33246	2.663
PLA/vetiver (after injection)	91601	31448	2.913	87153	29318	2.973

The digital camera taken pictures of polypropylene (PP), PLA, PLA/NR, PLA/NR/NR-g-GMA, PLA/vetiver, PLA/vetiver/NR, PLA/vetiver/NR/NR-g-GMA, PLA/vetiver2/NR/NR-g-GMA and PLA/vetiver3/NR/NR-g-GMA before and after burial in soil for 180 days are shown in Figure 6.1. It was found that the color of PP has not changed after burial in soil. The change in color of PLA, PLA blends and PLA composites after burial in soil was clearly observed. Moreover, a lot of fungi can be found on the surface of PLA blends and PLA composites specimens. This

confirmed that PLA, PLA blends and PLA composites can be degraded by bacteria and fungi in the soil environment.

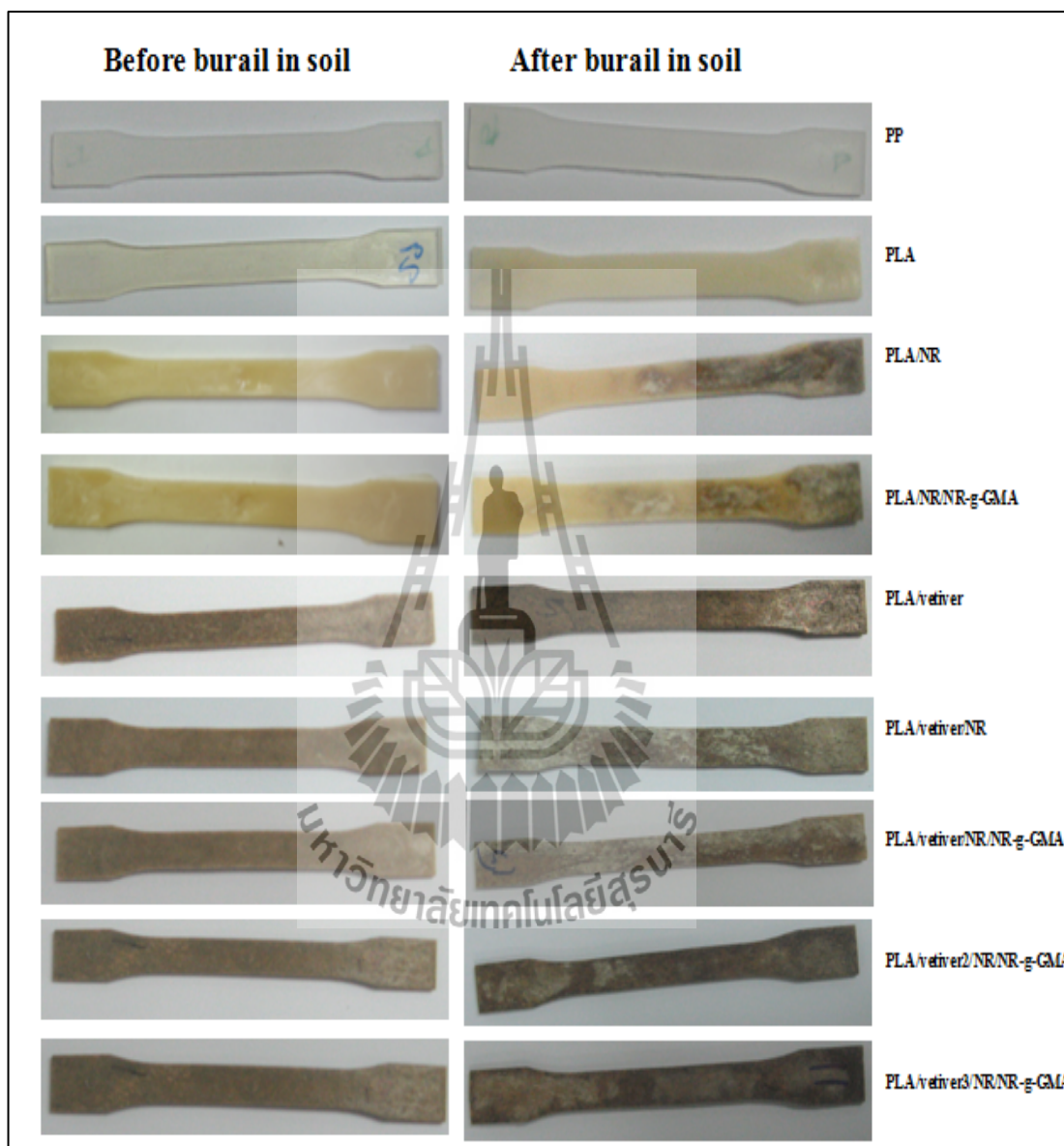
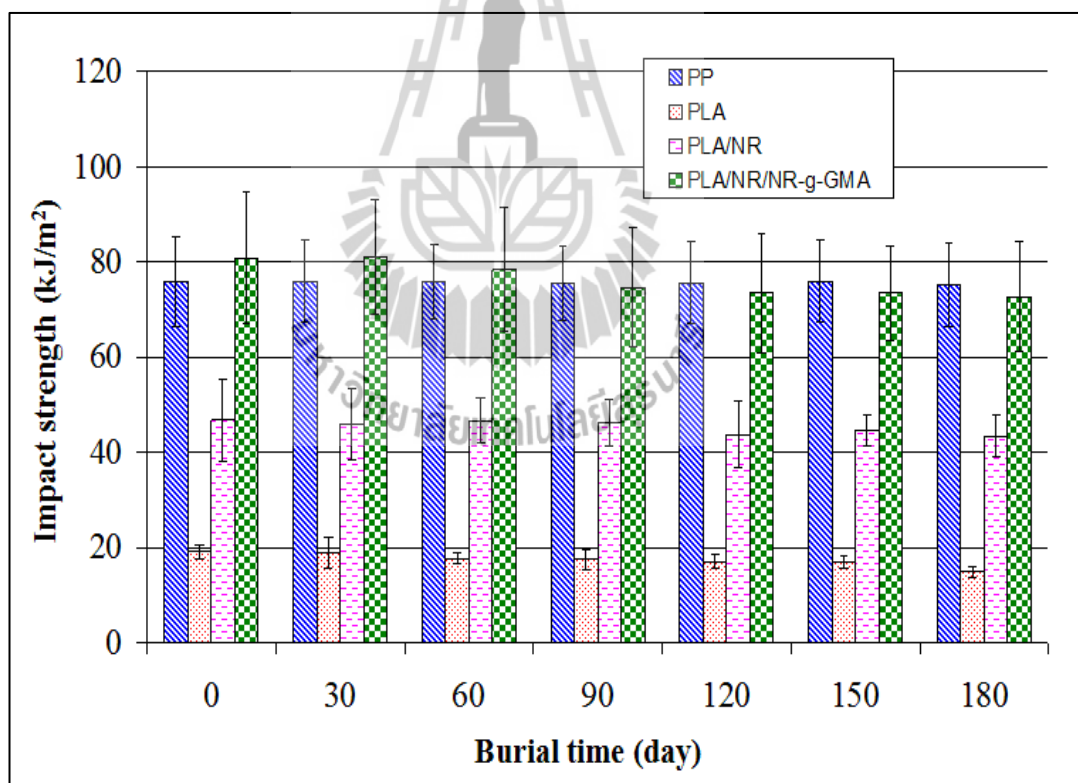


**Figure 6.1** Pictures of PP, PLA, PLA/NR, PLA/NR/NR-g-GMA, PLA/vetiver, PLA/vetiver/NR, PLA/vetiver/NR/NR-g-GMA, PLA/vetiver2/NR/NR-g-GMA and PLA/vetiver3/NR/NR-g-GMA before and after burial in soil for 180 days.

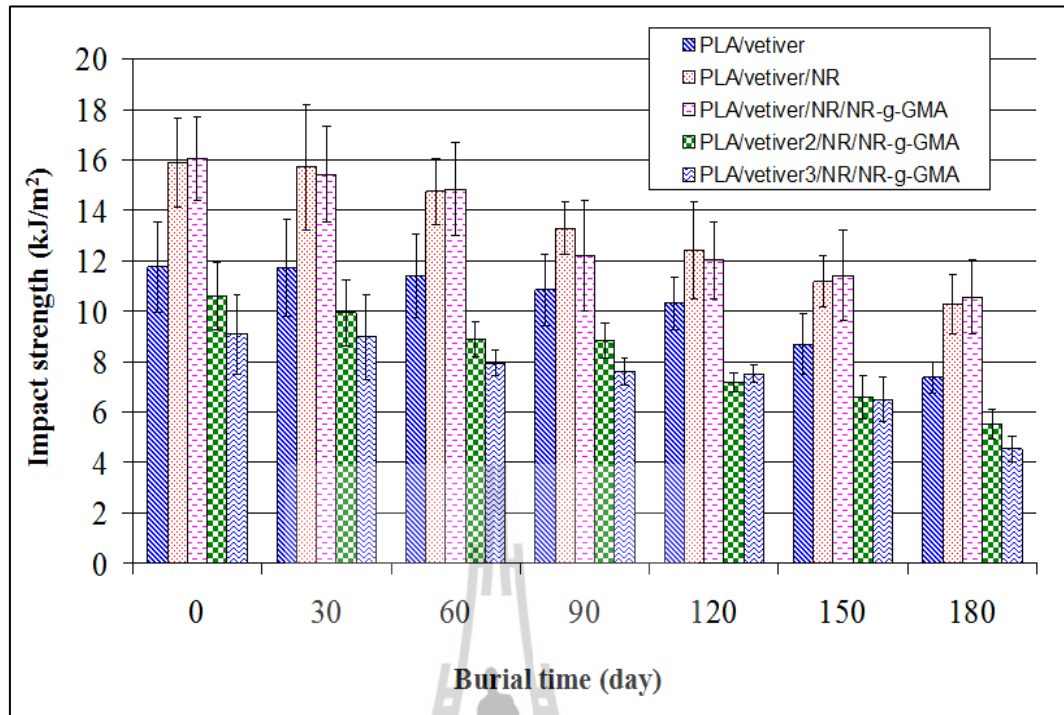
Figure 6.2 shows the comparison of impact strength of PP, PLA, PLA/NR and PLA/NR/NR-g-GMA as a function of burial time. PLA showed much lower impact strength than PP. When adding NR into PLA, impact strength of PLA was improved but still lower than that of PP. With the addition of NR-g-GMA into PLA/NR blend the impact strength of PLA/NR blend was significantly increased. The impact strength of PLA/NR/NR-g-GMA was comparable to that of PP. After burial in soil for 180 days, the impact strength of PP has not changed. For PLA, the impact strength was slightly decreased. A decrease in impact strength after burial in soil was also observed in PLA/NR and PLA/NR/NR-g-GMA.

Figure 6.3 shows impact strength of PLA/vetiver, PLA/vetiver/NR, PLA/vetiver/NR/NR-g-GMA, PLA/vetiver2/NR/NR-g-GMA and PLA/vetiver3/NR/NR-g-GMA as a function of burial time. It was observed that with the addition of vetiver grass fiber into PLA, impact strength of PLA/vetiver was lower than that of PLA. The lower impact strength of natural fiber reinforced polymer composite compared to virgin polymer is generally observed in other studies (Wan, Luo, He, Liang, Huang, and Li, 2009); (Masud, Lawrence, Amar, and Manjusri, 2006) and (Nina, Axel, and Jorg, 2009). However, with the addition of NR, the impact strength of the composite was improved. This result was resembled with our previous study (Ruksakulpiwat, Srideea, Suppakarn, and Sutapun, 2009). It was found that the addition of rubber in natural fiber-PP composite can improve the impact strength of the composites. When using NR-g-GMA as compatibilizer in PLA/vetiver/NR, it was observed that impact strength of PLA/vetiver/NR/NR-g-GMA was slightly higher than that of PLA/vetiver/NR. With increasing vetiver grass fiber content in PLA/vetiver/NR/NR-g-GMA up to 20 and 30% (wt/wt), impact strength of the

composites was decreased. After burial in soil, impact strength of all PLA composites with vetiver grass decreased significantly with increasing burial time. Impact strength of PLA/vetiver after burial in soil for 180 days was decreased about 37%. Impact strength of PLA/vetiver/NR and PLA/vetiver/NR/NR-g-GMA after burial in soil for 180 days was decreased about 35% and 34%, respectively. With increasing vetiver grass fiber content upto 20 and 30% (wt/wt), impact strength of PLA composites after burial in soil for 180 days was greatly decreased (48 and 50%). This result indicated that the biodegradability of PLA was significantly affected by the addition of the vetiver grass fiber.



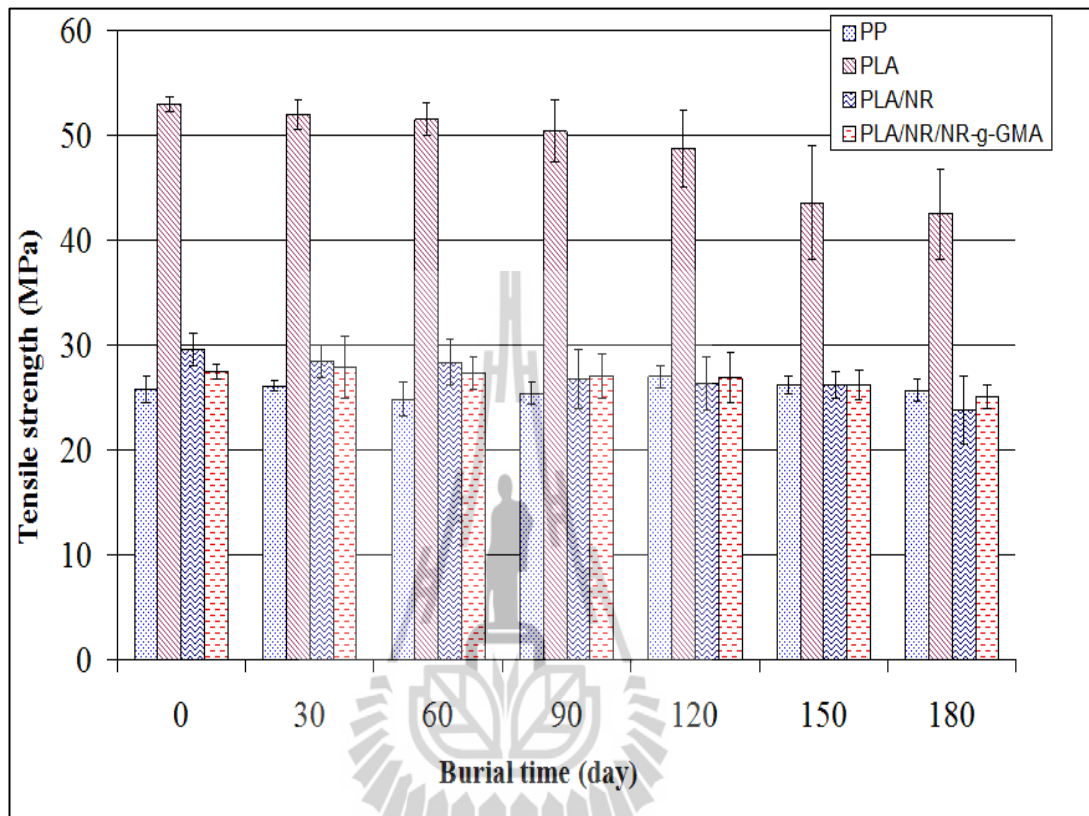
**Figure 6.2** Impact strength of PP, PLA, PLA/NR and PLA/NR/NR-g-GMA.



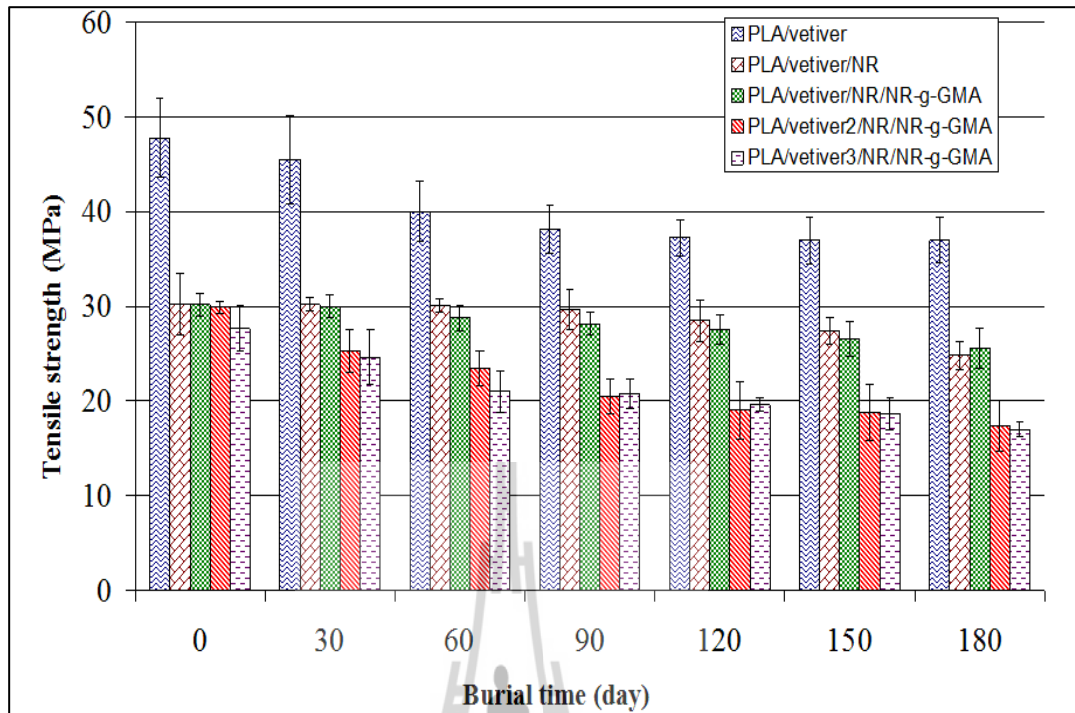
**Figure 6.3** Impact strength of PLA/vetiver, PLA/ vetiver /NR, PLA/vetiver /NR/NR-g-GMA, PLA/ vetiver 2/NR/NR-g-GMA and PLA/vetiver3 /NR/NR-g-GMA.

Tensile strength of PP, PLA, PLA/NR and PLA/NR/NR-g-GMA as a function of burial time are shown in Figure 6.4. PLA showed much higher tensile strength than PP. When adding NR and NR-g-GMA into PLA, tensile strength of PLA was decreased but still higher than PP. After burial in soil, tensile strength of PP did not change, due to its non-biodegradability, whereas those of PLA, PLA/NR and PLA/NR/NR-g-GMA slightly decreased after 180 days. However, with the addition of vetiver grass fiber, tensile strength of PLA/vetiver, PLA/vetiver/NR, PLA/vetiver/NR/NR-g-GMA, PLA/vetiver2/NR/NR-g-GMA and PLA/vetiver3-

/NR/NR-g-GMA significantly decreased after burial in soil for 180 days as shown in Figure 6.5.



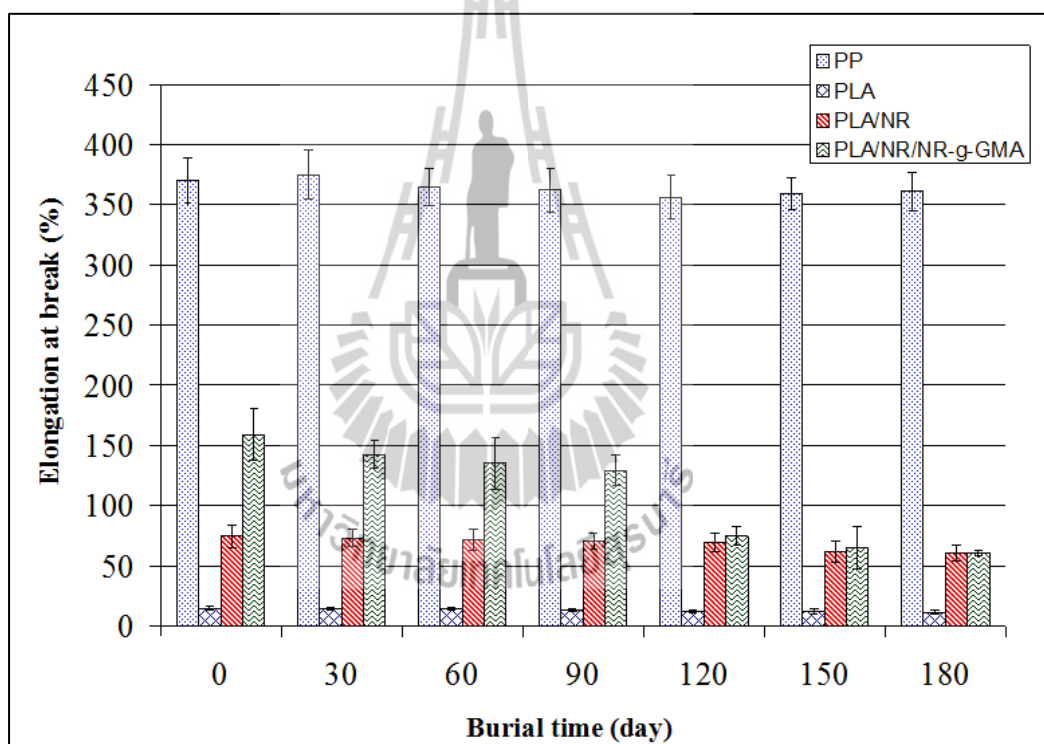
**Figure 6.4** Tensile strength of PP, PLA, PLA/NR and PLA/NR/NR-g-GMA.



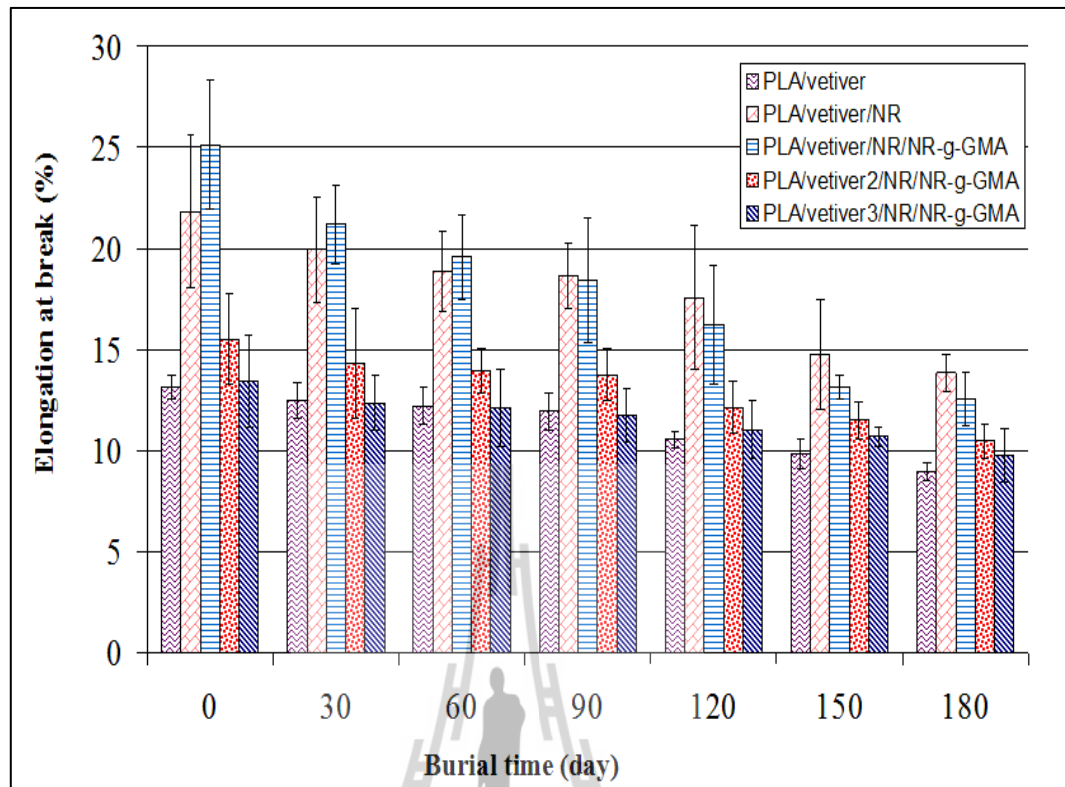
**Figure 6.5** Tensile strength of PLA/vetiver, PLA/ vetiver /NR, PLA/vetiver/NR/NR-g-GMA, PLA/vetiver2/NR/NR-g-GMA and PLA/vetiver 3/NR/NR-g-GMA.

Figure 6.6 shows elongation at break of PP, PLA, PLA/NR and PLA/NR/NR-g-GMA. Elongation at break of PLA was much lower than that of PP. With the addition of NR into PLA, elongation at break of PLA was improved. When adding NR-g-GMA into PLA/NR blend elongation at break of PLA/NR blend was significantly increased. After burial in soil elongation at break of pure PP did not change but elongation at break of pure PLA and PLA blend were decreased. Elongation at break of PLA/vetiver, PLA/vetiver/NR, PLA/vetiver/NR/NR-g-GMA, PLA/vetiver2/NR/NR-g-GMA and PLA/vetiver3/NR/NR-g-GMA are illustrated in Figure 6.7. It was found that elongation at break of PLA/vetiver was lower than that

of PLA. With the addition of NR, elongation at break of PLA/vetiver/NR was higher than that of PLA/vetiver. Further improvement in elongation at break was shown with the addition of NR-g-GMA into PLA composite (PLA/vetiver/NR/NR-g-GMA). This was attributed to the enhanced compatibility between PLA, vetiver grass fiber and NR by NR-g-GMA. Furthermore, it was observed that with the addition of vetiver grass, elongation at break of PLA composite were greatly decreased after burial in soil. This confirmed that vetiver grass fiber had great influences on biodegradability of PLA.



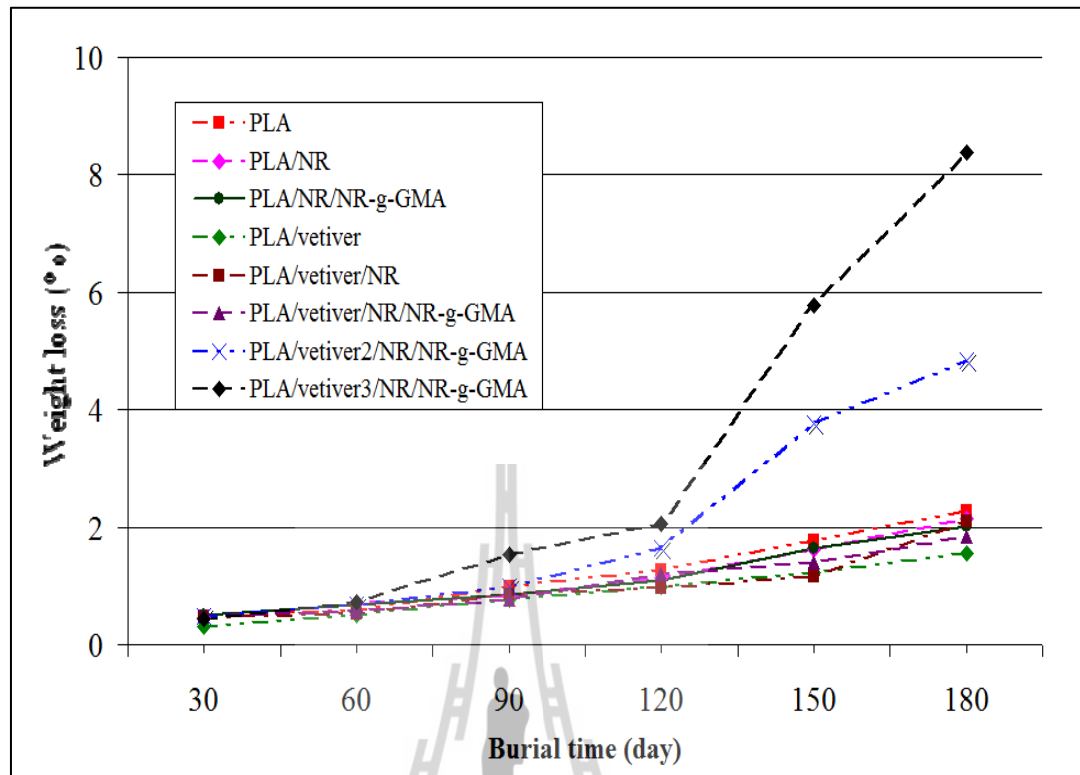
**Figure 6.6** Elongation at break of PP, PLA, PLA/NR and PLA/NR/NR-g-GMA.



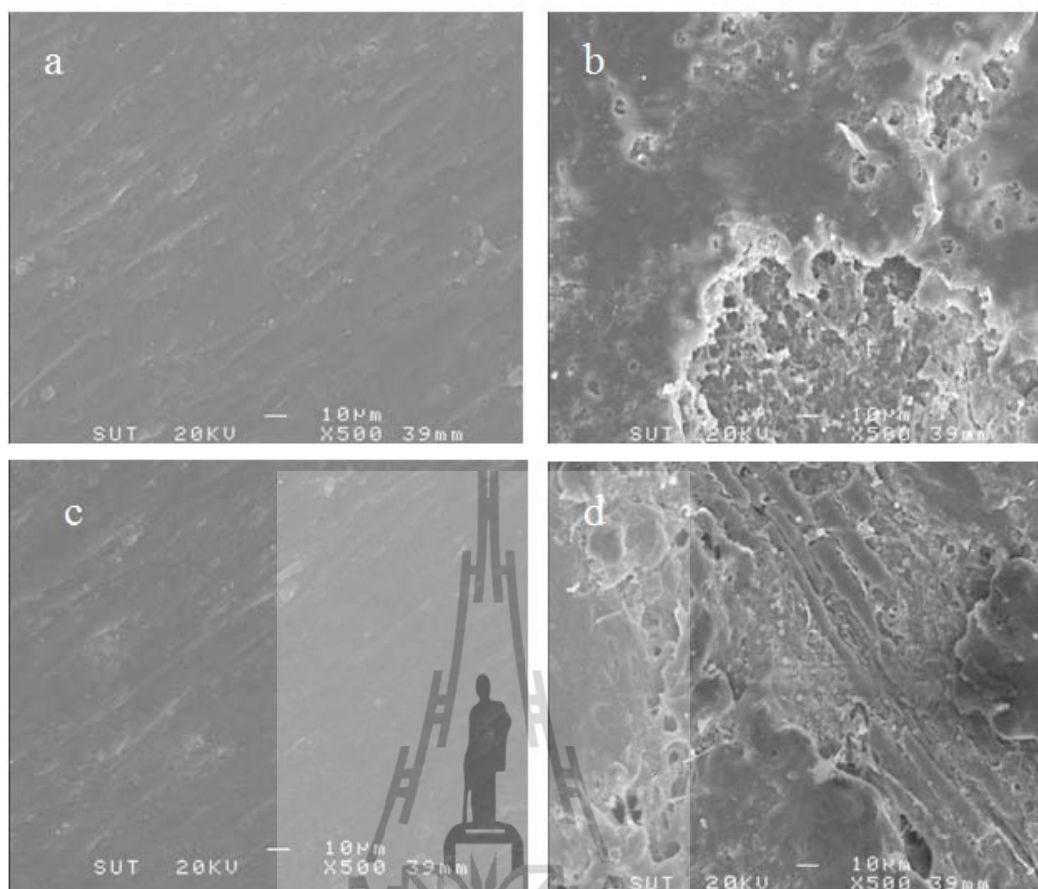
**Figure 6.7** Elongation at break of PLA/vetiver, PLA/ vetiver /NR, PLA/vetiver/NR/NR-g-GMA, PLA/vetiver2/NR/NR-g-GMA and PLA/vetiver3/NR/NR-g-GMA.

Figure 6.8 shows weight loss of PLA, PLA blends and PLA composites after burial in soil at various times. It was shown that PLA exhibited about 2% mass loss after burial in soil for 180 days. The presence of NR, NR-g-GMA and vetiver grass fiber 10% (wt/wt) did not pronouncedly affect the change in weight loss after burial in soil for the period of study. However, the addition of 20 and 30% (wt/wt) of vetiver grass fiber caused significantly increase in weight loss of the specimens with increasing burial time. SEM micrographs (500x magnification) of PLA blend and PLA composite are shown in Figure 6.9 (a-d). Before burial in soil,

the smooth surface of PLA/NR/NR-g-GMA can be observed (Figure 6.9 (a)). After burial in soil for 180 days, the surface of PLA was eroded due to the bacteria and fungi contained in soil (Figure 6.9 (b)). The smooth surface of PLA/vetiver2/NR/NR-g-GMA before burial in soil was also observed (Figure 6.9 (c)). After burial in soil for 180 days, vetiver grass fiber was degraded and the surface of PLA was eroded especially around the vetiver grass fiber. This confirmed that the addition of vetiver grass fiber enhanced the biodegradability of PLA. Vetiver grass fiber was mainly composed of cellulose (Ruksakulpiwat et al., 2007). These constituents of vetiver grass fiber can be degraded by many bacteria and fungi in the soil environment. The degradation of vetiver grass fiber was faster than that of PLA matrix because the cellulosic materials can be easily attacked by microorganisms (Singh, Pandey, Rutot, Degee, and Dubois, 2003). After vetiver grass fiber consumption by microorganisms, the increased polymer surface was created. Kim et al. found that the addition of natural fiber (rice-husk flour, RHF) also enhanced the biodegradability of poly(butylene succinate) (PBS) mainly because of the increased polymer surface by the degradation of RHF. The biodegradability of PBS would be controlled by the bioflour content because it is more easily degradable than PBS in soil environment (Kim, Kim, and Lee, 2006). Moreover, vetiver grass fiber is a water absorption material, the addition of vetiver grass fiber in PLA might enhance the hydrolysis reaction of PLA. This resulted in the faster degradation of PLA composite with vetiver grass fiber than that of pure PLA and PLA blend without vetiver grass fiber.



**Figure 6.8** Weight loss of PLA, PLA blends and PLA composites during the burial in soil.



**Figure 6.9** SEM micrographs (500x magnification) of surface morphology of PLA/NR/NR-g-GMA before burial in soil (a), PLA/NR/NR-g-GMA after burial in soil (b), PLA/vetiver2/NR/NR-g-GMA before burial in soil (c) and PLA/vetiver2/NR/NR-g-GMA after burial in soil (d) prepared from compression molding.

## 6.5 Conclusions

The addition of vetiver grass fiber in PLA and PLA blend significantly enhanced the biodegradability of PLA after burial in soil. This was shown by the great reduction in impact strength, tensile strength and elongation at break of PLA composites with the addition of vetiver grass. Moreover it was observed that the addition of vetiver grass fiber content more than 20% (wt/wt) in PLA/NR blend with NR-g-GMA, weight loss of samples after burial in soil for 120 days increased dramatically.

## 6.6 References

- Broz, M. E., VanderHart, D. L., and Washburn, N. R. (2003). Structure and mechanical properties of poly (d,l-lactic acid)/poly ( $\epsilon$ -caprolactone) blends. **Biomaterials**, 24: 4181-4190.
- Gu, S.Y., Zhang, K., Ren, J., and Zhan, H. (2008). Melt rheology of polylactide/poly (butylene adipate-co-terephthalate) blends. **Carbohyd. Polym.** 74: 79-85.
- Kim, H. S., Kim, H. J., and Lee, J. W. (2006). Biodegradability of bio-flour filled biodegradable poly (butylene succinate) bio-composites in natural and compost soil. **Polym. Degrad. Stab.** 91: 1117-1127.
- Long, J., Michael, P. W., and Jinwen, Z. (2006). Study of Biodegradable Polylactide/Poly (butylenes adipate-co-terephthalate) Blends. **Biomacromolecules**. 7: 199-207.

- Lunt, J. (1998). Large-scale production, properties and commercial applications of polylactic acid polymers. **Polym. Degrad. Stab.** 59: 145-152.
- Masud, S.H., Lawrence, T.D., Amar, K.M., and Manjusri, M. (2006). Chopped glass and recycled newspaper as reinforcement fibers in injection molded poly(lactic acid) (PLA) composites: A comparative study. **Compos. Sci. Technol.** 66: 1813-1824.
- Nina, G., Axel, S.H., and Jorg, M. (2009). Natural and man-made cellulose fibre-reinforced poly(lactic acid) (PLA) composites: An overview about mechanical characteristics and application areas. **Compos. Part A.** 40: 810-821.
- Oksman, K., Skrifvars, M., and Selin, J. F. (2003). Natural fibres as reinforcement in polylactic acid (PLA) composites. **Compos. Sci. Technol.** 63: 1317-1324.
- Ochi, S. (2008). Mechanical properties of kenaf fibers and kenaf/PLA composites. **Mech. Mater.** 40: 446-452.
- Ratto, J.A., Stenhouse, P.J., Auerbach, M., Mitchell, J., and Farrell, R. (1999). Processing, performance and biodegradability of a thermoplastic aliphatic polyester starch system. **Polymer.** 40: 6777-6788.
- Ruksakulpiwat, Y., Suppakarn, N., Sutapun, W., and Thomthong, W. (2007). Vetiver–polypropylene composites: Physical and mechanical properties. **Compos. Part A.** 38: 590-601.
- Ruksakulpiwat, Y., Srideea, J., Suppakarn, N., and Sutapun, W. (2009). Improvement of impact property of natural fiber–polypropylene composite by using natural rubber and EPDM rubber. **Compos. Part B.** 40: 619-622.

- Sarazin, P., Li, G., Orts, W. J., and Favis, B. D. (2008). Binary and ternary blends of polylactide, polycaprolactone and thermoplastic starch. **Polymer**. 49: 599-609.
- Shibata, M., Inoue, Y., and Miyoshi, M. (2006). Mechanical properties, morphology, and crystallization behavior of blends of poly(L-lactide) with poly(butylene succinate-co-L-lactate) and poly(butylene succinate). **Polymer**. 47: 3557-3564.
- Singh, R. P., Pandey, J. K., Rutot, D., Degee, P.H., and Dubois, P.H. (2003). Biodegradation of Poly(3-caprolactone)/starch blends and composites in composting and culture environment: the effect of compatibilization on the inherent biodegradability of the host polymer. **Carbohydr. Res.** 338: 1759-1769.
- Somnuk, U., and Eder, G., Phinyocheep, P., Suppakarn, N., Sutapun, W., and Ruksakulpiwat, Y. (2007). Quiescent crystallization of natural fibers polypropylene composites. **J. Appl. Polym. Sci.** 106: 2997-3006.
- Teramoto, N., Urata, K., Ozawa, K., and Shibata, M. (2004). Biodegradation of aliphatic polyester composites reinforced by abaca fiber. **Polym. Degrad. Stab.** 86: 401- 409.
- Tserki, V., Matzinos, P., and Panayiotou, C. (2003). Effect of compatibilization on the performance of biodegradable composites using cotton fiber waste as filler. **J. Appl. Polym. Sci.** 88: 1825-1835.
- Wan, Y.Z., Luo, H., He, F., Liang, H., Huang, Y., and Li, X. L. (2009). Mechanical, moisture absorption, and biodegradation behaviours of bacterial cellulose fibre-reinforced starch biocomposites. **Compos. Sci. Technol.** 69: 1212-1217.

- Wu, D., Zhang, Y., Zhang, M., and Zhou, W. (2008). Phase behavior and its viscoelastic response of polylactide/poly(e-caprolactone) blend. **Euro. Polym. J.** 44: 2171-2183.
- Yokohara, T., and Yamaguchi, M. (2008). Structure and properties for biomass-based polyester blends of PLA and PBS. **Euro. Polym. J.** 44: 677-685.



# **CHAPTER VII**

## **COMPARISON BETWEEN MECHANICAL PROPERTIES OF POLYLACTIC ACID AND NATURAL RUBBER BLEND USING CALCIUM CARBONATE AND VETIVER GRASS FIBER AS FILLER**

### **7.1 Abstract**

In this study, calcium carbonate ( $\text{CaCO}_3$ ) and vetiver grass fiber were used as fillers in PLA/NR blend. With the addition of  $\text{CaCO}_3$  into PLA/NR blend with NR-g-GMA, impact strength and modulus of the composite were further increased with a loss in tensile strength. In contrast, the addition of vetiver grass fiber into PLA/NR blend with NR-g-GMA led to an increase in tensile strength and modulus and a decrease in impact strength and elongation at break. The onset degradation temperatures of PLA composites were lower than that of PLA and PLA/NR blend.

### **7.2 Introduction**

From Chapter 4, natural rubber (NR) was used to improve toughness of poly (lactic acid) (PLA). Impact strength and elongation at break of PLA was increased when adding NR. Moreover, by using NR-g-GMA as a compatibilizer for PLA and NR blend, impact strength and elongation at break was improved. However, tensile strength and modulus of PLA/NR blend with and without NR-g-GMA were

decreased. Vetiver grass fiber was used as filler in PLA/NR blends to improve mechanical properties. The result showed that with the addition of vetiver grass fiber into PLA/NR with NR-g-GMA led to a slightly increase in tensile strength and modulus and a decrease in impact strength and elongation at break, which can greatly limit its engineering applications. Therefore, these properties needed to be improved for many potential applications.  $\text{CaCO}_3$  was widely used as a filler to improve mechanical properties of PLA blends. Mechanical properties of PLA blends using  $\text{CaCO}_3$  as filler were improved. In this study, mechanical properties of PLA/NR blend using calcium carbonate ( $\text{CaCO}_3$ ) and vetiver grass fiber as filler were compared. It was expected that mechanical properties of PLA/NR blend were improved. Thermal properties of PLA, PLA blends and PLA composites were also studied.

## **7.3 Experimental**

### **7.3.1 Materials**

A commercial grade of PLA (PLA 4042D) was purchased from NatureWorks LLC. Thai natural rubber (grade STR 5L) were purchased from Thaihua Latex Co., Ltd. NR-g-GMA was prepared in our laboratory. The details on synthesis and characterization of NR-g-GMA were given in Chapter 3. Vetiver grass fiber, with 2 mm in length and its aspect ratio of 6.15 was modified by heat treatment method using the temperature of 180°C for 4 hours before mixing.  $\text{CaCO}_3$  (Hicoat 801) was provided by Sand and Soil Co., Ltd. and it was dried in an oven at 70 °C for 6 hours to eliminate moisture before used.

### 7.3.2 Blends and composites preparation

The compositions of PLA blends and PLA composites are shown in Table 7.1. Before mixing, PLA was dried in an oven at 70 °C for 4 hours to eliminate moisture. All compositions of each PLA blends and PLA composites were mixed using an internal mixer (Hakke Rheomix, 3000p) at temperature of 170 °C with a rotor speed of 60 rpm for 10 min. Compression molding (LabTech, LP20-B) were used to prepare the specimens. The melting temperature of 165 °C and mold temperature of 25 °C were used. The impact test was performed according to ASTM D256 using an Atlas testing machine (model BPI). Tensile properties were obtained according to ASTM D638 using an Instron universal testing machine (UTM, model 5565) with a load cell of 5 kN. Thermo gravimetric analysis (TGA) was performed using a TA Instrument thermo gravimetric analyzer (TGA, Mettler Toledo model TGA/DSC 1) by heating the sample from room temperature to 600 °C at a heating rate of 20 °C/min under a nitrogen atmosphere. Differential scanning calorimetry (DSC : Mettler Toledo Version STARe SW 8.1) was used to obtain thermal properties of specimens by heating the specimens from 30 °C to 200 °C at the rate of 5 °C/min (First heating scan). After keeping the specimens at 200 °C for 3 min they were cooled to 30 °C at 5 °C/min. Then they were heated again to 200 °C at 5 °C/min (Second heating scan). The degree of crystallinity, %X<sub>C</sub>, of the composites can be obtained by:

$$\%X_C = \frac{\Delta H_m}{\Delta H_{mo}(\text{Ø}_{PLA})} \times 100$$

In which  $\Delta H_m$  was the measured melting enthalpy,  $\Delta H_{m0}$  was the melting enthalpy of purely crystalline sample (93 J/g for PLA) (Cheung, Lau, Tao, and Hui, 2008) and  $\phi_{PLA}$  was the PLA weight fraction in the composites.

**Table 7.1** Blends and composites composition.

Symbols	PLA (wt%)	NR (wt%)	NR-g-GMA (wt%)	Vetiver grass fiber (phr)	CaCO <sub>3</sub> (phr)
PLA	100	-	-	-	-
PLA/NR	90	10	-	-	-
A	90	9	1	-	-
B	90	9	1	10	-
C	90	9	1	-	5
D	90	9	1	-	10
E	90	9	1	-	20

#### 7.4 Results and discussion

Table 7.2 shows impact strength, tensile strength, elongation at break and modulus of PLA, PLA blends and PLA composites. It was shown that with the addition of CaCO<sub>3</sub> (5 phr) into PLA/NR/NR-g-GMA blend, impact strength of the composite was increased. With increasing CaCO<sub>3</sub> content to 10 and 20 phr, impact strength of PLA composites decreased. This may be related to agglomeration of CaCO<sub>3</sub>, resulting in a poor dispersion of CaCO<sub>3</sub> on the PLA matrix. Moreover, it was found that with increasing CaCO<sub>3</sub> content modulus of the composite was increased but tensile strength and elongation at break were decreased. However, elongation at

break of this composite was still higher than that of neat PLA and PLA/NR blend without NR-g-GMA. In contrast, the addition of vetiver grass fiber into PLA/NR blend with NR-g-GMA led to the decrease of impact strength. This may be due to the fact that the addition of vetiver grass fiber was possibly increased the number of void in PLA composites. Therefore, these voids were served as a local area for crack initiation and caused the failure at lower stress. Somnuk et.al (2007) also observed this behavior in vetiver grass fiber - PP composite.

**Table 7.2** Impact strength, tensile strength, modulus and elongation at break of PLA, PLA blends and PLA composites.

<b>Samples</b>	<b>Impact strength (kJ/m<sup>2</sup>)</b>	<b>Tensile strength (MPa)</b>	<b>Elongation at break (%)</b>	<b>Modulus (GPa)</b>
PLA	19.06±0.50	52.99±0.65	10.84±1.64	0.63±0.04
PLA/NR	39.70±4.50	29.66±1.56	74.51±9.06	0.51±0.04
A	69.83±10.49	28.3±0.99	403.45±23.50	0.52±0.02
B	15.40±2.31	30.65±1.50	24.10±3.62	0.61±0.04
C	99.75±7.58	24.38±0.54	278.64±17.32	0.62±0.03
D	82.48±14.52	25.94±0.43	244.75±19.41	0.64±0.02
E	81.98±11.27	26.14±0.61	232.23±19.46	0.68±0.04

TGA curves of NR, PLA, PLA blends and PLA composites are shown in Figure 7.1. The onset degradation temperature of PLA/NR was 294.20 °C, which is about 4°C higher than PLA (290.76 °C). The slightly increase in thermal stability of PLA/NR has been attributed to the higher thermal stability of NR. Moreover,

PLA/NR blend with NR-g-GMA showed higher onset degradation temperatures (301.59°C) than that of PLA/NR. The increase in thermal stability of PLA/NR when using NR-g-GMA as compatibilizer might be attributed to the higher interaction and better dispersion of NR in PLA matrix. An increase in thermal stability of PLA due to the good interaction between the blend components was also reported in other PLA blends and composites (Girija, Sailaja, and Giridhar, 2005). The onset degradation temperature of PLA composite was lower than that of PLA and PLA blend. Moreover, it was found that the onset degradation temperature was decreased with increasing CaCO<sub>3</sub> content (Figure 7.2). This may be due to the fact that the basic nature of CaCO<sub>3</sub> may have catalyzed the depolymerization of the ester bonds of PLA, and thus, it was thought to be responsible for the reduced thermal stability (Kim, Park, Choi, and Yoon, 2008). DSC curves of PLA, PLA blends and PLA composites obtained from the second heating scan are shown in Figure 7.3 and Figure 7.4. The glass transition temperature ( $T_g$ ), the crystallization temperature ( $T_c$ ) (indicated by exothermic peak) and melting temperature ( $T_m$ ) (indicated by endothermic peak) of PLA, PLA blends and PLA composites could be observed. The double melting endotherms for neat PLA were observed. This indicated that several crystallite forms of PLA were taken place. From the DSC curves, it was found that  $T_g$  of PLA blends and PLA composites were not changed comparing to that of neat PLA.  $T_m$  of PLA blends and PLA composites were shifted to higher temperature compared to that of neat PLA. Moreover, degree of crystallinity ( $\%X_C$ ) of PLA composites was lower than that of neat PLA (Table 7.3). This could be due to the fact that the addition of CaCO<sub>3</sub> and vetiver grass fiber in PLA may hinder the migration and diffusion of PLA molecular chains to the surface of the nucleus in the composite.

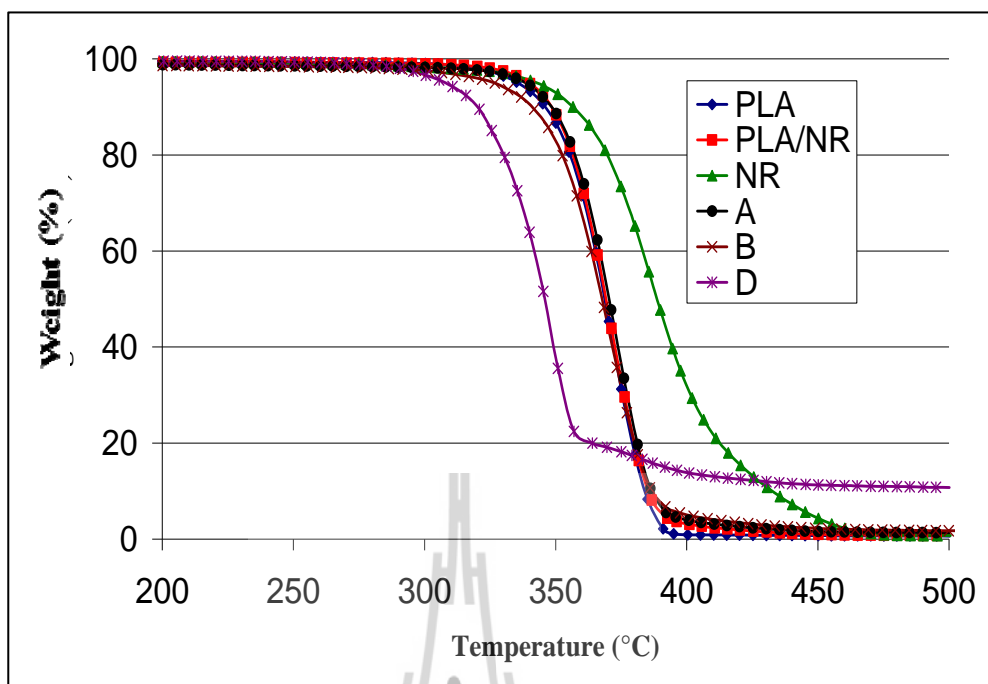


**Figure 7.1** TGA curves of PLA blends and PLA composites.

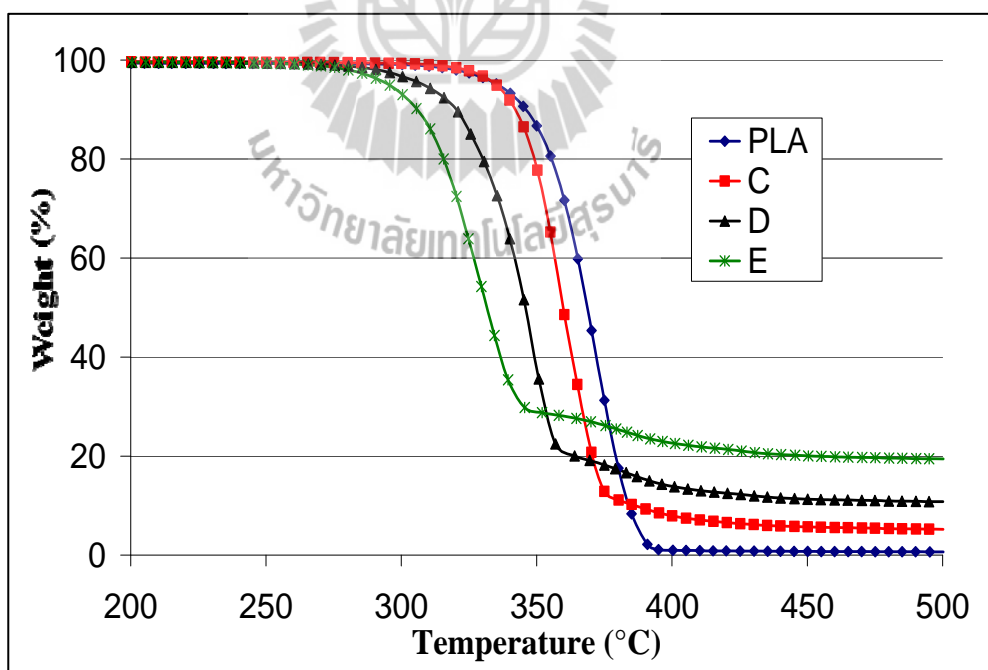


**Figure 7.2** TGA curves of PLA blends and PLA composites at various  $\text{CaCO}_3$  contents.

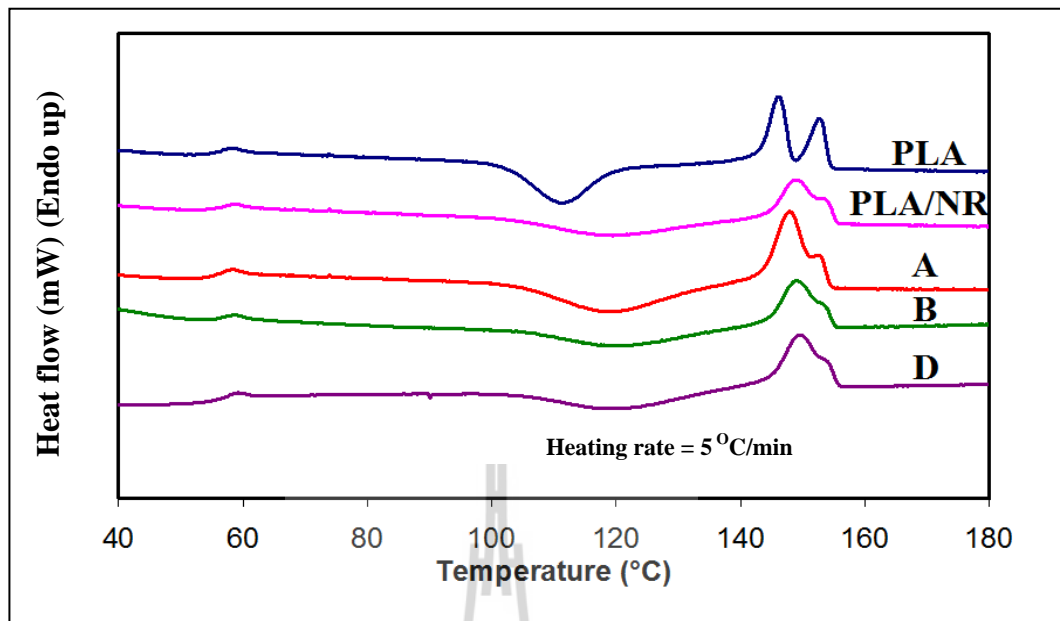


**Figure 7.3** DSC curves of PLA, PLA blends and PLA composites (Second heating scan).

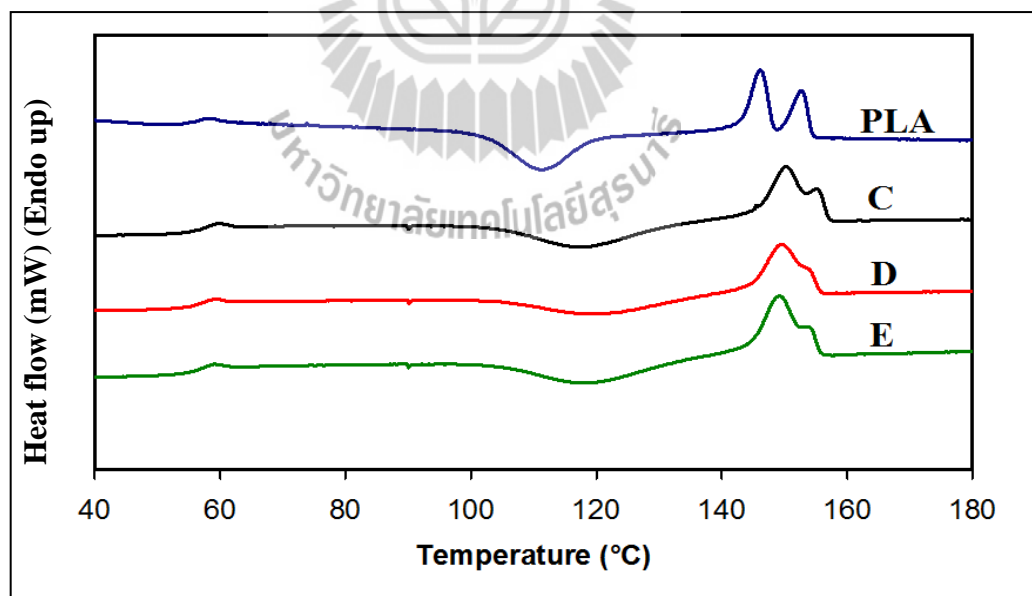


**Figure 7.4** DSC curves of PLA, PLA blends and PLA composites at various  $\text{CaCO}_3$  contents (Second heating scan).

**Table 7.3**  $T_g$ ,  $T_c$ ,  $\Delta H_c$ ,  $T_m$ ,  $\Delta H_m$  and  $\%X_C$  of PLA, PLA blends and PLA composites.

Samples	$T_g$ ( $^{\circ}\text{C}$ )	$T_c$ ( $^{\circ}\text{C}$ )	$\Delta H_c$ (J/g)	$T_m$ ( $^{\circ}\text{C}$ )		$\Delta H_m$ (J/g)	$\%X_C$
				1	2		
PLA	57.3	111.5	30.0	146.0	152.7	29.8	32.1
PLA/NR	57.2	119.4	26.7	149.1	-	22.5	26.9
A	57.2	119.4	26.1	147.9	-	27.4	32.8
B	56.7	119.3	23.6	149.3	-	21.5	28.3
C	58.5	117.7	20.9	150.3	-	24.0	30.1
D	57.0	118.7	13.4	149.5	-	20.4	26.8
E	57.3	117.8	14.1	149.2	-	20.0	28.7

## 7.5 Conclusions

With the addition of  $\text{CaCO}_3$  into PLA/NR blend with NR-g-GMA, impact strength and modulus of the composite were further increased with a loss in tensile strength. In contrast, the addition of vetiver grass fiber into PLA/NR blend with NR-g-GMA led to an increase in tensile strength and modulus and a decrease in impact strength and elongation at break. The thermal stability of PLA/NR blend was improved when using NR-g-GMA as a compatibilizer. However, thermal stability of PLA composite was lower than those of PLA and PLA blend. The  $T_g$  of PLA blends and PLA composites were not changed while  $T_c$  and  $T_m$  were shifted to higher temperature compared to that of neat PLA.

## 7.6 References

- Cheung, H. Y., Lau, K. T., Tao, X. M., and Hui, D. (2008). A potential material for tissue engineering: silkworm silk/PLA biocomposite. **Comp. Part B: Eng.** 39: 1026-1033.
- Girija, B.G., Sailaja, R.R.N., and Giridhar, M. (2005). Thermal degradation and mechanical properties of PET blends. **Polym. Degrad. Stab.** 90: 147-153.
- Kim, H. S., Park, B. H., Choi, J. H. and Yoon, J. S. (2008). Mechanical Properties and Thermal Stability of Poly(L-lactide)/Calcium Carbonate Composites. **J. Appl. Polym. Sci.** 109: 3087-3092,
- Lunt, J. (1998). Large-scale production, properties and commercial applications of polylactic acid polymers. **Polym. Degrad. Stab.** 59: 145-152.
- Somnuk, U., Eder, G., Phinyocheep, P., Suppakarn, N., Sutapun, W., and Ruksakulpiwat, Y. (2007). Quiescent crystallization of natural fibers/polypropylene composites. **J. Appl. Polym. Sci.** 106:2997-3006.

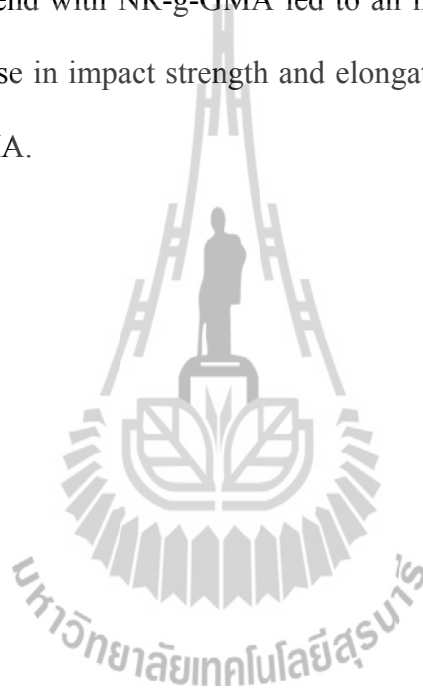
## CHAPTER VIII

### CONCLUSIONS

In this study, GMA can be grafted onto NR by emulsion polymerization method using cumene hydroperoxide (CHP) and tetraethylenepentamine (TEPA) as the initiators. The appropriate temperature and time for preparation of the graft copolymer was 30°C and 8 hours. NR-g-GMA was used as a compatibilizer for PLA/NR blend and PLA composite. The effects of NR-g-GMA on mechanical, rheological, morphological and thermal properties of PLA/NR blends and PLA composites were studied. NR-g-GMA was shown to be an effective compatibilizer for PLA/NR blend. From FT-IR results, it was confirmed that the epoxy group in NR-g-GMA can react with the carboxyl groups of PLA chain ends during blending. This results in improved compatibility between PLA and NR. With the addition of NR-g-GMA, better dispersion and distribution of NR in PLA matrix can be observed by SEM micrographs. This led to a significant increase in impact strength and elongation at break without significantly loss in tensile strength and modulus of PLA/NR blend with NR-g-GMA. Moreover, an increase in thermal stability of PLA/NR when using NR-g-GMA as a compatibilizer was observed. Shear viscosities of PLA/NR and PLA/NR blend with NR-g-GMA were quite similar and they were lower than those of neat PLA. The effects of content and %grafting of NR-g-GMA on mechanical properties of PLA/NR blend were elucidated. With increasing NR-g-GMA content up to 1% (wt/wt), impact strength and elongation at break of PLA/NR blend increased

about 2 times and 2.5 times, respectively. Moreover, with increasing %grafting of NR-g-GMA up to 2.3, the impact strength and elongation at break of PLA/NR/NR-g-GMA were increased. The compatibility between PLA, NR and vetiver grass fiber was also improved by using NR-g-GMA as a compatibilizer. Comparisons between the mechanical properties of the PLA composites prepared from injection molding and compression molding were made in this study. Injection molded PLA showed lower tensile strength, elongation at break and impact strength. However, it was observed that injection molded PLA composites showed higher tensile strength and impact strength than those of compression molded PLA composites. This is due to the higher orientation of vetiver grass fiber in injection molding than in compression molding as shown in SEM micrographs. PLA/vetiver/NR/NR-g-GMA from both injection molding and compression molding showed higher elongation at break and impact strength than those of PLA/vetiver/NR without significant lost in tensile strength. With increasing vetiver grass fiber content from 10% to 20%, tensile strength of injection molded PLA composite slightly increased. For compression molded specimens, tensile strength as well as elongation at break and impact strength of PLA composite decreased with increasing vetiver grass fiber content. The biodegradability of PLA blends and PLA composites was evaluated by soil burial test. The comparison of mechanical properties of PP, PLA, PLA blends and PLA composites as a function of burial time were made. After burial in soil for 180 days, the impact strength of PP has not changed. For PLA and PLA blends, the mechanical properties were slightly decreased. In contrast, the mechanical properties of PLA composites were dramatically decreased. This indicated that vetiver grass fiber showed a significant role in the biodegradability of PLA composites. Moreover, the

addition of vetiver grass fiber at 20 and 30% (wt/wt) content led to a significant increase in weight loss of the specimens with increasing burial time. Additionally, mechanical properties of PLA/NR blend using calcium carbonate ( $\text{CaCO}_3$ ) and vetiver grass fiber as filler were also compared. With the addition of  $\text{CaCO}_3$  into PLA/NR/NR-g-GMA blend, impact strength and modulus of the composite were higher than those of PLA/NR/NR-g-GMA. In contrast, the addition of vetiver grass fiber into PLA/NR blend with NR-g-GMA led to an increase in tensile strength and modulus and a decrease in impact strength and elongation at break compare to those of PLA/NR/NR-g-GMA.



**APPENDIX A**  
**GRAFTING EFFICIENCY, %GRAFTING,**  
**%CONVERSION AND CURE CHARACTERISTICS**  
**OF NR-g-GMA**

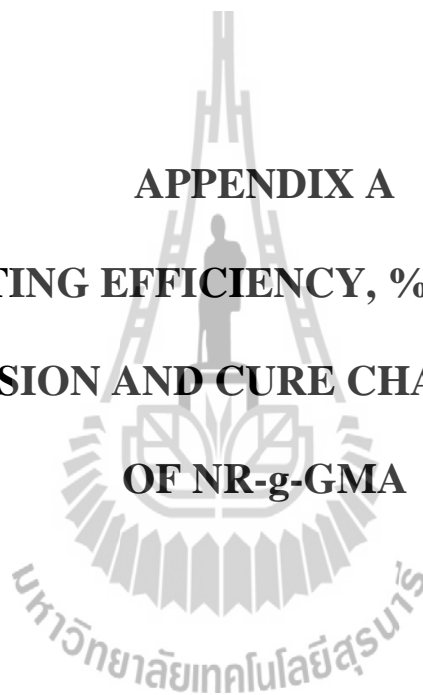


**Table A1** Grafting efficiency, %grafting and %conversion of NR-g-GMA at various reaction temperature.

<b>Temperature (°C)</b>	<b>Dried NR (g)</b>	<b>GMA (g)</b>	<b>GMA grafted (g)</b>	<b>GMA Homopolymer (g)</b>	<b>%grafting</b>	<b>Grafting efficiency</b>	<b>%conversion</b>
10	4.8860	2.0405	1.2816	0.2103	26.2300	85.9039	73.1144
30	4.8929	2.0056	1.6671	0.3114	34.0718	84.2608	98.6488
50	4.8993	2.0796	1.7349	0.3438	35.4112	83.4608	99.9567
70	4.9121	2.0778	1.7639	0.3105	35.9093	85.0318	99.8364



**Table A2** Grafting efficiency, %grafting and %conversion of NR-g-GMA at various reaction time.

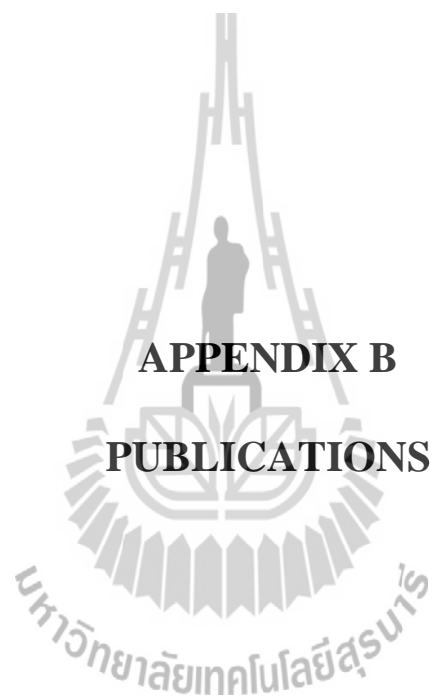
<b>Time (hours)</b>	<b>Dried NR (g)</b>	<b>GMA (g)</b>	<b>GMA grafted (g)</b>	<b>GMA homopolymer (g)</b>	<b>%grafting</b>	<b>Grafting efficiency</b>	<b>%conversion</b>
1	0.2230	0.0920	0.0394	0.0068	17.6682	85.2814	50.2174
2	0.2235	0.0922	0.0532	0.0091	23.8031	85.3933	67.5705
3	0.2285	0.0943	0.059	0.0096	25.8206	86.0058	72.7466
4	0.2284	0.0942	0.0598	0.0099	26.1821	85.7963	73.9915
6	0.2272	0.0937	0.0665	0.0108	29.2694	86.0285	82.4973
8	0.2227	0.0919	0.0779	0.0138	34.9798	84.9509	99.7824
10	0.2275	0.0909	0.0775	0.0128	34.0659	85.8250	99.3399
12	0.2241	0.0925	0.0778	0.0138	34.7166	84.9345	99.0270
18	0.2248	0.0929	0.0797	0.0131	35.4537	85.8836	99.8924
24	0.2226	0.0919	0.0766	0.0143	34.4115	84.2684	98.9119

**Table A3** Grafting efficiency, %grafting and %conversion of NR-g-GMA at various GMA content.

<b>GMA contents (phr)</b>	<b>Dried NR (g)</b>	<b>GMA (g)</b>	<b>GMA grafted (g)</b>	<b>GMA homopolymer (g)</b>	<b>%grafting</b>	<b>Grafting efficiency</b>	<b>%conversion</b>
1	4.8853	0.0515	0.0371	0.0143	0.7594	72.1790	99.8058
3	4.8903	0.1554	0.1127	0.0426	2.3046	72.5692	99.9356
5	4.8855	0.2921	0.2126	0.0791	4.3517	72.8831	99.8631
10	4.8907	0.5501	0.4109	0.1387	8.4017	74.7635	99.9091
20	4.8863	1.0482	0.816	0.2305	16.6998	77.9742	99.8378
30	4.8866	1.6302	1.2896	0.3384	26.3905	79.2138	99.8650
40	4.8905	2.0404	1.7102	0.3231	34.9698	84.1096	99.6520
50	4.8867	2.5800	1.8116	0.7331	37.0721	71.1900	99.6318

**Table A4** Cure characteristics of NR and NR-g-GMA at various %grafting, expressed in term of scorch time, cure time, maximum torque (MH), minimum torque (ML) and torque difference (MH-ML).

<b>Samples</b>	<b>Scorch time (min)</b>	<b>Cure time (min)</b>	<b>MH (dNm)</b>	<b>ML (dNm)</b>	<b>MH-ML (dNm)</b>
NR	4.22	7.97	17.060	4.900	12.160
NR-g-GMA (%grafting 4.35)	4.45	8.70	33.565	9.793	23.772
NR-g-GMA (%grafting 8.40)	4.70	9.12	34.537	10.071	24.466
NR-g-GMA (%grafting 16.70)	4.55	9.12	35.118	9.450	25.668



**APPENDIX B**  
**PUBLICATIONS**

## List of publications

- Juntuek, P., Ruksakulpiwat, C., Chumsamrong P., and Ruksakulpiwat Y. (2010). Mechanical properties of polylactic acid and natural rubber blends using vetiver grass fiber as filler. **Adv. Mat. Res.** 123-125: 1167-1170.
- Juntuek, P., Ruksakulpiwat, C., Chumsamrong, P., and Ruksakulpiwat, Y. (2011). Glycidyl methacrylate grafted natural rubber: Synthesis, Characterization, and Mechanical Property. **J. Appl. Polym. Sci.** 122, 3152-3159.
- Juntuek, P., Ruksakulpiwat, C., Chumsamrong P., and Ruksakulpiwat Y. (2012). Comparison between mechanical and thermal properties of polylactic acid and natural rubber blend using calcium carbonate and vetiver grass fiber as fillers. **Adv. Mat. Res.** 410: 59-62.
- Juntuek, P., Ruksakulpiwat, C., Chumsamrong, P., and Ruksakulpiwat, Y. Effect of glycidyl methacrylate-grafted natural rubber on physical properties of polylactic acid and natural rubber blends. **J. Appl. Polym. Sci.** (In publication).
- Juntuek, P., Ruksakulpiwat, C., Chumsamrong, P., and Ruksakulpiwat, Y. Effect of vetiver grass fiber and molding techniques on biodegradability and mechanical property of PLA/NR composites. **Polym. Degrad. Stab.** (Submitted).
- Juntuek, P., Ruksakulpiwat, C., Chumsamrong P., and Ruksakulpiwat Y. (2009). The study of grafting glycidyl methacrylate onto natural rubber. **The International Conference on Advances in Materials and Processing Technologies (AMPT 2009)**, Kuala Lumpur, Malaysia, October 26-29.

- Juntuek, P., Ruksakulpiwat, C., Chumsamrong P., and Ruksakulpiwat Y. (2010). The study of using glycidyl methacrylate grafted natural rubber as an impact modifier of polylactic acid. **Proceedings of Clean Technology Conference**, Anaheim, California, U.S.A, June 21-25.
- Juntuek, P., Ruksakulpiwat, C., Chumsamrong P., and Ruksakulpiwat Y. (2011). Mechanical properties of polylactic acid and natural rubber blend using Calcium carbonate and vetiver grass fiber as filler. **The 18<sup>th</sup> International Conference on Composite Materials (ICCM18)**, Jeju Island, Korea, August 21-26.
- Juntuek, P., Ruksakulpiwat, C., Chumsamrong P., and Ruksakulpiwat Y. (2011). Effect of vetiver grass fiber on biodegradability of polylactic acid and natural rubber blend. **The 3<sup>rd</sup> International Conference on Biodegradable and Biobased Polymers (BIOPOL-2011)**, ECPM, University of Strasbourg, France, August 29-31.
- Juntuek, P., Ruksakulpiwat, C., Chumsamrong P., and Ruksakulpiwat Y. Glycidyl methacrylate grafted natural rubber. **patent pending: 1101000734.**
- Juntuek, P., Ruksakulpiwat, C., Chumsamrong P., and Ruksakulpiwat Y. Polylactic acid (PLA) and natural rubber (NR) blend using glycidylmethacrylate as a compatibilizer. **patent pending: 1101000735.**
- Juntuek, P., Ruksakulpiwat, C., Chumsamrong P., and Ruksakulpiwat Y. Polylactic acid (PLA), natural rubber (NR) and vetiver grass fiber composite. **patent pending: 11010003625.**

## **BIOGRAPHY**

Miss Punmanee Juntuek was born on September 12, 1982 in Chaiyaphum, Thailand. She finished primary school from Ban Huiyang School and secondary school from Huitonpittayakom School. After that, she continued her study in Faculty of Science at Khon Kaen University (KKU), Khon Kaen and earned her Bachelor's degree in Chemistry in 2006. Then, she continued with her graduate study in Polymer Engineering Program, Institute of Engineering, Suranaree University of Technology. Her expertise is in the field of polymer synthesis, polymer characterization, and polymer composites. During her doctoral degree study, she published five papers in international journal as shown in Appendix B. She also presented four papers in abroad. During her graduate study, she got a research assistant scholarship from Center of Excellence on Petrochemical and Materials Technology.

